International Journal of Endocrinology

Primary Hyperparathyroidism: Diagnosis, Management, and Therapy

Lead Guest Editor: Maria G. Chiofalo
Guest Editors: Giorgio Borretta, Juan P. Dueñas, and Vito Guarnieri

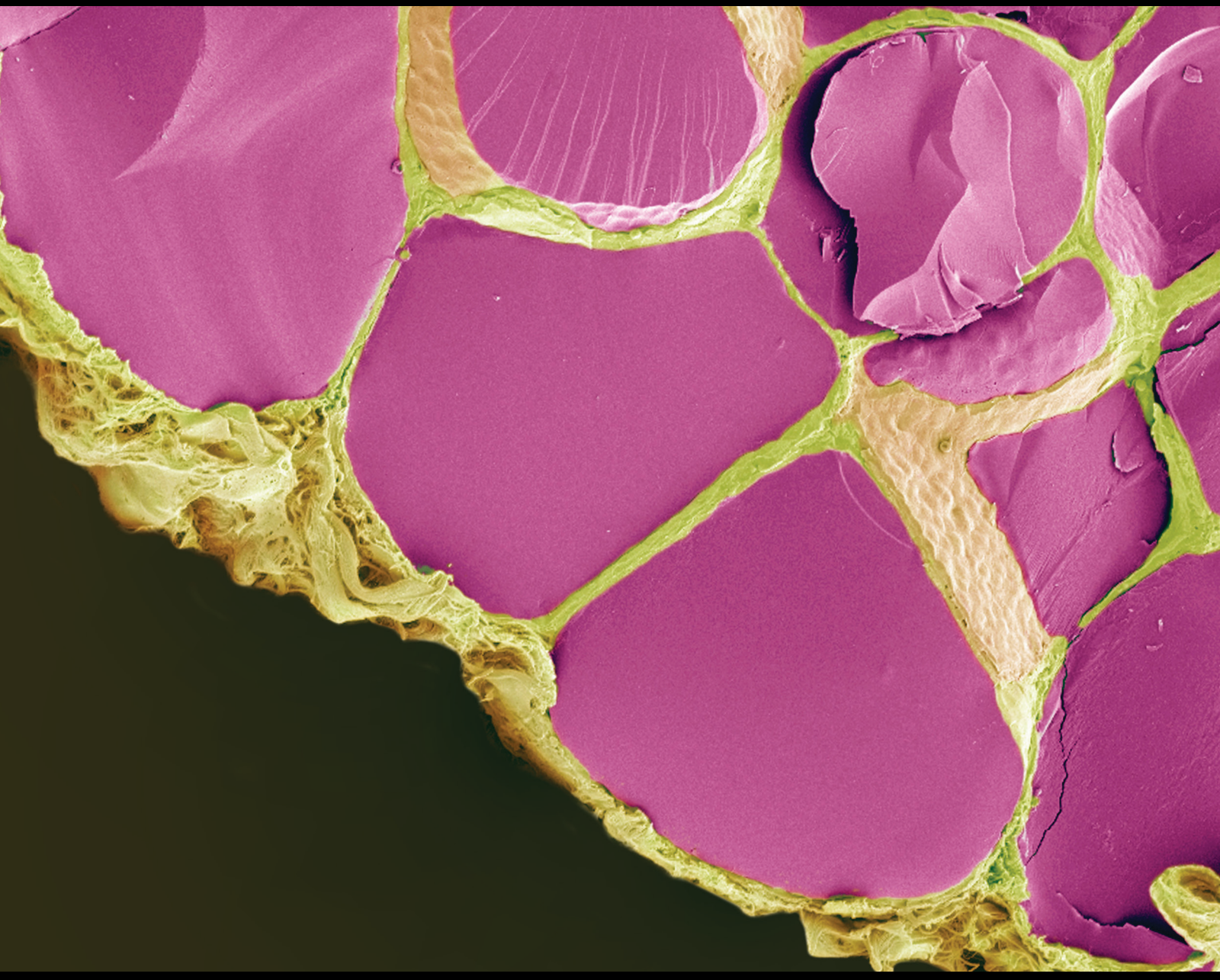

Primary Hyperparathyroidism: Diagnosis, Management, and Therapy

International Journal of Endocrinology

Primary Hyperparathyroidism: Diagnosis, Management, and Therapy

Lead Guest Editor: Maria G. Chiofalo
Guest Editors: Giorgio Borretta, Juan P. Dueñas, and Vito Guarnieri

Chief Editor

Academic Editors

Contents

Hindawi
International Journal of Endocrinology
Volume 2020, Article ID 2080797, 5 pages
https://doi.org/10.1155/2020/2080797

Research Article

Rare Somatic MEN1 Gene Pathogenic Variant in a Patient Affected by Atypical Parathyroid Adenoma

Luigia Cinque,[1] Flavia Pugliese,[2] Celeste Clemente,[3] Stefano Castellana,[4] Maria Pia Leone,[1] Danilo de Martino,[5] Teresa Balsamo,[6] Claudia Battista,[2] Tommaso Biagini,[7] Paolo Graziano,[3] Marco Castori,[1] Alfredo Scillitani,[2] and Vito Guarnieri[1]

[1]*Division of Medical Genetics, Fondazione IRCCS Casa Sollievo Della Sofferenza, San Giovanni Rotondo (FG), Italy*
[2]*Unit of Endocrinology, Fondazione IRCCS Casa Sollievo Della Sofferenza, San Giovanni Rotondo (FG), Italy*
[3]*Unit of Pathology, Fondazione IRCCS Casa Sollievo Della Sofferenza, San Giovanni Rotondo (FG), Italy*
[4]*Bioinformatic Unit, Fondazione IRCCS Casa Sollievo Della Sofferenza, San Giovanni Rotondo (FG), Italy*
[5]*Unit of General Surgery 2nd and Thoracic Surgery, Fondazione IRCCS Casa Sollievo Della Sofferenza, San Giovanni Rotondo (FG), Italy*
[6]*Laboratory of Oncology, Fondazione IRCCS Casa Sollievo Della Sofferenza, San Giovanni Rotondo (FG), Italy*
[7]*Bioinformatic Unit, Istituto Mendel-CSS, Rome, Italy*

Correspondence should be addressed to Vito Guarnieri; v.guarnieri@operapadrepio.it

Received 13 November 2019; Revised 14 February 2020; Accepted 6 March 2020; Published 27 April 2020

Academic Editor: Per Hellström

Objective. Atypical parathyroid adenoma is a rare neoplasm, showing atypical histological features intermediate between classic benign adenoma and the rarest parathyroid carcinoma, whose the clinical behaviour and outcome is not yet understood or predictable. Up to date only two cases of atypical adenoma were found associated to a MEN1 syndrome, and only one was proved to carry a pathogenic variant of the MEN1 gene. *Design*. We report the clinical, histologic, and molecular findings of a 44-year-old woman, presenting with a histologically proved atypical parathyroid adenoma with an apparent aggressive behaviour. *Methods and Results*. CDC73 gene was screened at germline and somatic levels with no results. Whole exome sequencing performed on DNA extracted from blood leukocytes and tumour tissue revealed a somatic MEN1 gene heterozygous variant, c.912+1G > A, of the splicing donor site of exon 6. On immunohistochemistry, downregulation of the menin protein expression in the neoplastic cells was also observed. *Conclusions*. We report the second case of a rare association of a somatic MEN1 gene mutation in a patient with atypical parathyroid adenoma. We suggest that MEN1 gene could be an underestimate genetic determinant of these rare histological entities, and we highlight the utility of a complete genetic screening protocol, by the use of next-generation sequencing technology in such undetermined clinical cases with no frank clinical presentation.

1. Introduction

Primary hyperparathyroidism (pHPT) is the third most common endocrine disease after diabetes and thyroid disorders [1]. It is characterized by hypercalcemia sustained by inappropriate high parathyroid hormone (PTH) levels, the latter due to a parathyroid neoplasm. Benign parathyroid adenoma (PA) is the main common cause of pHPT in up to 85% of cases, and the remaining 15% by hyperplasia [1]. Less than 1% of cases includes the rare parathyroid carcinoma (PC), while an intermediate histology entity, between the PA and the PC, defined as atypical adenoma (AA) has been reported with a frequency ranging from 0.5% to 4.4% with highest frequency for the selected ethnic group [1, 2]. Recognizing both PC, especially in absence of metastases, and AA is not clear-cut in all cases. The PC presents with severe hypercalcemia (>14 mmg/dL), with a parathyroid lesion of 3 cm in average (from 2 to 10 g) [3] with a firm adherence and invasion of surrounding structures [4]. In 70% of sporadic PC cases, as well as in 15–20%, associated to

hyperparathyroidism with jaw tumour syndrome (HPT-JT), pathogenic variants of the CDC73 gene were found, with the corresponding loss of expression of the encoded parafibromin protein, on the tumour tissues [5–7].

In fact, in absence of a well-defined vascular invasion and/or metastasis, differential diagnosis between AA and PC might be challenging. Histological criteria observed in AA are represented by cellular atypia together with solid growth pattern, fibrous septa, and adherence to surrounding thyroid tissue, with or without the so called capsule pseudoinvasion [8]. Moreover, no specific molecular markers are available, taking into account that, despite many efforts spent in this specific field, a handful of pathogenic CDC73 variants have been reported in AA [9–11].

Thus, the AA can be considered a challenge not only for the expert pathologist but also for the endocrinologist. Because of the rarity, its natural history is unknown, postsurgical management of these patients is not predictable, and few anecdotal information are available about the outcome [12, 13]. Whether, in terms of origin and prognosis, AA is more similar to PA remains likewise to be evaluated: in this case, a possible molecular marker could be the MEN1 gene, that results mutated in the namesake syndrome, characterized by familial HPT, benign parathyroid adenoma or hyperplasia, gastro-entero-pancreatic and pituitary tumors (the latter 40% and 30% of cases, respectively) and less frequently by adrenocortical and thyroid carcinoids and lipomas [14, 15]. Interestingly, although in MEN1 pHPT is almost always associated with benign parathyroid lesions, adenoma, or hyperplasia [1, 2], mutations of the gene have been found in 35% of PA and 6% of PC [16–18], but also in a small series of AA, in 1 out of 10 cases (10%) [2]. This could suggest a wider presentation of parathyroid disease in this condition.

We report a 44-year-old woman with pHPT and severe hypercalcemia due to AA. Whole exome sequencing (WES) revealed a previously known MEN1 variant that occurred somatically in the parathyroid lesion.

2. Material and Methods

2.1. Clinical History. An apparently healthy 44-year-old woman was admitted for recurrent bilateral renal colic, with an ultrasound picture of bilateral renal stones with hydronephrosis. The blood chemistry performed for diagnostic analysis showed a picture of primary hyperparathyroidism with severe hypercalcemia (14 mg/dL, n.r. = 8.4–10.2 mg/dL) and very high parathormone values (1347 pg/mL, n.r. = 10–65 pg/mL). On neck ultrasound, a richly vascularized hypoechoic parathyroid lesion of 1.5 cm in diameter was detected inferiorly to the lower left thyroid pole. Due to high levels of serum calcium, she was hydrated with 4 L of intravenous physiological solution and 3 L of water "per os." However, normocalcaemia was not reached, and 4 mg of intravenous zoledronic acid was administered. She underwent surgery with removal of the lower left parathyroid and left thyroid lobe, with macroscopic histological finding of parathyroid carcinoma. After parathyroidectomy, serum calcium levels returned to normal and no biochemical or instrumental signs of recurrence have been observed to date (10 years of follow-up).

2.2. Molecular Study. After informed consent, DNA was extracted from peripheral blood and the protocol was approved by our local ethic committee (*Prot-Familia*-16/CE/2016). The work was done according to the 1984 Helsinki declaration and its subsequent versions.

Due to the severity of the biochemical profile and the original histological suspect, Sanger sequencing for both the CDC73 and MEN1 genes and the search for large deletions at the CDC73 locus were attempted [19]. Then, in search of a possible alternative genetic explanation, WES was performed on DNA extracted from blood and paraffin-embedded tumoral lesions. Briefly, gDNA concentration was determined with the Qubit dsDNA BR Assay (Invitrogen, Carlsbad, CA, USA), and the fluorescence was measured using the Qubit Fluorometer (Invitrogen, Carlsbad, CA, USA). A total of 50 ng of gDNA was used for library preparation. The library was prepared using Agilent SureSelect QXT Clinical Research Exome kit (Agilent Technologies, Santa Clara, CA), according to SureSelect QXT Target Enrichment for Illumina Multiplexed Sequencing protocol. gDNA was enzimatically fragmented, and adaptors were ligated to the DNA fragments. The fragments were purified with AMPure beads and PCR amplified. The library was used in the hybridization and captured with the biotinylated SureSelect bait. The SureSelect-enriched DNA libraries were purified according to the manufacturer's recommendations and PCR amplified using an appropriate pair of dual indexing primers. The amplified indexed DNA products were checked for quality (2200 Tape Station and High Sensitivity D1000 ScreenTape, Agilent Technologies, Santa Clara, CA), normalized, pooled, and sequenced using the NextSeq500 platform (Illumina, San Diego, CA) at an average coverage depth of 70X. *In silico* analysis was carried out comparing variants found on constitutional and somatic DNAs (i.e., occurring in the paraffin-embedded lesion, but absent in the peripheral blood). In particular, genes affecting the parathyroid function and neoplasms, CDC73, MEN1, CDKN1B, and GCM2, were screened.

The presence of the variant was confirmed by Sanger sequencing on somatic DNA: the PCR was carried out to amplify both exons 5 and 6 (which located close to each other) of the MEN1 gene, using the following forward 5′-tgcccgataggctaaggac-3′ and reverse 5′-actgttagggtctcccttct-3′ primers. The PCR product was purified (ExoSAP-IT, Thermo Fisher Scientific, Waltham, MA, USA) and sequenced (ABI Prism 3100 Genetic Analyzer, Thermo Fisher Scientific Waltham, Massachusetts, USA) using the BigDye Terminator v1.1 sequencing kit (Applied Biosystems, Foster City, CA, USA).

2.3. Immunohistochemistry. 3-μm thick representative parathyroid tumor tissue sections were deparaffinized in xylene, rehydrated in graded alcohols, washed in double-distilled water, and treated with DAKO solution (EnVision FLEX Target Retrieval Solution) for antigen retrieval. The

slides were treated with primary anti-menin monoclonal antibody (clone B-9, diluted 1 : 200, Santa Cruz Biotechnology) for 30 min. Antigen-antibody reaction was visualized using the EnVision FLEX kit (Dako Agilent) with diaminobenzidine as chromogen. After counterstaining with hematoxylin, the slides were covered.

3. Results

3.1. Molecular Findings. We did not find any deleterious germline variants in both the CDC73 and MEN1 genes. Conversely, at the somatic level, the WES revealed a previously reported MEN1 gene splicing nucleotidic change, namely, c.912+1G > A, in heterozygosity, affecting the donor site of exon 6 and predicted to cause the skipping of exon 6 with the insertion of a premature stop codon, p.(Tyr276Arg ∗ 62) (see [14] and reference therein). As stated above, the variant was not present on germline DNA (Figure 1), thus confirming the sporadic nature of the clinical case.

3.2. Pathologic Findings and IHC for MEN1 Protein. Grossly, surgical specimen consisted of left thyroid lobe strictly adhering to a solid, capsulated parathyroid neoplasm (1.5 cm in diameter).

Microscopically, parathyroid lesions showed a trabecular growth pattern and thick fibrous septa and separated solid nests of clear tumor cells. Moreover, some aggregates of neoplastic cells entrapped in the context of the tumor capsule were observed, and focal infiltration of thyroid tissue was also identified (Figure 2(a)). Neither obvious mushroom-like infiltration of the capsule nor vascular invasion was demonstrated. Mitoses were present in a number less than 1 per 10 high-power field.

While positivity for parafibromin antibody was observed (data not shown), menin immunoreactivity was reduced in neoplastic cells (Figures 2(b) and 2(c)).

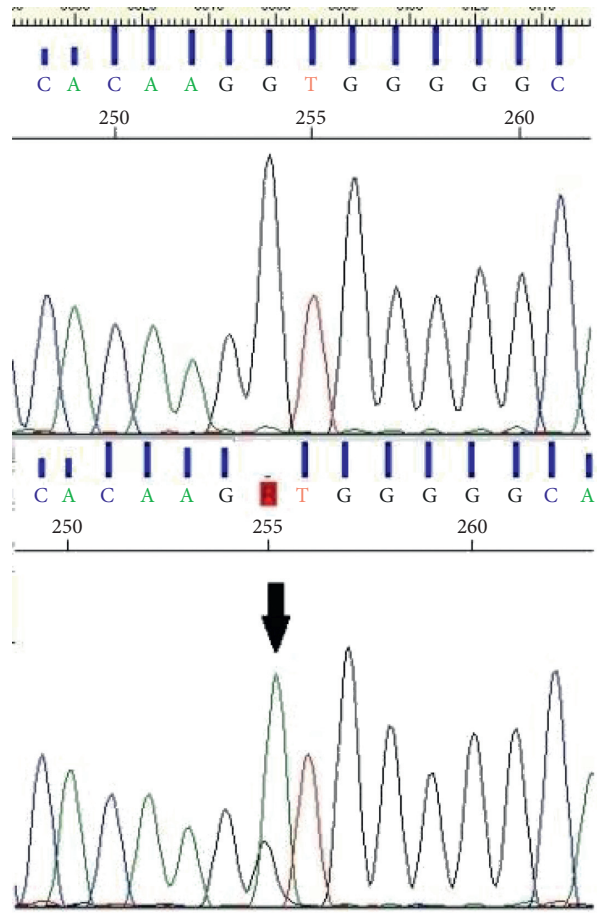

Figure 1: Electropherograms showing the splicing pathogenic variant G > A (arrow). On the top: germline DNA; on the bottom: somatic DNA.

4. Discussion

To our knowledge, the case here presented is the second reporting an AA due to a MEN1 gene mutation. AA is a histology entity thought to be located in an intermediate position between the more aggressive and rare PC and the common PA. Due to its rarity, the lack of information about the origin, the potential malignity and, mostly, of the possible outcome, make the AA a challenging tumor to deal with, that requires a strict follow-up. Several molecular attempts have been made in search of possible genetic or histological determinants for a better classification, recognition, and prognosis; however, these studies were not definitive, since they confirmed the partial overlapping with PC and PA. The CDC73 gene, the main gene of sporadic and familial PC, resulted mutated only in few cases of AA [9–11], and this initially suggested that the AA may be an intermediate progression step towards the full malignity. However, metanalyses on the use of the parafibromin protein expression and on the follow-up of patients with AA and CDC73 deleterious variants provided controversial results (see [2] and references therein). Conversely, involvement of MEN1 was not systematically investigated in AA. This because MEN1 is only rarely mutated in malignant parathyroid lesions (~0.5%) [17, 20, 21], since, on the contrary, the CDC73 gene is considered the candidate gene for parathyroid lesions of uncertain malignity. Up to date, only two cases of AA were associated to MEN1 syndrome, and only one a germline mutation was also identified [2, 17]. However, at variance with our case who presented only nephrolythiasis and hypercalcemia associated to the parathyroid lesion, previously a clear landscape of clinical MEN1 syndrome was recognizable, being the patients affected by other related tumors, such as pancreas, adrenal, or thymic carcinoids (Table 1).

The case here showed is instructive for the following reasons: (i) the clinical presentation featured by severe hypercalcemia as well as the subsequent macroscopic observation at the surgery of the parathyroid lesion; both were evocative of a more aggressive disease (HPT-JT or sporadic PC); (ii) although the subsequent pathologic diagnosis lowered the malignant grade from PC to AA, it still prompted to search for a CDC73 gene involvement, resulted negative (along with the MEN1 gene), at germline level; and

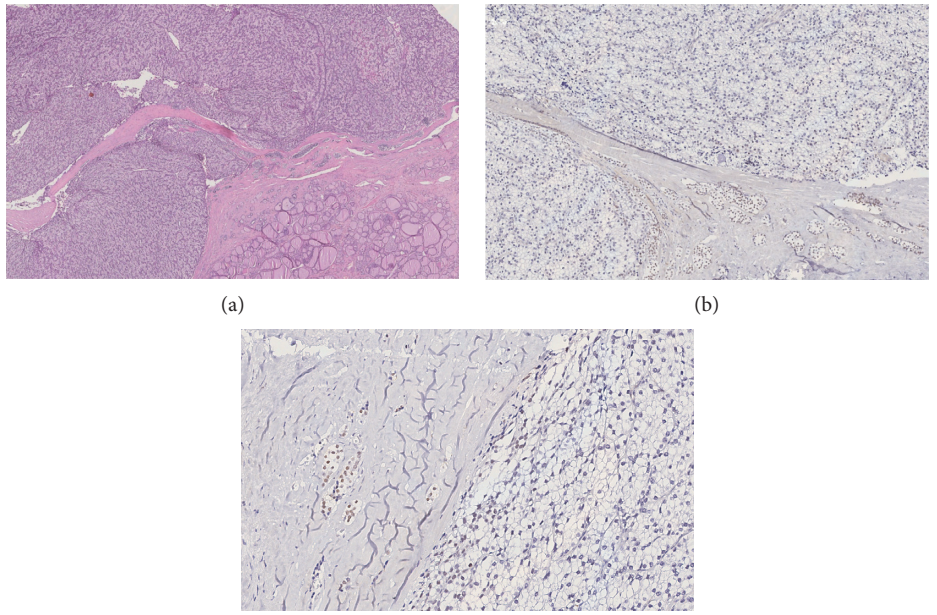

(a) (b) (c)

Figure 2: (a) Parathyroid adenoma: on hematoxylin-eosin tissue sections, the pushing growth pattern of the tumor and the strict adherence to thyroid tissue is observed. (b). Reduction of nuclear immunoreactivity of menin protein was observed in the neoplastic cell. (c). High-power view (X30) highlights decreased menin expression in neoplastic cells, whereas entrapped parathyroid normal cells maintain strong nuclear menin immunoreactivity.

Table 1: Clinical features of the three subjects reported in the literature with MEN1 syndrome and AA.

	Sex	Age	Ca[a]	PTH[b]	Parathyroid	Nephrolythiasis	MEN1 mutation	Other MEN1-related tumors	Others	Ref.
ID1	M	50	3.22 nmol/L	215 pmol/L	2 × 2.9 cm, 14 g	Bilateral	c.253A>T	Acromegalia, pituitary and adrenal, lipomas	CKD	Christakis et al. [18]
ID2	F	32	12 mg/dL	NA	0.7 cm	No	NA	Pancreas and thymus	No	Pal et al. [20]
ID3	F	44	14 mg/dL	1347 pg/mL	2 cm	Bilateral	c.912+1G>A	No	No	Present work

[a]Normal range: 1.12–1.32 mmol/L or 8.4–10.2 mg/dL; [b]normal range 15–65 pg/mL; CKD = chronic kidney disease.

(iii) high-throughput technologies are now available at relatively low price and represent the good choice to gain the molecular answer for not clear-cut cases as the one here reported.

However, the limit of our work is related just to the rarity of AA: whether our finding would suggest that also the MEN1 gene can play a role in the onset of the AA, at the same time, it would will be hard to be confirmed due to the paucity of samples worldwide available, although the AA is more common that the rarest PC.

We confirmed that, in the absence of any reliable histological or molecular signature, the management of individuals with a previous AA is based on periodic clinical assessment. However, we believe that an extensive molecular testing including all known genes associated with parathyroid hyperplastic/neoplastic disorders [22–24] might support the clinicians in the management of these patients. This study, in particular, demonstrates that next generation sequencing technologies are helping in translating high-throughput molecular screening on both blood and paraffin-embedded lesions into clinical practice.

Data Availability

This work does not include data that strictly require to be published in a public database.

Disclosure

The funders had no role in study design, data collection and analysis, decision to publish, or preparation of the manuscript.

Conflicts of Interest

The authors have no conflicts of interest to disclose.

Acknowledgments

The authors gratefully acknowledge the family involved in this study. This work was funded by the Ricerca Finalizzata (GR-2011-02351489), funding granted by the Italian Ministry of Health (to VG), Ricerca Corrente 2019 (to AS), and the "5 × 1000" voluntary contributions.

References

[1] J. P. Bilezikian, L. Bandeira, A. Khan, and N. E. Cusano, "Hyperparathyroidism," *The Lancet*, vol. 391, no. 10116, pp. 168–178, 2018.

[2] F. Cetani, C. Marcocci, L. Torregrossa, and E. Pardi, "Atypical parathyroid adenomas: challenging lesions in the differential diagnosis of endocrine tumors," *Endocrine-Related Cancer*, vol. 26, no. 7, pp. R441–R464, 2019.

[3] O. Clark, "Parathyroid carcinoma," in *Current Surgical Diagnosis and Treatment*, G. M. Doherty and L. W. Way, Eds., pp. 284–293, McGraw-Hill Companies, Chelsea, MI, USA, 2006.

[4] S. E. Rodgers and N. D. Perrier, "Parathyroid carcinoma," *Current Opinion in Oncology*, vol. 18, no. 1, pp. 16–22, 2006.

[5] J. D. Carpten, C. M. Robbins, A. Villablanca et al., "HRPT2, encoding parafibromin, is mutated in hyperparathyroidism-jaw tumor syndrome," *Nature Genetics*, vol. 32, no. 4, pp. 676–680, 2002.

[6] T. M. Shattuck, S. Välimäki, T. Obara et al., "Somatic and germ-line mutations of theHRPT2 gene in sporadic parathyroid carcinoma," *New England Journal of Medicine*, vol. 349, no. 18, pp. 1722–1729, 2003.

[7] C. C. Juhlin, A. Villablanca, K. Sandelin et al., "Parafibromin immunoreactivity: its use as an additional diagnostic marker for parathyroid tumor classification," *Endocrine-Related Cancer*, vol. 14, no. 2, pp. 501–512, 2007.

[8] R. A. DeLellis, "Parathyroid carcinoma," *Advances in Anatomic Pathology*, vol. 12, no. 2, pp. 53–61, 2005.

[9] K. J. Bradley, B. M. Cavaco, M. R. Bowl, B. Harding, A. Young, and R. V. Thakker, "Utilisation of a cryptic non-canonical donor splice site of the gene encoding PARAFIBROMIN is associated with familial isolated primary hyperparathyroidism," *Journal of Medical Genetics*, vol. 42, no. 8, p. e51, 2005.

[10] T. G. Kelly, T. M. Shattuck, M. Reyes-Mugica et al., "Surveillance for early detection of aggressive parathyroid disease: carcinoma and atypical adenoma in familial isolated hyperparathyroidism associated with a germline HRPT2 mutation," *Journal of Bone and Mineral Research*, vol. 21, no. 10, pp. 1666–1671, 2006.

[11] V. Guarnieri, C. Battista, L. A. Muscarella et al., "CDC73 mutations and parafibromin immunohistochemistry in parathyroid tumors: clinical correlations in a single-centre patient cohort," *Cellular Oncology*, vol. 35, no. 6, pp. 411–422, 2012.

[12] I. Christakis, N. Bussaidy, C. Clarke et al., "Differentiating atypical parathyroid neoplasm from parathyroid cancer," *Annals of Surgical Oncology*, vol. 23, no. 9, pp. 2889–2897, 2016.

[13] E. M. Ryhänen, H. Leijon, S. Metso et al., "A nationwide study on parathyroid carcinoma," *Acta Oncologica*, vol. 56, no. 7, pp. 991–1003, 2017.

[14] M. C. Lemos and R. V. Thakker, "Multiple endocrine neoplasia type 1 (MEN1): analysis of 1336 mutations reported in the first decade following identification of the gene," *Human Mutation*, vol. 29, no. 1, pp. 22–32, 2008.

[15] D. Trump, B. Farren, C. Wooding et al., "Clinical studies of multiple endocrine neoplasia type 1 (MEN1)," *Qjm*, vol. 89, no. 9, pp. 653–670, 1996.

[16] K. Brewer, J. Costa-Guda, and A. Arnold, "Molecular genetic insights into sporadic primary hyperparathyroidism," *Endocrine-Related Cancer*, vol. 2, pp. R53–R72, 2019.

[17] I. Christakis, N. L. Busaidy, G. J. Cote et al., "Parathyroid carcinoma and atypical parathyroid neoplasms in MEN1 patients; A clinico-pathologic challenge. The MD Anderson case series and review of the literature," *International Journal of Surgery*, vol. 31, pp. 10–16, 2016.

[18] L. Cinque, A. Sparaneo, A. S. Salcuni et al., "MEN1 gene mutation with parathyroid carcinoma: first report of a familial case," *Endocrine Connections*, vol. 6, no. 8, pp. 886–891, 2017.

[19] L. A. Muscarella, D. Turchetti, A. Fontana et al., "Large deletion at the CDC73 gene locus and search for predictive markers of the presence of a CDC73 genetic lesion," *Oncotarget*, vol. 9, no. 29, pp. 20721–20733, 2018.

[20] M. C. Lemos and R. V. Thakker, "Multiple endocrine neoplasia type 1 (*MEN1*): analysis of 1336 mutations reported in the first decade following identification of the gene," *Human Mutation*, vol. 29, no. 1, pp. 22–32, 2008.

[21] R. Pal, S. K. Bhadada, P. Dutta et al., "Ectopic atypical parathyroid neoplasm in a patient with Multiple Endocrine Neoplasia type I," *AACE Clinical Case Reports*, vol. 4, no. 5, pp. e383–e387, 2018.

[22] N. Singh Ospina, T. J. Sebo, G. B. Thompson, B. L. Clarke, and W. F. Young Jr., "Prevalence of parathyroid carcinoma in 348 patients with multiple endocrine neoplasia type 1 - case report and review of the literature," *Clinical Endocrinology*, vol. 84, no. 2, pp. 244–249, 2016.

[23] M. Kutahyalioglu, H. T. Nguyen, L. Kwatampora et al., "Genetic profiling as a clinical tool in advanced parathyroid carcinoma," *Journal of Cancer Research and Clinical Oncology*, vol. 145, no. 8, pp. 1977–1986, 2019.

[24] L. Cardoso, M. Stevenson, and R. V. Thakker, "Molecular genetics of syndromic and non-syndromic forms of parathyroid carcinoma," *Human Mutation*, vol. 38, no. 12, pp. 1621–1648, 2017.

Hindawi
International Journal of Endocrinology
Volume 2020, Article ID 3801902, 11 pages
https://doi.org/10.1155/2020/3801902

Research Article

Shear Wave Elastography versus Strain Elastography in Diagnosing Parathyroid Adenomas

Laura Cotoi,[1] **Daniela Amzar**,[2] **Ioan Sporea**,[3] **Andreea Borlea**,[1] **Dan Navolan**,[4] **Flore Varcus**,[5] **and Dana Stoian**[2]

[1]*PhD School Department, "Victor Babes" University of Medicine and Pharmacy, Timisoara, Romania*
[2]*Department of Endocrinology, "Victor Babes" University of Medicine and Pharmacy, Timisoara, Romania*
[3]*Department of Gastroenterology and Hepatology, "Victor Babes" University of Medicine and Pharmacy, Timisoara, Romania*
[4]*Department of Obstetrics and Gynecology III, "Victor Babes" University of Medicine and Pharmacy, Timisoara, Romania*
[5]*Department of Surgery II, "Victor Babes" University of Medicine and Pharmacy, Timisoara, Romania*

Correspondence should be addressed to Daniela Amzar; amzar.danielageorgiana@gmail.com

Received 13 September 2019; Revised 27 December 2019; Accepted 28 January 2020; Published 17 March 2020

Academic Editor: Giorgio Borretta

Objectives. The aim of the study was to compare elastographic means in parathyroid adenomas, using shear wave elastography and strain elastography. *Methods*. This prospective study examined 20 consecutive patients diagnosed with primary hyperparathyroidism and parathyroid adenoma, confirmed by biochemical assay, technetium-99 sestamibi scintigraphy, and pathology report, after parathyroid surgery. All patients were examined on conventional 2B ultrasound, 2D shear wave elastography, and strain elastography. We determined using 2D shear wave elastography (SWE) the elasticity index (EI) in parathyroid adenoma, thyroid parenchyma, and surrounding muscle and examined using strain elastography the parathyroid adenoma, and determined the strain ratio with the thyroid tissue and muscle tissue. *Results*. All patients had positive sestamibi scintigraphy and underwent surgery, with confirmation of parathyroid adenoma in all cases. The mean parathormone (PTH) value before surgery was 153.29 pg/ml (36.5, 464.8) and serum calcium concentration was 10.5 mg/dl (9, 11.5). We compared using 2D-SWE and strain elastography parathyroid adenoma with thyroid tissue and with surrounding muscle. The mean EI measured by SWE in parathyroid adenoma was 4.74 ± 2.74 kPa and in thyroid parenchyma was 11.718 ± 4.206 kPa (mean difference = 6.978 kPa, $p < 0.001$), and the mean EI value in muscle tissue was 16.362 ± 3.829 kPa (mean difference = 11.622, $p < 0.001$). Using ROC analysis, we found that an EI below 7 kPa correctly identifies parathyroid tissue. We evaluated parathyroid adenomas using strain elastography by color mapping and strain ratio as a semiquantitative measurement; however, we could not find any statistical correlation comparing the strain ratio obtained from the parathyroid adenoma with the thyroid tissue ($p = 0.485$). *Conclusion*. Ultrasound elastography is a helpful tool in identifying parathyroid adenomas. A cutoff value below 7 kPa can be used in 2D-SWE. Color maps in strain elastography without adding strain ratio can be used, parathyroid adenoma being identified as score 1 in the Rago criteria.

1. Introduction

Primary hyperparathyroidism (PHPT) is the third most frequent endocrinopathy, after type 2 diabetes mellitus and thyroid disease. It is most commonly caused by an overactive parathyroid gland resulting in high serum parathormone (PTH) concentrations and consequent high serum calcium concentrations [1–7]. PHPT is nowadays commonly asymptomatic, with high prevalence among postmenopausal women (female–male ratio 3–4 : 1) [8–11], routine serum calcium evaluation contributing to an increase in disease diagnosis [6].

The most common PHPT cause is unique parathyroid adenoma [12]. Sporadic parathyroid adenomas represent 85–90% of cases [3], a smaller percentage is accounted for multiglandular disease and less than 1% is due to parathyroid carcinoma [2–4].

Active screening has increased the incidence of PHPT, as European studies have shown [5, 13]. A Swedish study

showed that 3% of women and 0.7% of men over the age of 60 will present PHPT [14]. A prevalence study of PHPT conducted in Denmark evaluated that over a period of 11 years, there was an annual rate of 16 per 100.000 cases [15].

Primary hyperparathyroidism can be surgically treated, requiring accurate preoperative localization of the adenoma [16]. Most available preoperative localization techniques for PHPT are ultrasonography (US) and technitium-99 m sestamibi scintigraphy scan [17]. US is widely available, non-invasive, cheap, and repeatable [18, 19], and it can be used for positive diagnosis and also for therapeutic interventions (fine-needle aspiration and percutaneous interventions–ethanol, radio frequency, or laser ablation) [20]. Additional applications of US such as color and power Doppler, 3D imaging, contrast-enhanced ultrasonography, and elastography have increased the diagnostic value of ultrasound in diagnosing hyperparathyroidism [18], by decreasing the false-positive cases.

Important literature studies have concluded that the diagnostic value of US in parathyroid adenomas has a sensitivity of up to 76% and a specificity of 93.2% [21].

Elastography is a relatively novel technique, complementary to conventional ultrasonography. It can be used to assess tissue stiffness [22] with the potential of differentiating benign from malignant tissues [23].

Complementary to conventional ultrasound, elastography can be used to assess quantitative and qualitative information about tissue stiffness and can make the correlation between healthy tissue and pathological tissue. By measuring tissue elasticity, elastography has been validated as a marker of pathological states in many clinical areas [24], by improving diagnostic methods and establishing its role in breast tumours characterization [25], thyroid nodules [22], testicular cancer [26, 27], and liver pathology [28]. There are also studies conducted on primary and secondary hyperparathyroidism [29–32].

Elastography's efficacy in parathyroid disease is less studied, the major impediment being the lack of visualisation of normal parathyroid glands on conventional ultrasound. Elastographic measurements are not able to compare normal parathyroid tissue with hypertrophic or hyperplastic parathyroid lesions, thus using surrogate markers, such as thyroid tissue or sternocleidomastoid muscle.

1.1. Principle of Elastography. Elastography estimates tissue stiffness by applying compression force and measuring the distortion degree of the tissue [33]. Tissue strain is estimated by finite difference estimation of echo time-delays obtained cross-correlating processing before and after compression echo signals [34].

The distortion degree can be obtained using two methods, applying external pressure manually or via ultrasound transducer [33]. Shear waves are generated by short-duration acoustic beam or by converged ultrasound beams. They generate shear waves that diffuse transversally through the tissue.

Qualitative information are acquired through color maps, semiquantitative information through strain ratio (SR), and qualitative information through measurements (numerical values) [22].

1.1.1. Strain Elastography. Real-time elastography (RTE) is an elastographic technique that requires external pressure in order to produce deformation of subjacent tissue. After applying a controlled external pressure, elastographic map is added on grey-scale conventional ultrasound mode and displayed as color maps (red for liquids, green for soft tissue, and blue for hard tissue), giving the physician qualitative information about the tissue stiffness [22].

Semiquantitative information can be obtained using strain elastography, by comparing tissue strain in the region of interest (ROI) of targeted tissue with another adjacent healthy tissue, computing a SR.

1.1.2. Shear Wave Elastography. SWE assesses tissue stiffness by evaluating shear wave attenuation. Shear waves are induced vibrations by acoustic radiation force through a focused ultrasound beam, making it a more operator-independent technique [22, 35, 36]. Analyzing with ultrafast ultrasound acquisition sequence the particle displacements, quantitative measurements of tissue elasticity can be obtained [35].

Two elastographic methods use SWE: supersonic shear wave and acoustic radiation force impulse (ARFI) [37].

In supersonic shear wave, focused ultrasound beam is used and particle displacements of tissue can be measured with wave velocity (m/s) or by direct measurement in the ROI (kilopascals-kPa), acquiring quantitative data. Qualitative data are also available through color maps. In comparison to strain elastography, supersonic software displays a different color code—soft tissues are blue and stiff tissues are red [22, 38].

2. Objective

The objective of this prospective study was to determine, using SWE and RTE, the characteristics of parathyroid adenomas and to determine whether the techniques add information in the preoperative diagnosis of primary hyperparathyroidism cases.

3. Materials and Methods

This prospective study evaluated 20 consecutive patients diagnosed with primary hyperparathyroidism, from October 2018 to June 2019. All cases were patients aged over 18 years who presented solitary parathyroid adenoma, confirmed by biochemical evaluation, localization with technetium sestamibi scintigraphy (MIBI) and certified by pathology report after surgery (parathyroid adenoma excision). The study was approved by the Ethics Committee of our hospital and all patients signed a written informed consent. The study was in accordance with the Ethics Code of the World Medical Association.

3.1. Inclusion Criteria. All patients were adults with confirmed primary hyperparathyroidism. After performing all measurements, to conclude if there are any differences between patients with primary hyperparathyroidism and consequent autoimmune thyroid disease, we divided our study group into 2 subgroups. One group of patients with parathyroid adenoma and thyroid autoimmune disease (11 patients) and another group of patients with parathyroid adenoma, but without thyroid disease (9 patients). Only patients who underwent surgery were considered in the final analysis, with pathology report of parathyroid adenoma being the golden standard for diagnosis.

3.2. Exclusion Criteria. Ectopic parathyroid adenoma diagnosed by means of MIBI scintigraphy was excluded. Secondary cases of hyperparathyroidism were also not considered in the evaluation, regardless of whether the etiology was renal or digestive.

3.3. Conventional Ultrasound. Conventional B-mode parathyroid ultrasound was performed in all cases on two different ultrasound systems, with an Aixplorer system (SuperSonic Imagine, France) using a high-resolution linear transducer of 15–4 MHz and with Hitachi Preirus (Hitachi Medical Corporation, Tokyo, Japan) machine with a 6- to 13-MHz linear probe. Using grey-scale US, we evaluated the following parameters: thyroid dimensions (two dimensions in transverse scan and one dimension in longitudinal), thyroid volume, parathyroid adenoma dimensions, parathyroid adenoma volume, shape, and echogenity. Doppler US was performed in order to observe the presence of the peripheral vascular rim as a landmark sign for parathyroid adenomas. All patients were clinically and ultrasonographically evaluated by two practitioners, one with over a 15-year experience in thyroid, parathyroid, and neck ultrasound.

3.4. Shear Wave Elastography. After performing conventional ultrasound, 2D-SWE was performed with an Aixplorer system (SuperSonic Imagine, France) using a high-resolution multifrequency linear transducer of 15–4 MHz. Patients remained in the supine position, with hyperextension of the neck; the examiner maintained precise adherence of the probe to the examined area, without applying any manual compression, permitting the transducer to automatically induce vibrations in the tissue and avoiding any movements while waiting for image stabilization.

Qualitative assessment was first obtained using real-time elastograms. Quantitative information was later obtained using a special software program. We determined the parameters identified as the elasticity index (EI). Default settings for parathyroid 2D-SWE evaluation are not established, and for the study, we used 2D-SWE thyroid settings (range 0–100 kPa). In SWE, quantitative measurements for determining tissue elasticity properties can be obtained within a ROI. On the Aixplorer system, the ROI is quantified as quantification box (Q-Box) (Figure 1). Q-Box is available only on frozen image and provides quantitative information about tissue stiffness. The summary of tissue elasticity properties is automatically displayed using machine software: mean stiffness value (SWE-mean), maximum stiffness value (SWE-max), minimum stiffness value (SWE-min), standard deviation (SWE-SD), and the diameter of the ROI. A ratio between two different areas of interest on the same image can be obtained using Q-Box ratio. The numerical parameter obtained—SWE ratio—allows the practitioner to compare the stiffness of two areas on the same image [7].

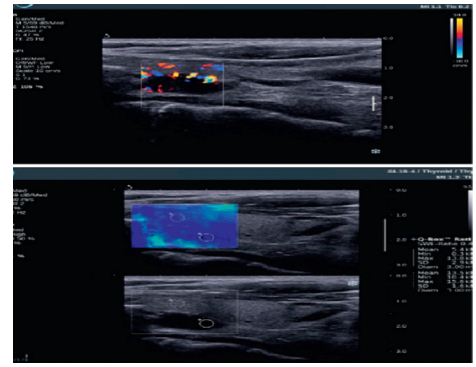

Figure 1: US and 2D-SWE evaluation of parathyroid adenoma.

We compared the EI using the Q-Box ratio of parathyroid adenomas with thyroid tissue and also with sternocleidomastoid muscle tissue (Figure 2). For each parathyroid adenoma, we performed five measurements and compared them with the measurements obtained from the thyroid parenchyma and surrounding muscle tissue.

3.5. Strain Elastography. RTE was performed after conventional ultrasound evaluation using a Hitachi Preirus (Hitachi Medical Corporation, Tokyo, Japan) machine with a 6- to 13-MHz linear probe.

Strain elastography depends upon externally induced deformation on the tissue. The stiff tissue has a lower degree of deformation and movement, compared with normal (elastic) tissue. Color elastograms (red—soft tissue to blue—stiff tissue) are displayed along with 2B-mode conventional ultrasound, giving qualitative information about tissue elasticity [22] (Figure 3).

Rago criteria [22, 39] used for thyroid nodular pathology was applied to the qualitative strain elastography evaluation: score 1—elasticity in the whole lesion, score 2—mostly soft, score 3—soft in the peripheral part of the lesion, score 4—the entire lesion is stiff, and score 5—stiffness that extends beyond the lesion's margins, infiltration in the surrounding tissue.

The main limitation of this qualitative analysis is the depth of the lesions, giving incomplete colored maps. Most of the parathyroid adenomas evaluated were score 1 according to the Rago criteria (Figure 4).

Semiquantitative information can also be obtained using strain elastography, by comparing tissue strain in the ROI of the parathyroid adenoma parenchyma to the thyroid tissue or muscle. The result is an automatic SR.

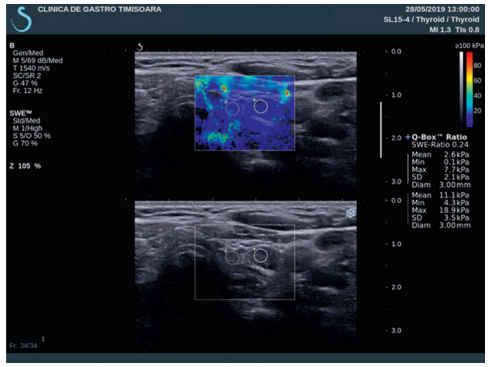

Figure 2: Q-Box ratio of parathyroid adenoma with thyroid tissue.

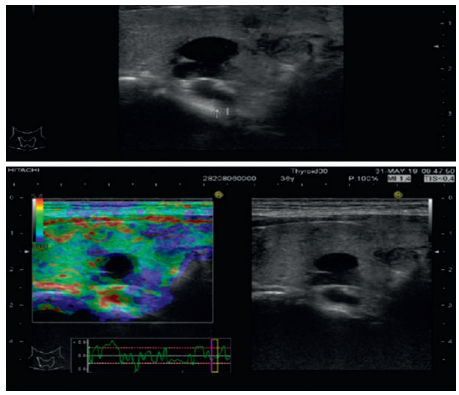

Figure 3: US and strain elastography of parathyroid adenoma.

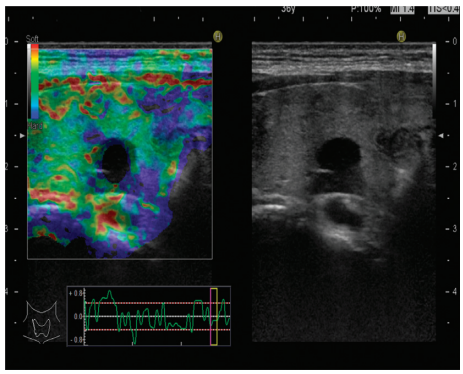

Figure 4: Color map on strain elastography with Hitachi machine. Score 1 on Rago criteria for qualitative strain elastography images.

We performed semiquantitative measurement (SR) for parathyroid adenoma versus thyroid parenchyma and, respectively, parathyroid adenoma versus sternocleidomastoid muscle.

3.6. Statistical Analysis. Data were collected and analyzed using SPSS v.25 (Statistical Package for the Social Sciences, Chicago, IL, USA). Continuous variables were presented as mean and standard deviation (SD), and categorical variables were presented as frequency and percentages.

We performed descriptive and inferential statistics analysis to summarize the characteristics of the study population. To compare patients with or without autoimmune thyroiditis, specific group-pairs with each other, we used the *t* test. For comparing the three measurements and to assess the EI (thyroid, parathyroid, and muscle), we used the ANOVA test, followed by a post hoc analysis with Tukey's HSD test.

The receiver operating characteristic (ROC) curve was employed to illustrate the diagnostic ability and the thresholds to discriminate between the parathyroid, and other structures (thyroid and muscle) were determined with the Youden index.

A p value of <0.05 was considered to indicate a statistically significant difference.

4. Results

We evaluated 20 patients (male to female ratio 1/19) with a mean age of 57.3 ± 13.33 years, mostly postmenopausal women, with confirmed primary hyperparathyroidism. Conventional ultrasound examination and both 2D-SWE and strain elastography were performed. Baseline characteristics of the study group are presented in Table 1.

Anatomical location of parathyroid adenoma can be a bias when using ultrasound for preoperative localization of the adenoma. In our study, we excluded ectopic localization of the parathyroid gland. Parathyroid adenomas in patients from our study were mostly found near the right superior thyroid lobe (9 adenomas), 3 were located near the right inferior thyroid lobe, 3 were located near the left superior lobe, and 5 near the left inferior lobe. The localization on ultrasound, compared with localization on scintigraphy and intraoperative findings, are depicted in Table 2.

On ultrasound findings, the mean parathyroid adenoma dimensions were 0.776 ± 0.50 cm, the maximum size found on ultrasound was 2.46 cm, and the minimum dimension was 0.34 mm. We found 13 parathyroid adenomas with cystic appearance (65%), 5 parathyroid adenomas with homogeneously solid and hypoechoic appearance (25%), and 2 adenomas had a mixed appearance (10%)—mostly cystic and one with an elongated shape (Figure 5).

4.1. 2B-SWE Results. In total, 20 patients were evaluated using 2D-SWE, and five measurements were made for each comparison. We noted our SWE result in Table 3, considering the minimum SWE value, the maximum SWE value, and the mean SWE value for each analyzed tissue.

One-way ANOVA test demonstrated a statistically significant difference between parathyroid elasticity (kPa) and thyroid and muscle elasticity, when measured by 2D-SWE ($p < 0.001$) (Figure 6). Post hoc analysis with *T* test was conducted and a Bonferroni correction was applied, resulting in a significance level at $p < 0.008$, with higher parathyroid elasticity (4.74 ± 2.745 kPa) compared with normal thyroid tissue (11.718 ± 4.206 kPa), and respectively surrounding muscles (16.362 ± 3.829 kPa). The difference is significant when comparing SWE mean values of

Table 1: Baseline characteristics of the study.

Characteristic	Study group
F/M	19/1
Age (years)	57.3 ± 13.33
Adenoma volume (ml)	0.21 ± 0.32
Parathormone (pg/ml)	153.29 ± 118.43
Ionized serum calcium (mmol/l)	1.23 ± 0.2
Total serum calcium (mg/dl)	10.5 ± 0.96
Urinary calcium (mg/24 h)	225.89 ± 105.33
Urinary phosphorus (g/24 h)	0.74 ± 0.16
Diuresis (ml)	1966.5 ± 393.73
Glomerular filtration rate (ml/min/1.73 m)	104.74 ± 17.42
25-OH vitamin D (ng/ml)	23.07 ± 8.77
TSH (μU/ml)	3.32 ± 4.05
FT4 (pmol/ml)	15.52 ± 2.92
Presence of autoimmune thyroid disease	11 (55%)
Thyroid volume (ml)	11.24 ± 5.37
Presence of osteoporosis	10 (50%)
T-score spine	−1.43 ± 1.32
T-score hip	−1.72 ± 1.18
Bone density mass (spine)	0.95 ± 0.21
Bone density mass (hip)	0.77 ± 0.17

F, female; M, male.

parathyroid adenomatous tissue with thyroid parenchyma (mean difference = −6.978 kPa, $p < 0.001$), respectively with mean SWE muscle values (mean difference = 11.622, $p < 0.001$).

The results summarizing AUROC, sensitivity, and specificity for each quantitative parameter are presented in Table 4. The best sensitivity and specificity are observed for SWE-mean value. By analyzing the parameters given by the ultrasound machine, we have found that the best accuracy is by analyzing the SWE-mean value, with a value of 92.5% for parathyroid/thyroid couple and 97.5% for parathyroid/muscle couple, followed by the SWE-min value with an accuracy of 90.0%, respectively 97.5%. SWE-min and SWE-max values could also be useful tools whenever borderline values are found, helping to discriminate structures and positively identify parathyroid adenomas.

We observed significant difference between the mean SWE ratio of parathyroid/thyroid compared with parathyroid/muscle SWE ratio ($p = 0.047$) (Figure 7).

Evaluating the impact of parathyroid adenoma location on SWE measurement, we obtained the following results: anterior adenomas: mean SWE = 4.74 ± 2.75 kPa, SWE-max = 11.45 ± 6.19 kPa, and SWE-min = 1 ± 1.74 kPa; posterior adenomas: mean SWE = 4.66 ± 2.88 kPa, SWE-max = 11.62 ± 6.94 kPa, and SWE-min = 0.80 ± 1.42 kPa. We did not find significant differences related to the location of the parathyroid adenomas.

There were no differences in SWE ratio of parathyroid adenoma, compared to healthy thyroid tissue (9/20 cases), mean SWE ratio = 0.418 ± 0.230, and the ratio of parathyroid adenoma compared to autoimmune thyroid tissue (11/20 cases), mean SWE ratio = 0.416 ± 0.186, $p = 0.570$.

Even if there are significant differences when using SWE ratio to determine the parathyroid adenomatous tissue, the SWE ratio values—parathyroid/thyroid and parathyroid/muscle, are similar to one another, and there is no clear delimitation between the two reports. Because of the contiguity of the SWE ratio values, we cannot determine the best SWE ratio to use. The most reliable method to differentiate the parathyroid tissue from surrounding tissues is by using the mean SWE value.

4.2. Strain Elastography Results. The initial qualitative analysis found 15 of 20 cases with score 1 on color map evaluation, according to the Rago criteria. Two cases had blue/green/red (BGR) sign due to lack of wave transmission.

Data obtained through the semiquantitative analysis using the strain elastography technique are summarized in Table 5. Using the *T* test, we found no significant differences in the SR value of parathyroid versus thyroid tissue compared with the SR value of parathyroid versus muscle tissue ($p = 0.485$). Evaluation was possible in 18 cases. Two cases had a negative scan due to the depth of the parathyroid lesion.

There were also no differences in the SR of parathyroid adenoma versus healthy thyroid tissue (9/20 cases), mean SR = 1.465 ± 1.458, and the SR of parathyroid adenoma versus autoimmune thyroid disease tissue (11/20 cases), mean SR = 1.656 ± 1.746, $p = 0.481$.

4.3. Comparing SWE and RTE. With histopathological results of the parathyroid adenomas as gold standard, ROC curve was used to evaluate the discriminative power of elastography US examination. Comparing the mean SWE value of parathyroid with the mean SWE value of surrounding muscle, the area under the curve (AUC) was 0.997 (95% CI [0.990; 0.999]) (Figure 8). A value over 10.47 kPa has a specificity of 95% and a sensitivity of 100% in identifying muscle tissue, using parathyroid adenoma as reference.

The mean SWE of parathyroid adenoma was compared to the mean SWE of thyroid tissue, regardless of whether the patient presents with an autoimmune thyroid disease, and the ROC curve obtained after evaluating the parameters, with AUC of 0.950 (95% CI [0.886; 0.999]) (Figure 9). A value over 7.28 kPa has a specificity of 90% and sensitivity of 95% in differentiating thyroid parenchyma, using parathyroid adenomatous tissue as reference.

When comparing the two elastographic methods for identifying parathyroid adenomas, we compared the two ROC curves. The SWE method has a higher sensitivity and specificity, if parathyroid adenoma is compared with thyroid tissue (regardless of the presence of autoimmune thyroid disease) or surrounding muscle–AUC curve 0.70 (95% CI [0.544; 0.876]) (Figure 10), compared with the specificity and sensitivity of strain elastography–AUC curve 0.646 (95% CI [0.442; 0.850]) (Figure 11). The optimal point on SWE ratio parathyroid/thyroid can be set at 0.3030 with a sensitivity of 75% and a specificity of 60%.

The same point was set for RTE elastography using SR, with a point set at 1.4 using the Youden index, with a sensitivity of 75% and a specificity of 66.7%.

Table 2: Location on ultrasound, scintigraphy, and intraoperative findings of parathyroid adenoma.

Parathyroid adenoma location	Ultrasound	Scintigraphy	Intraoperative findings
Right superior lobe	9	7	8
Right inferior lobe	3	5	4
Left superior lobe	3	2	3
Left inferior lobe	5	6	5

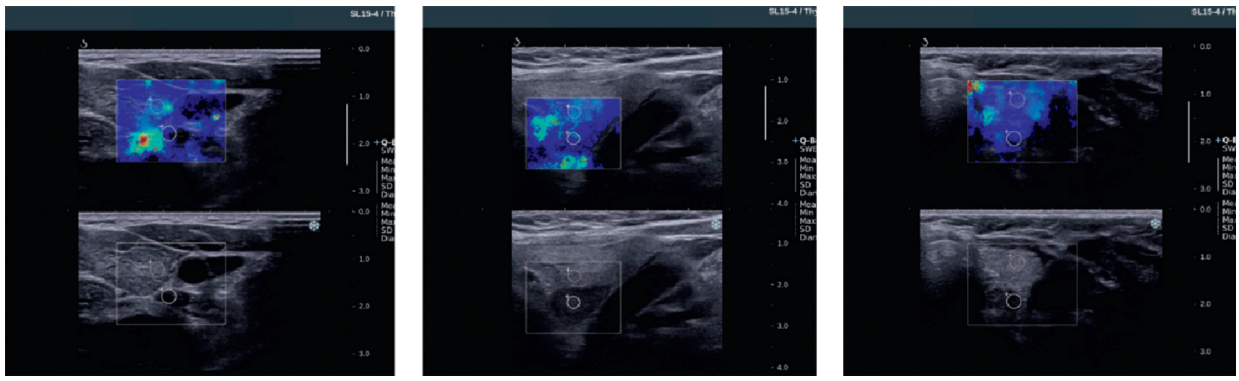

(a) (b) (c)

Figure 5: Image (a) –ultrasound appearance of hypoechoic cystic nodule; (b) –ultrasound appearance of hypoechoic homogeneously solid nodule; (c) –ultrasound appearance of mixed nodule.

Table 3: 2D-SWE results: mean value ± SD.

	Mean SWE (kPa)	Min SWE (kPa)	Max SWE (kPa)
Parathyroid adenoma	4.74 ± 2.745	1 ± 0.434	11 ± 6.266
Thyroid tissue	11.718 ± 4.206	7.013 ± 4.532	18.133 ± 7.789
Muscle tissue	16.362 ± 3.829	11.412 ± 4.097	25.518 ± 7.933

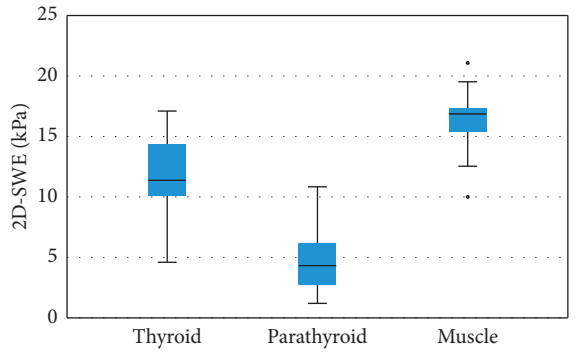

Figure 6: Comparison of mean SWE between parathyroid, thyroid, and muscle.

Table 4: Sensitivity, specificity, and AUROC for measured SWE-min, SWE-max, and SWE-mean.

	SWE-min PTX/T	SWE-mean PTX/T	SWE-max PTX/T	SWE-min PTX/M	SWE-mean PTX/M	SWE-max PTX/M
Area under curve (AUC) value	0.957	0.950	0.765	0.998	0.997	0.955
Specificity	85%	90.0%	70.0%	95.0%	95.0%	80.0%
Sensitivity	95%	95.0%	80.0%	100%	100%	100%
PPV	86.4%	*90.5%*	72.7%	95.2%	*95.2%*	83.3%
NPV	94.4%	*94.7%*	77.8%	100%	*100%*	100%
Accuracy	90.0%	*92.5%*	75.0%	97.5%	*97.5%*	90.0%
p value	*<0.001*	*<0.001*	*<0.001*	*<0.001*	*<0.001*	*<0.001*
Cutoff value	<3.14 kPa	<*7.28* kPa	<9.14 kPa	<5.32 kPa	<*10.47* kPa	<15.16 kPa

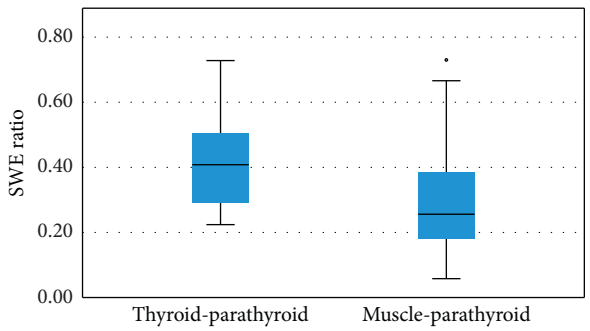

Figure 7: Values of SWE ratio of parathyroid versus thyroid elasticity, respectively parathyroid versus muscle elasticity.

Table 5: RTE results: SR values.

	Min SR	Max SR	Mean SR
Parathyroid/thyroid SR	0.01	5.82	1.46 ± 1.45
Parathyroid/muscle SR	0.5	3.5	1.79 ± 0.90

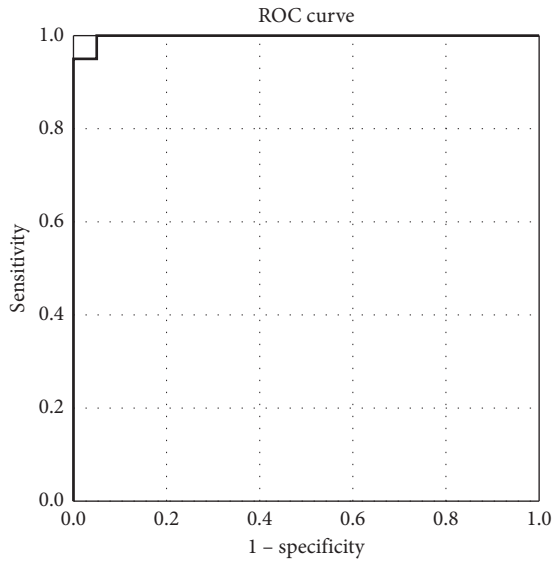

Figure 8: AUC for prediction of parathyroid adenoma using mean SWE for parathyroid (muscle as reference tissue).

5. Discussion

In this prospective study, we compared elastographic features, both in SWE and strain elastography of confirmed parathyroid adenomas with surrounding thyroid tissue and sternocleidomastoid muscle. The study included only solitary parathyroid adenomas that were initially localized in conventional B-mode ultrasonography. Our study included mostly female patients, empowering the fact that single parathyroid adenomas are more prevalent among postmenopausal women [14].

The role of elastographic measurements in the parathyroid field is advancing, as several studies on the elasticity of parathyroid adenomas have been conducted and have shown that elastography is a helpful technique in differentiating parathyroid pathology [19, 29–31, 40–42].

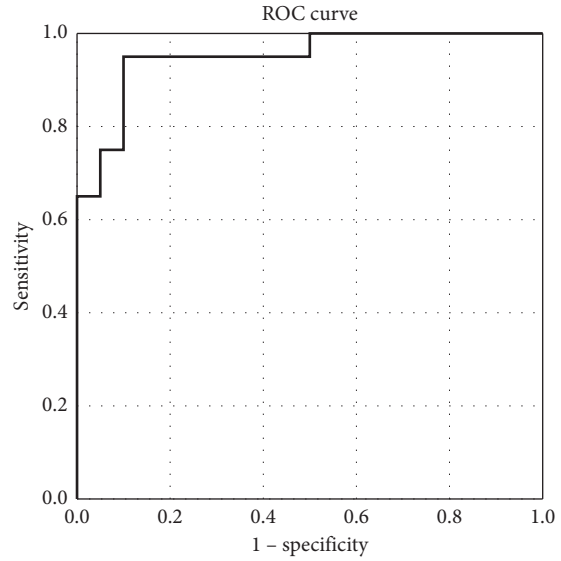

Figure 9: AUC for prediction of parathyroid adenoma using mean SWE for parathyroid (thyroid tissue as reference).

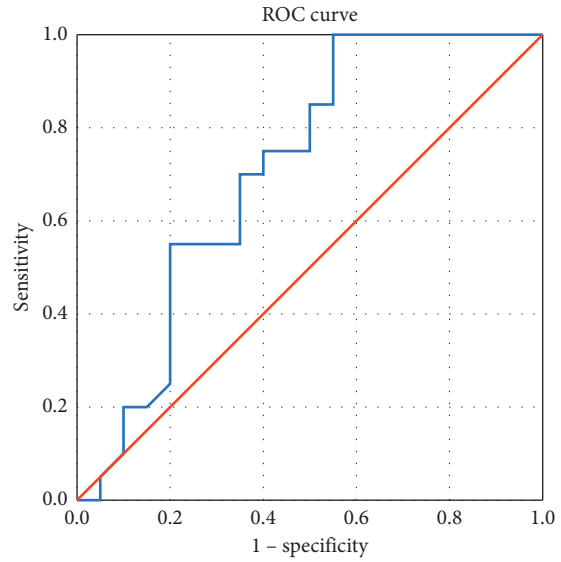

Figure 10: AUC for prediction of parathyroid adenoma using SWE (SWE ratio parathyroid/thyroid).

In our study, tissue stiffness of parathyroid adenoma was best assessed by measuring mean SWE, providing quantitative information that may be useful in localizing parathyroid adenomas. The mean (±SD) SWE value assessed was 4.74 ± 2.745 kPa for all parathyroid adenomas enrolled in the study. Compared with thyroid parenchyma (mean SWE value 11.718 ± 4.206 kPa) and surrounding muscle (mean SWE value 16.362 ± 3.829 kPa), the elasticity of parathyroid adenoma was significantly lower than both thyroid and muscle tissue. Taking into account that our study included a limited number of patients, we evaluated using cross-tabulation on ROC curves that the best mean SWE cut-off value for predicting parathyroid adenomas should be below 7 kPa.

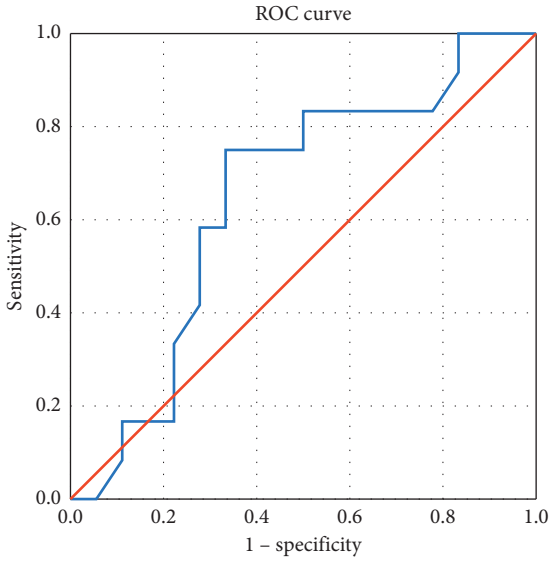

Figure 11: AUC for prediction of parathyroid adenoma using strain elastography (SR parathyroid/thyroid).

Polat et al. [19] examined parathyroid lesions using the SWE virtual touch imaging quantification (VTIQ) method and compared the shear wave velocity (SWV) of parathyroid lesions with inflammatory cervical lymph nodes. The mean SWV of parathyroid adenomas (2.16 ± 0.33 m/s) was higher than the mean SWV of parathyroid hyperplasia (1.75 ± 0.28 m/s) and higher than that of cervical lymph nodes (1.86 ± 0.37 m/s). They established a cut-off value greater than 1.92 m/s for diagnosing parathyroid adenoma.

Azizi et al. [29] compared parathyroid adenomas using SWE VTIQ with thyroid tissue. They found that parathyroid adenomas have a lower SWV mean of 2.01 m/s (±0.24) than the normal thyroid tissue of 2.77 m/s.

Batur et al. [40] measured the elasticity of parathyroid adenomas using ARFI imaging 2D-SWE and compared it to benign and malignant thyroid pathology. The reported results showed that parathyroid adenomas (mean SWV value of 3.09 ± 0.75 m/s) have a lower elasticity than benign thyroid nodules (2.20 ± 0.39 m/s) and a higher elasticity than malignant thyroid lesions (3.59 ± 0.43 m/s).

Stangierski et al. [41] measured using the 2D-SWE elastographic method parathyroid adenomas and compared elasticity with benign thyroid nodules. Parathyroid adenomas had a mean SWE value of 5.2 ± 7.2 kPa, which was significantly lower than that of thyroid nodules of 24.3 ± 33.8 kPa, showing that parathyroid adenomas have a significantly lower EI than benign thyroid nodules.

The difference between parathyroid and thyroid parenchyma elasticity was significant, regardless of whether we compared parathyroid adenomatous tissue with healthy thyroid tissue or with autoimmune thyroid tissue. On ultrasound examination, most lesions were cystic (nine nodules), and we also found solid and mixed adenomas (five and two nodules), but we did not find any significant differences on elastography examination regarding the EI, both on shear wave and on strain elastography. Also, the location of the parathyroid adenoma had no influence on the elastographic measurements.

Thyroid nodules are extremely common in the general population, up to 5% prevalence on palpation and over 50% discovered in autopsies [43]. Elastography has found its place in differentiating thyroid nodules, with a general consensus in major guidelines [44–46] and important papers in the field [47–49]. Thyroid nodules frequently pose a dilemma to the clinician, first in respect to the nature of the nodule and also when faced with patients with parathyroid adenomas. In our study, we did not compare parathyroid adenoma elasticity with thyroid nodule elasticity because of the small number of thyroid nodules present in examined patients.

Literature studies conducted on thyroid nodules on SWE have found EI values of 150 ± 95 kPa [38], 30.7 kPa [50], and 115 ± 60.4 kPa [51] for malignant nodules, and values of 36 ± 30 kPa [38], 18.7 kPa [50], and 41 ± 25.8 kPa [51] for benign nodules. EI values reported for normal thyroid tissue were 15.9 ± 7.6 kPa [38], 13.6 kPa [50]. Therefore, the EI index of malignant and also benign nodules is higher than the EI of normal thyroid tissue; thus, we could conclude that the EI of parathyroid adenoma should be lower than the EI of both normal thyroid tissue and thyroid nodules.

We also evaluated patients using strain elastography, resulting in qualitative and semiquantitative data. We found a mean SR of 1.46 for parathyroid/thyroid and 1.8 ± 0.9 for parathyroid/muscle and no significant statistic difference in SR between the two groups.

Because autoimmune thyroid disease does alter the elasticity of the thyroid tissue [52, 53], we compared the SR for the two subgroups formed–normal thyroid and chronic autoimmune thyroiditis, and did not find any significant differences between the two groups. We did not find any articles addressing this particular aspect.

RTE can be a useful tool in differentiating thyroid nodules [54]. RTE studies have found different SR cut-off values ranging from 2 to 4 [55], with lower values for benign nodules and higher values for malignant nodules [49]. We did not compare the SR of parathyroid adenoma and thyroid nodules.

Literature reports have studied and compared the elasticity of parathyroid pathology using strain elastography. In the first study conducted on 72 patients by Ünlütürk et al. [56], they found that parathyroid adenomas appear as stiff lesions (median SR = 3.56) and parathyroid hyperplasia have a lower stiffness and a higher elasticity score (median SR = 1.49). Isidori et al. [42] evaluated 79 patients with parathyroid disorders on Elastoscan Core Index (ECI) and compared parathyroid elasticity with lymph node and thyroid nodule elasticity. They found that ECI was significantly higher in malignant lesions than in benign lesions. Combining the ECI with conventional US, and in particular with shape and vascularization, can improve the differentiation of parathyroid lesions from lymph nodes and thyroid nodules.

We observed that 2D-SWE evaluation had better results in identifying parathyroid adenomas. The best diagnosis performance is observed using mean SWE parathyroid/

muscle (AUROC = 0.997, Sn = 100%, Sp = 95%), followed by mean SWE parathyroid/thyroid (AUROC = 0.950, Sn = 95% Sp = 90%). RTE has lower diagnosis performance (AUROC = 0.646, Sn = 75%, Sp = 66.7%). To our best knowledge, this is the first study that used two major elastographic techniques to investigate parathyroid lesions and compared the accuracy of the methods, in order to determine the best method to localize parathyroid adenomas. The majority of literature studies had a small series of cases comparing parathyroid adenomas with normal thyroid tissue—57 patients [29], 36 patients [30], 21 patients [40], and 65 patients [41], or lymph nodes—66 patients [19]. Our study had a limited number of patients because of the small amount of time between diagnosis and surgery. We compared two important elastographic methods, in an effort to determine the most valuable method of determining the presence of parathyroid adenomas and differentiating parathyroid adenomas from surrounding tissue. We found that the best accuracy is obtained by analyzing the mean SWE—92.5%, followed by SWE-min—90% when compared with the thyroid tissue. When finding borderline values of mean SWE, SWE-min, SWE-max, and SWE ratio values could be useful tools to positively identify the parathyroid adenoma.

The study had certain limitations. First is the small number of patients enrolled in the study. In spite of the small number of patients, all patients underwent surgery, thus confirming by histopathological examination of the parathyroid lesions. The depth of parathyroid adenomas was also a limitation; it did not allow positive results on strain elastography scans in all cases. Based on the elastography studies in the literature [29] and the current study on parathyroid pathology, we could consider elastography as an useful tool in correctly identifying parathyroid adenoma, considering also the different tissue composition, vascularity pattern, and subsequent tissue stiffness in comparison to surrounding tissue. There are clinical implications regarding the use of elastography in diagnosing primary hyperparathyroidism. It is a simple, noninvasive, operator-independent, repeatable, and reproducible method, which can be used complementary to conventional ultrasound and scintigraphy examination, distinguishing between parathyroid adenoma, and thyroid and muscle tissue. It could furnish relevant information regarding parathyroid elasticity and could be a useful tool in localizing parathyroid adenomas in patients with primary hyperparathyroidism.

6. Conclusion

To conclude, the aim of this prospective study was to quantify the value of strain elastography and 2D-SWE in localizing parathyroid pathology. Although strain elastography can be a useful qualitative tool by using color mapping, 2D-SWE can offer a better differentiation on tissue elasticity when diagnosing parathyroid adenomas. By using this elastographic technique, a value less than 7 kPa for mean EI is suggestive for parathyroid adenoma. Also, when using the SWE ratio, a value less than 0.3030 when comparing with thyroid tissue, regardless of whether the patient is healthy or with autoimmune disease, is highly suggestive for parathyroid adenomas.

Abbreviations

PTH: Parathyroid hormone
SR: Strain ratio
PHPT: Primary hyperparathyroidism
VTIQ: Virtual touch imaging quantification
ARFI: Acoustic radiation force impulse
MIBI: Technetium sestamibi scintigraphy
RTE: Real-time elastography
SD: Standard deviation
SWV: Shear wave velocity
2D-SWE: 2 dimensional shear wave elastography
US: Ultrasonography
Sn: Sensibility
ROI: Region of interest
Sp: Specificity
EI: Elasticity index
SWE: Shear wave elastography.

Data Availability

The data that support the findings of this study are available from the corresponding author upon reasonable request.

Conflicts of Interest

The authors declare that they have no conflicts of interest.

References

[1] F. Bandeira, L. Griz, N. Chaves et al., "Diagnosis and management of primary hyperparathyroidism: a scientific statement from the department of bone metabolism, the Brazilian society for endocrinology and metabolism," *Arquivos Brasileiros de Endocrinologia & Metabologia*, vol. 57, no. 6, pp. 406–424, 2013.

[2] M. Mizamtsidi, C. Nastos, G. Mastorakos et al., "Diagnosis, management, histology and genetics of sporadic primary hyperparathyroidism: old knowledge with new tricks," *Endocrine Connections*, vol. 7, no. 2, pp. R56–R68, 2018.

[3] R. Rahbari, A. K. Holloway, M. He, E. Khanafshar, O. H. Clark, and E. Kebebew, "Identification of differentially expressed microRNA in parathyroid tumors," *Annals of Surgical Oncology*, vol. 18, no. 4, pp. 1158–1165, 2011.

[4] E. Kebebew and O. H. Clark, "Parathyroid adenoma, hyperplasia, and carcinoma: localization, technical details of primary neck exploration, and treatment of hypercalcemic," *Surgical Oncology Clinics of North America*, vol. 7, no. 4, pp. 721–748, 1998.

[5] J. P. Bilezikian, N. E. Cusano, A. A. Khan, J.-M. Liu, C. Marcocci, and F. Bandeira, "Primary hyperparathyroidism," *Nature Reviews Disease Primers*, vol. 2, no. 1, Article ID 16033, 2016.

[6] C. Eufrazino, A. Veras, and F. Bandeira, "Epidemiology of primary hyperparathyroidism and its non-classical manifestations in the city of Recife, Brazil," *Clinical Medicine Insights: Endocrinology and Diabetes*, vol. 6, pp. 69–74, 2013.

[7] L. Cotoi, D. Stoian, A. Borlea, and F. Varcus, "Ultrasonographic and elastographic diagnostic of parathyroid lesions–a

literature review," *Austin Journal of Endocrinology and Diabetes*, vol. 6, no. 2, 2019.

[8] L. Bandeira and J. Bilezikian, "Primary hyperparathyroidism," *F1000Research*, vol. 5, pp. 1–11, 2016.

[9] R. W. Gasser, "Clinical aspects of primary hyperparathyroidism: clinical manifestations, diagnosis, and therapy," *Wiener Medizinische Wochenschrift*, vol. 163, no. 17-18, pp. 397–402, 2013.

[10] U. E. M. Oliveira, M. N. Ohe, R. O. Santos et al., "Analysis of the diagnostic presentation profile, parathyroidectomy indication and bone mineral density follow-up of Brazilian patients with primary hyperparathyroidism," *Brazilian Journal of Medical and Biological Research*, vol. 40, no. 4, pp. 519–526, 2007.

[11] R. Arrangoiz, F. Cordera, F. Lambreton, E. L. De Leon, and E. Moreno, "Current thinking on primary hyperparathyroidism," *JSM Head & Neck Cancer-Cases and Reviews*, vol. 1, pp. 1–15, 2016.

[12] J. P. Bilezikian, M. L. Brandi, M. Rubin, and S. J. Silverberg, "Primary hyperparathyroidism: new concepts in clinical, densitometric and biochemical features," *Journal of Internal Medicine*, vol. 257, no. 1, pp. 6–17, 2005.

[13] N. Yu, P. T. Donnan, M. J. Murphy, and G. P. Leese, "Epidemiology of primary hyperparathyroidism in tayside, Scotland, UK," *Clinical Endocrinology*, vol. 71, no. 4, pp. 485–493, 2009.

[14] M. Palmér, S. Jakobsson, G. Åkerström, and S. Ljunghall, "Prevalence of hypercalcaemia in a health survey: a 14-year follow-up study of serum calcium values," *European Journal of Clinical Investigation*, vol. 18, no. 1, pp. 39–46, 1988.

[15] A. Abood and P. Vestergaard, "Increasing incidence of primary hyperparathyroidism in Denmark," *Danish Medical Journal*, vol. 60, no. 2, Article ID A4567, 2013.

[16] R. Udelsman, "Six hundred fifty-six consecutive explorations for primary hyperparathyroidism," *Annals of Surgery*, vol. 235, no. 5, pp. 665–672, 2002.

[17] F. Varcus, J. L. Peix, N. Berger, and D. Bordos, "La scintigraphie thyroïdienne: quelle place dans le bilan préopératoire des nodules thyroïdiens?" *Annales de Chirurgie*, vol. 127, no. 9, pp. 685–689, 2002.

[18] M. Ruchała and E. Szczepanek, "Endokrynologia polska," *Endokrynologia Polska*, vol. 61, no. 3, pp. 330–344, 2010.

[19] A. V. Polat, M. Ozturk, B. Akyuz, C. Celenk, M. Kefeli, and C. Polat, "The diagnostic value of shear wave elastography for parathyroid lesions and comparison with cervical lymph nodes," *Medical Ultrasonography*, vol. 19, no. 4, pp. 386–391, 2017.

[20] J. H. Lee and Y. Anzai, "Imaging of thyroid and parathyroid glands," *Seminars in Roentgenology*, vol. 48, no. 1, pp. 87–104, 2013.

[21] K. Cheung, T. S. Wang, F. Farrokhyar, S. A. Roman, and J. A. Sosa, "A meta-analysis of preoperative localization techniques for patients with primary hyperparathyroidism," *Annals of Surgical Oncology*, vol. 19, no. 2, pp. 577–583, 2012.

[22] D. Stoian, T. Bogdan, and M. Craina, "Elastography : a new ultrasound technique in nodular thyroid pathology," in *Thyroid Cancer—Advances in Diagnosis and Therapy*, IntechOpen, London, UK, 2016.

[23] C. F. Dietrich, R. G. Barr, A. Farrokh et al., "Strain elastography—how to do It? Authors introduction to elastography what elastography techniques are Used? Definition of color coding, Why? Strain-based elastography—how does it Work? Technical principles of tissue elastography," *Ultrasound Int Open*, vol. 3, no. 4, pp. E137–E149, 2017.

[24] R. J. Dewall, "Ultrasound elastography: principles, techniques, and clinical applications," *Critical Reviews in Biomedical Engineering*, vol. 41, no. 1, pp. 1–19, 2013.

[25] D. Stoian, B. Timar, M. Craina, E. Bernad, I. Petre, and M. Craciunescu, "Qualitative strain elastography—strain ratio evaluation—an important tool in breast cancer diagnostic," *Medical Ultrasonography*, vol. 18, no. 2, pp. 195–200, 2016.

[26] A. Marsaud, M. Durand, X. Carpentier et al., "Elastography shows promise in testicular cancer detection," *Progrès en Urologie*, vol. 25, no. 2, pp. 75–82, 2010-2015.

[27] S. M. Dudea, A. Ciurea, A. Chiorean, and C. Botar-Jid, "Doppler applications in testicular and scrotal disease," *Medical Ultrasonography*, vol. 12, no. 1, pp. 43–51, 2010.

[28] S. Bota, H. Herkner, I. Sporea et al., "Meta-analysis: ARFI elastography versus transient elastography for the evaluation of liver fibrosis," *Liver International*, vol. 33, no. 8, pp. 1138–1147, 2013.

[29] G. Azizi, K. Piper, J. M. Keller et al., "Shear wave elastography and parathyroid adenoma: a new tool for diagnosing parathyroid adenomas," *European Journal of Radiology*, vol. 85, no. 9, pp. 1586–1593, 2016.

[30] S. Hattapoğlu, C. Göya, C. Hamidi et al., "Evaluation of parathyroid lesions with point shear wave elastography," *Journal of Ultrasound in Medicine*, vol. 35, no. 10, pp. 2179–2182, 2016.

[31] A. Chandramohan, M. Therese, D. Abhraham, T. V. Paul, and P. J. Mazhuvanchary, "Can ARFI elastography be used to differentiate parathyroid from thyroid lesions?" *Journal of Endocrinological Investigation*, vol. 41, no. 1, pp. 111–119, 2018.

[32] L. Cotoi, F. Borcan, I. Sporea et al., "Shear wave elastography in diagnosing secondary hyperparathyroidism," *Diagnostics*, vol. 9, no. 4, p. 213, 2019.

[33] G. Cannataro and D. Mastrodicasa, "Strain elastosonography of thyroid nodules: a new tool for malignancy prediction? Overview of literature," *Endocrinology & Metabolic Syndrome*, vol. 5, no. 3, pp. 12–15, 2016.

[34] I. Cespedes, M. Insana, and J. Ophir, "Theoretical bounds on strain estimation in elastography," *IEEE Transactions on Ultrasonics, Ferroelectrics and Frequency Control*, vol. 42, no. 5, pp. 969–972, 1995.

[35] J. H. Yoon, K. H. Ko, H. K. Jung, and J. T. Lee, "Qualitative pattern classification of shear wave elastography for breast masses: how it correlates to quantitative measurements," *European Journal of Radiology*, vol. 82, no. 12, pp. 2199–2204, 2013.

[36] M. Paridah, A. Moradbak, A. Mohamed, O. F. A. Taiwo, M. Asniza, and S. H. Abdul Khalid, *We are IntechOpen, the World's Leading Publisher of Open Access Books Built by Scientists, for Scientists TOP 1%*, IntechOpen, London, UK, 2016.

[37] Y. F. Zhang, H. X. Xu, Y. He et al., "Virtual touch tissue quantification of acoustic radiation force impulse: a new ultrasound elastic imaging in the diagnosis of thyroid nodules," *PLoS One*, vol. 7, no. 11, Article ID e49094, 2012.

[38] F. Sebag, J. Vaillant-Lombard, J. Berbis et al., "Shear wave elastography: a new ultrasound imaging mode for the differential diagnosis of benign and malignant thyroid nodules," *The Journal of Clinical Endocrinology & Metabolism*, vol. 95, no. 12, pp. 5281–5288, 2010.

[39] T. Rago, F. Santini, M. Scutari, A. Pinchera, and P. Vitti, "Elastography: new developments in ultrasound for predicting malignancy in thyroid nodules," *The Journal of*

Clinical Endocrinology & Metabolism, vol. 92, no. 8, pp. 2917–2922, 2007.

[40] A. Batur, M. Atmaca, A. Yavuz et al., "Ultrasound elastography for distinction between parathyroid adenomas and thyroid nodules," *Journal of Ultrasound in Medicine*, vol. 35, no. 6, pp. 1277–1282, 2016.

[41] A. Stangierski, K. Wolinski, and M. Ruchala, "Shear wave elastography in the diagnostics of parathyroid adenomas-new application of the method," *Endocrine*, vol. 60, no. 2, pp. 240–245, 2018.

[42] A. M. Isidori, V. Cantisani, E. Giannetta et al., "Multiparametric ultrasonography and ultrasound elastography in the differentiation of parathyroid lesions from ectopic thyroid lesions or lymphadenopathies," *Endocrine*, vol. 57, no. 2, pp. 335–343, 2017.

[43] J. D. Mortensen, L. B. Woolner, and W. A. Bennett, "Gross and microscopic findings in clinically normal thyroid glands," *The Journal of Clinical Endocrinology & Metabolism*, vol. 15, no. 10, pp. 1270–1280, 1955.

[44] D. Cosgrove, R. Barr, J. Bojunga et al., "WFUMB guidelines and recommendations on the clinical use of ultrasound elastography: Part 4. Thyroid," *Ultrasound in Medicine & Biology*, vol. 43, no. 1, pp. 4–26, 2017.

[45] G. Russ, S. J. Bonnema, M. F. Erdogan, C. Durante, R. Ngu, and L. Leenhardt, "European thyroid association guidelines for ultrasound malignancy risk stratification of thyroid nodules in adults: the EU-TIRADS," *European Thyroid Journal*, vol. 6, no. 5, pp. 225–237, 2017.

[46] J. Bamber, D. Cosgrove, C. Dietrich et al., "EFSUMB guidelines and Recommendations on the clinical use of ultrasound elastography. Part 1: basic principles and technology," *Ultraschall in der Medizin—European Journal of Ultrasound*, vol. 34, no. 2, pp. 169–184, 2013.

[47] V. Cantisani, H. Grazhdani, E. Drakonaki et al., "Strain US elastography for the characterization of thyroid nodules: advantages and limitation," *International Journal of Endocrinology*, vol. 2015, Article ID 908575, 8 pages, 2015.

[48] P. Trimboli, G. Treglia, R. Sadeghi, F. Romanelli, and L. Giovanella, "Reliability of real-time elastography to diagnose thyroid nodules previously read at FNAC as indeterminate: a meta-analysis," *Endocrine*, vol. 50, no. 2, pp. 335–343, 2015.

[49] G. Russ, B. Royer, C. Bigorgne, A. Rouxel, M. Bienvenu-Perrard, and L. Leenhardt, "Prospective evaluation of thyroid imaging reporting and data system on 4550 nodules with and without elastography," *European Journal of Endocrinology*, vol. 168, no. 5, pp. 649–655, 2013.

[50] K. S. S. Bhatia, C. S. L. Tong, C. C. M. Cho, E. H. Y. Yuen, Y. Y. P. Lee, and A. T. Ahuja, "Shear wave elastography of thyroid nodules in routine clinical practice: preliminary observations and utility for detecting malignancy," *European Radiology*, vol. 22, no. 11, pp. 2397–2406, 2012.

[51] J. B. Veyrieres, F. Albarel, J. V. Lombard et al., "A threshold value in Shear wave elastography to rule out malignant thyroid nodules: a reality?" *European Journal of Radiology*, vol. 81, no. 12, pp. 3965–3972, 2012.

[52] F. Magri, S. Chytiris, V. Capelli et al., "Shear wave elastography in the diagnosis of thyroid nodules: feasibility in the case of coexistent chronic autoimmune Hashimoto's thyroiditis," *Clinical Endocrinology*, vol. 76, no. 1, pp. 137–141, 2012.

[53] I. Kim, E. K. Kim, J. H. Yoon et al., "Diagnostic role of conventional ultrasonography and shearwave elastography in asymptomatic patients with diffuse thyroid disease: initial experience with 57 patients," *Yonsei Medical Journal*, vol. 55, no. 1, p. 247, 2014.

[54] P. Trimboli, R. Guglielmi, S. Monti et al., "Ultrasound sensitivity for thyroid malignancy is increased by real-time elastography: a prospective multicenter study," *The Journal of Clinical Endocrinology & Metabolism*, vol. 97, no. 12, pp. 4524–4530, 2012.

[55] V. Cantisani, P. Lodise, H. Grazhdani et al., "Ultrasound elastography in the evaluation of thyroid pathology. Current status," *European Journal of Radiology*, vol. 83, no. 3, pp. 420–428, 2014.

[56] U. Ünlütürk, M. F. Erdoğan, Ö. Demir, C. Çulha, S. Güllü, and N. Başkal, "The role of ultrasound elastography in preoperative localization of parathyroid lesions: a new assisting method to preoperative parathyroid ultrasonography," *Clinical Endocrinology*, vol. 76, no. 4, pp. 492–498, 2012.

Hindawi
International Journal of Endocrinology
Volume 2020, Article ID 5230985, 8 pages
https://doi.org/10.1155/2020/5230985

Research Article

Comparison between Second- and Third-Generation PTH Assays during Minimally Invasive Parathyroidectomy (MIP)

Marie-Hélène Gannagé-Yared,[1] **Nada Younès**,[1] **Anne-Sophie Azzi**,[1] **and Ghassan Sleilaty**[2,3]

[1]*Endocrinology Department, Faculty of Medicine, Saint Joseph University, Beirut, Lebanon*
[2]*Department of Biostatistics, Faculty of Medicine, Saint-Joseph University, Beirut, Lebanon*
[3]*Clinical Research Center, Faculty of Medicine, Saint-Joseph University, Beirut, Lebanon*

Correspondence should be addressed to Marie-Hélène Gannagé-Yared; mariehelene.yared@usj.edu.lb

Received 12 November 2019; Revised 22 January 2020; Accepted 18 February 2020; Published 14 March 2020

Academic Editor: Maria G. Chiofalo

Context. Intraoperative PTH (IOPTH) drop of more than 50% during minimally invasive parathyroidectomy (MIP) predicts the surgery success. Comparison between second- and third-generation PTH assays (PTH 2G and PTH 3G) on IOPTH decline is scarce. The aim of this study is to compare both assays and to determine the predictors of IOPTH decline. *Methods.* 112 patients (of which 72.3% females) underwent MIP by the same surgeon. Age, sex, body mass index (BMI), pre- and postoperative serum calcium, creatinine, 25(OH)D levels, PTH at baseline (PTH T0), and PTH at 10 minutes after adenoma resection (PTH T10) were recorded. Both PTH 2G and PTH 3G assays were assessed using the Diasorin assays. *Results.* The mean age was 56.1 ± 14.7 years. Mean value of BMI, preoperative calcium, 25(OH)D, and CKD-EPI-eGFR were, respectively, 26.8 ± 4.8 kg/m^2, 110.9 ± 7.9 mg/L, 19.3 ± 9.2 ng/mL, and 88.6 ± 25.6 mL/min/1.73 m^2. PTH 2G and PTH 3G assays were well correlated at PTH T0 and PTH T10 (respectively, correlation coefficient 0.74 and 0.72 for intraclass correlation type 3). The median PTH fall was, respectively, of 79.9% and 82.5% for PTH 2G and PTH 3G. Multivariate analysis using the combined PTH 2G and PTH 3G as a dependent variable with 2 repeated measurements (at PTH 0 and PTH 10) showed a significant effect of preoperative calcium on IOPTH fall ($p = 0.001$, effect size 0.13), while no significant effects were observed for sex, age, BMI, and 25(OH)D. *Conclusion.* PTH 2G and PTH 3G assays resulted in a similar drop in IOPTH values. Elevated preoperative calcium levels are the only independent predictor of IOPTH decline. Further studies are needed to determine other factors that can influence PTH kinetics.

1. Introduction

Primary hyperparathyroidism (PHPT) is most frequently caused by a single adenoma localized in one of the parathyroid glands [1]. Surgery remains the only definitive cure of the disease. Previously managed by bilateral surgical neck exploration, PHPT is nowadays treated by minimally invasive parathyroidectomy (MIP). This change was primarily driven by the accuracy of preoperative localization tests allowing a unilateral neck exploration with a limited operative time, sometimes using just a cervical block with sedation [1–3]. The incorporation of intraoperative measurements of PTH (IOPTH) has facilitated MIP and reduced the need for further unnecessary explorations [4]. The Miami criterion for a successful parathyroidectomy was defined as a fall of IOPTH by more than 50% of its initial value, within 10 to 15 minutes after removal of the adenoma [5]. The IOPTH value drawn at 10 minutes following parathyroidectomy is the most accurate predictor of a successful MIP [6, 7]. Age, impaired renal function [8], race (African American vs. others) [9], and high BMI [10] were shown to be negative predictors of IOPTH decline following MIP, while low 25 hydroxyvitamin D (25(OH)D) levels have been shown to either increase IOPTH drop [11] or have no effect [12, 13].

Different generations of parathormone (PTH) assays are present in the market. The older ones, called "intact" PTH or

second-generation PTH assays (PTH 2G) cross-react with an N-terminal truncated PTH fragment called (7–84) PTH or non-(1–84) PTH [14–17]. The more recent ones called third-generation assays (PTH 3G) do not detect the non-(1–84) PTH but measure a post-translational form called amino-PTH [18, 19]. Despite lower values in PTH 3G assays compared to PTH 2G (approximately 30 to 50% lower) [17, 20–22], both assays demonstrated a strong correlation in patients with normal renal function [20, 23] and on hemodialysis [22, 24], even if the difference between both methods increases when PTH values are high [23, 24].

It has been shown that during MIP a greater IOPTH drop was observed 10 minutes after excision in the PTH 3G compared to the PTH 2G assay [25, 26] in both primary [26] and secondary hyperparathyroidism [25]. Because of the lack of consistent data on this subject, we aimed to compare both PTH assays during MIP in patients with an estimated Chronic Kidney Disease Epidemiology Collaboration (CKD-EPI) equation > 30 mL/min/1.73 m^2 and to identify the predictors of IOPTH decline.

2. Materials and Methods

2.1. Subjects. One hundred and twelve patients underwent MIP. The MIP surgeries were performed by the same surgeon at the department of general surgery of Hotel-Dieu de France university hospital, Beirut. MIP was performed only in cases with clearly positive localization on ultrasound or scan. Subjects with a family history of hyperparathyroidism or a personal or family history of multiple endocrine neoplasia or recurrent hyperparathyroidism after surgery were also excluded.

The following clinical data were retrospectively collected from the patients' records: age, sex, weight, height, body mass index (BMI) (calculated as weight in kilograms (kg) over the square of height in square meter (m^2)), history of diabetes or hypertension, and bisphosphonate use. Prior to surgery, PHPT was diagnosed according to the following criteria: combined elevation of PTH and calcium levels for the hypercalcemic PHPT; elevated PTH level combined with a normal calcium and 25(OH)D levels (25(OH)D ≥ 20 ng/mL) for normocalcemic PHPT. Normocalcemic PHPT was found in 9 subjects (8% of the sample).

2.2. Surgical Procedure. Surgery was performed under local anesthesia (0.5–1% xylocaine with 1 : 200,000 adrenaline) assisted with an intravenous sedation. Propofol was given intravenously for sedation with titration according to the need of the patient. In addition, an intravenous bolus of fentanyl of 50 to 100 μg was given before the incision to insure analgesia. A focused lateral approach through a 2 cm transverse skin mini incision was done directly over the parathyroid gland localized by preoperative imaging. Then the sternomastoid muscle was mobilized laterally, and the identified adenoma was removed and sent to pathology for extemporaneous analysis. The surgery time was 30 ± 8 min (range 15–55 min).

2.3. Laboratory Analysis

2.3.1. Biochemistry Assessment. Fasting serum preoperative calcium, phosphorus, and creatinine levels were repeated on the day of the surgery between 08 : 00 and 09 : 00 AM and measured on dry chemistry by using a Kodak automate. Postoperatively on day 1, fasting calcium and phosphorus were also measured. The respective normal values for calcium and phosphorus were 2.1–2.56 mmol/L and 0.84–1.45 mmol/L. In addition to creatinine measurements, CKD-EPI equation was used for glomerular filtration rate estimation (eGFR). Results are expressed in mL/min/1.73 m^2.

2.3.2. PTH and 25(OH)D Measurements. PTH was measured intraoperatively at baseline (preincision or PTH T0) and at 10 minutes following surgical removal of the parathyroid adenoma (PTH T10), with both PTH 2G and PTH 3G assays. The PTH 2G was measured using the chemiluminescent Diasorin assay on the Liaison automate (Stillwater, USA). This method uses a monoclonal antibody specific for the central and C-terminal part of the molecule (amino acids 34–84) and a second polyclonal antibody recognizing the N-terminal part of the PTH. It recognizes both the PTH 1–84 and the peptide 7–84. The lower limit of detection is 3 pg/mL and the measurement range between 3 and 1900 pg/mL. The PTH 3G was also measured with a chemiluminescent Diasorin assay on the Liaison automate (Stillwater, USA). This assay allows the determination of the PTH 1–84 without cross-reactivity with the PTH 7–84 fragment, using two polyclonal antibodies, the first one specific to the N-terminal extremity of the peptide and the second specific to the C-terminal part ensuring 100% specificity for the whole PTH molecule. The minimal detectable level is 1.7 pg/mL. The respective normal values for healthy subjects are 7 to 36 pg/mL for PTH 3G assay and 11 to 62 pg/mL for PTH 2G. 25-(OH)D was measured using the Diasorin chemiluminescent automate Liaison (Stillwater, USA). Measurements of PTH 2G and 25(OH)D were delayed and measured on serum previously frozen at −80°C.

2.3.3. Statistical Analysis. The distributions of quantitative variables were assessed with Q-Q plots. Shapiro–Wilk and Kolmogorov–Smirnov tests were used to check departure from normality. Continuous variables overtly nonnormal were expressed as median with its interquartile range (1^{st} quartile–3^{rd} quartile). Continuous variables not departing from normality were expressed as mean and its standard deviation. PTH assay distributions are expectedly heavily skewed motivating an inverse normal transform (INT) approach, using Van der Waerden ranks. A 2-way MANCOVA model was applied, using the INT of PTH 2G and PTH 3G assays as a combined dependent variable for multivariate analysis, followed by INT of PTH 2G and PTH 3G separately for post-MANCOVA univariate analysis. Two repeated measurements were specified (at baseline PTH T0 and at 10 min PTH T10), gender was taken as between-subject independent factor, and age, CKD-EPI-eGFR, BMI,

preoperative calcium, and 25(OH)D levels were taken as covariates. Type III sum of squares was used, and a 2-way time by factor interactions were included in the model.

Agreement between the PTH 2G and PTH 3G assays was calculated using intraclass correlation coefficient type 3 (ICC [3], 95% confidence provided), assuming a 2-way mixed effects model where the subjects' effects are random, and measures' effects are fixed. Results were considered statistically significant for p values under 0.05.

Analyses were run using SPSS software (IBM Corp. Released 2013, SPSS Statistics for Windows Version 22.0, Armonk, NY).

3. Results

A total of 112 patients were included in this study, with a mean age of 56.1 ± 14.7 years (range 23–86 years). 72.3% of the subjects were females, 17.9% had diabetes, 42.9% had hypertension, and 6.3% were taking bisphosphonates. The mean BMI was 26.8 ± 4.8 kg/m^2 (range 18.6–44.9 kg/m^2).

3.1. Biochemical Measurements. The respective pre- and postoperative mean calcium levels were 110.9 ± 7.9 (range 97.2–156 mg/L) and 90.7 ± 7.4 mg/L (range 70.8–114 mg/L). The mean CKD-EPI-eGFR was 88.6 ± 25.6 mL/min/1.73 m^2 (range 30.0–164.2 mL/min/1.73 m^2) with 95 patients (84.8%) having a CKD-EPI-eGFR ≥ 60 mL/min/1.73 m^2 and 17 (15.2%) between 30 and 60 mL/min/1.73 m^2. The mean 25(OH)D level was 19.3 ± 9.2 ng/mL (range 4–44.6 ng/mL).

3.2. IOPTH Drop in PTH 2G and PTH 3G Assays. The median and interquartile values of baseline PTH (PTH T0) using the PTH 2G and PTH 3G assays were, respectively, 121.5 pg/mL (89.5–172.5 pg/mL) (range 17.4–992 pg/mL) and 64.2 pg/mL (48.7–90.5 pg/mL) (range 27.8–538 pg/mL). There was no difference in PTH 2G and PTH 3G between subjects who took bisphosphonates and those who did not ($p = 0.990$ and $p = 0.696$, respectively). Ten minutes after the adenoma removal, the median and interquartile values of PTH (PTH T10) were 24.1 pg/mL (16.8–37.91 pg/mL) (range 3.3–172 pg/mL) for PTH 2G and 12.3 pg/mL (8.4–19.2 pg/mL) (range 4–119 pg/mL) for PTH 3G. The median IOPTH drop was 79.9% (71.4%–85.8%) for the PTH 3G and 82.5% (72.9%–87.9%) for the PTH 2G ($p = 0.566$) (data shown in Table 1).

There was a good agreement between the 2 assays for both baseline PTH T0 and PTH T10 (ICC [3] 0.735 (95% CI 0.311–0.871) and 0.722 (95% CI 0.157–0.876), respectively).

3.3. Uni- and Multivariate Analysis Studying the Relationship between Baseline PTH Values and Other Variables. MANCOVA analysis revealed that 25(OH)D and preoperative calcium levels are independently associated with the combined PTH 2G and PTH 3G assay variable ($p = 0.016$, effect size 0.094 for 25(OH)D; $p = 0.017$, effect size 0.093 for preoperative calcium levels), while the other variables did not achieve significance (age, BMI, and CKD-EPI-eGFR) (data not shown in tables).

Table 1: Pre- and postoperative values of the assessed biochemical variables.

Preoperative calcium (mg/L)	110.9 ± 7.9
Postoperative calcium (mg/L)	90.7 ± 7.4
Preoperative phosphorus (mmol/L)	1.00 ± 0.16
Postoperative phosphorus (mmol/L)	1.26 ± 0.25
CKD-eGFR (ml/min/1.73 m^2)	88.6 ± 25.6
PTH 3G T0 (pg/mL)	64.2 [48.7–90.5]
PTH 3G T10 (pg/mL)	12.3 [8.4–19.2]
PTH 2G T0 (pg/mL)	121.5 [89.5–172.5]
PTH 2G T10 (pg/mL)	24.1 [16.8–37.91]
Percentage of IOPTH 2G decrease	79.9% [71.4%–85.5%]
Percentage of IOPTH 3G decrease	82.5% [72.9%–87.9%]
25(OH)D level (ng/mL)	19.3 ± 9.2

Data are expressed as mean ± SD or median and its interquartile range.

In univariate analysis following MANCOVA, studying separately PTH 2G and PTH 3G, the effect of 25(OH)D levels was similar for PTH 2G and 3G (for PTH 2G, $p = 0.013$, effect size 0.070; for PTH 2G, $p = 0.004$, effect size 0.094). The preoperative calcium was also significant for the PTH 2G ($p = 0.009$, effect size 0.078) and for PTH 3G ($p = 0.004$, effect size 0.092) (Table 2).

3.4. Uni- and Multivariate Analysis Studying the Predictors of IOPTH Fall. MANCOVA of the combined PTH 2G and PTH 3G as a dependent variable with 2 repeated measurements (at PTH T0 and PTH T10) showed a significant effect of preoperative calcium on IOPTH fall ($p = 0.007$, effect size 0.110), with no significant effects of the other factors (age, sex, CKD-EPI-eGFR, BMI, and 25(OH)D) (Table 3).

The univariate analysis studying separately PTH 2G and PTH 3G, showed that only the preoperative calcium levels had a significant effect on IOPTH fall in both assays ($p = 0.015$, effect size 0.067 for PTH 2G; $p = 0.002$, effect size 0.109 for PTH 3G) (Table 3).

When analyzed separately according to 25(OH)D levels, the magnitude of the PTH drop was inversely correlated with 25(OH)D levels for PTH 3G (Spearman's rho = −0.076, $p = 0.050$) but not for PTH 2G (Spearman's rho = −0.025, $p = 0.524$), as shown in Figure 1. The magnitude of PTH drop was also correlated with the preoperative calcium level for both PTH 2G and PTH 3G (Spearman's rho = 0.254, $p = 0.007$ for PTH 3G; Spearman's rho = 0.228, $p = 0.017$ for PTH 2G) as shown in Figure 2.

4. Discussion

The purpose of our study was to compare the IOPTH decline using 2 different PTH assays in 112 patients undergoing MIP and to determine the predictors of this decline. Our results showed a respective IOPTH fall of 79.9% and 82.5% for the PTH 3G and PTH 2G assay, with no significant difference between both assays. Two previous groups, the first one from Japan [25, 26] and the second one from Austria [27, 28], reported a quicker drop of the IOPTH using a PTH 3G assay compared to a PTH 2G one. The difference between both assays could be explained by the cross-reactivity of PTH 2G

Table 2: Univariate analysis studying the relationship between baseline PTH values and other variables (a) computed at alpha 5%).

Univariate between subjects F tests	Variable	p value	Effect size (partial eta squared)	Power
Intercept	PTH_3G	0.035	0.052	0.565
	PTH_2G	0.058	0.042	0.476
Age	PTH_3G	0.109	0.030	0.360
	PTH_2G	0.370	0.009	0.145
CKD-EPI-eGFR	PTH_3G	0.974	0.000	0.050
	PTH_2G	0.583	0.004	0.085
BMI	PTH_3G	0.690	0.002	0.068
	PTH_2G	0.225	0.017	0.227
25(OH)D	PTH_3G	0.004	0.094	0.836
	PTH_2G	0.013	0.070	0.709
Preoperative calcium	PTH_3G	0.004	0.092	0.825
	PTH_2G	0.009	0.078	0.758
Gender	PTH_3G	0.979	0.000	0.050
	PTH_2G	0.788	0.001	0.058

Table 3: Uni- and multivariate analysis studying the predictors of IOPTH fall (a) computed at alpha 5%).

	Wilk's lambda	p value	Effect size (partial eta squared)	Power
Multivariate tests within subjects				
Time	0.908	0.018	0.092	0.727
Time ∗ age	0.991	0.683	0.009	0.110
Time ∗ CKD-EPI-eGFR	0.980	0.427	0.020	0.193
Time ∗ BMI	0.981	0.443	0.019	0.187
Time ∗ 25(OH)D	0.987	0.583	0.013	0.137
Time ∗ preoperative calcium	0.890	0.007	0.110	0.816
Time ∗ gender	0.949	0.110	0.051	0.449
Univariate within subjects F tests				
	Variable			
Time	PTH_3G	0.005	0.091	0.822
	PTH_2G	0.013	0.070	0.708
Time ∗ age	PTH_3G	0.477	0.006	0.109
	PTH_2G	0.381	0.009	0.140
Time ∗ CKD-EPI-eGFR	PTH_3G	0.393	0.009	0.136
	PTH_2G	0.206	0.019	0.242
Time ∗ BMI	PTH_3G	0.203	0.019	0.245
	PTH_2G	0.331	0.011	0.162
Time ∗ 25(OH)D	PTH_3G	0.944	0.000	0.051
	PTH_2G	0.596	0.003	0.082
Time ∗ preoperative calcium	PTH_3G	0.002	0.109	0.890
	PTH_2G	0.015	0.067	0.687

assays with non-(1–84) PTH fragments of longer half-lives [26], resulting in a slower IOPTH drop. However, the abovementioned studies were mainly performed on a small sample of subjects with renal hyperparathyroidism (rHPT) [25, 27, 28], either secondary to hemodialysis [25, 27, 28] or following renal transplantation [27, 28]. The only study that included a subgroup of subjects with PHPT was the Japanese one [26] in which 74 patients with PHPT were enrolled. The authors of the latter study found a greater difference in IOPTH fall between both assays in hemodialysis subjects compared to subjects with PHPT, suggesting that renal function affects the IOPTH drop. The difference between these studies and our study could be explained by the normal renal function in the majority of the current sample (84.8% of our sample had a CKD-EPI-eGFR ≥ 60 mL/min/1.73 m^2), the use of different PTH assays in our study, and more importantly, the timing of sampling during the surgery. In fact, in both the Japanese [25, 26] and Austrian studies [27, 28], the Quick Roche Elecsys PTH assay was used for the 2G assay, while either the Scantibodies Laboratory assay [25, 26] or the Nichols assay [27, 28] was used for the 3G assay. Subsequently, one could speculate that different PTH kinetics exist between these 3 assays and the Diasorin assays that were used in our study. In fact, it is possible that the short turnout of the Quick Roche Elecsys PTH 2G assay, which is of 6 minutes, does not allow the achievement of the same IOPTH fall observed with the PTH 3G assay. In addition, the IOPTH value at 10 minutes after excision of adenoma was used in our study as a predictive value for surgical cure, as established by the Miami criterion [5]. Collecting a sample at a later timing, for example at 15 minutes [25, 26] or even later at a maximum of 50 minutes [26] could have led to a divergence between both assays.

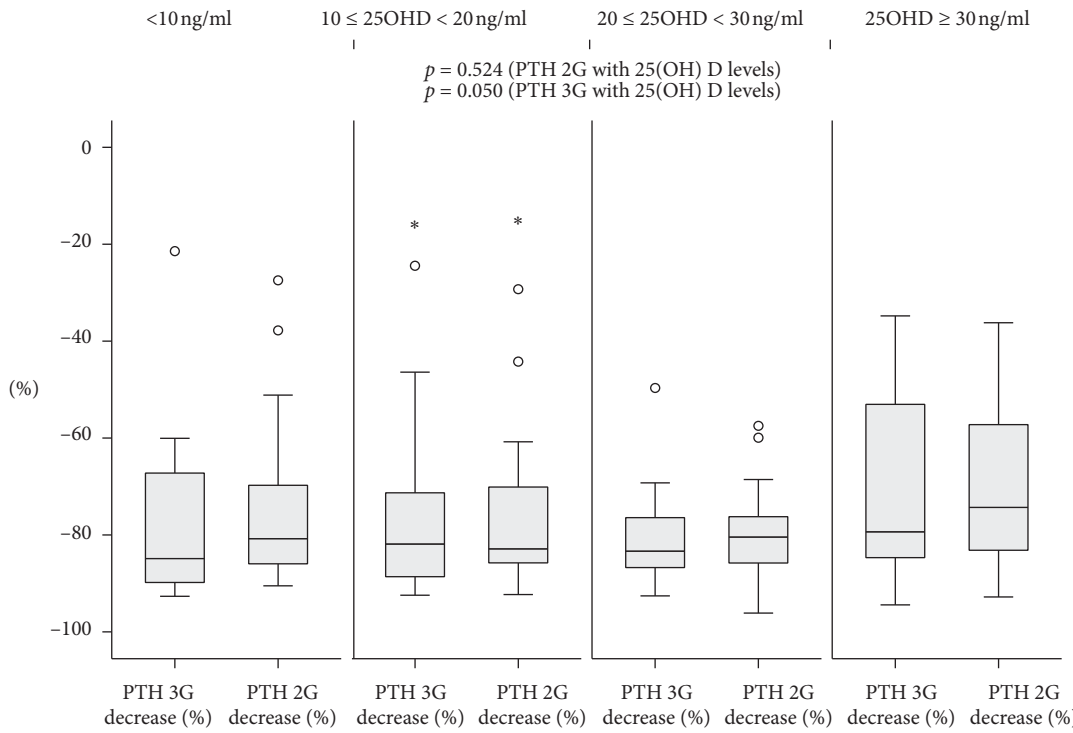

Figure 1: Effect of 25(OH)D on IOPTH decline, using PTH 2G and PTH 3G assays. PTH 2G, 2nd generation PTH assay; PTH 3G, 3rd generation PTH assay; IOPTH, Intraoperative PTH decline. Drop of PTH 2G and PTH 3G results are shown as boxplots. p values correspond to those of the Spearman correlation coefficient between PTH 2G and PTH 3G on one hand and 25(OH) D on the other hand. Small circles correspond to outliers, and stars correspond to extreme outliers.

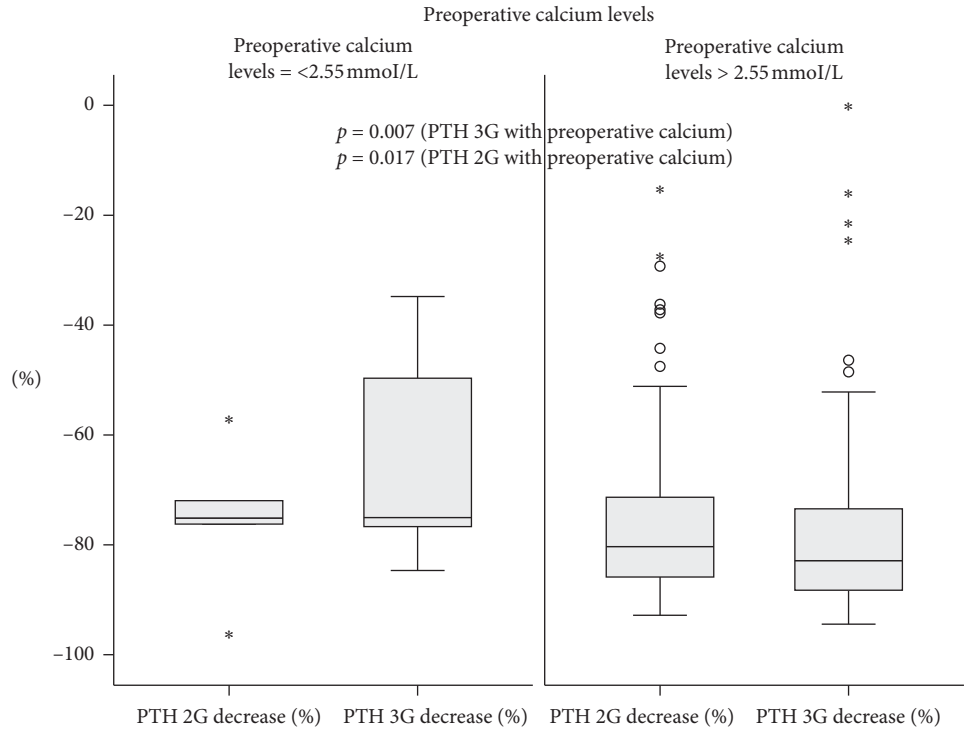

Figure 2: Effect of preoperative calcium (preoperative calcium ≤ 2.55 mmol/L vs >2.55 mmol/L) on IOPTH decline, using PTH 2G and PTH 3G assays. PTH 2G, 2nd generation PTH assay; PTH 3G, 3rd generation PTH assay; IOPTH, Intraoperative PTH decline. Drop of PTH 2G and PTH 3G results are shown as boxplots. p values correspond to those of the Spearman correlation coefficient between PTH 2G and PTH 3G on one hand and preoperative calcium levels on the other hand. Small circles correspond to outliers and stars correspond to extreme outliers.

We then studied the effect of gender, age, BMI, CKD-EPI-eGFR, preoperative calcium, and 25(OH)D levels on IOPTH decline. On one hand, we found that the only predictor of IOPTH fall was the preoperative calcium level, the presence of elevated levels being associated with a greater IOPTH decrease, no matter the used assay. Those results are in line with two other studies demonstrating that subjects with the normocalcemic variant of PHPT have a slower drop in their IOPTH [10, 29]. On the other hand, gender, age, and BMI did not affect the IOPTH decline. Similarly to our results, another study did not find that gender influences the IOPTH drop [10]. In addition, in our previous report [8], age but not gender was a predictor of IOPTH decline, since an inverse relationship between age and IOPTH was noted. Also, another study showed an inverse relation between BMI and IOPTH in patients younger than 55 years [10]. Of note, we found that the CKD-EPI-eGFR was not a predictor of the IOPTH contrary to our previous study demonstrating an inverse relationship between the CKD-EPI-eGFR and IOPTH decline [8]. The reason behind these different results could be related to other characteristics of our population (age being slightly younger age and majority of patients having a normal renal function) or to different used PTH assays.

Finally, we analyzed the effect of 25(OH)D levels on the IOPTH decline. In addition to being inversely correlated with PTH values in uni- and multivariate analysis, 25(OH) D was found to have an effect on IOPTH decline. Because vitamin D deficiency stimulates parathyroid hyperplasia and is associated with larger parathyroid adenomas and higher levels of PTH before and after surgery for PHPT [30], one could speculate that the IOPTH decline is slower in vitamin D deficient patients [31, 32]. However, results of studies looking at the impact of 25(OH)D status on IOPTH kinetics are controversial. While one study has shown an inverse relationship between 25(OH)D levels and IOPTH decline [11], others did not find the same results [12, 13, 33–35]. We also found a significant drop in IOPTH regardless of 25(OH)D classes. The drop in PTH 3G was significantly and inversely correlated with 25(OH)D, a finding that is in line with the Agarwal et al. study [11], but the small effect size precludes any meaningful inference, noting that in univariate F tests following MANCOVA (Table 3), the effect of 25(OH)D was not found to be significant.

The strength of our study is that it is the first one to compare PTH 2G and PTH 3G assays in a large sample of subjects undergoing a MIP. Unfortunately, both the Diasorin PTH 2G and PTH 3G used assays in our study need an approximate complete turnout of 50 minutes compared to the only two other available QUICK PTH assays (Siemens Immulite® Turbo PTH and Roche Elecsys) which need less than 15 minutes. Subsequently, the surgical decision-making process requires a longer time during which the patient is still in the operative room. This is the reason why an IOPTH sampling was not performed at a later time than 10 minutes in our institution. Our surgeon relies solely on the extemporaneous pathology in order to extend the surgical procedure. Nevertheless, our results confirm the fact that developing a quick third-generation assay may not be an added value compared to the second-generation assays.

5. Conclusion

In conclusion, our study shows that PTH 2G and PTH 3G assays resulted in a similar drop in IOPTH values. Eelevated preoperative calcium level was an independent predictor of IOPTH while age, sex, BMI, CKD-EPI-eGFR, and 25 (OH)D levels were not. Our results suggest that current criteria for IOPTH monitoring are applicable regardless of the used PTH assay and the clinical characteristics of the patients.

Abbreviations

PTH: Parathormone
25(OH)D: 25-hydroxyvitamin D
IOPTH: Intraoperative parathormone.

Data Availability

The excel data used to support the findings of this study are available from the corresponding author upon request.

Conflicts of Interest

The authors declare that they have no conflicts of interest.

Authors' Contributions

Marie-Hélène Gannagé-Yared conceptualized the study and reviewed and edited the manuscript. Nada Younes and Anne-Sophie Azzi performed the data curation and wrote the original draft. Ghassan Sleilaty performed statistical analysis and wrote the statistical results.

Acknowledgments

This work was supported by the Conseil de Recherche de l'Université Saint-Joseph. The authors thank Mrs. Rima Chedid for her careful reading of the article.

References

[1] K. L. Insogna, "Primary hyperparathyroidism," *New England Journal of Medicine*, vol. 379, no. 11, pp. 1050–1059, 2018.
[2] W. R. Sackett, B. Barraclough, T. S. Reeve, and L. W. Delbridge, "Worldwide trends in the surgical treatment of primary hyperparathyroidism in the era of minimally invasive parathyroidectomy," *Archives of Surgery*, vol. 137, no. 9, pp. 1055–1059, 2002.
[3] R. Udelsman, "Six hundred fifty-six consecutive explorations for primary hyperparathyroidism," *Annals of Surgery*, vol. 235, no. 5, pp. 665–672, 2002.
[4] M. L. Richards, G. B. Thompson, D. R. Farley, and C. S. Grant, "An optimal algorithm for intraoperative parathyroid hormone monitoring," *Archives of Surgery*, vol. 146, no. 3, pp. 280–285, 2011.
[5] G. L. Irvin, C. C. Solorzano, and D. M. Carneiro, "Quick intraoperative parathyroid hormone assay: surgical adjunct to allow limited parathyroidectomy, improve success rate, and

predict outcome," *World Journal of Surgery*, vol. 28, no. 12, pp. 1287–1292, 2004.

[6] G. L. Irvin, V. D. Dembrow, and D. L. Prudhomme, "Clinical usefulness of an intraoperative "quick parathyroid hormone" assay," *Surgery*, vol. 114, no. 6, pp. 1019–1022, 1993.

[7] L. J. Sokoll, H. Drew, and R. Udelsman, "Intraoperative parathyroid hormone analysis: a study of 200 consecutive cases," *Clinical Chemistry*, vol. 46, no. 10, pp. 1662–1668, 2000.

[8] M. H. Gannagé-Yared, B. Abboud, M. Amm-Azar et al., "Predictors of intra-operative parathyroid hormone decline in subjects operated for primary hyperparathyroidism by minimally invasive parathyroidectomy," *Journal of Endocrinological Investigation*, vol. 32, no. 2, pp. 160–164, 2009.

[9] R. M. Cisco, J. H. Kuo, L. Ogawa et al., "Impact of race on intraoperative parathyroid hormone kinetics," *Archives of Surgery*, vol. 147, no. 11, pp. 1036–1040, 2012.

[10] A. J. Leiker, T. W. F. Yen, D. C. Eastwood et al., "Factors that influence parathyroid hormone half-life," *JAMA Surgery*, vol. 148, no. 7, pp. 602–606, 2013.

[11] G. Agarwal, D. Sadacharan, P. Ramakant, M. Shukla, and S. K. Mishra, "The impact of vitamin D status and tumor size on the intraoperative parathyroid hormone dynamics in patients with symptomatic primary hyperparathyroidism," *Surgery Today*, vol. 42, no. 12, pp. 1183–1188, 2012.

[12] M. M. Statham, N. B. Watts, and D. L. Steward, "Intraoperative PTH: effect of sample timing and vitamin D status," *Otolaryngology—Head and Neck Surgery: Official Journal of American Academy of Otolaryngology-Head and Neck Surgery*, vol. 136, no. 6, pp. 946–51, 2007.

[13] C. E. Graves, C. M. McManus, J. A. Chabot, J. A. Lee, and J. H. Kuo, "Vitamin D does not affect intraoperative parathyroid hormone kinetics: a mixed linear model analysis," *Journal of Surgical Research*, vol. 241, pp. 199–204, 2019.

[14] P. D'Amour, J.-H. Brossard, L. Rousseau et al., "Structure of non-(1-84) PTH fragments secreted by parathyroid glands in primary and secondary hyperparathyroidism," *Kidney International*, vol. 68, no. 3, pp. 998–1007, 2005.

[15] R. Lepage, L. Roy, J.-H. Brossard et al., "A non-(1-84) circulating parathyroid hormone (PTH) fragment interferes significantly with intact PTH commercial assay measurements in uremic samples," *Clinical Chemistry*, vol. 44, no. 4, pp. 805–809, 1998.

[16] V. P. Michelangeli, P. Heyma, P. G. Colman, and P. R. Ebeling, "Evaluation of a new, rapid and automated immunochemiluminometric assay for the measurement of serum intact parathyroid hormone," *Annals of Clinical Biochemistry: An International Journal of Biochemistry and Laboratory Medicine*, vol. 34, no. 1, pp. 97–103, 1997.

[17] M. A. Smit, C. M. J. van Kinschot, J. van der Linden, C. van Noord, and S. Kos, "Clinical guidelines and PTH measurement: does assay generation matter?" *Endocrine Reviews*, vol. 40, no. 6, pp. 1468–1480, 2019.

[18] J. C. Souberbielle, P. Boudou, and C. Cormier, "Lessons from second- and third-generation parathyroid hormone assays in primary hyperparathyroidism," *Journal of Endocrinological Investigation*, vol. 31, no. 5, pp. 463–469, 2008.

[19] P. D'Amour, J.-H. Brossard, L. Rousseau, L. Roy, P. Gao, and T. Cantor, "Amino-terminal form of parathyroid hormone (PTH) with immunologic similarities to hPTH(1-84) is overproduced in primary and secondary hyperparathyroidism," *Clinical Chemistry*, vol. 49, no. 12, pp. 2037–2044, 2003.

[20] P. Boudou, F. Ibrahim, C. Cormier, A. Chabas, E. Sarfati, and J.-C. Souberbielle, "Third- or second-generation parathyroid hormone assays: a remaining debate in the diagnosis of primary hyperparathyroidism," *The Journal of Clinical Endocrinology & Metabolism*, vol. 90, no. 12, pp. 6370–6372, 2005.

[21] N. Ljungdahl, M. Haarhaus, C. Linder, and P. Magnusson, "Comparison of 3 third-generation assays for bio-intact parathyroid hormone," *Clinical Chemistry*, vol. 52, no. 5, pp. 903-904, 2006.

[22] M. L. Melamed, J. A. Eustace, L. C. Plantinga et al., "Third-generation parathyroid hormone assays and all-cause mortality in incident dialysis patients: the CHOICE study," *Nephrology Dialysis Transplantation*, vol. 23, no. 5, pp. 1650–1658, 2008.

[23] A. M. Dupuy, A. S. Bargnoux, M. Morena et al., "Moving from the second to the third generation Roche PTH assays: what are the consequences for clinical practice?" *Clinical Chemistry and Laboratory Medicine (CCLM)*, vol. 57, no. 2, pp. 244–249, 2018.

[24] M.-H. Gannagé-Yared, C. Farès, T. Ibrahim, Z. A. Rahal, M. Elias, and D. Chelala, "Comparison between a second and a third generation parathyroid hormone assay in hemodialysis patients," *Metabolism*, vol. 62, no. 10, pp. 1416–1422, 2013.

[25] H. Yamashita, T. Cantor, S. Uchino et al., "Sequential changes in plasma intact and whole parathyroid hormone levels during parathyroidectomy for secondary hyperparathyroidism," *World Journal of Surgery*, vol. 29, no. 2, pp. 169–173, 2005.

[26] H. Yamashita, P. Gao, T. Cantor et al., "Comparison of parathyroid hormone levels from the intact and whole parathyroid hormone assays after parathyroidectomy for primary and secondary hyperparathyroidism," *Surgery*, vol. 135, no. 2, pp. 149–156, 2004.

[27] K. Kaczirek, G. Prager, P. Riss et al., "Novel parathyroid hormone (1-84) assay as basis for parathyroid hormone monitoring in renal hyperparathyroidism," *Archives of Surgery*, vol. 141, no. 2, pp. 129–134, 2006.

[28] C. Bieglmayer, K. Kaczirek, G. Prager, and B. Niederle, "Parathyroid hormone monitoring during total parathyroidectomy for renal hyperparathyroidism: pilot study of the impact of renal function and assay specificity," *Clinical Chemistry*, vol. 52, no. 6, pp. 1112–1119, 2006.

[29] C. E. Graves, C. M. McManus, J. A. Chabot, J. A. Lee, and J. H. Kuo, "Biochemical profile affects IOPTH kinetics and cure rate in primary hyperparathyroidism," *World Journal of Surgery*, vol. 44, no. 2, pp. 488–495, 2020.

[30] M. Carsote, D. Paduraru, A. Nica, and A. Valea, "Parathyroidectomy: is vitamin D a player for a good outcome?" *Journal of Medicine and Life*, vol. 9, no. 4, pp. 348–352, 2016.

[31] S. E. Carty, M. M. Roberts, M. A. Virji, L. Haywood, and J. H. Yim, "Elevated serum parathormone level after "concise parathyroidectomy" for primary sporadic hyperparathyroidism," *Surgery*, vol. 132, no. 6, pp. 1086–1093, 2002.

[32] N. Özbey, Y. Erbil, E. Ademoğlu, S. Özarmağan, U. Barbaros, and A. Bozbora, "Correlations between vitamin D status and biochemical/clinical and pathological parameters in primary hyperparathyroidism," *World Journal of Surgery*, vol. 30, no. 3, pp. 321–326, 2006.

[33] J. T. Adler, R. S. Sippel, and H. Chen, "25-hydroxyvitamin D status does not affect intraoperative parathyroid hormone dynamics in patients with primary hyperparathyroidism," *Annals of Surgical Oncology*, vol. 17, no. 11, pp. 2958–2962, 2010.

[34] B. R. Untch, M. E. Barfield, M. Dar, D. Dixit, G. S. Leight, and J. A. Olson, "Impact of 25-hydroxyvitamin D deficiency on perioperative parathyroid hormone kinetics and results in

patients with primary hyperparathyroidism," *Surgery*, vol. 142, no. 6, pp. 1022–1026, 2007.

[35] D. N. Singh, S. K. Gupta, G. Chand et al., "Intra-operative parathyroid hormone kinetics and influencing factors with high baseline PTH: a prospective study," *Clinical Endocrinology*, vol. 78, no. 6, pp. 935–941, 2013.

Hindawi
International Journal of Endocrinology
Volume 2020, Article ID 7048185, 5 pages
https://doi.org/10.1155/2020/7048185

Research Article

Parathyroid Carcinoma: An Up-to-Date Retrospective Multicentric Analysis

Francesco Quaglino,[1] Luca Manfrino ,[1] Luca Cestino,[1] Massimo Giusti,[2] Enrico Mazza,[3] Alessandro Piovesan,[4] Nicola Palestini,[5] Corrado Lauro,[6] and Elena Castellano[7]

[1]*Department of General Surgery, "Maria Vittoria" Hospital ASL Città di Torino, Turin 10144, Italy*
[2]*Department of Internal Medicine, "San Giovanni Bosco" Hospital ASL Città di Torino, Turin 10154, Italy*
[3]*Department of Endocrinology, "Maria Vittoria" Hospital ASL Città di Torino, Turin 10144, Italy*
[4]*Department of Endocrinology, A. O. U. Città della Salute della Scienza di Torino, Turin 10126, Italy*
[5]*Thyroid and Parathyroid Surgery, Candiolo Cancer Institute I. R. C. C. S., Candiolo 10060, Italy*
[6]*Department of General Surgery, "Santa Croce e Carle" Hospital, Cuneo 12100, Italy*
[7]*Department of Endocrinology, Diabetes and Metabolism, "Santa Croce e Carle" Hospital, Cuneo 12100, Italy*

Correspondence should be addressed to Luca Manfrino; manfrino.luca@gmail.com

Received 13 November 2019; Revised 28 January 2020; Accepted 11 February 2020; Published 6 March 2020

Academic Editor: Maria G. Chiofalo

Parathyroid carcinoma (PC) is a rare disease responsible for about 1% of primary hyperparathyroidism (PHPT) cases. PC usually has an indolent course, tough to differentiate from the benign causes of PHPT, and the only certain diagnosis is histologic. The gold standard surgical treatment is the en bloc resection associated with the homolateral thyroid loboistmectomy. The aim of this study was to underline the main differences between PC and benign PHPT, along with gathering epidemiological knowledge relative to PC in our region. Data from the regional cancer network (Rete Oncologica del Piemonte e della Valle d'Aosta) since 2007 have been reported, including 21 patients from three hospitals (AO S. Croce e Carle of Cuneo, AOU Città della Salute of Turin, and ASL Città di Torino). The incidence of the disease, gender, age at time of diagnosis, presence of renal and bone symptoms, serum calcium and PTH levels, surgical technique performed, and percentage of recurrence were analysed. PC data were than compared with a series of patients affected by benign PHPT, referred to ASL Città di Torino, Maria Vittoria Hospital, from 2007 to 2019. A PC incidence of 0.05 cases per 100,000 inhabitants was found in our region. Benign forms occurred more frequently in females ($p = 0.0002$), while PC equally occurred in males and females and affected younger patients ($p = 0.026$). Serum calcium and PTH levels were significantly higher in PC patients; accordingly, typical PHPT symptoms were more frequently reported in PC than in benign PHPT. In the PC group, the en bloc resection shows a 13 times lower risk for relapse compared with all the other surgical techniques. PC is equally gender distributed, and the average patients' age is in the fifth decade of life. It is usually functioning, with greater biochemical activity and multiple symptoms. A not-radical surgical resection is associated with a higher recurrence rate. A meticulous presurgical evaluation of PHPT patients showing PC's evocative features is mandatory to obtain a complete disease extirpation.

1. Introduction

Parathyroid carcinoma (PC) is a rare disease responsible for about 1% of primary hyperparathyroidism (PHPT) cases and represents 0.005% of all tumours [1, 2]. PC is usually sporadic, but it can be associated with genetic syndromes [3]. Its aetiology is unknown, but a correlation with radiation exposure and with secondary and tertiary hyperparathyroidism associated with renal failure has been reported [4].

Parathyroid carcinomas usually have an indolent course [5, 6], and given the extreme clinical difficulty in differentiating them from the benign causes of primary

hyperparathyroidism, to date, the only certain diagnosis is histologic.

An important characteristic of PC is the recurrence rate which stands at a value of 50% [7]. Furthermore, relapse seems to be related to the surgical technique used to remove the tumour [8]. The gold standard surgical treatment is the en bloc resection associated with the homolateral thyroid loboistmectomy [9, 10].

However, this technique is not always performed because physicians often underestimate the possibility of the lesion's malignancy.

The association of prophylactic central neck dissection with the en bloc resection seems to be controversial. Lymph node involvement is documented in the literature in 6.5% of patients [11], and its prognostic role is not clarified. The studies on this topic show different recommendations: some suggest a central neck dissection while others do not [12–18].

Therefore, the aim of this study was to highlight the main clinical and biochemical differences between PC and benign causes of PHPT. A further purpose was to gather epidemiological knowledge relative to PC in our region in the interest to support the regional cancer network "Rete Oncologica del Piemonte e della Valle d'Aosta" [19].

Moreover, the en bloc resection was compared with other less radical surgical techniques in order to look for consequences on relapse probability.

2. Materials and Methods

30 patients were diagnosed with PC during the last 12 years (from January 2007 to July 2019), and most of their data were inserted in the regional cancer network. Complete information was available only for 21 patients which were included in the study.

The patients were treated in three different hospitals: AOU Città della Salute e della Scienza di Torino, ASL City of Turin (Maria Vittoria Hospital), and AO Santa Croce e Carle of Cuneo.

All patients underwent parathyroid resection surgery with subsequent histologic diagnosis.

The pathological criteria considered suggestive of PC were [20, 21] capsule and surrounding structures' invasion, vascular invasion, and presence of metastases.

None of the patients examined had lymph node involvement and/or distant metastasis.

A comparison was then performed with a series of 92 patients with a clinical evidence of PHPT without malignancy characteristics diagnosed in a period from January 2007 to July 2019 at Maria Vittoria hospital (ASL City of Turin). Among these 92 subjects, 50 underwent surgery in our surgical service and had a histologic diagnosis confirmation of single parathyroid adenoma. PHPT patients have been addressed to surgical treatment if symptomatic or asymptomatic, meeting the surgical criteria reported by the latest international guidelines [22].

Regarding PC, the following characteristics were examined: sex, age at the time of diagnosis, symptoms, serum calcium level, PTH (normal values, 16–75 pg/ml [10]), side of the lesion, size of the tumour, surgical technique used, and disease recurrence.

The comparison with the population affected by benign PHPT concerns the following characteristics: sex, age, symptoms, serum calcium level, and PTH.

Renal (nephrolithiasis, nephrocalcinosis, and renal insufficiency) and bone (osteoporosis, fractures, brown tumours, and cystic fibrous osteitis) involvement were reported.

3. Statistical Analysis

Variables were preliminarily tested for normal distribution with the Shapiro–Wilk test, and data were expressed as mean ± SD when normally distributed and as median and interquartile range (IQR) when not normally distributed. The chi-squared test was used for the categorical variables, except when the contingency tables presented values ≤5 where the Fisher test was employed. For noncategorical variables, the Shapiro–Wilk test was used to verify the normal distribution of the sample, in which case the data were compared with the Student's t-test and expressed as mean ± standard deviation.

In the event of a not normal distribution, the data were compared with the Wilcoxon rank-sum test and described as median and interquartile range. The significance levels considered for two-sided P values were 0.05 in all tests.

4. Results and Discussion

4.1. Results. Table 1 summarizes the characteristics of the whole series of PC patients, while Table 2 shows the comparison with patients with benign PHPT.

First of all, the incidence in our region resulted to be of 0.05 cases per 100,000 inhabitants.

As far as sex and age are concerned, benign forms seem to occur more frequently in the female sex ($P = 0.0002$) and in older persons, while PC affects younger patients ($P = 0.026$) without substantial differences in incidence between the two genders.

19 out of the 21 (90.5%) PC patients presented symptoms at the time of the diagnosis, while only 40 out of 92 (43.5%) patients suffering from benign forms on PHPT were symptomatic.

It is interesting to note that, in malignant tumours, both kidney and bone symptoms are reported.

Also taking singularly the bone and then the renal symptoms, a significant difference between the two populations can be noted ($P = 0.0002$ and $P = 0.0001$).

Serum calcium and PTH values resulted significantly higher in the PC group.

The relationship between the type of surgical technique used and the percentage of relapse is summarized in Table 3.

In 4 patients, the mutation of CDC73 was investigated and none of them displayed abnormalities.

The gold standard surgical technique (en bloc resection) was used only on 10 (47.6%) patients, none of whom developed recurrence. The other 11 (52.4%) were treated with less radical resections, and in 6 of them, the tumour relapsed (54.5%).

Table 1: Characteristics and treatment of patients affected by PC.

Patient no.	Sex	Age	Symptoms	Ca (mg/dl)	PTH (pg/ml)	Side	Size (cm)	Surgical technique	Relapse
1	F	60	B, K	13	1195	L	5.7	En bloc	No
2	F	70	B, K	12.8	1170	R	na	Other	Yes
3	M	37	No	13.4	602	R	na	En bloc	No
4	F	82	K	9.6	501	L	2	En bloc	No
5	F	38	K	12.6	353	R	4	Other	No
6	F	76	No	13.3	675	L	2	Other	Yes
7	F	57	B, K	12.6	1497	R	4.5	Other	No
8	M	59	B	13	667	R	6	Other	No
9	M	49	B, K	15.4	1140	L	5	Other	No
10	M	50	B, K	15	900	R	na	Other	Yes
11	M	61	B, K	12	464	L	2	En bloc	No
12	M	82	B	12.8	427	na	1.5	Other	Yes
13	M	38	B, K	8, 3	692	R	5	En bloc	No
14	F	67	B, K	13	700	R	1.5	En bloc	No
15	F	32	B	10	758	na	4	Other	No
16	F	76	B, K	13.6	1916	L	3.2	Other	Yes
17	M	33	B, K	16.9	3050	R	2.5	En bloc	No
18	M	77	B	11	915	R	3	En bloc	No
19	M	67	K	12.8	683	L	4	En bloc	No
20	F	45	B	13.6	908	R	4.9	En bloc	No
21	M	59	B, K	10.5	920	L	5.5	Other	Yes

F = female, M = male, B = bone involvement, K = kidney involvement, L = left, R = right, and NA = not available.

Table 2: Comparison between PC and benign PHPT populations.

Variable	PC	Benign PHPT	P value
No. of cases	21	92	—
Sex, M/F	11/10	16/76	0.0002
Age			
Median (IQR)	59 (27.5)	68 (14.5)	0.026
Mean ± SD	57.96 ± 16.61	65.98 ± 12.26	—
Patient with symptoms	19	40	0.0001
Bone involvement	16	27	0.0002
Kidney involvement	14	16	0.0001
Ca (mg/dl)			
Mean ± SD	12.63 ± 1.97	10.69 ± 1.14	10^{-9}
PTH (pg/ml)			
Median (IQR)	758 (473)	137.5 (100.5)	10^{-6}
Side, R/L	11/8	—	—
Size (cm)			
Mean	3.63	—	—

Ca = calcium, R = right, L = left, IQR = interquartile range, and SD = standard deviation.

Table 3: Comparison between the en bloc resection and less radical resections.

	En bloc resection	Other resection	P value	OR
No. of patients	10	11	0.0152	13
Relapse	0	6	—	—
No relapse	10	5	—	—

The disease recurrence was significantly lower in the patients undergoing en bloc resection compared with all the others techniques ($P = 0.0152$; OR 13).

The univariate linear regression model (Table 4), used to establish the level of correlation between the PC and presence of symptoms and serum calcium and PTH levels, showed a positive correlation with all the examined parameters, being moderate-strong only for PTH ($R = 0.689$ and $R^2 = 0.475$).

Table 4: Univariate linear regression.

Variable	R	R^2	P value
Symptoms	0.369	0.136	<0.0001
Calcium	0.493	0.243	0.005
PTH	0.689	0.475	<0.0001

4.2. Discussion. Parathyroid carcinoma is a rare tumour, and it is difficult to assert a clinical diagnosis based only on symptoms and biochemical characteristics.

In the literature, there is a lack of studies with a relevant number of patients because of the epidemiological features of the disease.

In our study, the main characteristics of PC in our region's population were defined and compared with benign forms of PHPT in order to highlight the main differences and help the diagnostic process.

A study of RARECAREnet Project [2] indicates an incidence of PC in Europe of 0.03/100,000.

Some features were found to be helpful with the diagnosis of PC. Benign PHPT showed a greater incidence in females, while PC's incidence is similar in the two genders [13, 23, 24].

This hallmark was confirmed in our study. Moreover, the mean age of PC presentation is usually lower than benign PHPT [10]. This finding has been confirmed in our study, even if a little older compared with the statistics found in the literature [4].

Most of the PCs are functioning [13, 25], causing a great PTH elevation and multiple symptoms. The main districts interested are the bones and kidneys. In our PC population,

over 90% patients presented symptoms and more than half of them had a multiple district involvement.

On the other hand, in the benign PHPT population, just under half patients presented symptoms and mostly with only one district affected.

Serum calcium and PTH levels in PC are usually higher than those in benign PHPT [3, 26–28]. This finding was confirmed in our study; in particular, PTH shows 3 or more times higher levels in PC, significantly higher than the values reported in our benign PHPT cases.

According to the results obtained, the en bloc resection appears to be associated with a lower risk of recurrence, while a less radical resection with a 13 times higher relapse risk.

An additional interesting feature concerning PC is the relation with germline mutations of CDC73, a gene that encodes a protein known as parafibromin [10]; anomalies in this gene associate with higher probability to suffer PC-isolated or in the context of hyperparathyroidism-jaw tumour syndrome or familial-isolated primary hyperparathyroidism [29].

Unfortunately, as this evaluation was available only in 4 patients, no statistical analysis was performed.

In this study, all the three regional hub centres for PC were included; for this reason, it is likely that all the PC regional cases were included. Therefore, our PC rate may be affected by selection bias.

The main limitation of the study is that the benign PHPT patients were selected only from one hospital, so they may not be totally representative of the regional population.

5. Conclusion

Investigating all the clinical features that could differentiate PC from benign PHPT is crucial to ensure a correct surgical approach, reducing the risk of recurrence and the necessity of reoperation, which is burdened by a higher frequency of surgery-related complications.

Furthermore, it is difficult to eradicate the disease completely after recurrence, forcing the patient to live with a hard-to-treat severe hypercalcemia syndrome [30].

Data Availability

The patient data used to support the findings of this study are available from the corresponding author upon request.

Conflicts of Interest

The authors declare that they have no conflicts of interest.

References

[1] N. Kolsi, S. Jellali, and J. Koubaa, "Parathyroid carcinoma: about a case and review of the literature," *Pan African Medical Journal*, vol. 27, pp. 27–85, 2017.

[2] G. Gatta, R. Capocaccia, L. Botta et al., "Burden and centralised treatment in Europe of rare tumours: results of RARECAREnet-a population-based study," *The Lancet Oncology*, vol. 18, no. 8, pp. 1022–1039, 2017.

[3] J. Goswamy, M. Lei, and R. Simo, "Parathyroid carcinoma," *Current Opinion in Otolaryngology & Head and Neck Surgery*, vol. 24, no. 2, pp. 155–162, 2016.

[4] G. L. Irvin 3rd, V. D. Dembrow, and D. L. Prudhomme, "Operative monitoring of parathyroid gland hyperfunction," *The American Journal of Surgery*, vol. 162, no. 4, pp. 299–302, 1991.

[5] C. Marcocci, F. Cetani, M. R. Rubin, S. J. Silverberg, A. Pinchera, and J. P. Bilezikian, "Parathyroid carcinoma," *Journal of Bone and Mineral Research*, vol. 23, no. 12, pp. 1869–1880, 2008.

[6] A. S. Salcuni, F. Cetani, V. Guarnieri et al., "Parathyroid carcinoma," *Best Practice & Research Clinical Endocrinology & Metabolism*, vol. 32, no. 6, pp. 877–889, 2018.

[7] J. H. Robert, A. Trombetti, A. Garcia et al., "Primary hyperparathyroidism: can parathyroid carcinoma Be anticipated on clinical and biochemical grounds? Report of nine cases and review of the literature," *Annals of Surgical Oncology*, vol. 12, no. 7, pp. 526–532, 2005.

[8] S. Xue, H. Chen, C. Lv et al., "Preoperative diagnosis and prognosis in 40 parathyroid carcinoma patients," *Clinical Endocrinology*, vol. 85, no. 1, pp. 29–36, 2016.

[9] G. Randolph, *Surgery of the Thyroid and Parathyroid Glands*, Saunders, Philadelphia, WB, USA, 2003.

[10] F. Cetani and C. Marcocci, "Parathyroid carcinoma," in *The Parathyroids*, J. P. Bilezikian, Ed., pp. 409–421, Elsevier, Amsterdam, Netherlands, 3rd edition, 2015.

[11] K.-M. Schulte, N. Talat, J. Miell, C. Moniz, P. Sinha, and S. Diaz-Cano, "Lymph node involvement and surgical approach in parathyroid cancer," *World Journal of Surgery*, vol. 34, no. 11, pp. 2611–2620, 2010.

[12] G. L. Clayman, H. E. Gonzalez, A. El-Naggar, and R. Vassilopoulou-Sellin, "Parathyroid carcinoma: evaluation and interdisciplinary management," *Cancer*, vol. 100, no. 5, pp. 900–905, 2004.

[13] T. Obara, T. Okamoto, M. Kanbe, and M. Iihara, "Functioning parathyroid carcinoma: clinicopathologic features and rational treatment," *Seminars in Surgical Oncology*, vol. 13, no. 2, pp. 134–141, 1997.

[14] S. R. Rao, A. R. Shaha, B. Singh, A. Rinaldo, and A. Ferlito, "Management of cancer of the parathyroid," *Acta Oto-Laryngologica*, vol. 122, no. 4, pp. 448–452, 2002.

[15] R. A. DeLellis, P. Mazzaglia, and S. Mangray, "Primary hyperparathyroidism: a current perspective," *Archives of Pathology & amp; Laboratory Medicine*, vol. 132, no. 132, pp. 1251–1262, 2008.

[16] A. G. Wynne, J. V. Heerden, J. A. Carney, and L. A. Fitzpatrick, "Parathyroid carcinoma," *Medicine*, vol. 71, no. 4, pp. 197–205, 1992.

[17] T. Okamoto, M. Iihara, T. Obara, and T. Tsukada, "Parathyroid carcinoma: etiology, diagnosis, and treatment," *World Journal of Surgery*, vol. 33, no. 11, pp. 2343–2354, 2009.

[18] K. Enomoto, S. Uchino, A. Ito et al., "The surgical strategy and the molecular analysis of patients with parathyroid cancer," *World Journal of Surgery*, vol. 34, no. 11, pp. 2604–2610, 2010.

[19] http://www.reteoncologica.it/area-operatori/gruppi-per-patologie/patologie/tumori-della-tiroide-e-delle-ghiandole-endocrine.

[20] K. Duan and Ö Mete, "Parathyroid carcinoma: diagnosis and clinical implications," *Turkish Journal of Pathology*, vol. 31, no. 1, pp. 80–97, 2015.

[21] R. A. Delellis, "Challenging lesions in the differential diagnosis of endocrine tumors: parathryoid carcinoma," *Endocrine Pathology*, vol. 19, no. 4, pp. 221–225, 2008.

[22] J. P. Bilezikian, M. L. Brandi, R. Eastell et al., "Guidelines for the management of asymptomatic primary hyperparathyroidism: summary statement from the Fourth International Workshop," *The Journal of Clinical Endocrinology & Metabolism*, vol. 99, no. 10, pp. 3561–3569, 2014.

[23] J. M. P. Fernandes, C. Paiva, R. Correia et al., "Parathyroid carcinoma: from a case report to a review of the literature," *International Journal of Surgery Case Reports*, vol. 42, pp. 214–217, 2018.

[24] A. A. Khan, D. A Hanley, R Rizzoli et al., "Primary hyperparathyroidism: review and recommendations on evaluation, diagnosis, and management. A Canadian and international consensus," *Osteoporosis International*, vol. 28, no. 28, pp. 1–19, 2017.

[25] J. Cao, C. Chen, Q.-L. Wang, J.-J. Xu, and M.-H. Ge, "Parathyroid carcinoma: a report of six cases with a brief review of the literature," *Oncology Letters*, vol. 10, no. 6, pp. 3363–3368, 2015.

[26] E. A. Asare, C. Sturgeon, D. J. Winchester et al., "Parathyroid carcinoma: an update on treatment outcomes and prognostic factors from the national cancer data base (NCDB)," *Annals of Surgical Oncology*, vol. 22, no. 12, pp. 3990–3995, 2015.

[27] D. Betea, I. Potorac, and A. Beckers, "Parathyroid carcinoma: challenges in diagnosis and treatment," *Annales d'Endocrinologie*, vol. 76, no. 2, pp. 169–177, 2015.

[28] F. Quaglino, V. Marchese, R. Lemini et al., "Parathyroid carcinoma. A single Institution experience and a review of the international literature," *Annali Italiani di Chirurgia*, vol. 89, pp. 295–304, 2018.

[29] L. Cardoso, M. Stevenson, and R. V. Thakker, "Molecular genetics of syndromic and non-syndromic forms of parathyroid carcinoma," *Human Mutation*, vol. 38, no. 12, pp. 1621–1648, 2017.

[30] C. H. Wei and A. Harari, "Parathyroid carcinoma: update and guidelines for management," *Current Treatment Options in Oncology*, vol. 13, no. 1, pp. 11–23, 2012.

Hindawi
International Journal of Endocrinology
Volume 2020, Article ID 2182539, 6 pages
https://doi.org/10.1155/2020/2182539

Research Article

Surgical Approach to Primary Hyperparathyroidism in Patients with Concomitant Thyroid Diseases: A Retrospective Single Center Study

Elena Castellano,[1] **Paolo Benso**,[2] **Roberto Attanasio**,[3] **Alberto Boriano**,[4] **Corrado Lauro**,[2] **Giorgio Borretta**,[1] **and Felice Borghi**[2]

[1]*Department of Endocrinology, Diabetes and Metabolism, Santa Croce and Carle Hospital, Cuneo, Italy*
[2]*Unit of General and Oncological Surgery, Department of Surgery, Santa Croce and Carle Hospital, Cuneo, Italy*
[3]*IRCCS Orthopedic Institute Galeazzi, Endocrinology Service, Milan, Italy*
[4]*Medical Physics Department, Santa Croce and Carle Hospital, Cuneo, Italy*

Correspondence should be addressed to Elena Castellano; castellano.elena@libero.it

Received 30 September 2019; Revised 23 January 2020; Accepted 31 January 2020; Published 22 February 2020

Academic Editor: Małgorzata Kotula-Balak

Background. Primary hyperparathyroidism (PHPT) and thyroid diseases are a frequent concomitant occurrence, but the surgical approach to associated disease is still debated. *Methods*. We retrospectively evaluated a series of PHPT patients focusing on thyroid disease and surgery. *Results*. Among 238 PHPT patients undergoing parathyroidectomy (PTX) between 2002 and 2017, 128 were affected also by a benign thyroid disease, namely, goiter in 118 (76 multinodular (MNG) and 42 uninodular (UNG)), autoimmune thyroiditis in 10, and hyperthyroidism in 21. Surgical approach was unilateral neck exploration (UNE) in 59 patients and bilateral neck exploration (BNE) in 69. The PHPT cure rate was 94%. On comparing patients submitted to PTX only and PTX plus thyroidectomy (TX), in the latter MNG and hyperthyroidism were more frequent, and surgical time and length of stay were longer. No difference in surgical complications was found between patients undergoing UNE and BNE. *Conclusion*. PHPT patients with a concomitant thyroid disease underwent double surgery in almost two-thirds of the cases, mostly by BNE. The main factors driving the decision to perform concomitant PTX and TX were the presence of thyroid nodular disease with the nodule site ipsilateral to the presurgically localized parathyroid adenoma.

1. Introduction

Primary hyperparathyroidism (PHPT) and thyroid diseases are common in the general population (1–3), and a higher probability of identifying thyroid diseases in PHPT patients is probably due to the anatomic proximity of thyroid and parathyroid glands. The reported prevalence of the concomitant occurrence of these two clinical conditions is widely scattered (17–84%) (4–9), and we reported recently that the majority of PHPT patients resident in an endemic goiter area had a thyroid disease (10).

Despite the reported high prevalence of this association, the proper surgical approach when PHPT and thyroid diseases coexist is still a matter of debate. Recently, the American Association of Endocrine Surgeons (AAES) guidelines (11) recommended that thyroidectomy (TX) should be performed concomitantly with parathyroidectomy (PTX) whenever PHPT patients meet evidence-based surgical criteria for isolated thyroid disease.

We evaluated retrospectively a series of patients with PHPT looking for (1) the surgical approach performed in those with associated thyroid diseases and (2) the factors driving the decision to perform both PTX and TX.

2. Methods

2.1. Design. We retrospectively evaluated a surgical monocentric series of 238 patients with PHPT, undergoing PTX

at our hospital between 2002 and 2017, focusing on concomitant thyroid disease, not suspicious for malignancy. In the selected period, the same team was in charge for neck surgery.

The study was conducted in accordance with the Declaration of Helsinki and was approved by the Institutional Review Board and the Ethical Committee of our institution. No informed consent was required for this study because we only retrospectively accessed a de-identified database for analysis purposes. All data were collected as part of routine clinical and psychological procedures.

2.2. Patients. Patients had been referred by general practitioners, primary care clinics, and subspecialty clinics. The diagnosis of PHPT had been established by the presence of hypercalcemia and concomitant inappropriately raised serum parathyroid hormone (PTH) levels on at least two separate occasions (reference range for calcium levels 8.4–10.2 mg/dL, for PTH vide infra). Patients diagnosed with multiple endocrine neoplasm, hyperparathyroidism-jaw tumor syndrome, or familial hypocalciuric hypercalcemia were excluded, as well as those with thyroid nodules cytologically suspicious for malignancy (Tir 4 and Tir 5, according to ATA guidelines—12).

No patient had been treated with drugs known to interfere with thyroid function (interferon, lithium, amiodarone, or immune checkpoint inhibitors).

All patients underwent imaging by neck ultrasonography (US) and ^{99m}Tc-MIBI scintigraphy. Presurgical PHPT localization was considered positive if a single adenoma was disclosed by at least one of the two studies.

The US thyroid pattern was considered abnormal if nodules or features of chronic lymphocytic thyroiditis were found, defined as nodular or autoimmune disease, respectively.

According to history, ongoing therapy, and US results, patients were diagnosed with unilateral or bilateral goiter, hyperthyroidism, or chronic lymphocytic thyroiditis.

Depending on the extent of surgery, patients were grouped as follows: group 1, patients who underwent only PTX; group 2, patients who underwent both PTX and TX. Groups 1 and 2 were compared for demographic characteristics, PHPT biochemical markers, thyroid diseases, surgical approach, and length of hospital stay.

2.3. Methods. Calcium levels were assayed by automated analysis using colorimetric and enzymatic methods, while ionized serum calcium was analyzed by a specific probe after correction for pH.

Serum intact PTH concentrations were measured up to 2012 using a 2-site immunochemiluminometric assay (Immulite 2000; DPC, Los Angeles, CA) with inter- and intra-assay variation coefficients of 6.3 to 8.8% and 4.2 to 5.7%, respectively. Thereafter, serum intact PTH concentrations were measured using a new second-generation immunochemiluminometric assay (COBAS e411; ROCHE Diagnostics, Risch-Rotkreuz, Switzerland) with inter- and intra-assay variation coefficients of 3.1 to 6.5% and 1.4 to 3.2%, respectively. The corresponding normal ranges are 20 to 65 ng/L and 15 to 65 ng/L.

An intraoperative PTH (ioPTH) fall ≥50% at ten minutes vs. baseline was considered adequate for PHPT cure.

After primary surgery, PHPT was considered persistent if hypercalcemia recurred within 6 months or recurrent if hypercalcemia relapsed after at least 6 months of normocalcemia.

2.4. Statistical Analysis. Variables were preliminarily tested for normal distribution with the Shapiro–Wilks W-test, and data were expressed as mean ± SD when normally distributed as median and interquartile range (IQR) when not normally distributed.

Continuous variables with nonnormal and normal distribution were analyzed by Mann–Whitney U test and t-test for unpaired samples, respectively, as appropriate. Differences in categorical variables were analyzed by χ^2 or Fisher's test as appropriate.

Logistic regression analysis was used to evaluate the correlations between the surgical approach and the other variables. Variables that were significant in univariate analysis were entered into multiple regression analysis.

The level of statistical significance was set at $p < 0.05$. The calculations were performed using SPSS (IBM SPSS Statistics, Version 21).

3. Results

Among the 238 PHPT patients undergoing PTX at our hospital in the considered period, 128 (53.8%) fulfilled the inclusion criteria.

Table 1 summarizes the characteristics of the whole series. The presurgical imaging resulted positive for a single adenoma in 101 patients (78.9%). Multinodular goiter (MNG), uninodular goiter (UNG), autoimmune thyroiditis (AIT), and hyperthyroidism were diagnosed in 76 (59.4%), 42 (32.8%), 10 (7.8%), and 21 (16.4%) patients, respectively. All 21 patients with hyperthyroidism had toxic MNG.

When thyroid nodules were ipsilateral to the parathyroid adenoma, PTX + TX was performed in the majority of patients (71%), and in 81% of them the surgical approach was unilateral; on the other hand, when thyroid nodules were contralateral, the combined surgery was performed only for 46.8% of patients, all of them with bilateral surgical approach. The mean diameter of thyroid nodules contralateral to parathyroid adenoma was 20 mm. Local compressive symptoms and hyperthyroidism were the most frequent causes driving concomitant PTX and TX.

Eighty percent of patients bearing bilateral thyroid nodules underwent concomitant PTX and TX, with BNE in the large majority of the cases (90%).

Surgical approach was thus unilateral neck exploration (UNE) in 59 (46.1%) patients and bilateral neck exploration (BNE) in 69 (53.9%). The PHPT cure rate was 94%.

Patients undergoing bilateral surgery had thyroid nodules contralateral to parathyroid adenoma (15/38) or bilateral nodular goiter (18/38) in the large majority of cases (33/38, 87%).

Table 1: Demographic, biochemical, and clinical characteristics of patients with PHPT and concomitant thyroid disease with the comparison between patients undergoing only PTX (group 1) or PTX + TX (group 2).

	Whole series ($n = 128$)	Group 1 ($n = 44$)	Group 2 ($n = 84$)	p^*
Age (years)	64.1 ± 9.8	63.1 ± 9.5	64.6 ± 9.9	0.411
Males	28 (21.9%)	9 (20.5%)	19 (22.6%)	0.955
PHPT clinics:				
Symptomatic	73 (57%)	27 (61.4%)	46 (54.8%)	0.597
Asymptomatic meeting surgical criteria	55 (43%)	17 (38.6%)	38 (45.2%)	
Serum total calcium (mg/dL)	11.1 ± 1.2	11.4 ± 1.6	11 ± 0.9	0.071
PTH (ng/L)	144 [115]	136 [92.5]	144 [118.9]	0.96
Thyroid disease:				
MNG	76 (59.4%)	16 (36.4%)	60 (71.4%)	**<0.0001**
UNG	42 (32.8%)	20 (45.4%)	22 (26.2%)	
AIT without nodules	10 (7.8%)	8 (18.2%)	2 (2.4%)	
Hyperthyroidism	21 (16.4%)	2 (4.5%)	19 (22.6%)	**0.018**
Presurgical localization:				
Positive for a single adenoma	101 (78.9%)	36 (81.8%)	65 (77.4%)	0.722
Negative or suspicious for multiglandular disease	27 (21.1%)	8 (18.2%)	19 (22.6%)	
Surgery:				
UNE	59 (46.1%)	36 (81.8%)	23 (27.4%)	**<0.0001**
BNE	69 (53.9%)	8 (18.2%)	61 (72.6%)	
ioPTH fall	85.9%	84.1%	86.9%	0.867
Persistent PHPT	6 (4.7%)	2 (4.5%)	4 (4.8%)	0.700
Recurrent PHPT	2 (1.6%)	1 (2.3%)	1 (1.2%)	0.778
Postsurgical hypocalcemia:				
Transient	13 (10.2%)	3 (6.8%)	10 (11.9%)	
Persistent	1 (0.8%)	0	1 (1.2%)	
Surgical site infection	3 (2.3%)	1 (2.3%)	2 (2.4%)	0.172°
RLN monolateral palsy:				
Transient	3 (2.3%)	0	3 (3.6%)	
Persistent	1 (0.8%)	0	1 (1.2%)	
Procedure length (minutes)	104 ± 47 [15–290]	79 ± 34 [15–190]	119 ± 48 [35–290]	**<0.0001**
Hospital stay (days)	2.4 ± 1.5 [0–9]	1.6 ± 1 [0–5]	2.8 ± 1.5 [1–9]	**<0.0001**

Abbreviations: AIT = autoimmune thyroiditis; BNE = bilateral neck exploration; MNG = multinodular goiter; ioPTH = intraoperative PTH; RLN = recurrent laryngeal nerve; UNG = uninodular goiter; UNE = unilateral neck exploration. Data are expressed as mean ± SD when normally distributed, median and (interquartile range) when not normally distributed, and as percentage and absolute number when categorical. *The comparison between group A and group B. °Refers to the comparison of the whole incidence of surgical complications.

The comparison between group 1 and group 2 disclosed no differences for age, sex distribution, PHPT characteristics, and presurgical localization rate. In group 2 MNG and hyperthyroidism were significantly more frequent, and surgical time and length of stay were significantly longer ($p < 0.0001$).

In group 2, seven patients (8.3%) had an incidental identification of a thyroid cancer. It was a papillary microcarcinoma in 6 patients (mean diameter 5 mm; range 2–8 mm) and a 24 mm follicular carcinoma, associated to a 2 mm papillary microcarcinoma in the last patient. In none of them there was a preoperative suspicion of cancer.

Table 2 shows the comparison between patients undergoing surgery by UNE or BNE among group 2 patients. No differences were found in the demographic characteristics of patients. The type of thyroid disease significantly differs between the two subgroups, being UNG and AIT more frequent in patients submitted to UNE and MNG more frequent in patients undergoing BNE ($p < 0.0001$). The procedure length and the length of stay were significantly higher in patients submitted to BNE ($p < 0.0001$ and =0.011, respectively), while no difference in the complication rate was found between the two subgroups.

In univariate analysis, double surgery resulted significantly related to the type of thyroid disease, to the presence of hyperthyroidism, and to nodule site (ipsilateral or contralateral to the parathyroid adenoma). As reported in Table 3, in multiple analysis, only the type of thyroid disease and thyroid nodule site maintained statistical significance ($p = 0.05$ and =0.044, respectively).

In univariate analysis, the unilateral approach resulted significantly correlated to the type of thyroid disease, to the presence of hyperthyroidism, and to the positive presurgical PHPT localization. In multiple analysis (Table 4), only the presurgical PHPT localization maintained statistical significance ($p < 0.0001$).

Table 2: Comparison between UNE and BNE in patients of group 2.

	UNE ($n = 23$)	BNE ($n = 61$)	p^*
Age (years)	63.9 ± 10.5	64.9 ± 9.8	0.681
Males	7 (30.4%)	12 (19.7%)	0.448
Thyroid disease:			
MNG	11 (47.8%)	49 (80.3%)	**<0.0001**
UNG	10 (43.5%)	12 (19.7%)	
AIT without nodules	2 (8.7%)	0	
Hyperthyroidism	3 (13%)	16 (26.2%)	0.319
Tir3 at FNAB	2 (8.7%)	5 (8.2%)	0.787
Presurgical localization:			
Positive for a single adenoma	21 (91.3%)	44 (72.1%)	0.114
Negative or suspicious for multiglandular disease	2 (8.7%)	17 (27.9%)	
Partial TX	23 (100%)	27 (44.3%)	**<0.0001**
ioPTH fall >50% at 10 min	22 (95.7%)	51 (83.6%)	0.272
Persistent PHPT	0	4 (6.6%)	—
Recurrent PHPT	0	1 (1.6%)	
Postsurgical hypocalcemia:			
Transient	2 (8.7%)	8 (13.1%)	0.418°
Persistent	0	1 (1.6%)	
Surgical site infection	0	2 (3.3%)	
RLN monolateral palsy:			
Transient	0	3 (4.9%)	
Persistent	0	1 (1.6%)	
Procedure length (minutes)	84 ± 23 [35–150]	130 ± 50 [19–290]	**0.0001**
Hospital stay (days)	2.2 ± 0.7 [1–4]	3.1 ± 1.6 [1–9]	**0.011**

Abbreviations: AIT = autoimmune thyroiditis; BNE = bilateral neck exploration; FNAB = fine needle aspiration biopsy; MNG = multinodular goiter; ioPTH = intraoperative PTH; RLN = recurrent laryngeal nerve; TX = thyroidectomy; UNG = uninodular goiter; UNE = unilateral neck exploration. Data are expressed as mean ± SD when normally distributed, median and interquartile range when not normally distributed, and as percentage and absolute number when categorical. *The comparison between group A and group B. °Refers to the comparison of the whole incidence of surgical complications.

Table 3: Multiple logistic regression analysis for TX.

	p	ODDS	95% CI
Type of thyroid disease MNG UNG AIT	**0.05**	**0.38**	**0.14–1.00**
Hyperthyroidism (yes)	0.418	2.66	0.49–14.42
Thyroid nodule site: Bilateral Ipsilateral Contralateral	**0.044**	**0.49**	**0.25–0.95**

Abbreviations: AIT = autoimmune thyroiditis; MNG = multinodular goiter; TX = thyroidectomy; UNG = uninodular goiter; UNE = unilateral neck exploration.

Table 4: Multiple logistic regression analysis for BNE.

	p	ODDS	95% CI
Type of thyroid disease MNG UNG AIT	0.09	0.38	0.11–1.02
Hyperthyroidism (yes)	0.418	1.66	0.49–5.66
Parathyroid presurgical localization Positive for single adenoma Negative or multiglandular	**0.001**	**0.14**	**0.04–0.45**
Thyroid nodule site Bilateral Ipsilateral Contralateral	0.537	0.84	0.48–1.47

Abbreviations: AIT = autoimmune thyroiditis; BNE = bilateral neck exploration; MNG = multinodular goiter; UNG = uninodular goiter.

4. Discussion

Synchronous thyroid pathology has been reported to occur in 17 to 84% of patients with PHPT [1–5]. More than half of surgically treated PHPT patients of our cohort had a concomitant thyroid disease.

About two-thirds of our PHPT patients with concomitant thyroid disease without any suspicion of malignancy underwent simultaneous thyroid and parathyroid surgery. Patients undergoing combined surgery were submitted to BNE more frequently than patients undergoing PTX alone, which in turn were submitted to unilateral approach in most cases. The combined surgery was associated to the type of thyroid disease and to the contralateral nodule site relative to parathyroid adenoma, while UNE was associated to the positive presurgical localization of parathyroid adenoma.

The combined thyroid and parathyroid surgery had similar cure rate and complication rate despite longer procedure length and hospital stay than PTX alone.

PHPT is very frequently associated with thyroid abnormalities [6–8] and, on the other hand, the reported

prevalence of PHPT in patients bearing any thyroid disease is three times higher than in healthy subjects [7]. In an unselected series in an endemic goiter area, we recently reported that 60% of our PHPT patients had also a thyroid disease, which was unknown prior to PHPT diagnosis in almost one-third of cases [10].

The association between PHPT and thyroid disease still remains to be fully understood. Some authors suggested that it may be coincidental due to close surveillance of the thyroid gland during PTX, while others postulated a goitrogen role of the long-term exposure to elevated calcium levels [9, 11].

Regardless of any causal association, the presence of a thyroid disease plays a relevant role in the clinical management of PHPT patients. Actually, a lower sensitivity and specificity of preoperative parathyroid adenoma localization in patients with coexisting thyroid disease has been extensively reported [5, 9, 12, 13]. In addition, hyperthyroidism could worsen some PHPT features, such as hypercalcemia and osteoporosis [10]. Moreover, the prevalence of thyroid cancer seems to be higher in patients with PHPT, with thyroid malignancy reported in 2 to 12% of PHPT surgical patients [13, 14].

Finally, the surgical approach to PHPT may be changed if thyroid disease is also present [9, 15, 16]. While the simultaneous TX and PTX are mandatory in case of malignancy suspicion, the surgical approach in case of concomitant thyroid disease unsuspected for malignancy is still debated [9, 15, 16]. Italian AME guidelines [17] in 2012 suggested to treat nodular thyroid disease concomitantly to PHPT, in order to avoid repetitive surgery that would be more worrisome owing to postsurgical adhesions. More recently, AAES [18] recommended that TX should be performed concomitantly with PTX whenever PHPT patients meet evidence-based surgical criteria for isolated thyroid disease.

Few surgical series [12, 15, 19] of PHPT patients with concomitant thyroid disease reported an extensive use of simultaneous surgery, with BNE more frequently performed in comparison to patients without thyroid disease. Although the majority of concurrent thyroid disease resulted was benign, a not negligible prevalence of incidentally discovered thyroid malignancy was previously reported. In particular, papillary microcarcinoma was disclosed in 12% of the series of 103 patients reported by Bentrem et al. [12], 17.6% among the 51 patients reported by Kösem et al. [19], 13% among the 85 patients reported by Latina et al. [10], and 32.2% of the 231 patients belonging to a series by Scerrino et al. [15].

In agreement with previous data, in our retrospective study, simultaneous surgery was performed in the majority of cases, mostly with the bilateral approach. This decision has a number of possible explanations. First, some PHPT patients with benign nodular goiter have undergone thyroid surgery for hyperthyroidism or symptoms of tracheal compression. Nodular goiter complications are a common occurrence in endemic goiter areas [20], so that a simultaneous surgery could avoid costs and risks associated with neck reexploration. Finally, this approach can detect unsuspected occult thyroid cancers that are more prevalent in PHPT patients than in general population [13, 14].

In conclusion, this retrospective study showed that PHPT patients with a concomitant thyroid disease underwent simultaneous parathyroid and thyroid excision in almost two-thirds of the cases. In these patients, the BNE is performed more frequently than in patients undergoing PTX alone, with similar cure rate and incidence of permanent surgical complication. The main factors driving the decision to perform associated PTX and TX are thyroid nodular disease and nodule site ipsilateral to presurgically localized parathyroid adenoma.

Abbreviations

AAES: American Association of Endocrine Surgeons
AIT: Autoimmune thyroiditis
ATA: American thyroid association
BNE: Bilateral neck exploration
FNAB: Fine needle aspiration biopsy
ioPTH: Intraoperative PTH
IQR: Interquartile range
MIBI: Methoxyisobutylisonitrile
MNG: Multinodular goiter
PHPT: Primary hyperparathyroidism
PTH: Parathyroid hormone
PTX: Parathyroidectomy
RLN: Recurrent laryngeal nerve
TX: Thyroidectomy
UNE: Unilateral neck exploration
UNG: Uninodular goiter
US: Ultrasonography.

Data Availability

The datasets generated during and/or analyzed during the current study are not publicly available but are available from the corresponding author upon reasonable request.

Conflicts of Interest

The authors declare that they have no conflicts of interest.

References

[1] S. H. Golden, K. A. Robinson, I. Saldanha, B. Anton, and P. W. Ladenson, "Prevalence and incidence of endocrine and metabolic disorders in the United States: a comprehensive review," *The Journal of Clinical Endocrinology & Metabolism*, vol. 94, no. 6, pp. 1853–1878, 2009.

[2] E. Lundgren, J. Rastad, E. Thurfjell, G. Åkerström, and S. Ljunghall, "Population-based screening for primary hyperparathyroidism with serum calcium and parathyroid hormone values in menopausal women," *Surgery*, vol. 121, no. 3, pp. 287–294, 1997.

[3] A. Garmendia Madariaga, S. Santos Palacios, F. Guillén-Grima, and J. C. Galofré, "The incidence and prevalence of thyroid dysfunction in Europe: a meta-analysis," *The Journal of Clinical Endocrinology & Metabolism*, vol. 99, no. 3, pp. 923–931, 2014.

[4] A. Panarese, V. D'Andrea, S. Pontone et al., "Management of concomitant hyperparathyroidism and thyroid diseases in the

elderly patients: a retrospective cohort study," *Aging Clinical and Experimental Research*, vol. 29, no. S1, pp. 29–33, 2017.

[5] O. Heizmann, C. T. Viehl, R. Schmid, J. Müller-Brand, B. Müller, and D. Oertli, "Impact of concomitant thyroid pathology on preoperative workup for primary hyperparathyroidism," *European Journal of Medical Research*, vol. 14, pp. 37–41, 2009.

[6] S. Y. Morita, H. Somervell, C. B. Umbricht, A. P. B. Dackiw, and M. A. Zeiger, "Evaluation for concomitant thyroid nodules and primary hyperparathyroidism in patients undergoing parathyroidectomy or thyroidectomy," *Surgery*, vol. 144, no. 6, pp. 862–867, 2008.

[7] M. Regal, C. Páramo, R. L. Cano et al., "Coexistence of primary hyperparathyroidism and thyroid disease," *Journal of Endocrinological Investigation*, vol. 22, no. 3, pp. 191–197, 1999.

[8] T. Masatsugu, H. Yamashita, S. Noguchi et al., "Significant clinical differences in primary hyperparathyroidism between patients with and those without concomitant thyroid disease," *Surgery Today*, vol. 35, no. 5, pp. 351–356, 2005.

[9] S. Ryan, D. Courtney, and C. Timon, "Co-existent thyroid disease in patients treated for primary hyperparathyroidism: implications for clinical management," *European Archives of Oto-Rhino-Laryngology*, vol. 272, no. 2, pp. 419–423, 2015.

[10] A. Latina, E. Castellano, F. Cesario, A. Boriano, R. Attanasio, and G. Borretta, "Unknown and already known thyroid abnormalities in primary hyperparathyroidism," *Endocrine Practice*, vol. 24, no. 7, pp. 628–633, 2018.

[11] E. O. Onkendi, M. L. Richards, G. B. Thompson, D. R. Farley, P. J. Peller, and C. S. Grant, "Thyroid cancer detection with dual-isotope parathyroid scintigraphy in primary hyperparathyroidism," *Annals of Surgical Oncology*, vol. 19, no. 5, pp. 1446–1452, 2012.

[12] D. J. Bentrem, P. Angelos, M. S. Talamonti, and R. Nayar, "Is preoperative investigation of the thyroid justified in patients undergoing parathyroidectomy for hyperparathyroidism?" *Thyroid*, vol. 12, no. 12, pp. 1109–1112, 2002.

[13] J. N. Attie and R. Vardhan, "Association of hyperparathyroidism with nonmedullary thyroid carcinoma: review of 31 cases," *Head & Neck*, vol. 15, no. 1, pp. 20–23, 1993.

[14] L. A. Burmeister, M. Sandberg, S. E. Carty, and C. G. Watson, "Thyroid carcinoma found at parathyroidectomy," *Cancer*, vol. 79, no. 8, pp. 1611–1616, 1997.

[15] G. Scerrino, G. Melfa, C. Raspanti et al., "The prevalence of post-thyroidectomy chronic asthenia: a prospective cohort study," *Langenbeck's Archives of Surgery*, vol. 402, no. 7, pp. 1095–1102, 2017.

[16] M. Milas, A. Mensah, M. Alghoul et al., "The impact of office neck ultrasonography on reducing unnecessary thyroid surgery in patients undergoing parathyroidectomy," *Thyroid*, vol. 15, no. 9, pp. 1055–1059, 2005.

[17] M. Zini, R. Attanasio, R. Cesareo et al., "AME position statement: primary hyperparathyroidism in clinical practice," *Journal of Endocrinological Investigation*, vol. 35, no. 7 Suppl, pp. 2–21, 2012.

[18] S. M. Wilhelm, T. S. Wang, D. T. Ruan et al., "The American association of endocrine Surgeons guidelines for definitive management of primary hyperparathyroidism," *JAMA Surgery*, vol. 151, no. 10, pp. 959–968, 2016.

[19] M. Kösem, E. Algün, Ç. Kotan, M. Harman, and M. Öztürk, "Coexistent thyroid pathologies and high rate of papillary cancer in patients with primary hyperparathyroidism: controversies about minimal invasive parathyroid surgery," *Acta Chirurgica Belgica*, vol. 104, no. 5, pp. 568–571, 2004.

[20] W. Attaallah, S. Erel, N. Z. Canturk et al., "Is hemithyroidectomy a rational management for benign nodular goitre? A Multicentre Retrospective Single Group Study," *The Netherlands Journal of Medicine*, vol. 73, no. 1, pp. 17–22, 2015.

Hindawi
International Journal of Endocrinology
Volume 2020, Article ID 6302861, 7 pages
https://doi.org/10.1155/2020/6302861

Research Article

Parathormone Levels in a Middle-Eastern Healthy Population Using 2nd and 3rd Generation PTH Assays

Marie-Hélène Gannagé-Yared,[1] **Marie-Noëlle Kallas-Chémaly**,[1] **and Ghassan Sleilaty**[2,3]

[1]*Endocrinology Department, Faculty of Medicine, Saint Joseph University, Beirut, Lebanon*
[2]*Department of Biostatistics, Faculty of Medicine, Saint-Joseph University, Beirut, Lebanon*
[3]*Clinical Research Center, Faculty of Medicine, Saint-Joseph University, Beirut, Lebanon*

Correspondence should be addressed to Marie-Hélène Gannagé-Yared; mariehelene.yared@usj.edu.lb

Received 9 October 2019; Revised 15 December 2019; Accepted 23 January 2020; Published 21 February 2020

Academic Editor: Giorgio Borretta

Background. The purpose of the current study is to determine PTH reference values in vitamin-D-replete Lebanese adults using 2nd and 3rd generation PTH assays and to look at the factors that affect PTH variations. *Methods*. Fasting PTH was measured using 2nd and 3rd generation Diasorin PTH assays in 339 vitamin-D-replete healthy subjects aged 18 to 63 years (230 men and 109 women) who have normal calcium levels and an eGFR ≥60 ml/mn. 25-OH vitamin D (25(OH)D) was measured using the Diasorin assay. *Results*. For the 2nd PTH generation, median (IQR) levels were 48.9 (34.9–66.0) pg/ml, and its 2.5th–97.5th percentile values were 19.7–110.5 pg/ml for 25(OH)D values between 20 and 30 ng/ml, and 19.7–110.7 pg/ml for 25(OH)D values ≥30 ng/ml. For the 3rd PTH generation, the median (IQR) values were 23.9 (17.7–30.5) pg/ml, and its 2.5th–97.5th percentile values were, respectively, 9.2 and 50.2 pg/ml for 25(OH) D values between 20 and 30 ng/ml, and 8.4 and 45.4 pg/ml for 25(OH)D values ≥30 ng/ml. The median (IQR) serum 25(OH)D levels were 27.5 (23.8–32.7) ng/ml. 2nd and 3rd generation PTH values are strongly correlated ($r = 0.96$, $p < 0.0001$), but poorly concordant (Lin's concordance coefficient 0.365, 95% CI: 0.328–0.401) with observations beyond the 95% Bland–Altman limits of agreement. 2nd and 3rd generation PTH levels did not differ according to gender and were significantly correlated with age but not with 25(OH)D and serum calcium levels. *Conclusion*. Lebanese adult healthy subjects have higher 2nd and 3rd generation PTH levels compared with the reference range provided by the manufacturer. The reference range was not influenced by changing the 25(OH)D cutoff. The clinical significance of the higher PTH levels in our population should be investigated.

1. Introduction

In clinical practice, assessing parathormone (PTH) concentration is important in exploring calcium/phosphorus metabolism disorders and in monitoring patients suffering from chronic kidney disease. Unfortunately, this task is complex despite the advent of automated laboratory assays. In fact, there are considerable variations in PTH values obtained from different assays, even when provided by the same manufacturer [1, 2]. This variability is mainly related to the assay measurement of different PTH fragments. Older PTH assays, called second (2nd) generation assays or "intact" PTH, are known to measure not only the 84 amino acid molecules but also to cross-react with a truncated PTH fragment called the 7–84 PTH, whereas the more recently introduced assays, named the third (3rd) generation assays, do not measure this truncated fragment, but may cross-react with another fragment called amino-PTH [3]. This difference explains the higher PTH values obtained with 2nd generation assays compared with the 3rd generation ones in healthy subjects [4, 5] as well as in subjects with chronic renal failure [4, 6, 7].

Establishing a normal reference range for PTH is usually based on the values measured in 95% of healthy individuals after ruling out potential confounding factors since the PTH level is affected by multiple factors, such as vitamin D status, age, and renal function [1, 8–10]. Therefore, vitamin D deficiency as well as renal failure, both conditions leading to

secondary hyperparathyroidism, should be ruled out or taken into consideration when establishing a reference range of PTH [11]. Other interfering factors such as calcium/phosphorus disorders should be also excluded [12]. Reference values for PTH are available in European [13, 14], United States [15], and Chinese populations [16]. However, normative PTH values are lacking in the Middle-East, more particularly in Lebanon, a part of the world known for its high prevalence of vitamin D deficiency [17, 18]. In addition, reference values were mainly established using either 2nd or 3rd generation PTH assays. Few studies compared both assays in healthy adults [4, 5, 19] and included only a small number of subjects [4, 19]. It is thus unclear if there is a difference in normative values between both assays. Moreover, the concordance between both assays has only been studied in one study with a good concordance in healthy patients [4].

The purpose of the current study is first to determine PTH reference values in Lebanese adults who are vitamin-D-replete and have a normal renal function using both 2nd and 3rd generation PTH assays; the second is to identify factors that may affect PTH variations.

2. Materials and Methods

2.1. Patients. The study included a total of 339 subjects (230 women and 109 men) aged 18 to 63 years, who presented at the Laboratory of Hôtel-Dieu de France Hospital (one of the biggest university hospitals in the Beirut area) for a routine biochemistry evaluation including calcium, creatinine, and 25(hydroxyvitamin) D (25(OH)D) measurements. Inclusion criteria to measure PTH in these subjects were normal serum calcium (values between 2.10 and 2.56 mmol/L), estimated glomerular filtration rate (eGFR) ≥60 mL/min/1.73 m^2, and 25(OH)D levels ≥20 ng/ml. The 20 ng/ml cutoff value supported by the Institute of Medicine (IOM) report was used to define optimal vitamin D status [20].

2.2. Biochemical Measurements. Morning fasting blood specimens were collected in dry tubes, then centrifuged within 30 min after venipuncture, and analyzed the day of sampling for calcium, creatinine, and 25(OH)D measurements. Part of the serum was immediately frozen and stored at −20°C for later PTH measurements. Only samples with a 25(OH)D ≥20 ng/ml were subsequently analyzed within one month for both 2nd and 3rd PTH measurements. Measurements of total calcium and creatinine levels were performed using a Vitros 5.1 FS automate (Ortho-Clinical Diagnostics, Inc. Raritan, New Jersey). The eGFR was assessed using the Chronic Kidney Disease Epidemiology Collaboration (CKD-EPI) equation [21].

2.3. 25(OH)D and PTH Assays. PTH and 25(OH)D measurements were done in batches on the LIAISON XL (DiaSorin, Stillwater, MN, USA). Serum 25(OH)D was measured using a direct competitive chemiluminescence immunoassay (CLIA). The observed reference range is 9.3–47.9 ng/ml. The lowest reported value is 4 ng/mL, and the interassay coefficient of variation (CV) <20%. The DiaSorin Liaison PTH 2nd and 3rd generation assays were used to measure PTH values. The PTH 2nd generation assay is a modified 2-step, 2-site sandwich assay using 2 polyclonal antibodies to detect intact PTH, and the expected range provided by the kit comprised between 14.5 and 87.1 pg/ml corresponding to the 2.5th and the 97.5th percentiles. The DiaSorin Liaison PTH 3rd generation or 1–84 PTH assay is also a 2-step, 2-site sandwich assay that uses a first antibody that is highly specific for the N terminus of 1–84 PTH to ensure no cross reactivity with fragments such as 7–84 PTH, while the second polyclonal antibody is targeted against the C-terminal region of the 1–84 molecule. The expected reference range provided by the kit comprises between 6.5 and 36.8 pg/ml. Interassay CV was less than 15% for both PTH assays.

2.4. Statistical Analysis. The distribution of 2nd and 3rd generation PTH values was checked using Kolmogorov–Smirnov (KS) and Shapiro–Wilk (SW) tests, with additional visual inspection of quartile-quartile (Q-Q) plots. Logarithmic transformation (natural logarithm) was applied to 2nd and 3rd generation PTH values (labeled Ln (PTH 2G) and Ln (PTH 3G), respectively).

The native variables with skewed distribution were expressed as median with its interquartile range (quartile 1–quartile 3) (Table 1) and percentiles 2.5% and 97.5% (Table 2). For the transformed variables satisfying normality assumptions, the mean and the standard deviation were calculated.

Correlation between Ln (PTH 2G) and Ln (PTH 3G) was estimated using Pearson correlation coefficient, and its 95% confidence interval was calculated by bootstrapping performed on 1000 samples. R^2 was also calculated.

Agreement between Ln (PTH 2G) and Ln (PTH 3G) was studied using Bland–Altman method, and Lin's concordance correlation coefficient was calculated using a macro developed by M. Garcia-Granero (http://gjyp.nl/marta/Lin.sps), providing an asymptotic 95% confidence interval.

The distributions of 2nd and 3rd generation PTH values were compared for 25(OH)D values between 20 and 30 ng/ml and values ≥30 ng/ml using Mann–Whitney U test. Percentiles 2.5% and 97.5% of PTH 2G and PTH 3G of the current study were further compared with expected values provided with the kits by the manufacturers, respectively, using 95% bias corrected accelerated (BCa) confidence intervals built by bootstrapping on 1000 samples. Correlation between 2nd and 3rd generation PTH values and 25(OH)D, serum calcium levels, and CKD EPI eGFR values relied on Spearman's correlation coefficient and its BCa 95% confidence interval. Kappa statistic for agreement between nominal variables was also calculated.

The statistical analysis was performed using IBM SPSS (IBM Corp.; SPSS Statistics for Windows v22.0, Armonk, NY, USA).

2.5. Ethical Issues. The study was approved by the Ethics Committee of our university hospital (CEHDF 1247). The

Table 1: Baseline clinical and biological characteristics of the overall sample, men, and women.

	Overall sample $N = 341$	Men $N = 110$	Women $N = 231$	Test	p value
Age (years)	43.6 ± 11.8	45.7 12.2	42.5 ± 11.5	T	0.021
Creatinine (μmol/L)	64.3 ± 13.1	76.2 ± 12.6	58.6 ± 9.0	T	<0.001
eGFR (ml/mn)	105.4 ± 13.7	102.5 ± 13.9	106.7 ± 13.4	T	0.008
Calcium (mmol/L)	2.40 ± 0.08	2.42 ± 0.07	2.40 ± 0.08	T	0.047
PTH 2nd G (pg/mL)*	48.9 [34.9–66.0]	46.5 [37.8–66]	51.2 [33.5–68.0]	U	0.788
PTH 3rd G (pg/mL)*	23.9 [17.6–30.5]	23.1 [18.6–30.6]	24.5 [17.2–30.4]	U	0.798
25(OH) D (ng/mL)*	27.5 [23.9–32.6]	27.2 [24–32.6]	27.6 [23.8–32.8]	U	0.840

Data are expressed as mean ± SD or median and its interquartile range (Q1–Q3) PTH and 25(OH)D. *denotes variables with a significant departure of normality as detected by Kolmogorov–Smirnov and Shapiro–Wilk test and inspected graphically by quartile-quartile plots. T test: independent samples T test; U test: Mann–Whitney U test.

Table 2: Distributions of 2nd generation PTH and 3rd generation PTH according to dichotomized 25-OH vitamin D values (between 20 and 30 ng/ml and ≥30 ng/ml, respectively).

	2nd generation PTH (pg/mL)		3rd generation PTH (pg/mL)	
	20 < 25(OH)D < 30 (ng/mL)	25(OH)D ≥ 30 (ng/mL)	20 < 25(OH)D < 30 (ng/mL)	25(OH)D ≥ 30 (ng/mL)
Percentiles				
2.5	19.7	19.7	9.1	8.4
5	23.2	24.9	9.9	12.6
10	28.0	28.2	13.2	13.4
25	35.5	33.7	17.6	17.7
50	50.7	48.4	24.0	23.5
75	66.0	67.5	30.5	30.5
90	88.1	84.8	38.3	37.0
95	103.0	92.3	44.0	41.7
97.5	110.5	110.7	50.2	45.4
p value (U test)	0.696		0.917	

U test: Mann–Whitney U test.

authors have complied with the World Medical Association Declaration of Helsinki regarding ethical conduct of research involving human subjects.

3. Results

The baseline characteristics of the sample are shown in Table 1. Female subjects were slightly younger than males (42.5 ± 11.5 vs. 45.7 ± 12.2 years, $p = 0.021$), with a lower serum creatinine (58.6 ± 9.0 μmol/L vs. 76.2 ± 12.6 μmol/L, $p < 0.001$) and marginally higher eGFR (106.7 ± 13.4 vs. 102.5 ± 13.9 mL/min/1.73 m^2, $p = 0.008$) that disappeared after adjusting for age ($p = 0.135$). In the overall sample, the mean serum calcium level was 2.40 ± 0.08 mmol/L.

3.1. 25(OH)D and PTH Measurements and Reference Range of Serum PTH Concentrations. The median serum 25(OH)D value was 27.5 (23.8–32.7) ng/ml with no significant difference according to gender ($p = 0.840$). 64.6% of the subjects had 25(OH)D values between 20 and 30 ng/ml, and 35.6% had 25(OH)D values ≥30 ng/ml.

2nd and 3rd generation PTH showed a significant departure from normality and a right-skewed distributions (Figure 1). Therefore, their natural logarithm transforms (Ln (PTH 2G) and Ln (PTH 3G)), which satisfied normality assumptions, were used in subsequent analysis (Figure 2).

The medians of 2nd and 3rd generation PTH assays were 48.9 (34.9–66.0) pg/ml and 23.9 (17.7–30.5) pg/ml, respectively (Table 1).

The percentiles 2.5% and 97.5% for 2nd and 3rd generation PTH were (19.7–110.5) pg/ml and (9.2–46.6) pg/ml, respectively (Table 2). The distributions of 2nd and 3rd generation PTH according to dichotomized 25(OH)D values (between 20 and 30 ng/ml and ≥30 ng/ml) showed no statistical difference between both groups ($p = 0.696$ and $p = 0.917$, respectively) (Table 2). When compared to the reference 97.5% percentile values provided by the manufacturer, respectively, 10.0% and 11.2% of the subjects had their 2nd and 3rd generation PTH values beyond the reference percentile (respectively, 95% CI: 7.4%–13.0% and 8.1%–14.4%), both comparable but significantly different from the threshold specified by the manufacturer. Out of the 34 subjects with 2nd generation PTH above the reference 97.5% percentile, 4 (11.8%) had normal 3rd generation PTH values. Conversely, out of the 38 subjects with 3rd generation PTH above the reference 97.5% percentile, 8 (21.1%) had normal 2nd generation PTH values (Kappa measure of agreement = 0.814 ± 0.052), corroborating the Bland–Altman method findings. None of the subjects had both 2nd and 3rd generation PTH values below the 2.5% percentile reference values.

While the Pearson correlation coefficient between Ln (PTH 2G) and Ln (PTH 3G) was high, reaching 0.957 (95% CI: 0.945–0.968, $p < 0.0001$) as shown in Figure 3, the

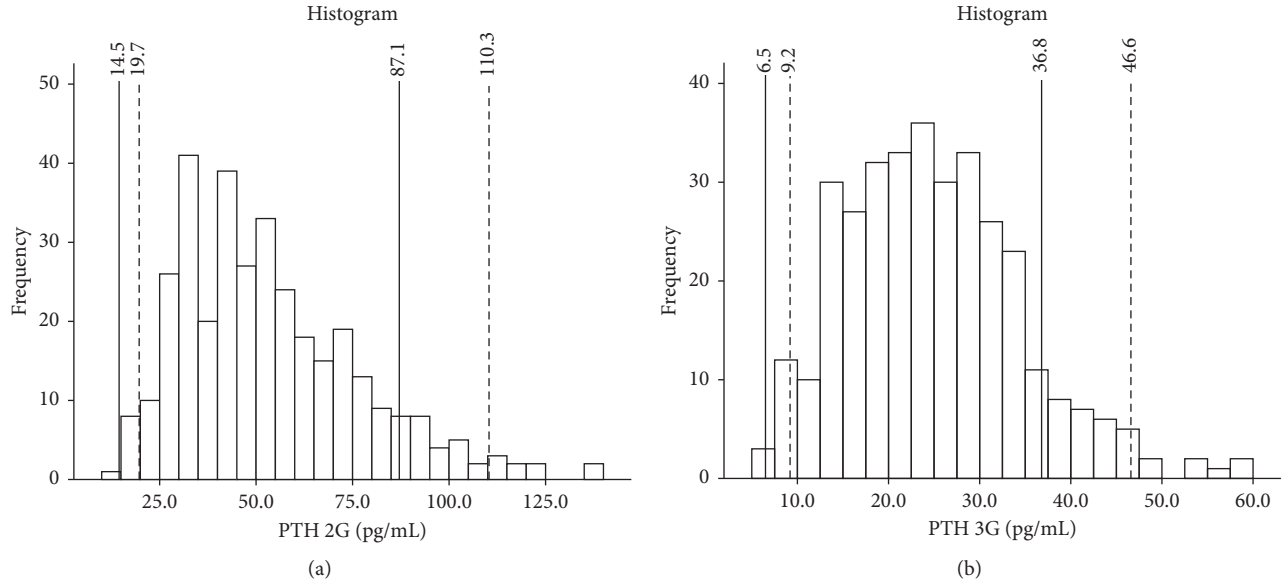

Figure 1: Histograms showing the distribution of 2nd generation PTH values (a) and 3rd generation PTH values (b). Uninterrupted vertical lines represent percentiles 2.5% and 97.5% as provided by the manufacturer. Dashed vertical lines represent actual percentiles 2.5% and 97.5% from the current series.

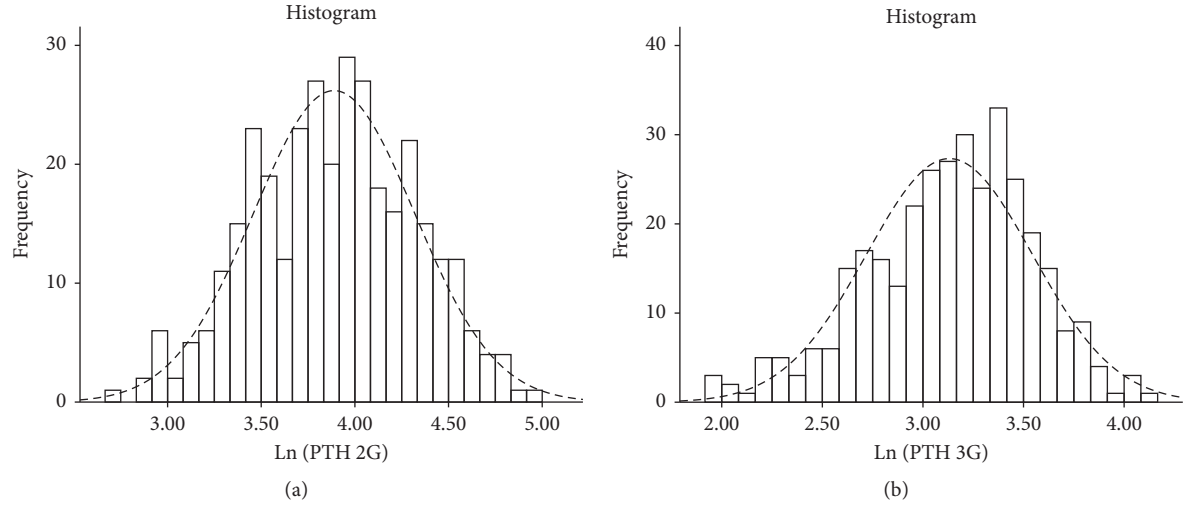

Figure 2: Histograms showing the distribution of log-transformed values of 2nd generation PTH values (a) and 3rd generation PTH values (b). Dashed lines represent a superimposed normal distribution.

agreement between Ln (PTH 2G) and Ln (PTH 3G) was low since Lin's concordance correlation coefficient was only 0.365 (95% CI: 0.328–0.401). The Bland–Altman graphical analysis is consistent with these findings since a significant number of pairs of observations are beyond 95% limits of agreement (Figure 4), with a mean bias of 0.758 on the logarithmic scale (2.13 pg/ml on natural scale).

3.2. Relationship of Serum PTH Level with Gender and Age. No significant differences in 2nd and 3rd generation PTH levels were observed according to gender ($p = 0.788$ and $p = 0.798$, respectively, Table 1). There was a significant correlation between 2nd generation PTH levels and age (Pearson correlation coefficient for age and Ln (PTH 2G) = 0.270 (95% CI: 0.170–0.370, $p < 0.001$)), as well as between 3rd generation PTH levels and age (Pearson correlation coefficient for age and Ln (PTH 3G) = 0.267 (95% CI: 0.161–0.373, $p < 0.001$)).

3.3. Relationship of Serum PTH Level with 25(OH)D and Other Biological Parameters. There was no significant correlation between 2nd generation PTH levels and 25(OH)D (Spearman's correlation coefficient = −0.030, 95% CI: −0.137–0.073, $p = 0.584$) nor between 3rd generation PTH levels and 25(OH)D (Spearman's correlation coefficient −0.002, 95% CI: −0.108–0.094, $p = 0.968$).

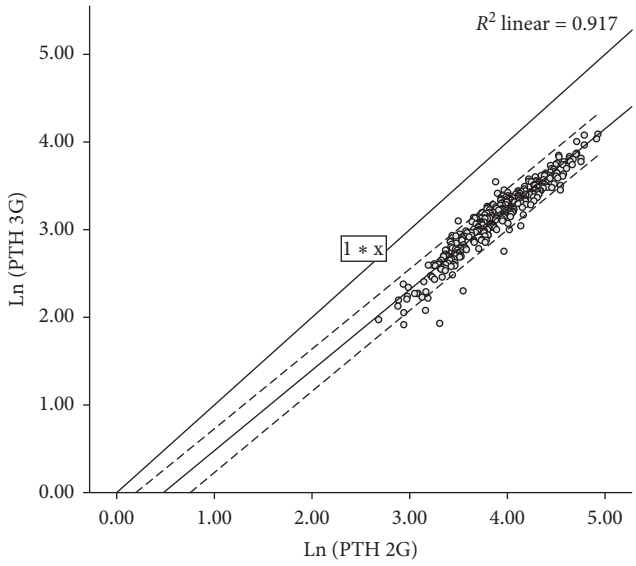

Figure 3: Scatterplot showing the correlation between log(2nd generation PTH) (Ln (PTH 2G)) values and log(3rd generation PTH) (Ln (PTH 3G)) values. The dashed lines represent 95% confidence limits for correlation. The $(1 * x)$ line represents the line of perfect concordance (that is, $y = x$, where Lin's coefficient equals 1).

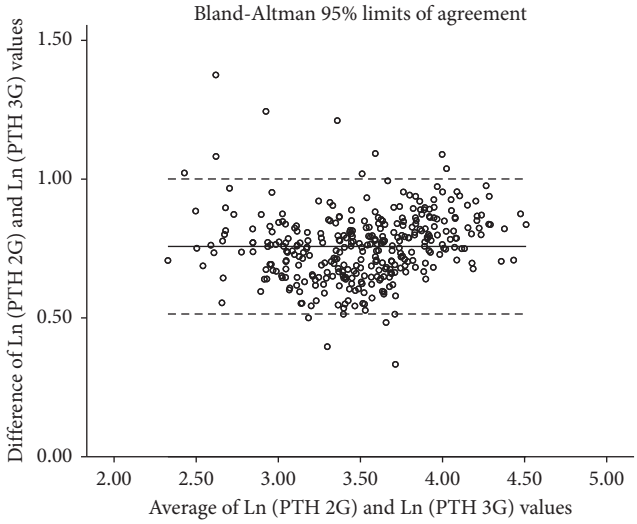

Figure 4: Bland–Altman plot showing the agreement between log(2nd generation PTH) (Ln (PTH 2G)) values and log(3rd generation PTH) (Ln (PTH 3G)) values. Central horizontal line represents the mean bias. The dashed horizontal lines represent 95% limits of agreement.

Likewise, there was no significant correlation between 2nd generation PTH levels and serum calcium levels (Spearman's correlation coefficient = −0.087, 95% CI: −0.192–0.024, $p = 0.109$), nor between 3rd generation PTH levels and serum calcium levels (Spearman's correlation coefficient = −0.094, 95% CI: −0.199–0.019, $p = 0.085$). There was a weak but statistically significant inverse correlation between CKD-EPI eGFR levels and both 2nd and 3rd generation PTH levels (Spearman's correlation coefficients were −0.107, 95% CI: −0.207–0.001, $p = 0.049$ and −0.111, 95% CI: −0.205–0.002, $p = 0.042$, respectively).

4. Discussion

In this study, we established the reference ranges for PTH in 339 Lebanese subjects using the Diasorin 2nd and 3rd generation PTH assays. These reference ranges were established in vitamin-D-replete subjects (25(OH)D ≥20 ng/ml) after excluding subjects with abnormal calcium levels and low eGFR. We found that the 97.5% percentiles for 2nd and 3rd generation PTH are, respectively, 110.5 and 46.6 pg/ml, that is, 26.8% higher than the upper limit of normal (ULN) reference values of 87.1 and 36.8 pg/ml provided by the manufacturer.

Different authors evaluated the reference values for PTH in vitamin-D-replete subjects. As an example, using the Cobas/Elecsys Roche 2nd generation PTH kit, Cavalier et al. [22] found in 240 healthy Belgian subjects a ULN PTH value of 50 pg/ml which is lower than the 65 pg/ml value provided by the manufacturer. Similarly, using the same assay, Touvier et al. [10] found that the plasma PTH ULN is of 45.3 pg/ml in 1824 French adults recruited from the SUVIMAX study. In contrast, two other studies found higher ULN reference values with the same assay. The first one [8] was performed on a Danish population composed of 2316 women and reported a ULN of 67 pg/ml, while the second one [16] was performed on 1436 healthy Chinese subjects, and the ULN reference value was 70 pg/ml. Moreover, using the 3rd PTH Diasorin assay, Souberbielle [13] found in 898 healthy French adults that the ULN value was 28.9 pg/ml, a value that is also lower than the value provided by the manufacturer. Finally, in a United States (US) study [15], the authors compared the performance characteristics of six 2nd PTH assays and found that the ULN values of their population are comparable or higher than the one established by the manufacturers. The differences between the French and Belgian studies [10, 13, 22] on one side and the other studies on the other are unclear. Since age is a significant determinant of PTH, that difference could be explained by the wider age range of the Danish study [8] (which includes women aged up to 84) compared with the French studies [10, 13] in which none [10] or very few [13] of the included subjects were older than 65. Other factors such as a later daytime and a nonfasting blood collection could also contribute to the higher PTH levels in the Danish study. Finally, ethnic differences could explain the higher PTH values observed in the Chinese study [16] as well as in the present study. Consequently, PTH ULN reference values seems to differ between different countries, with the lowest reference values being observed in Belgium and France. In our opinion, the higher ULN reference values observed in our sample as compared with western countries might be related to the higher prevalence of vitamin D deficiency [17, 18]. In fact, it is possible that in some patients, a persistent vitamin D deficiency and long-lasting secondary hyperparathyroidism induces an autonomous secretion of PTH (i.e., tertiary hyperparathyroidism) leading to parathyroid adenoma or hyperplasia [23]. The mechanism behind this finding could be, as suggested by Souberbielle [23], the desensitization of parathyroid vitamin D receptor leading to a decreased expression of the calcium sensor

receptor and therefore to a shift in the calcium set-point. The reason why some but not others may develop this secondary parathyroid growth is unclear.

When comparing the 2 different PTH generation assays in our sample, a strong positive correlation was noted, but the agreement between them was low according to Lin's concordance correlation coefficient, thus suggesting that the assays are not interchangeable. Few studies compared the two PTH generations in the same sample: in French healthy subjects [4] PTH concentration did not differ according to the generation of the used kits, except for an overestimation with the 2nd generation assays for values beyond 200 pg/ml. In another study [5], there was poor concordance between the methods; moreover, this worsened in the higher range of measurements.

Because PTH may be increased in patients with vitamin D deficiency and decreased in vitamin-D-replete subjects, exclusion of patients with vitamin D insufficiency from the reference population for PTH values is mandatory. Since the 25(OH)D cutoff that should be used (20 versus 30 ng/ml) is not clearly established, we compared the reference values based on both 25(OH)D cutoffs. We found that the PTH ULN did not differ no matter they used cutoff, corroborating the US study by La'ulu [15] in which the Diasorin assay was also used. The fact that no significant inverse relationship was found between 25(OH)D and PTH might be due to a vitamin-D-replete status in our population and suggests that a cutoff of 20 ng/ml might be enough to decrease PTH levels until it is stabilized. This does not exclude the possibility that higher 25(OH)D levels are requested to ensure this decrease.

We finally searched for a possible relationship between PTH and both age and gender. Similarly to other studies [8], we found a positive relationship between age and PTH without any difference according to gender. Other studies found an increase in PTH values with age in both Turkish [24] and US populations [25]. In addition, in Turkish females, PTH values were higher than those in males [24] while other studies, similarly to ours, did not show this gender difference [10].

The reason why PTH is higher in our population compared to western population is unclear. As explained above, and since the Lebanese population is at a high risk for vitamin D deficiency [17, 18], prolonged secondary hyperparathyroidism may lead to higher PTH values in our population even after vitamin D repletion. As a result, adopting different reference range values in our population may modify our therapeutic decisions. The obvious consequence of this finding is that, in clinical practice, much less patients will be detected as having normocalcemic primary hyperparathyroidism (PHPTH). Another possibility could be the presence of patients with normocalcemic PHPTH amongst our study population. Here, the only way to rule out early PHPTH would be the follow-up of our subjects in time. Further follow-up of our study population might therefore be necessary to give a clearer answer.

One main limitation of this study is the lack of anthropometric and social information (body mass index (BMI) and income level). This limits the interpretation of the results since obesity is known to increase PTH levels [10, 26]. In addition, dietary vitamin D and calcium intakes and the use of vitamin D supplements or of medications that can effect vitamin D metabolism were not recorded. However, the abovementioned factors seems to have little impact on the interpretation of the results since in a large cross-sectional Danish study, only 16% of the variability of PTH is explained by 25(OH)D, age, BMI, and daily calcium intake [8]. Finally, and because our study includes only subjects with an eGFR ≥60 ml/mn, no further ascertainment can be made regarding reference PTH values in patients with CKD.

5. Conclusion

A reference value for PTH was established for the first time in a sample of the Lebanese population using two different generation of PTH assays after excluding vitamin-D-deficient subjects. With both methods, the Lebanese subjects had higher PTH compared with the reference range provided by the manufacturer. We also confirmed that using a 25(OH)D cutoff of 20 ng/ml instead of 30 ng/ml did not change the reference range. Our study highlights the fact that, regardless of the assay used, each laboratory should establish its own normative PTH values in collaboration with clinicians in order to avoid under- or overestimation of PHPTH diagnosis. Since several studies have indicated that PTH levels in the upper limit of the normative reference level have a harmful effect on cardiovascular risk [27] and mortality [28], the clinical significance of the higher PTH levels in our population should be further investigated.

Abbreviations

PTH: Parathormone
25(OH)D: 25(hydroxyvitamin) D
BMI: Body mass index.

Data Availability

The data used to support the findings of this study are available from the corresponding author upon request.

Conflicts of Interest

The authors declare that they have no conflicts of interest.

Acknowledgments

The authors thank Mrs Rima Chedid for her careful reading of the article. This work was supported by the Conseil de recherche de l'Université Saint-Joseph, Beirut.

References

[1] J.-C. Souberbielle, F. Brazier, M.-L. Piketty, C. Cormier, S. Minisola, and E. Cavalier, "How the reference values for serum parathyroid hormone concentration are (or should be) established?" *Journal of Endocrinological Investigation*, vol. 40, no. 3, pp. 241–256, 2017.

[2] E. Cavalier, M. Plebani, P. Delanaye, and J. C. Souberbielle, "Considerations in parathyroid hormone testing," *Clinical*

Chemistry and Laboratory Medicine (CCLM), vol. 53, no. 12, p. 1913, 2015.

[3] P. D'Amour, J. H. Brossard, L. Rousseau, L. Roy, P. Gao, and T. Cantor, "Amino-terminal form of parathyroid hormone (PTH) with immunologic similarities to hPTH(1–84) is overproduced in primary and secondary hyperparathyroidism," *Clinical Chemistry*, vol. 49, no. 12, pp. 2037–2044, 2003.

[4] A. M. Dupuy, A. S. Bargnoux, M. Morena et al., "Moving from the second to the third generation Roche PTH assays: what are the consequences for clinical practice?" *Clinical Chemistry and Laboratory Medicine (CCLM)*, vol. 57, no. 2, pp. 244–249, 2018.

[5] T. C. P. Bonanséa, M. N. Ohe, C. Brandão et al., "Experience with a third-generation parathyroid hormone assay (BIO-PTH) in the diagnosis of primary hyperparathyroidism in a Brazilian population," *Archives of Endocrinology and Metabolism*, vol. 60, no. 5, pp. 420–425, 2016.

[6] M. Hecking, A. Kainz, B. Bielesz et al., "Clinical evaluation of two novel biointact PTH(1–84) assays in hemodialysis patients," *Clinical Biochemistry*, vol. 45, no. 18, pp. 1645–1651, 2012.

[7] M.-H. Gannagé-Yared, C. Farès, T. Ibrahim, Z. A. Rahal, M. Elias, and D. Chelala, "Comparison between a second and a third generation parathyroid hormone assay in hemodialysis patients," *Metabolism*, vol. 62, no. 10, pp. 1416–1422, 2013.

[8] L. Rejnmark, P. Vestergaard, L. Heickendorff, and L. Mosekilde, "Determinants of plasma PTH and their implication for defining a reference interval," *Clinical Endocrinology*, vol. 74, no. 1, pp. 37–43, 2011.

[9] A. Arabi, R. Baddoura, R. El-Rassi, and G. El-Hajj Fuleihan, "Age but not gender modulates the relationship between PTH and vitamin D," *Bone*, vol. 47, no. 2, pp. 408–412, 2010.

[10] M. Touvier, M. Deschasaux, M. Montourcy et al., "Interpretation of plasma PTH concentrations according to 25OHD status, gender, age, weight status, and calcium intake: importance of the reference values," *The Journal of Clinical Endocrinology & Metabolism*, vol. 99, no. 4, pp. 1196–1203, 2014.

[11] N.-S. Joo, B. Dawson-Hughes, Y.-S. Kim, K. Oh, and K.-J. Yeum, "Impact of calcium and vitamin D insufficiencies on serum parathyroid hormone and bone mineral density: analysis of the fourth and fifth Korea National Health and Nutrition Examination Survey (KNHANES IV-3, 2009 and KNHANES V-1, 2010)," *Journal of Bone and Mineral Research*, vol. 28, no. 4, pp. 764–770, 2013.

[12] R. Eastell, M. L. Brandi, A. G. Costa, P. D'Amour, D. M. Shoback, and R. V. Thakker, "Diagnosis of asymptomatic primary hyperparathyroidism: proceedings of the fourth international workshop," *The Journal of Clinical Endocrinology & Metabolism*, vol. 99, no. 10, pp. 3570–3579, 2014.

[13] J.-C. Souberbielle, C. Massart, S. Brailly-Tabard et al., "Serum PTH reference values established by an automated third-generation assay in vitamin D-replete subjects with normal renal function: consequences of diagnosing primary hyperparathyroidism and the classification of dialysis patients," *European Journal of Endocrinology*, vol. 174, no. 3, pp. 315–323, 2016.

[14] E. Cavalier, M. Salsé, A.-M. Dupuy et al., "Establishment of reference values in a healthy population and interpretation of serum PTH concentrations in hemodialyzed patients according to the KDIGO Guidelines using the Lumipulse G whole PTH (3rd generation) assay," *Clinical Biochemistry*, vol. 54, pp. 119–122, 2018.

[15] S. L. l La'ulu and W. L. Roberts, "Performance characteristics of six intact parathyroid hormone assays," *American Journal of Clinical Pathology*, vol. 134, no. 6, pp. 930–938, 2010.

[16] M. Li, F. Lv, Z. Zhang et al., "Establishment of a normal reference value of parathyroid hormone in a large healthy Chinese population and evaluation of its relation to bone turnover and bone mineral density," *Osteoporosis International*, vol. 27, no. 5, pp. 1907–1916, 2016.

[17] M. Chakhtoura, M. Rahme, N. Chamoun, and G. El-Hajj Fuleihan, "Vitamin D in the Middle East and North Africa," *Bone Reports*, vol. 8, pp. 135–146, 2018.

[18] M.-H. Gannagé-Yared, R. Chemali, N. Yaacoub, and G. Halaby, "Hypovitaminosis D in a sunny country: relation to lifestyle and bone markers," *Journal of Bone and Mineral Research*, vol. 15, no. 9, pp. 1856–1862, 2000.

[19] E. Cavalier, A. F. Daly, D. Betea et al., "The ratio of parathyroid hormone as measured by third- and second-generation assays as a marker for parathyroid carcinoma," *The Journal of Clinical Endocrinology & Metabolism*, vol. 95, no. 8, pp. 3745–3749, 2010.

[20] A. C. Ross, J. E. Manson, S. A. Abrams et al., "The 2011 report on dietary reference intakes for calcium and vitamin D from the Institute of medicine: what clinicians need to know," *The Journal of Clinical Endocrinology & Metabolism*, vol. 96, no. 1, pp. 53–58, 2011.

[21] A. S. Levey, L. A. Stevens, C. H. Schmid et al., "A New equation to estimate glomerular filtration rate," *Annals of Internal Medicine*, vol. 150, no. 9, pp. 604–612, 2009.

[22] E. Cavalier, P. Delanaye, L. Vranken et al., "Interpretation of serum PTH concentrations with different kits in dialysis patients according to the KDIGO guidelines: importance of the reference (normal) values," *Nephrology Dialysis Transplantation*, vol. 27, no. 5, pp. 1950–1956, 2012.

[23] J.-C. Souberbielle, F. Bienaimé, E. Cavalier, and C. Cormier, "Vitamin D and primary hyperparathyroidism (PHPT)," *Annales d'Endocrinologie*, vol. 73, no. 3, pp. 165–169, 2012.

[24] M. A. Serdar, B. B. Can, M. Kilercik et al., "Analysis of changes in parathyroid hormone and 25 (OH) vitamin D levels with respect to age, gender and season: a data mining study," *Journal of Medical Biochemistry*, vol. 36, no. 1, pp. 73–83, 2017.

[25] A. Valcour, F. Blocki, D. M. Hawkins, and S. D. Rao, "Effects of age and serum 25-OH-vitamin D on serum parathyroid hormone levels," *The Journal of Clinical Endocrinology & Metabolism*, vol. 97, no. 11, pp. 3989–3995, 2012.

[26] E. Kamycheva, J. Sundsfjord, and R. Jorde, "Serum parathyroid hormone level is associated with body mass index: the 5th Tromso study," *European Journal of Endocrinology*, vol. 151, pp. 167–172, 2004.

[27] A. J. van Ballegooijen, I. Reinders, M. Visser, and I. A. Brouwer, "Parathyroid hormone and cardiovascular disease events: a systematic review and meta-analysis of prospective studies," *American Heart Journal*, vol. 165, no. 5, pp. 655–664, 2013.

[28] B. Yang, C. Lu, Q. Wu, J. Zhang, H. Zhao, and Y. Cao, "Parathyroid hormone, cardiovascular and all-cause mortality: a meta-analysis," *Clinica Chimica Acta*, vol. 455, pp. 154–160, 2016.

Hindawi
International Journal of Endocrinology
Volume 2020, Article ID 1053719, 7 pages
https://doi.org/10.1155/2020/1053719

Research Article

PTH: Redefining Reference Ranges in a Healthy Population—The Role of Interfering Factors and the Type of Laboratory Assay

Simona Censi,[1] Maurizio Iacobone,[2] Stefano Simmini,[1] Jacopo Manso,[1] Giulio Franceschet,[1] Mario Plebani,[3] Anna Chiara Frigo,[4] Martina Zaninotto,[3] Francesca Torresan,[2] Giustina De Silvestro,[5] Carla Scaroni,[1] Caterina Mian,[1] and Valentina Camozzi[1]

[1]*Endocrinology Unit, Department of Medicine (DIMED), University of Padua, Padua, Italy*
[2]*Endocrine Surgery Unit, Department of Surgery, Oncology and Gastroenterology (DiSCOG), University of Padua, Padua, Italy*
[3]*Laboratory Medicine, Department of Medicine (DIMED), University of Padua, Padua, Italy*
[4]*Department of Cardiac, Thoracic and Vascular Sciences, Biostatistics, Epidemiology and Public Health Unit, University of Padua, Padua, Italy*
[5]*Department of Transfusion Medicine, Padua University Hospital, Padova, Italy*

Correspondence should be addressed to Maurizio Iacobone; maurizio.iacobone@unipd.it

Received 13 September 2019; Accepted 23 January 2020; Published 21 February 2020

Guest Editor: Vito Guarnieri

Introduction. Parathyroid hormone (PTH) is a linear peptide constituted by 84 amino acids and active in its 1–84 form, but a wide range of PTH forms produced by its post-transcriptional modifications are present in blood. Many assays with different specificities are commercially available. The aim of our study was to compare a 2nd and 3rd generation in healthy population in order to better define the reference range in the healthy population residing in our region. *Materials and Methods*. 108 subjects (53 females and 55 males) referring to the transfusion donor were enrolled in the study centre in April 2016 and underwent PTH levels measurements with a 3rd generation kit (chemiluminescent immunoassay DiaSorin Liaison) and with a 2nd generation kit (immunoradiometric assay Total Intact PTH Assay (Coated Tube), Scantibodies). Also calcium, phosphate, creatinine, and 25OHD3 were measured. A questionnaire on lifestyle and dietary habits was obtained. *Results*. The median PTH values obtained with the 2nd generation assay and the whole 3rd generation assay were 20.26 pg/ml and 23.11 pg/ml, respectively. Bland–Altman method showed substantial concordance between the two PTH assays, although with an overestimation of the 3rd generation method over the 2nd generation method. There was no correlation between 3rd generation PTH and 25OHD3 and creatinine. Calcium was negatively correlated with PTH only when measured with 3rd generation kit. *Conclusions*. On the basis of our data, obtained from healthy subjects, we can conclude that the reference range used by our laboratory was too narrow and was necessary to reestablish normal ranges according to our population. This is useful to avoid hyperparathyroidism misdiagnosis.

1. Introduction

Parathyroid hormone (PTH) is a linear peptide constituted by 84 amino acids and released by parathyroid glands. The PTH present in the circulation is very assorted, being present also PTH fragments, depending from post-transcriptional modifications occurring in parathyroid cells and in other tissues, mainly in the kidneys and in the liver [1]. As a consequence, there is a "pool" of PTH peptides, also in healthy people, but, in particular, in many clinical conditions. This phenomenon is particularly evident in patients with end-stage renal disease, where carboxy terminal PTH fragments are more abundant than the intact 1–84 PTH form, being half-life of the former (1-2 hours) and very longer than the latter (5–10 minutes) [1]. But the biological activity of this hormone is dependent from his intact form, particularly from its first N-terminal amino acids.

First generation assays consisted of competitive radioimmunoassay based on the use of polyclonal antibodies raised against PTH extracted from bovine or porcine

parathyroid glands in animal models. This method had interference with the specificity of the antibodies that mainly recognized carboxyl fragments, the PTH form predominant in the gland extracts used for immunization [2]. Afterwards, it was clarified that the N-terminal 1–34 PTH fragment is an isoform with the same biological activity of its complete 1–84 form [3], and thus, second-generation assays were developed, nowadays the most used worldwide. These second-generation methods consist in a noncompetitive assessment, "Sandwich" immunoassays, based on the use of two monoclonal antibodies, one directed against the N-terminal (aa 13–24) and one directed against the carboxyl amino-terminal (aa 39–84). Initially, these assays were thought to recognize the entire (1–84) PTH molecule, and they were considered the gold standard for PTH dosage [4]. Subsequently, it was demonstrated that this method is unable to distinguish between the intact (1–84) form from the other fragments without the very first amino acids (in particular the more abundant 7–84), devoid of any biological activity. This occurs because the antibody used has a higher affinity for amino acids around 20–25 and not for the first 4 amino acids, recognized by antibodies of the last generation [5]. Afterwards, assays with this specificity and commercially available were developed (third generation immunoassays) [6]. But also this technique has its pitfalls: these types of assays are not able to distinguish the biologically active molecule from a post-translational modified form with a phosphorylated serine (aa 17) known as nontruncated amino-terminal (NT-N) parathyroid hormone (NT-N PTH) [7]. NT-N PTH represents 10% of total PTH values and up to 15% in patients with end-stage renal disease or a severe hyperparathyroidism or parathyroid cancers [7]. Also within the commercial kit of the same generation, it is difficult to obtain comparable results, owing to different calibrations, matrix effect, and antibody avidity [8]; to obtain comparable results, it is fundamental to undergo a standardization, within healthy and affected (especially hemodialized and patients with primary hyperparathyroidism) subjects. Even more problematic is to compare assays of different generations, since nowadays lots of laboratories still use second-generation immunoassays.

In the literature, studies comparing the assays from the two generations in a healthy population are not available, and they would be useful to define the normal range for these assays and to understand their comparability.

The aim of our study was the assessment of the reference range for PTH values in a population of healthy blood donors, with the comparison of PTH values obtained with the second and third generation kits and the identification of the biological factors able to interfere with PTH values obtained with the two assays.

2. Materials and Methods

2.1. Patients. 114 people (56 males and 58 females, between 18 and 68 years) referring to the transfusion donor centre in April 2016 were enrolled in the study. The study was performed in accordance with the guidelines proposed in the Declaration of Helsinki, and all patients gave their written consent to the use of their blood for research purposes. The following exclusion criteria were considered: a history of acute or chronic diseases affecting bone, medical treatment interfering with skeletal metabolism in the previous 6 months, heavy smoking (more than 10 cigarettes/day), alcohol intake of more than 3 alcohol units/day, pregnancy, menopause within the previous 5 years, a personal or family history of pathological osteoporotic fractures, and extreme (very high or very low) values of 25OHD3. 5 females were excluded because they were using cholecalciferol supplement, and 1 male was excluded because of its vitamin D status, represented by circulating calcifediol level (25OHD3) was very higher than the other people included in the study (192 nmol/L). So, 108 subjects were finally included in the study (55 males and 53 females). All 108 subjects were assayed with the 3rd generation kit, while it was possible to use the 2nd generation kit in a maximum of 78 subjects, selected from the total population enrolled. Blood donors underwent a survey to collect individual lifestyle data, such as age, sex, nationality, solar light exposure (</≥30 minutes a day), physical exercise (yes/no), food calcium intake by a frequency validated questionnaire of dairy products, seafood, calcium-rich water consumption [9], reproductive state (years since the menopause, number of pregnancies, and miscarriages), medical and pharmacological history with particular attention to diseases and therapies interfering with bone metabolism (these blood donors were excluded from the study), and smoke habit. As regards nutritional calcium intake, a score <7 points was considered insufficient. Moreover, anthropometric characteristics were collected (weight, height, hip and waist circumference, and blood pressure). An 8.5 ml blood sample was collected from each patient.

2.2. Laboratory Assays. The third-generation PTH assay employed was a chemiluminescent immunoassay (CLIA) DiaSorin Liaison (Stillwater, USA) (reference range: 4.6–26.8 pg/ml) while the second-generation kit was an immunoradiometric assay (IRMA), Total Intact PTH Assay (Coated Tube), Scantibodies (Santee, USA) (reference range: 10–57 pg/ml). 25OHD3 was measured with a CLIA assay (DiaSorin, Stillwater, USA) (reference range: 75–250 nmol/L). Calcium (reference range: 2.10–2.55 mmol/l), phosphate (reference range: 0.87–1.45 mmol/L), and creatinine (reference range in male subjects 59–104 μmol/L, reference range in female subjects: 45–84 μmol/L) were measured using an enzymatic assay (Cobas 8000, Roche-Hitachi, GmbH, Mannheim, Germany).

2.3. Statistical Analysis. The Kolmogorov–Smirnov test was used to test the normal distribution of the variables. When a normal distribution was found, mean values and standard deviations were employed. When the distribution was not normal, the median values and interquartile ranges were used. Categorical variables (smoking habit and physical exercise) or quantitative categorized (sun exposure, calcium intake, dichotomized 25OHD, and 2nd and 3rd generation assays) were analysed using chi-square or Fisher exact test.

The eventual presence of linear correlation between variables (BMI, age, hip and waist circumference, calcium, phosphate, 25OHD3, and creatinine) and 25OHD3 and PTH measured with the 2 kits were analysed using the Spearman coefficient. The Bland–Altman plot was used to analyse the agreement between the two PTH methods. The concordance between the two assays was evaluated with Lin's concordance correlation coefficient, with a 95% confidence interval (IC) estimated with the Bootstrap method, carrying out 2000 resamples. A p value <0.05 was considered statistically significant.

3. Results

Patients' characteristics are summarized in Tables 1 and 2. In the population enrolled, 16 subjects were smokers (less than 10 cigarettes/day). In Table 3, mean values with relative standard deviation (SD) for calcium, phosphate, creatinine, 25OHD3, and PTH with the 2nd and 3rd generation assays in the entire population and in the population divided based on 25OHD3 levels are reported. The median PTH value obtained with the intact PTH assay (2nd generation assay) and the whole PTH assay (3rd generation assay) where 16.0 pg/ml (reference range: 4.6–26.8 pg/ml) and 20.9 pg/ml (reference range: 10–57 pg/ml), respectively. We found 2/78 (2.6%) cases of elevated PTH with the 2nd generation assay (being elevated values in these 2 patients 65 and 69 pg/ml) and 27/108 (25%) (range of elevated values: 28–70 pg/ml), with the third generation assay. The 2 patients that had high PTH levels with "intact" assay had elevated PTH levels also with the 3rd generation assay.

In the whole series, only 3/108 (2.7%) were found to have mildly elevated calcium levels, and none of these patients had elevated PTH values.

Analysing the association between solar exposition (</≥30 minutes/day) using the cutoff of 50 nmol/L (limit between deficiency and insufficiency) and the cutoff of 75 nmol/L (limit between insufficiency and sufficiency) for 25OHD3, we did not find any correlation between the two parameters. Moreover, 25OHD3 status was not associated with age, sex, and BMI in our series. There was no association between the 3rd generation abnormal PTH and 25OHD3 deficiency and insufficiency (Table 4). As regards the nutritional calcium intake and creatinine, there was no association with an elevated PTH, obtained with the 3rd generation kit. It was not possible to analyse the association of 25OHD3, nutritional calcium intake, and creatinine and an elevated PTH measured with the 2nd generation assay because subjects with a PTH found over the normality range with this kit were only 2/78, so the numerosity was not enough for a statistical analysis. On the contrary, there was a correlation between sex and PTH values obtained with both the kits: PTH values were significantly higher in males both with the 3rd generation kit (females: median value of 19.5 pg/ml, range: 10.4–9.4 pg/ml; males: median of 21.4 pg/ml, range: 8.1–70 pg/ml $p = 0.0454$) and the 2nd generation assay (females: median value of 13 pg/ml, range: 7.0–37.0 pg/ml and males: median value of 19.5 pg/ml, range: 7.0–69.0 pg/ml, $p = 0.0143$) (Table 5).

Age was found positively correlated with PTH when measured with both the kits; BMI is positively correlated with PTH when measured with the 2nd generation kit; hip and waist circumferences are negatively correlated with 25OHD3 and positively with PTH values measured with 2nd generation assay, while only waist circumference is positively correlated with PTH when measured with the 3rd generation kit. Calcium levels are negatively correlated with PTH only when measured with the 3rd generation kit, while phosphate is positively correlated only with 25OHD3. 25OHD3 is not correlated with PTH values, measured with both the assays. Creatinine is correlated only with 25OHD3, negatively. When the concordance between the two assays was analysed, the Bland–Altman method showed a mean error of 4.5 pg/ml, with an overestimation of the 3rd generation method over the 2nd generation method. Lin's concordance correlation coefficient was of 0.8917, with a 95% confidence interval of 0.8296 and 0.9387 (Figure 1).

4. Discussion

The study was inspired by the increasing number of asymptomatic patients with normal calcium concentrations referring to endocrinological consultation for increased PTH levels, when measured by our institutional laboratory. The problematic has emerged since the laboratory switched from an "intact" PTH second-generation assay kit to a "whole" third generation assay. PTH often resulted higher when obtained by our laboratory, when compared with laboratories that still used kits owning the previous generation. As a consequence, we wondered if the issue was due to the new assay kit used. Comparing PTH values obtained with different generation assays could be problematic. Tan and colleagues compared the third generation Roche Cobas Assay with four second-generation assays (Siemens ADVIA Centaur, OCD VITROS, Beckman Access 2, Abbott ARCHITECT, "intact" assays) in patients with renal disease. They concluded that Elycsys PTH (1–84) has a comparable precision and good correlation with "intact" assays; "intact" assays correlated well among each other but showed discrepancy with increasing PTH concentrations [10]. Another study compared a third-generation assay (Liaison, DiaSorin) with a second-generation assay (ELSA-PTH, Cis biomedical) in a population of dialyzed patients, and also, in this study, the two kits showed a good correlation, independently from age, sex, BMI, and blood pressure, but also, in this study, differences between the two assays increased with the rise of PTH values [11]. The aim of our study is to compare the two generations of PTH assays in healthy subjects, indeed this data is still not available in the literature.

So, a population of healthy subjects, with a personal and drug history negative for possible interference with bone metabolism, was enrolled. Then, the results on PTH values obtained with the two kits were compared. We chose to select our subjects among blood donors to have a healthy population, but many limitations remained. The limitations concerned the scarce representation of middle-aged people (30–40 years), having had this category of subjects a reduced availability to participate in the study and complete the

Table 1: Anthropometric characteristics of the enrolled population.

	All 108 (100%)	Females 53 (49.1%)	Males 55 (50.9%)
Age (years), median (range)	43.0 (18.0–68.0)	43.0 (18.0–59.0)	43.0 (20.0–68.0)
BMI (kg/m^2) median (range)	24.1 (18.7–40.1)	23.1 (18.7–35.0)	25.3 (20.2–40.1)
Weight (kg) median (range)	72.0 (49.0–130.0)	63.0 (49.0–94.0)	80.0 (62.0–130.0)
Height (cm) median (range)	172.0 (150.0–192.0)	165.0 (150.0–175.0)	178.0 (160.0–192.0)
Waist circumference (cm) median (range)	85.5 (65.0–125.0)	77.0 (65.0–112.0)	90.0 (70.0–125.0)
Hip circumference (cm) median (range)	102.0 (86.0–130.0)	100.0 (86.0–130.0)	103.0 (93.0–120.0)
Median systolic blood pressure (mmHg) (range)	120.0 (95.0–185.0)	120.0 (95.0–140.0)	125.0 (100.0–185.0)
Median diastolic blood pressure (mmHg) (range)	80.0 (65.0–105.0)	80.0 (65.0–95.0)	80.0 (70.0–105.0)

Table 2: Food and behavioural habits of the enrolled population.

	All 108 (100%)	Females 53 (49.1%)	Males 55 (50.9%)
Physical exercise (number of patients)			
Yes	84 (100.0%)	42 (50.0%)	42 (50.0%)
No	24 (100.0%)	11 (45.8%)	13 (54.2%)
Sun exposure (number of patients)			
<30 minutes	35 (100.0%)	17 (48.6%)	18 (51.4%)
≥30 minutes	73 (100%)	36 (49.3%)	37 (50.7%)
Daily calcium intake (points mean value ± SD and median with range)	5.4 ± 2.4 5.0 (0.0–11.0)	5.2 ± 2.2 5.0 (1.0–11.0)	5.7 ± 2.5 6.0 (0.0–11.0)
Daily calcium intake (number of patients)			
<7 points	69 (100.0%)	37 (53.6%)	32 (46.4%)
Daily calcium intake (number of patients)			
≥7 points	39 (36.1%)	16 (41.0%)	23 (59.0%)

Table 3: Laboratory data categorized on the basis of 25OHD3 levels deficiency (≥50 nmol/L) or sufficiency (≥75 nmol/L), expressed in mean ± standard deviation and median values and the range of the values. Reference ranges: calcium: 2.10–2.55 nmol/L; creatinine: male subjects: 59–104 μmol/L, female subjects: 45–84 μmol/L; phosphate: 0.87–1.45 mmol/L; 3rd generation PTH assay: 4.6–26.8 pg/ml; 2nd generation PTH assay: 10–57 pg/ml.

	All patients 108 (100%)	25OHD3 < 50 nmol/L 61 (56.5%)	25OHD3 ≥ 50 nmol/L 47 (43.5%)	p value	25OHD3 < 75 nmol/L 101 (93.5%)	25OHD3 ≥ 75 nmol/L 7 (6.5%)	p value
Calcium (mean values ± SD) (mmol/L)	2.4 ± 0.1	2.4 ± 0.1	2.4 ± 0.1	0.69	2.4 ± 0.1	2.4 ± 0.1	0.64
Phosphate (mean values ± SD) (mmol/L)	1.1 ± 0.2	1.1 ± 0.2	1.1 ± 0.2	0.12	1.1 ± 0.2	1.3 ± 0.1	0.03
Creatinine (mean values ± SD) (μmol/L)	77.4 ± 13.0	79.2 ± 14.1	74.9 ± 11.2	0.07	77.9 ± 13.1	70.4 ± 10.9	0.07
2nd generation (median values and range) (pg/ml) PTH	16.0 (7.0–69.0)	17.5 (7.0–69.0)	14.0 (7.0–48.0)	0.09	16.0 (7.0–69.0)	14.0 (8.4–36.0)	0.28
3rd generation (median values and range) (pg/ml) PTH	20.9 (8.1–70.0)	21.6 (11.0–70.0)	18.7 (8.1–54.9	0.19	20.7 (8.1–70.0)	22.0 (11.0–39.4)	0.96

Table 4: Blood donors divided according to the cutoffs of 25OHD3 levels, deficiency (≥50 nmol/L), and sufficiency (≥75 nmol/L) and according to PTH levels obtained with the third-generation assay (>26.8 pg/ml versus >4.6 and ≤26.8 pg/ml and <4.6 pg/ml).

	All patients 108 (100%)	PTH 3rd generation >26.8 pg/m 28/114 (25.0%)	PTH 3rd generation >4.6 and ≤26.8 pg/ml 86/114 (75.0%)	PTH 3rd generation <4.6 pg/ml 0/114 (0%)	p value
25OHD3 < 50 nmol/L	61 (100)	16 (26%)	45 (74%)	0 (0%)	0.74
25OHD3 ≥ 50 nmol/L	47 (100)	11 (23%)	36 (77%)	0 (0%)	
25OHD3 ≥ 75 nmol/L	7 (100)	2 (29%)	5 (71%)	0 (0%)	0.82
25OHD3 < 75 nmol/L	101 (100)	25 (25%)	76 (75%)	0 (0%)	

Table 5: PTH values measured with 2nd and 3rd generation assay according to sex. Reference ranges: 3rd generation PTH assay: 4.6–26.8 pg/ml; 2nd generation PTH assay: 10–57 pg/ml.

	All patients 108 (100%)	PTH 3rd generation (median and range) pg/ml	p value	All patients 75 (100%)	PTH 2nd generation (median and range) pg/ml	p value
Females	53 (49.1%)	19.5 (10.4–9.4)	0.0454	37 (49.3%)	13.0 (7.0–37.0)	0.0143
Males	55 (50.9%)	21.4 (8.1–70.0)		38 (50.7%)	19.5 (7.0–69.0)	

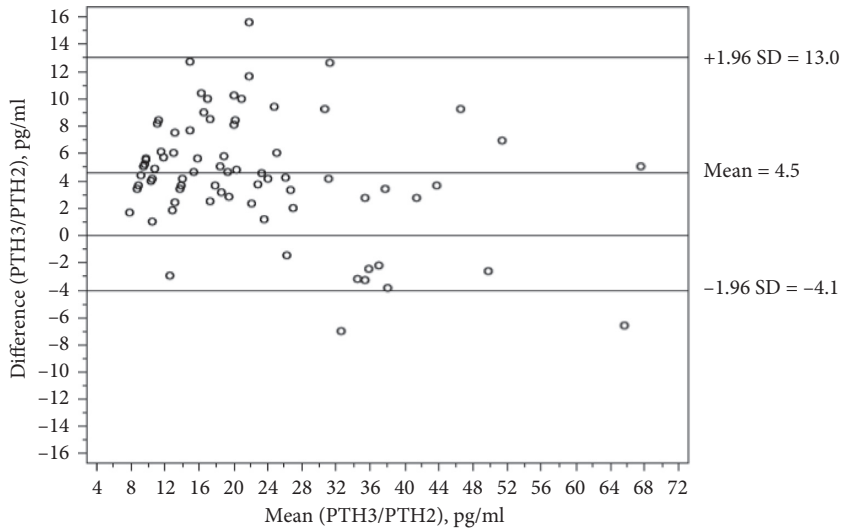

Figure 1: Bland–Altman plot analysing the agreement between the two PTH methods.

questionnaire. Another issue is the difficulty in obtaining an objective quantification of sun exposure and calcium nutritional intake. Moreover, among the 108 subjects enrolled, only 7 (6.5%) had levels of vitamin D sufficiency (≥75 nmol/L), 40/108 (37%) had insufficient levels (between 50 and 75 nmol/L), and 61/108 (56.6%) even had deficient levels (<50 nmol/L). This result is not surprisingly since the recruitment was done at the beginning of springtime, corresponding with the nadir of vitamin D status. This data could have affected the values of PTH found [12].

Older age and male sex were associated with higher PTH levels, maybe owing to a different sensitivity of parathyroid glands for serum calcium levels. Older age was found related to higher PTH values also in other studies [13], while gender and PTH association has obtained contrasting results in the literature, maybe owing to cultural issues and thus sun exposure [13]. It is possible that the PTH "resistance" develops with age and that a different PTH reference range should be adopted based on patients' age [14]. Moreover, also an impairment of renal function related with aging can contribute to this phenomenon. Thus, it is difficult to establish the ranges based on age, considering also other possible interfering factors that can play a role, from sun exposure, ethnicity, to menopause age [14, 15]. Based on these data, we can only say that the clinician should pay more attention to a slightly PTH elevation found in a young subject then to the same value documented in an elder.

Dietary habits and sun exposure did not influence PTH and 25OHD3 levels in our series, maybe owing to the daily variability of these parameters, and because of the difficulties related to its objective assessment.

No association was found between creatinine levels and PTH values, with both the assays. This result is probably due to the selection criteria including a population in good health.

Although the population considered was healthy, we found 2.6% of cases of elevated PTH with the 2nd generation assay and up to 25% with the 3rd generation assay, and all these patients had normal calcium levels. So, there is an

imbalance in subjects with elevated PTH values with the two assays. The statistical analysis demonstrates a good concordance between the two assays, but indeed, there is an overestimation of the PTH values found with the 3rd generation assay, and this discrepancy is more evident when low values (within the normal range) are considered. Maybe, for low PTH levels, 3rd generation assay undergoes some and still unknown interference. This discrepancy would confirm doubts about the interchangeability between the two generations, and it is quite surprising to find higher PTH values with an assay that should be more specific for the whole PTH and should not recognize its fragments. The overestimation we obtained with the 3rd generation assay is tolerable for low values but should not be acceptable for borderline values, situation in which a PTH overestimation should prompt mistaken clinical choices. A diagnosis of normocalcemic primary hyperparathyroidism can be made when the subject presents consistently elevated PTH concentrations in presence of normal calcium levels, after the exclusion of any cause of secondary PTH elevation (renal diseases, vitamin D insufficiency, etc) [15]. A narrow reference range can prompt the clinician to mistaken diagnosis and possibly to useless, time-consuming, and expensive diagnostic workout. Our laboratory adopted the normal range proposed by the literature obtained from an analogue Caucasian population (4.6–26.8 pg/ml) [16]. Based on our study, the normal range used in our laboratory was too narrow, with a highest value that should be raised to avoid a misdiagnosis of hyperparathyroidism, especially normocalcemic hyperparathyroidism, in healthy subjects. So, we suggest the normal laboratory range to be revised on the basis of these results, obtained in a population of healthy subjects residing in our region. However, the natural history of normocalcemic hyperparathyroidism is still unknown. Many patients become hypercalcemic and have evidence of organ damages, such as an impaired bone mineral density.

Another limit of the study could have been represented by the fact that our series included lot of people with insufficient vitamin D values, with possible consequently higher PTH values. By the way, this is not necessarily true in the healthy population. The Institute of Medicine (IOM) suggests there is no or only few evidence that, in the general population, a vitamin D level higher than 50 nmol/L is beneficial [17, 18], with acceptable levels for physiological functions in a healthy subject between 30 and 40 nmol/L, with a maximum calcium absorption capacity between 20 and 50 nmol/L [19]. IOM suggests that Endocrine Society guidelines on the treatment and prevention of vitamin D deficiency are based on weak and misinterpreted studies [20–22]. In conclusion, given the absence in our series of very high PTH values (we chose to consider a presumed healthy population), the scarce numerosity of subjects studied and the absence of important data for the evaluation of phosphocalcium metabolism (such as albumin and urinary calcium concentration), we cannot sustain the superiority of one assay on the other. Moreover, another limit of our study was the relatively scarce numerosity of patients in which we could obtain a PTH measurement with the 2nd generation assay (78 patients), since kit availability was limited. The patients were randomly chosen, but we should consider the possibility that this could have influenced the results obtained. By the way, since the correlation between the two assays was good, this possibility is unlikely.

Further studies are needed, based on a series of patients possibly with ascertained sufficient vitamin D levels and with the availability of other factors that interfere on bone metabolism (like urinary calcium levels and albumin concentrations).

In conclusion, the purpose of our study was to place the emphasis on the importance of the assay and proper range used when evaluating PTH, in order to properly interpret the results, avoiding successive cost- and time-consuming laboratory and radiological tests.

Data Availability

The biochemical data and questionnaires results used to support the findings of this study are available from the corresponding author upon request

Conflicts of Interest

The authors have no conflicts of interest.

References

[1] J. G. H. Vieira, "PTH assays: understanding what we have and forecasting what we will have," *Journal of Osteoporosis*, vol. 2012, Article ID 523246, 5 pages, 2012.

[2] S. A. Berson, R. S. Yalow, G. D. Aurbach, and J. T. Potts Jr., "Immunoassay of bovine and human parathyroid hormone," *Proceedings of the National Academy of Sciences*, vol. 49, no. 5, pp. 613–617, 1963.

[3] J. T. Potts, G. W. Tregear, H. T. Keutmann et al., "Synthesis of a biologically active N-terminal tetratriacontapeptide of parathyroid hormone," *Proceedings of the National Academy of Sciences*, vol. 68, no. 1, pp. 63–67, 1971.

[4] J. G. Vieira, S. K. Nishida, T. S. Kasamatsu, E. C. Amarante, and I. S. Kunii, "Development and clinical application of an immunofluorometric assay for intact parathyroid hormone," *Brazilian Journal of Medical and Biological Research*, vol. 27, no. 10, pp. 2379–2382, 1994.

[5] R. Lepage, L. Roy, J.-H. Brossard et al., "A non-(1-84) circulating parathyroid hormone (PTH) fragment interferes significantly with intact PTH commercial assay measurements in uremic samples," *Clinical Chemistry*, vol. 44, no. 4, pp. 805–809, 1998.

[6] P. Boudou, F. Ibrahim, C. Cormier, A. Chabas, E. Sarfati, and J.-C. Souberbielle, "Third- or second-generation parathyroid hormone assays: a remaining debate in the diagnosis of primary hyperparathyroidism," *The Journal of Clinical Endocrinology & Metabolism*, vol. 90, no. 12, pp. 6370–6372, 2005.

[7] P. Caron, W. F. Simonds, J.-C. Maiza et al., "Nontruncated amino-terminal parathyroid hormone overproduction in two patients with parathyroid carcinoma: a possible link to HRPT2 gene inactivation," *Clinical Endocrinology*, vol. 74, no. 6, pp. 694–698, 2011.

[8] M. Hecking, A. Kainz, B. Bielesz et al., "Clinical evaluation of two novel biointact PTH(1-84) assays in hemodialysis

patients," *Clinical Biochemistry*, vol. 45, no. 18, pp. 1645–1651, 2012.

[9] M. Montomoli, S. Gonnelli, M. Giacchi et al., "Validation of a food frequency questionnaire for nutritional calcium intake assessment in Italian women," *European Journal of Clinical Nutrition*, vol. 56, no. 1, pp. 21–30, 2002.

[10] K. Tan, L. Ong, S. K. Sethi, and S. Saw, "Comparison of the Elecsys PTH(1-84) assay with four contemporary second generation intact PTH assays and association with other biomarkers in chronic kidney disease patients," *Clinical Biochemistry*, vol. 46, no. 9, pp. 781–786, 2013.

[11] M.-H. Gannagé-Yared, C. Farès, T. Ibrahim, Z. A. Rahal, M. Elias, and D. Chelala, "Comparison between a second and a third generation parathyroid hormone assay in hemodialysis patients," *Metabolism*, vol. 62, no. 10, pp. 1416–1422, 2013.

[12] S. J. Khundmiri, R. D. Murray, and E. Lederer, "PTH and vitamin D," in *Comprehensive Physiology*, vol. 6, pp. 561–601, John Wiley & Sons, Hoboken, NJ, USA, 2016.

[13] M. A. Serdar, B. B. Can, M. Kilercik et al., "Analysis of changes in parathyroid hormone and 25 (OH) vitamin D levels with respect to age, gender and season: a data mining study," *Journal of Medical Biochemistry*, vol. 36, no. 1, pp. 73–83, 2017.

[14] A. Khan and J. P. Bilezikian, "Primary hyperparathyroidism," *Canadian Medical Association Journal*, vol. 163, no. 2, 2000.

[15] N. E. Cusano, S. J. Silverberg, and J. P. Bilezikian, "Normocalcemic primary hyperparathyroidism," *Journal of Clinical Densitometry*, vol. 16, no. 1, pp. 33–39, 2013.

[16] E. Cavalier, P. Delanaye, P. Lukas, A. Carlisi, R. Gadisseur, and J.-C. Souberbielle, "Standardization of DiaSorin and Roche automated third generation PTH assays with an international standard: impact on clinical populations," *Clinical Chemistry and Laboratory Medicine (CCLM)*, vol. 52, pp. 1137–1141, 2014.

[17] A. C. Ross, J. E. Manson, S. A. Abrams et al., "The 2011 report on dietary reference intakes for calcium and vitamin D from the institute of medicine: what clinicians need to know," *The Journal of Clinical Endocrinology & Metabolism*, vol. 96, no. 1, pp. 53–58, 2011.

[18] A. J. Sai, R. W. Walters, X. Fang, and J. C. Gallagher, "Relationship between vitamin D, parathyroid hormone, and bone health," *The Journal of Clinical Endocrinology & Metabolism*, vol. 96, no. 3, pp. E436–E446, 2011.

[19] C. J. Rosen, S. A. Abrams, J. F. Aloia et al., "IOM committee members respond to endocrine society vitamin d guideline," *The Journal of Clinical Endocrinology & Metabolism*, vol. 97, no. 4, pp. 1146–1152, 2012.

[20] M. C. Chapuy, A. M. Schott, P. Garnero, D. Hans, P. D. Delmas, and P. J. Meunier, "Healthy elderly French women living at home have secondary hyperparathyroidism and high bone turnover in winter. EPIDOS study group," *Journal of Clinical Endocrinology & Metabolism*, vol. 81, no. 3, pp. 1129–1133, 1996.

[21] M. F. Holick, E. S. Siris, N. Binkley et al., "Prevalence of vitamin D inadequacy among postmenopausal north American women receiving osteoporosis therapy," *The Journal of Clinical Endocrinology & Metabolism*, vol. 90, no. 6, pp. 3215–3224, 2005.

[22] M. K. Thomas, D. M. Lloyd-Jones, R. I. Thadhani et al., "Hypovitaminosis d in medical inpatients," *New England Journal of Medicine*, vol. 338, no. 12, pp. 777–783, 1998.

Hindawi
International Journal of Endocrinology
Volume 2020, Article ID 3146535, 10 pages
https://doi.org/10.1155/2020/3146535

Review Article

Osseous Manifestations of Primary Hyperparathyroidism: Imaging Findings

Jackson Bennett,[1] **James W. Suliburk**,[2] **and Fanny E. Morón**[3]

[1]*School of Medicine, Baylor College of Medicine, Houston, TX, USA*
[2]*Department of Surgery, Baylor College of Medicine, Houston, TX, USA*
[3]*Department of Radiology, Baylor College of Medicine, Houston, TX, USA*

Correspondence should be addressed to Fanny E. Morón; fmoron@bcm.edu

Received 13 September 2019; Revised 10 December 2019; Accepted 8 January 2020; Published 21 February 2020

Academic Editor: Giorgio Borretta

Primary hyperparathyroidism is a systemic endocrine disease that has significant effects on bone remodeling through the action of parathyroid hormone on the musculoskeletal system. These findings are important as they can aid in distinguishing primary hyperparathyroidism from other forms of metabolic bone diseases and inform physicians regarding disease severity and complications. This pictorial essay compiles bone-imaging features with the aim of improving the diagnosis of skeletal involvement of primary hyperthyroidism.

1. Introduction

Hyperparathyroidism (HPT) is an endocrine disorder defined by a state of inappropriately increased levels of parathyroid hormone (PTH) activity from one or more parathyroid glands [1]. Primary hyperparathyroidism (PHPT) is a main disease subtype with classical and normocalcemic variants. Hypercalcemia is evident in patients with classical PHPT, while the normocalcemic variant demonstrates normal total and ionized calcium levels after correcting for albumin [2–4]. Classical PHPT is most commonly asymptomatic and due to autonomous secretion of parathyroid hormone from a benign parathyroid adenoma in 80% of patients with lack of feedback inhibition of calcium [1, 4, 5]. Multigland disease (double adenoma, triple adenoma, and spontaneous four-gland hyperplasia), parathyroid carcinoma, and syndromic forms of PHPT typically comprise the remaining 20% of cases [5–7]. The normocalcemic variant is characterized by secondary elevations in PTH without an exact known etiology. This variant may represent a subclinical, asymptomatic early stage of PHPT, and it has the potential to progress to hypercalcemic status in 20% of cases and cause the target end organ damage seen in the symptomatic classical variant in some individuals [2, 4]. Other HPT disease subtypes include secondary and tertiary disease, which are primarily seen in patients with chronic renal disease and posttransplant patients [7].

Bone is a major target organ of PTH, and inappropriately elevated PTH levels in PHPT can lead to changes in the appearances of bones on a variety of diagnostic imaging evaluations. Metabolic bone disease is an established clinical manifestation of PHPT as PTH is a major regulator of osteoclast activity and bone remodeling [8]. In addition, the biomechanical properties of bone as seen in PHPT's variants, including fracture risk and protective bone treatment, are an area of ongoing scientific interest [3]. However, the clinical and physical symptoms as well as imaging findings that have been historically taught are considered relatively rare today in clinical presentation and context. This is thought to be due to earlier diagnosis and regular evaluations of calcium. From an epidemiological disease perspective of PHPT, the prevalence in the United States of the classical hypercalcemia form has been estimated to be 0.86% overall with a certain degree of variability [9, 10]. Many cases of Western PHPT are now initially identified in otherwise asymptomatic patients

through routine biochemical screening in up to 2% of patients over the age of 55 [1, 4, 11], while more severe, overt radiographical bone disease is rarer with potential to carry complications [1, 6, 12]. Widened prevalence estimates also exist for other disease phenotypes such as the normocalcemic form of PHPT (0.4–11%). Additionally, the modern incidence and prevalence estimates of PHPT have increased regionally in the USA, Europe, and China, which is thought to be attributed to a worldwide increase in routine biochemical disease screening. This is contrasted with developing countries in which PHPT presents with higher serum calcium levels and more symptomatic disease compared to the asymptomatic hypercalcemia seen in the USA, Europe, and China [9, 10].

There is an overlap regarding the bone imaging findings of primary and secondary HPT. While secondary HPT is not specifically discussed in depth here, it has a unique osteosclerotic effect on the axial skeleton that produces a classic "rugger-jersey spine" [13]. In this pictorial essay, we mainly focus on the skeletal findings of PHPT bone disease as seen on multiple imaging modalities. We present an organized discussion on subperiosteal bone resorption-acroosteolysis, subchondral bone resorption, brown tumors of the body, salt-and-pepper skull, and osteopenia associated with PHPT. The overall aim of this pictorial essay is to review this wide range of musculoskeletal imaging findings associated with PHPT in addition to common differential conditions to aid in diagnosing and enhancing our knowledge of this enigmatic disease.

1.1. Subperiosteal Bone Resorption. Subperiosteal bone resorption corresponds to destruction of the bone underneath the cortical periosteum of long bones; it is due to increased bone turnover. The mechanism of heightened levels of bone turnover is due to the unregulated effects of parathyroid hormone on bone calcium homeostasis as seen in PHPT [5]. Elevated PTH levels lead to upregulation of nuclear factor-$\kappa\beta$ ligand (RANKL), which interacts with its respective RANK receptor on osteoclast progenitor cells, leading to resorption via the indirect growth of bone-remodeling osteoclasts [8, 14]. These findings in the phalanges are defining, pathognomonic musculoskeletal imaging features of primary HPT [15].

The osseous changes most commonly occur at the proximal and middle phalanges located on the radial margins of the second and third fingers, and they are best viewed on radiographs [13]. On radiographs, subperiosteal bone resorption appears as lace-like subperiosteal/intracortical irregular margin of phalangeal cortical bone [5, 12] with thinned and feathery cortical bone (Figure 1). While elevated serum calcium levels in the setting of high PTH activity ensure a probable diagnosis of PHPT, a majority of patients who have skeletal changes associated with PHPT (up to 95% of patients) are best assessed radiographically at the hand, highlighting this location as a very specific osseous finding of the disease [5, 16]. Thus, when clinical findings suggest PHPT, radiography is the preferred imaging study, specifically at the hand, to look for subperiosteal resorption

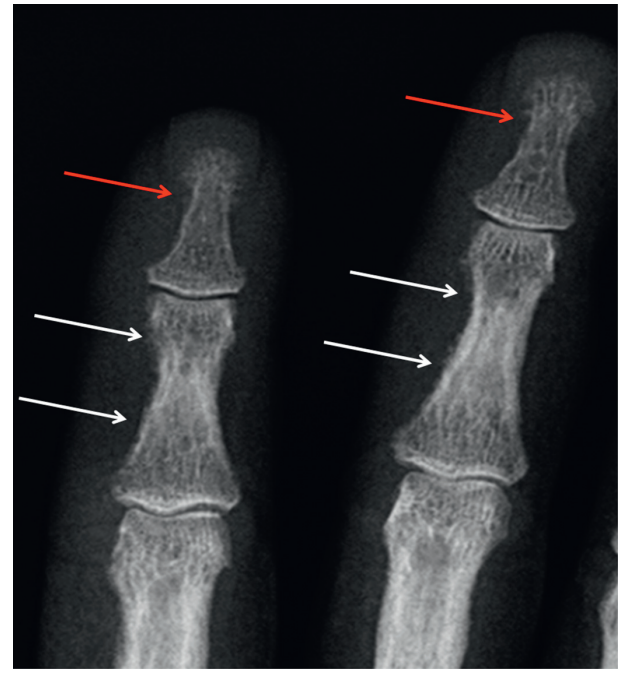

Figure 1: Subperiosteal resorption of the radial aspect of the middle phalanges of the second and third fingers (white arrows); feathery appearance and early tufts resorption-acroosteolysis (red arrows).

if osseous involvement is a concern [16]. In addition to the hand, subperiosteal resorption, cortical thinning, and acroosteolysis can also be seen in the long bones (Figures 2–4), the lamina dura of teeth and spine [5, 17]. Intracortical resorption can also occur and it appears on radiographs as cigar/oval-shaped or tunnel-shaped radiolucency within the cortex (Figure 3). In combination, subperiosteal bone resorption and the brown tumors of osteitis fibrosis cystica (OFC) contribute to 2% of symptomatic HPT manifestations on bone [18]. The radiographic differential diagnosis for subperiosteal arthritis, like changes in the hand, includes rheumatoid arthritis.

Acroosteolysis is a type of subperiosteal bone resorption pattern seen in PHPT and renal osteodystrophy that is located at the distal phalangeal tufts. Diffuse or "band-like" radiolucent patterns of resorption may occur, characteristically at the midshaft and distal phalanx of a single or multiple digits. Key radiological findings to note entail tuft destruction (Figure 1), soft tissue tapering and shortening at distal phalanx, a lucent line crossing the middle phalanx, calcifications, and arthritic changes. Other etiologies of this osseous finding include scleroderma, vascular, infectious, inflammatory, thermal injury, and traumatic and congenital causes of distal phalangeal shortening. Since acroosteolysis of the phalanges can occur in various other conditions, it is important to correlate these findings with other associated clinical and imaging features of HPT [5, 15].

1.2. Subchondral Resorption around Specific Joints. Subchondral resorption is an osseous abnormality with trabecular destruction underneath cartilage surfaces of

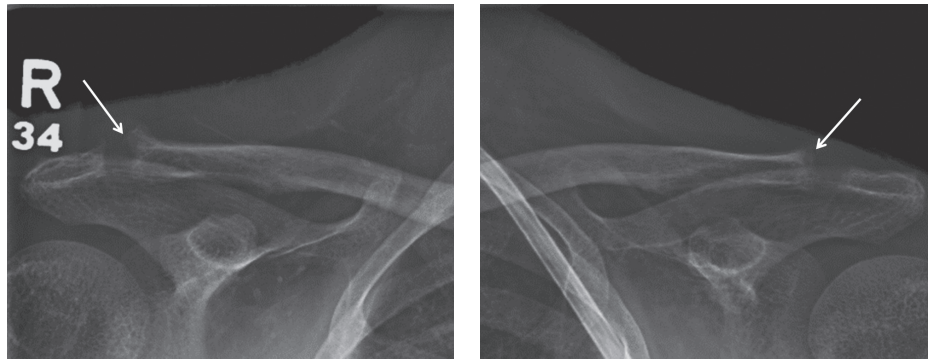

(a) (b)

Figure 2: Clavicular subchondral resorption (arrows), widening of the articular space and irregular-feathery articular surface bilaterally.

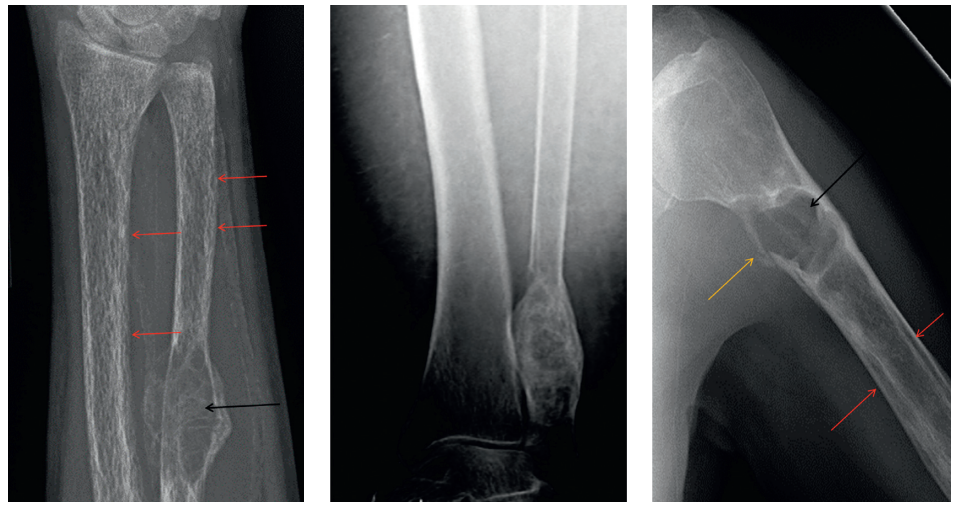

(a) (b) (c)

Figure 3: Additional cases of brown tumors (black arrows) in the ulna, fibula, and humerus. Prominent forearm demineralization with subperiosteal (red arrows), intracortical, and trabecular resorption in the forearm bones and humerus with resultant appearance of coarse internal trabeculation. Pathologic fracture at the humerus brown tumor (yellow arrow) and intracortical resorption with cigar/oval-shaped or tunnel-shaped radiolucency in the cortex (red arrows).

articular spaces; there is also fibrous replacement and new bone formation as well as juxta-articular erosions [13, 17]. The pathophysiology occurs due to PTH-mediated osteoclastic resorption of bone and surrounding cartilage [13]. Osteoclastic bone remodeling is upregulated by the resorption of PHPT, exerting its effect on joints with tight articulation, which are vulnerable to excessive shear stresses. Histologically, these changes may resemble woven bone in addition to fibrous tissue underneath cartilage [17]. Commonly affected joints comprise the acromioclavicular (Figure 2) and sternoclavicular joints, phalanges, pubic symphysis, and sacroiliac joints (Figure 5) [15].

On radiographs, subchondral resorption leads to widening of the articular space (as the result of collapsed resorted bone) and irregular appearance of the articular surfaces with indistinct articular margin [5, 15] (Figures 2 and 5). The erosions seen at the sacroiliac joint also tend to occur on the iliac sides [5, 15, 17] (Figure 5). In addition, at the acromioclavicular joint, bilateral erosions tend to affect the clavicular side more than the acromion (Figure 2), whereas the sternum and clavicle are equally affected at the sternoclavicular joint. Reactive sclerosis may additionally be present (Figure 5). The osseous changes at the hand, sacroiliac joints, and pubic symphysis may mimic the findings of other differential diagnoses such as the inflammatory arthridites and seronegative spondyloarthropathies [17].

1.3. Focal Lytic Lesions. A lytic lesion corresponds to localized bone loss creating an area of lucency in bone. The lytic lesions associated with HPT are named brown tumors, osteolytic aggregate of cyst-like entities seen in long-standing hyperparathyroidism termed OFC. The histology is

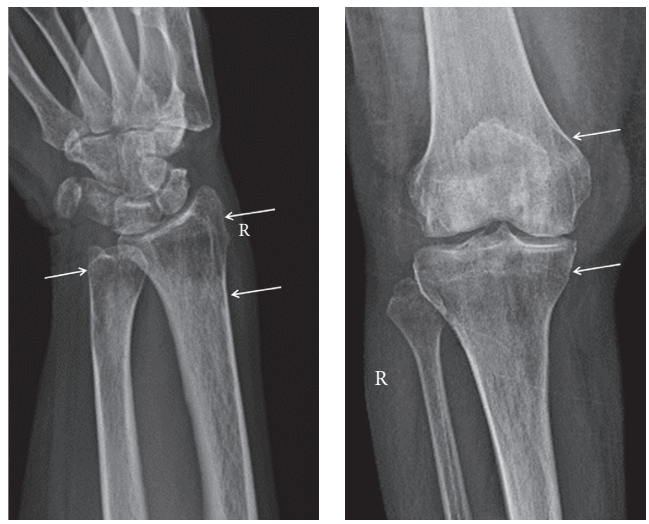

(a) (b)

Figure 4: Osteoporosis. Demineralization with predominance of the distal radius and ulna and around the knee, with cortical thinning due to subperiosteal resorption (arrows).

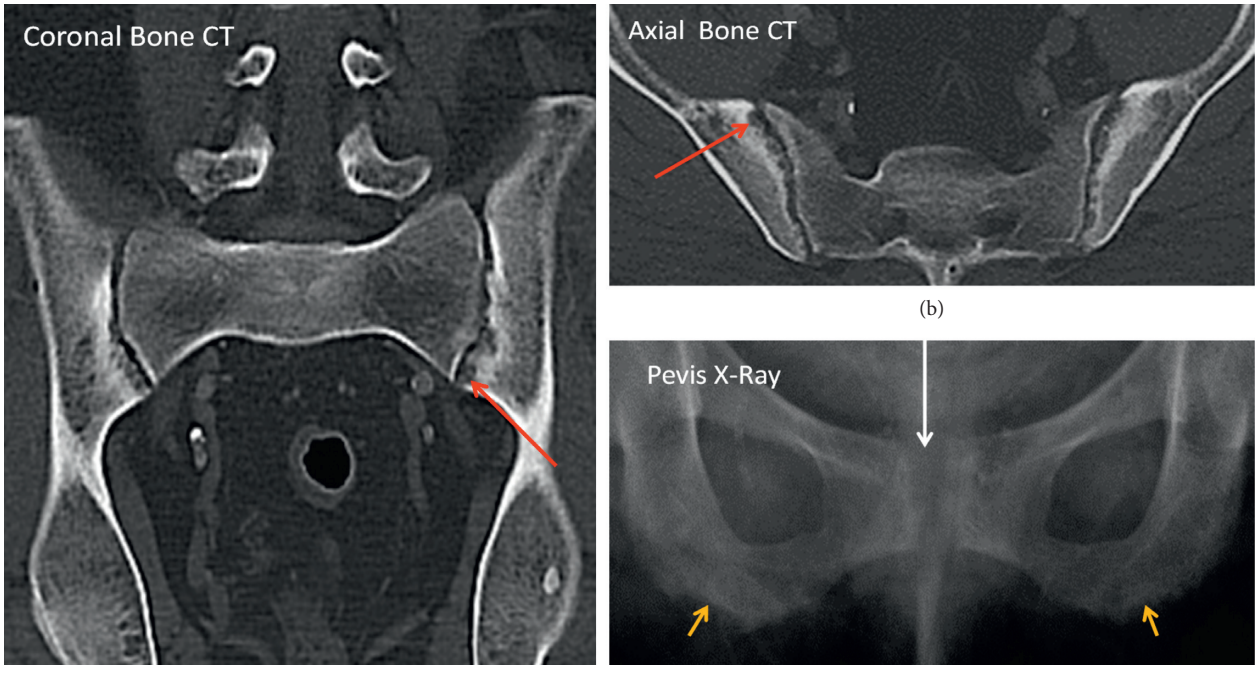

(a) (b) (c)

Figure 5: Subchondral resorption of the sacroiliac joints. Coronal and axial CT images show areas of subchondral lucency with irregular articular margin (red arrows), apparent widening of the joint space and surrounding hyperdense sclerosis. Pelvis X-ray symphysis pubis subchondral resorption (white arrow) with widening and also subligamentous resorption of the ischial tuberosities (yellow arrows). (a) Coronal bone CT. (b) Axial bone CT. (c) Pelvis X-ray.

similar to that of giant cell tumors, appearing as multinucleated giant cells; the bone marrow is replaced by reparative, richly vascularized connective tissue secondary to rapidly increased osteoclastic resorptive activity. Hemosiderin accumulation from hemorrhages associated with this vascularized tissue accounts for their characteristic brown color [18]. Brown tumors are associated with PHPT in up to 3% of patients [18, 19]. The incidence of brown tumors is now also increasingly common in secondary HPT (1.5–1.7% of patients) due to the prevalence of renal disease, dialysis, and this condition in comparison [5, 19, 20]. Brown tumors can be single or multiple and may be located in any site. The

most common sites of brown tumors associated with PHPT include the pelvis, mandibles, ribs, long bones, and hands in addition to the vertebrae [5, 18, 21].

On radiographs, brown tumors of PHPT appear as expansile, solitary, or multifocal well-defined soap-bubbly appearing lytic lesions with cortical thinning (without associated periotic reaction [20, 22]). Additionally, these lesions are characterized as having a narrow zone of transition into the normal bone but no reactive changes in the adjacent bone and well-defined sclerotic margins. There is adjacent cortical thinning but usually not frank destruction or breakthrough (Figure 6). Computed tomography (CT) further localizes the lesion in 3 planes within the bone marrow and proximity to the cortical bone or articular surfaces; CT better depicts cortical thinning and breakthrough as well as associated pathologic fractures. On CT, the lesion is expansile, lytic, and well circumscribed; the density varies depending on the relative proportion of its components. The lesions usually contain a combination of solid, cystic, and hemorrhagic components. The cystic component has lower attenuation (hypodense or darker density); the solid component has higher attenuation (hyperdense or whiter density) (Figure 7), and if there has been a recent bleed, the blood will be even denser, and adjacent soft tissue component may be present [5, 20]. Nuclear medicine bone scans can demonstrate intense brown tumor focal uptake [15]. Magnetic resonance imaging (MRI) is performed to further evaluate the extension of these lesions into adjacent compartments and associated complications such as pathologic fractures or spinal canal invasion and encroachment of the spinal cord. Traditional sequences include T1- and T2-weighted images (T1WI and T2WI, respectively) and fat-saturated sequences. The signal intensity of the lesion is inhomogeneous on MRI. Degraded blood products can cause high signal on T1WI and scattered areas of lower T2WI signal throughout the lesion (Figure 7). Like on CT, the lesion heterogeneity depends on the relative proportion of the lesion components. Solid component is similar to muscle on T1WI and T2WI; the cystic component is hyperintense on T2WI (Figure 6) and may also present with fluid-fluid levels on T2WI. Usually, the administration of contrast is not warranted; if administered, it may present inhomogeneous and peripheral enhancement [22] (Figure 6). The imaging differential diagnosis of brown tumors includes other lucent and lytic bone lesions, such as true giant cell tumors, multiple myeloma, fibrous dysplasia, and metastases [15]. Brown tumors can be clinically differentiated from these conditions based off of serum calcium, serum electrophoresis, and correlated with an isotope bone scan or other radiographic findings suggestive of PHPT [15, 23].

Spinal brown tumors represent a rare manifestation of OFC when compared to established locations such as the ribs, pelvis, mandible, and long bones [24]. The thoracic spine may be involved in up to 57% of spine cases [24]. Multilevel involvement of the spine affecting various vertebral bodies and posterior spinal elements has also been reported [24, 25]. Clinically, brown tumor spinal involvement is particularly significant because while it may present asymptomatically, it carries the extra potential complication of lesional growth and extension into the spinal canal. This can result in canal stenosis and compression of the spinal cord with frank neurological deficits at presentation requiring emergent decompressive surgery and parathyroidectomy [21, 24, 25]. The imaging findings of the spinal brown tumors are nonspecific and the same as elsewhere in the body (Figure 7). MRI is the preferred diagnostic imaging modality in evaluating spinal tumor location and extension. Solitary spinal lesions have a differential diagnosis of metastases, giant cell tumor, aneurysmal bone cyst, and giant cell reparative granuloma, which can be clinically and radiographically correlated with other findings of PHPT [26]. In addition, the typical CT and MRI findings in patients with a lytic lesion and known PHPT are highly suggestive of a brown tumor diagnosis as opposed to other conditions in the differential such as multiple myeloma [24, 27]. It is generally accepted that PHPT patients with overt symptomatic disease should undergo parathyroidectomy if they are reasonable surgical candidates [28]. From a treatment standpoint, parathyroidectomy has been shown to result in complete brown tumor regression [29, 30]. While parathyroidectomy is considered first line for treatment of OFC, surgical management of osseous lesions is debated and may be considered in certain patients [31]. These situations occur in the setting of misdiagnosis, delays in treatment, or lack of biochemical screening, which are more commonly seen in PHPT patient populations of developing countries [31]. Examples of lesions that may require surgery include those that fail to regress or have extensive brown tumor involvement of surrounding structures, for which local bone surgical intervention may be warranted [16, 29, 31]. Other cases entail large, aggressive brown tumors associated with severe pain, delayed treatment, pathological fractures leading to disability, or recurrence after parathyroidectomy [31].

1.4. Salt-and-Pepper Skull. Salt-and-pepper skull refers to diffuse, lytic foci interspersed between regular bone in the calvarium giving a granular skull appearance that occurs as a result of HPT [32]. In PHPT, the pathogenesis involves trabecular bone resorption that leads to decreased differentiation of the diploic space bone marrow and the inner and outer tables of the calvarium [5]. On imaging, bone demineralization and deossification create punctate, lucent foci and a generalized, ground-glass image associated with smudgy trabeculae and focal areas of patchy sclerosis described in combination as the "salt-and-pepper" skull appearance [5, 33] (Figure 8). These findings can be readily visualized on radiographs and CT. Altogether, these findings may be the first imaging change seen in patients presenting with HPT or as a component of OFC [33, 34]. The expanded differential diagnosis of skull demineralization includes osteoporosis associated with aging and less commonly anemias such as sickle cell and thalassemia, HPT, metastatic bone disease, multiple myeloma, and the lytic phase of Paget disease [35]. In differentiating the calvarium salt-and-pepper

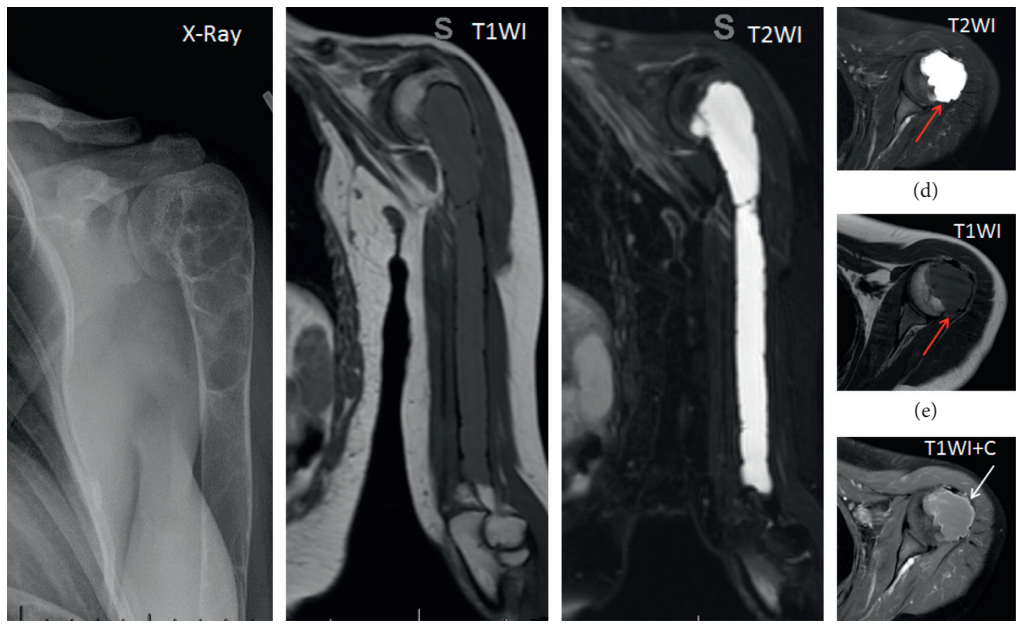

Figure 6: Left humerus brown tumor. X-Ray shows a large, well defined, multiloculated soap-bubbly lucent lesion. MRI T1W1 the lesion is similar to the muscle, on coronal and axial T2WI the lesion is hyperintense (very bright), axial T1WI without contrast the lesion is hypoinetense with prominent thinning of the cortical bone and minimal extension beyond the cortex (red arrows), axial T1WI + C with contrast and fat saturation shows diffuse and peripheral enhancement (white arrow).

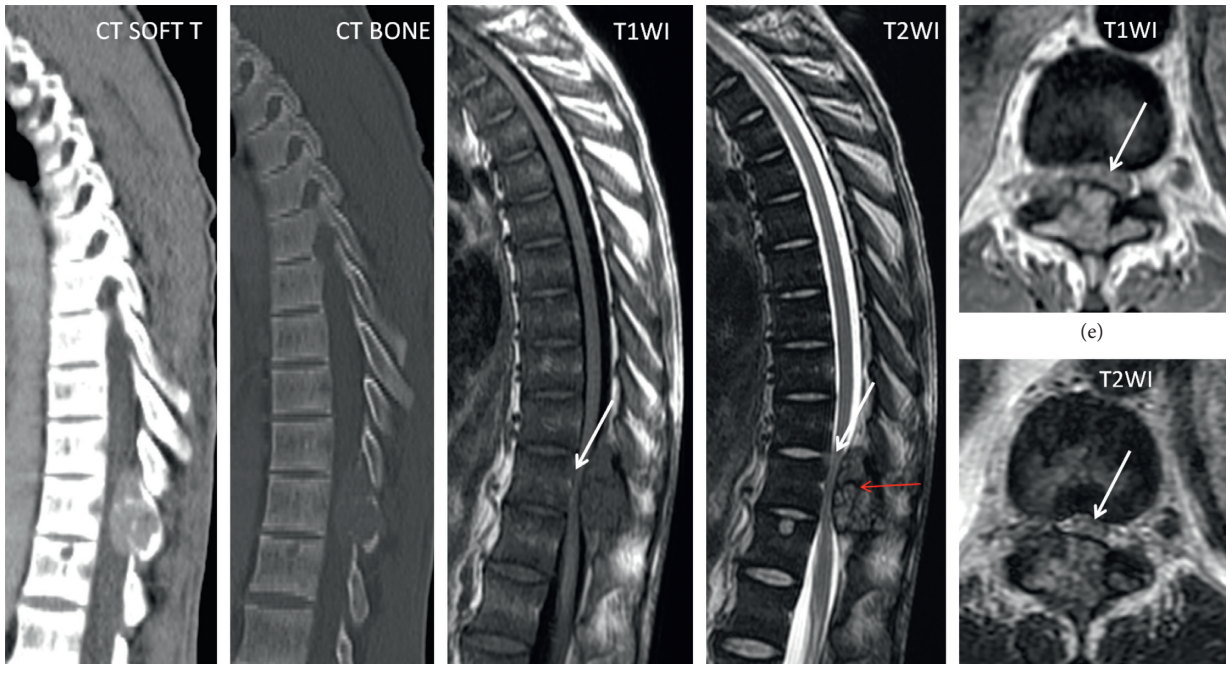

Figure 7: Thoracic spine brown tumor. Sagittal CT, sagittal T1WI/T2WI, and axial T1WI/T2WI MRI sequences show an expansible, well-circumscribed lesion in the posterior elements extending within the spinal canal, with severe spinal canal stenosis and compressed spinal cord (white arrow). Areas of low signal on T2W1 from hemosiderin are indicated by the red arrow.

skull of PHPT from other lesions of the calvarium, further confirmation with patient characteristics, clinical history, laboratory analysis, and imaging in combination is essential [32].

1.5. Osteopenia. Osteopenia is defined by the World Health Organization as a state of decreased bone density with a densitometry T-score of –1 to –2.5 standard deviations less than that of a young healthy reference

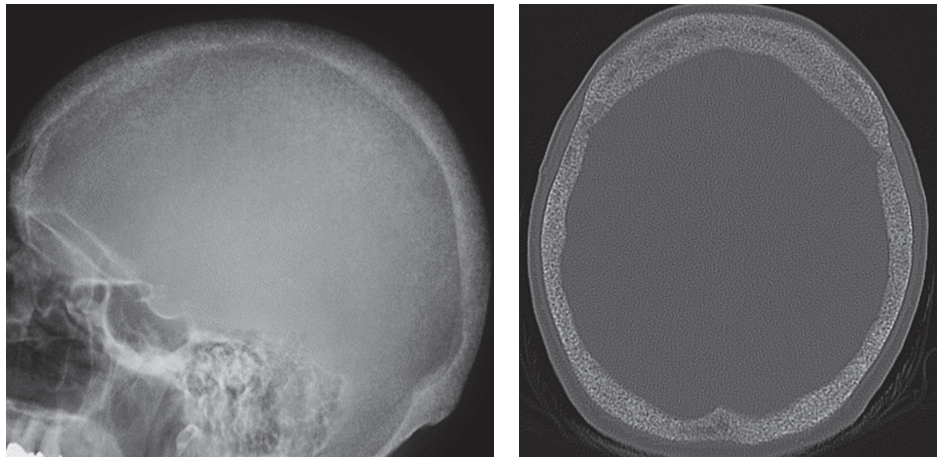

(a) (b)

Figure 8: "Salt-and-pepper-skull." Lateral skull X-ray and axial bone windows CT with salt-and-pepper appearance from trabecular bone resorption depicted as fine areas of lucency mixed with sclerotic radiopaque-denser-dot-like foci.

population [5, 36, 37]. In PHPT, mechanistically, there is resorption of secondary trabeculae (which corresponds to interlinking non-weight-bearing trabeculae) and accentuation of primary trabeculae (weight-bearing trabeculae) and overall decreased bone density due to the increased osteoclastic activity and vascularized fibrous tissue seen in PHPT. Generalized and asymmetric osteopenia is the most common skeletal finding in modern-day PHPT [7, 16, 31]. Recent studies cite the prevalence of osteoporosis in PHPT ranging from 39 to 62.9% [7]. The radiographic finding of decreased bone density (more lucent bones) requires 30–50% bone loss to be detected by human perception [14]. Other radiographic findings include accentuation vertical striation of primary trabeculae (coarse internal trabeculation (Figure 3)), which corresponds to weight-bearing vertically oriented ticked trabeculae within the lucent background. Cortical thinning appears as sharply demarcated distinction between cortex and medullary cavity due to accentuation of the cortical lining (Figures 3 and 4). It is important to note that decreased bone mineral density can also occur in senile, postmenopausal, and secondary causes of osteoporosis [38]. The osteopenia of PHPT preferentially affects the peripheral skeleton rather than the axial skeleton, which differs from the pattern seen in senile osteoporosis and postmenopausal women osteoporosis [38]. While PHPT is now commonly discovered as an asymptomatic disease, some studies have shown that bone mass loss in these patients is more than would be anticipated despite the lack of pathognomonic radiograph findings [12].

Currently, methods for assessing the severity of bone disease typically include radiographs, dual-energy and peripheral X-ray absorptiometry (DXA), and quantitative ultrasonography [39]. Additional technologies include high-resolution CT and a Trabecular Bone Score (TBS) to gauge osteoporotic fracture risk factors [40, 41]. Historically, the bone alterations seen in PHPT are described as having a predilection for cortical rather than trabecular osseous compartments. The mechanism of this finding is thought to be multifactorial, including an increased susceptibility of cortical bone to excess PTH over time and the nature of bone turnover in these regions [42, 43]. While trabecular bone has been previously viewed as relatively preserved in PHPT, emerging imaging techniques such as high-resolution CT suggest a significant correlation in conjunction with TBS in demonstrating both cortical and trabecular bone microalterations at sites such as the distal radius and tibia [44]. TBS is employed as an indirect measure of trabecular bone microarchitecture and is currently being researched as a useful complement to DXA measurements of bone [12, 45]. In a study of postmenopausal women with PHPT, TBS demonstrated trabecular network alterations in the presence of PHPT that are not readily directly detectable by DXA, notably in the microarchitectural analysis of the lumbar spine of asymptomatic patients with milder forms of disease [12, 44]. When correlated with transiliac bone biopsy in a cohort of male and female patients, TBS has also been shown to demonstrate value as a surrogate technique for analyzing trabecular bone microarchitecture alterations [46, 47].

Clinically, the bone demineralization seen in PHPT is important to recognize early on as osteopenia has potential to progress into frank osteoporosis and predispose patients to pathological fragility fractures in the spine and forearm [5, 14]. Of special consideration are fractures of the vertebrae, which are composed of roughly 70% cancellous bone and can be a presenting, clinically silent symptom in patients with mild, untreated PHPT despite a preference of PTH for cortical bone [7, 48, 49]. A population-based cohort study by Khosla et al. of patients diagnosed with PHPT showed that these patients exhibited increased vertebral, distal forearm, rib, pelvic, and overall risk of fracture with marginal increase in the risk of femoral fractures. This study supports the theory that excess levels of PTH have a significant effect on cancellous bone in addition to cortical bone [48]. The ability of trabecular imaging modalities to detect more extensive skeletal deterioration than previously demonstrated by conventional densitometric imaging is important, as it has led to discussions regarding expanding evaluation and

criteria for definitive parathyroidectomy in patients with PHPT [50].

In patients with decreased bone mineral density associated with PHPT (Figure 4), parathyroidectomy helps to restore bone health [12]. In a subset of patients with PHPT and low lumbar spine bone density, up to a 20% remineralization has been seen 4 years post-op from parathyroidectomy [14, 51]. At time frames of 6 months post-op, several studies have shown BMD improvements at the lumbar spine and hips [43, 52]. Additionally, PHPT's demineralizing effect on cortical bone at the femoral neck and distal one-third radius has been found to be at least partially reversible by parathyroidectomy 10–15 years post-op [14, 43]. There is evidence to suggest a sustained, gradual increase in femoral neck BMD that can occur after parathyroidectomy [46]. Overall, parathyroidectomy is seen as the curative and definitive treatment of this condition with significant improvements to BMD and reductions in nephrolithiasis, although it is unclear as to whether there are marked improvements in bone strength and fragility fracture risk [7, 14, 28].

2. Conclusion

The bone imaging manifestations of PHPT are diverse with skeletal findings on radiographs that are very characteristic of the disease. The common symptomatic osseous findings include subperiosteal and subchondral joint resorption, acroosteolysis, the salt-and-pepper skull, the brown tumors of OFC, and osteopenia. Knowledge of the classic imaging patterns and differential diagnosis in combination with the clinical picture of PHPT is invaluable for informing clinicians in preventing misdiagnosis, providing earlier intervention, and counseling patients on what is a curable disease with resultant improvement in imaging pathology.

Abbreviations

HPT:	Hyperparathyroidism
PTH:	Parathyroid hormone
PHPT:	Primary hyperparathyroidism
RANKL:	Nuclear factor-$\kappa\beta$ ligand
RANK:	Nuclear factor-$\kappa\beta$
OFC:	Osteitis fibrosa cystica
CT:	Computed tomography
MRI:	Magnetic resonance imaging
WI:	Weighted images
DXA:	Dual-energy X-ray absorptiometry
TBS:	Trabecular bone score
25(OH)D:	25-Hydroxy-vitamin D
1,25-(OH)2D:	1,25-Dihydroxy-vitamin D.

Conflicts of Interest

The authors declare that they have no conflicts of interest regarding the publication of this paper.

Acknowledgments

The authors acknowledge J. Szklaruk, Ph.D., M.D., at MD Anderson Cancer Center, Houston, TX, USA, for providing Figure 6 in this article.

References

[1] J. P. Bilezikian, N. E. Cusano, A. A. Khan, J.-M. Liu, C. Marcocci, and F. Bandeira, "Primary hyperparathyroidism nature reviews," *Disease Primers*, vol. 2, p. 16033, 2016.

[2] J. P. Bilezikian, M. L. Brandi, R. Eastell et al., "Guidelines for the management of asymptomatic primary hyperparathyroidism: summary statement from the fourth international workshop," *The Journal of Clinical Endocrinology & Metabolism*, vol. 99, no. 10, pp. 3561–3569, 2014.

[3] J. Bollerslev, C. Schalin-Jäntti, L. Rejnmark et al., "Unmet therapeutic, educational and scientific needs in parathyroid disorders: consensus statement from the first European society of endocrinology workshop (PARAT)," *European Journal of Endocrinology*, vol. 181, no. 3, 2019.

[4] M. Zini, R. Attanasio, R. Cesareo et al., "AME position statement: primary hyperparathyroidism in clinical practice," *Journal of Endocrinological Investigation*, vol. 35, no. 7, pp. 2–21, 2012.

[5] C. Y. Chang, D. I. Rosenthal, D. M. Mitchell, A. Handa, S. V. Kattapuram, and A. J. Huang, "Imaging findings of metabolic bone disease," *RadioGraphics*, vol. 36, no. 6, pp. 1871–1887, 2016.

[6] A. Khan and J. Bilezikian, "Primary hyperparathyroidism: pathophysiology and impact on bone," *CMAJ: Canadian Medical Association Journal*, vol. 163, no. 2, pp. 184–187, 2000.

[7] M. D. Walker and S. J. Silverberg, "Primary hyperparathyroidism," *Nature Reviews Endocrinology*, vol. 14, no. 2, pp. 115–125, 2018.

[8] L. Rolighed, L. Rejnmark, and P. Christiansen, "Bone involvement in primary hyperparathyroidism and changes after parathyroidectomy," *European Endocrinology*, vol. 10, no. 1, pp. 84–87, 2014.

[9] D. M. Press, A. E. Siperstein, E. Berber et al., "The prevalence of undiagnosed and unrecognized primary hyperparathyroidism: a population-based analysis from the electronic medical record," *Surgery*, vol. 154, no. 6, pp. 1232–1238, 2013.

[10] B. C. Silva, N. E. Cusano, and J. P. Bilezikian, "Primary hyperparathyroidism," *Best Practice & Research Clinical Endocrinology & Metabolism*, vol. 32, no. 5, pp. 593–607, 2018.

[11] P. V. Pradeep, B. Jayashree, A. Mishra, and S. K. Mishra, "Systematic review of primary hyperparathyroidism in India: the past, present, and the future trends," *International Journal of Endocrinology*, vol. 10, 2011.

[12] F. Bandeira, N. E. Cusano, B. C. Silva et al., "Bone disease in primary hyperparathyroidism," *Arquivos Brasileiros de Endocrinologia & Metabologia*, vol. 58, no. 5, pp. 553–561, 2014.

[13] M. D. Murphey, D. J. Sartoris, J. L. Quale, M. N. Pathria, and N. L. Martin, "Musculoskeletal manifestations of chronic renal insufficiency," *Radiographics*, vol. 13, no. 2, pp. 357–379, 1993.

[14] C. Marcocci, L. Cianferotti, and F. Cetani, "Bone disease in primary hyperparathyrodism," *Therapeutic Advances in Musculoskeletal Disease*, vol. 4, no. 5, pp. 357–368, 2012.

[15] B. J. Manaster, "Diagnostic imaging: non-traumatic disease," 2010.

[16] Imaging in primary hyperparathyroidism: practice essentials, radiography, magnetic resonance imaging," 2017.
[17] D. Resnick and G. Niwayama, "Subchondral resorption of bone in renal osteodystrophy," *Radiology*, vol. 118, no. 2, pp. 315–321, 1976.
[18] A. Jouan, L. Zabraniecki, V. Vincent, E. Poix, and B. Fournié, "An unusual presentation of primary hyperparathyroidism: severe hypercalcemia and multiple brown tumors," *Joint Bone Spine*, vol. 75, no. 2, pp. 209–211, 2008.
[19] T. Takeshita, H. Tanaka, A. Harasawa, T. Kaminaga, T. Imamura, and S. Furui, "Brown tumor of the sphenoid sinus in a patient with secondary hyperparathyroidism: CT and MR imaging findings," *Radiation Medicine*, vol. 22, no. 4, pp. 265–268, 2004.
[20] M. R. Khalatbari and Y. Moharamzad, "Brown tumor of the spine in patients with primary hyperparathyroidism," *Spine*, vol. 39, no. 18, pp. E1073–E1079, 2014.
[21] B. Solmaz, N. Tatarlı, F. Günver, and T. Emre, "A thoracic vertebral Brown tumor presenting with paraparesis in a patient with end-stage renal disease," *British Journal of Neurosurgery*, vol. 31, no. 6, pp. 635–637, 2017.
[22] W. S. Hong, M. S. Sung, K.-A. Chun et al., "Emphasis on the mr imaging findings of Brown tumor: a report of five cases," *Skeletal Radiology*, vol. 40, no. 2, pp. 205–213, 2011.
[23] R. Vaishya, K. Amit, and H. Singh, "Multiple "brown tumors" masquerading as metastatic bone disease," *World Neurosurgery*, vol. 12, 2019.
[24] K. M. Fargen, S. Christine, and J. A. Lin, "Vertebral Brown tumors causing neurologic compromise," *World Neurosurgery*, vol. 79, no. 1, 2013.
[25] D. Salamone, S. Muresan, M. Muresan, and N. Radu, "Multilevel Brown tumors of the spine in a patient with severe secondary hyperparathyroidism A case report and review of the literature," *Annali Italiani Di Chirurgia*, vol. 87, 2016.
[26] E. Sonmez, T. Tezcaner, I. Coven, and A. Terzi, "Brown tumor of the thoracic spine: first manifestation of primary hyperparathyroidism," *Journal of Korean Neurosurgical Society*, vol. 58, no. 4, pp. 389–392, 2015.
[27] N. G. Knowles, D. L. Smith, and E. K. Outwater, "MRI diagnosis of Brown tumor based on magnetic susceptibility," *Journal of Magnetic Resonance Imaging*, vol. 28, no. 3, pp. 759–761, 2008.
[28] A. A. Khan, D. A. Hanley, R. Rizzoli et al., "Primary hyperparathyroidism: review and recommendations on evaluation, diagnosis, and management. A Canadian and international consensus," *Osteoporosis International*, vol. 28, no. 1, pp. 1–19, 2017.
[29] J. A. Reséndiz-Colosia, S. A. Rodríguez-Cuevas, R. Flores-Díaz et al., "Evolution of maxillofacial Brown tumors after parathyroidectomy in primary hyperparathyroidism," *Head & Neck*, vol. 30, no. 11, pp. 1497–1504, 2008.
[30] Q. Yang, J. Li, Z. Yang et al., "Skeletal lesions in primary hyperparathyroidism," *The American Journal of the Medical Sciences*, vol. 349, no. 4, pp. 321–327, 2015.
[31] T. Glushko, S. S. A. Banjar, A. Nahal, and I. Colmegna, "Brown tumor of the pelvis," *Cleveland Clinic Journal of Medicine*, vol. 82, no. 12, pp. 799-800, 2015.
[32] C. K. Gomez, S. R. Schiffman, and A. A. Bhatt, "Radiological review of skull lesions," *Insights Into Imaging*, vol. 9, no. 5, pp. 857–882, 2018.
[33] D. Popovik-Monevska, S. Bozovik-Dvojakovska, V. Popovski, A. Benedetti, A. Grchev, and F. Koneski, "Brown tumour in the mandible and skull osteosclerosis associated with primary hyperparathyroidism—a case report," *Open Access Macedonian Journal of Medical Sciences*, vol. 6, no. 2, pp. 406–409, 2018.
[34] L. Bandeira and J. Bilezikian, "Primary hyperparathyroidism," *F1000Research*, vol. 5, 2016.
[35] D. M. Marchiori, "Chapter 16—skull patterns," *Clinical Imaging*, vol. 12, 2014.
[36] J. A. Kanis, D. Black, C. Cooper et al., "A new approach to the development of assessment guidelines for osteoporosis," *Osteoporosis International*, vol. 13, no. 7, pp. 527–536, 2002.
[37] S. Khosla and L. J. Melton, "Osteopenia," *New England Journal of Medicine*, vol. 356, no. 22, pp. 2293–2300, 2007.
[38] J. F. Griffith and H. K. Genant, "Chapter 64—imaging of osteoporosis," in *Osteoporosis*, Academic Press, San Diego, CA, USA, 2013.
[39] S. Minisola, L. Gianotti, S. Bhadada, and S. J. Silverberg, "Classical complications of primary hyperparathyroidism," *Best Practice & Research Clinical Endocrinology & Metabolism*, vol. 32, no. 6, pp. 791–803, 2018.
[40] B. C. Silva, S. B. Broy, S. Boutroy, J. T. Schousboe, J. A. Shepherd, and W. D. Leslie, "Fracture risk prediction by non-BMD DXA measures: the 2015 ISCD official positions Part 2: trabecular bone score," *Journal of Clinical Densitometry*, vol. 18, no. 3, pp. 309–330, 2015.
[41] S. Boutroy, M. L. Bouxsein, F. Munoz, and P. D. Delmas, "In VivoAssessment of trabecular bone microarchitecture by high-resolution peripheral quantitative computed tomography," *The Journal of Clinical Endocrinology & Metabolism*, vol. 90, no. 12, pp. 6508–6515, 2005.
[42] A. M. Parfitt, "Accelerated cortical bone loss: primary and secondary hyperparathyroidism," in *Current Concepts of Bone Fragility*, Springer, Berlin, Heidelberg, 1986.
[43] M. R. Rubin, J. P. Bilezikian, D. J. McMahon et al., "The natural history of primary hyperparathyroidism with or without parathyroid surgery after 15 years," *The Journal of Clinical Endocrinology & Metabolism*, vol. 93, no. 9, pp. 3462–3470, 2008.
[44] B. C. Silva, S. Boutroy, C. Zhang et al., "Trabecular bone score (TBS)-A novel method to evaluate bone microarchitectural texture in patients with primary hyperparathyroidism," *The Journal of Clinical Endocrinology & Metabolism*, vol. 98, no. 5, pp. 1963–1970, 2013.
[45] M. Warzecha, E. Czerwiński, J. Amarowicz, and M. Berwecka, "Trabecular bone score (TBS) in clinical practice—rewiev," *Ortopedia Traumatologia Rehabilitacja*, vol. 20, no. 5, pp. 347–359, 2018.
[46] C. Cipriani, A. Abraham, B. C. Silva et al., "Skeletal changes after restoration of the euparathyroid state in patients with hypoparathyroidism and primary hyperparathyroidism," *Endocrine*, vol. 55, no. 2, pp. 591–598, 2017.
[47] C. Muschitz, R. Kocijan, J. Haschka et al., "TBS reflects trabecular microarchitecture in premenopausal women and men with idiopathic osteoporosis and low-traumatic fractures," *Bone*, vol. 79, pp. 259–266, 2015.
[48] S. Khosla, L. J. Melton, R. A. Wermers, C. S. Crowson, W. M. O'Fallon, and B. L. Riggs, "Primary hyperparathyroidism and the risk of fracture: a population-based study," *Journal of Bone and Mineral Research*, vol. 14, no. 10, pp. 1700–1707, 1999.
[49] E. Vignali, G. Viccica, D. Diacinti et al., "Morphometric vertebral fractures in postmenopausal women with primary hyperparathyroidism," *The Journal of Clinical Endocrinology & Metabolism*, vol. 94, no. 7, pp. 2306–2312, 2009.

[50] M. D. Walker and J. P. Bilezikian, "Primary hyperparathyroidism," *Current Opinion in Rheumatology*, vol. 30, no. 4, pp. 427–439, 2018.

[51] S. J. Silverberg, F. G. Locker, J. P. Bilezikian et al., "Vertebral osteopenia: a new indication for surgery in primary hyperparathyroidism," *Journal of Clinical Endocrinology & Metabolism*, vol. 81, no. 11, pp. 4007–4012, 1996.

[52] N. E. Cusano, M. R. Rubin, and J. P. Bilezikian, "Skeletal microstructure and estimated bone strength improve following parathyroidectomy in primary hyperparathyroidism," *The Journal of Clinical Endocrinology & Metabolism*, vol. 103, no. 1, pp. 196–205, 2018.

Hindawi
International Journal of Endocrinology
Volume 2020, Article ID 9649564, 15 pages
https://doi.org/10.1155/2020/9649564

Review Article

Localization of Parathyroid Disease in Reoperative Patients with Primary Hyperparathyroidism

Aaroh M. Parikh[1,2] **Raymon H. Grogan**,[3] **and Fanny E. Morón**[4]

[1]*School of Medicine, Baylor College of Medicine, Houston, TX 77030, USA*
[2]*Department of Internal Medicine, Santa Clara Valley Medical Center, San Jose, CA 95128, USA*
[3]*Michael E. DeBakey Department of Surgery, Baylor College of Medicine, Houston, TX 77030, USA*
[4]*Department of Radiology, Baylor College of Medicine, Houston, TX 77030, USA*

Correspondence should be addressed to Fanny E. Morón; fmoron@bcm.edu

Received 22 August 2019; Accepted 20 November 2019; Published 25 January 2020

Academic Editor: Thomas J. Fahey

The localization of persistent or recurrent disease in reoperative patients with primary hyperparathyroidism presents challenges for radiologists and surgeons alike. In this article, we summarize the relevant imaging modalities, compare their accuracy in identifying reoperative disease, and outline their advantages and disadvantages. Accurate localization by preoperative imaging is a predictor of operative success, whereas negative or discordant preoperative imaging is a risk factor for operative failure. Ultrasound is a common first-line modality because it is inexpensive, accessible, and radiation-free. However, it is highly operator-dependent and less accurate in the reoperative setting than in the primary setting. Sestamibi scintigraphy is superior to ultrasound in localizing reoperative disease but requires radiation, prolonged imaging times, and reader experience for accurate interpretation. Like ultrasound, sestamibi scintigraphy is less accurate in the reoperative setting because reoperative patients can exhibit distorted anatomy, altered perfusion of remaining glands, and interference of radiotracer uptake. Meanwhile, four-dimensional computed tomography (4DCT) is superior to ultrasound and sestamibi scintigraphy in localizing reoperative disease but requires the use of radiation and intravenous contrast. Both 4DCT and magnetic resonance imaging (MRI) do not significantly differ in accuracy between unexplored and reoperative patients. However, MRI is more costly, inaccessible, and time-consuming than 4DCT and is inappropriate as a first-line modality. Hybrid imaging with positron emission tomography and computed tomography (PET/CT) may be a promising second-line modality in the reoperative setting, particularly when first-line modalities are discordant or inconclusive. Lastly, selective venous sampling should be reserved for challenging cases in which noninvasive modalities are negative or discordant. In the challenging population of reoperative patients with PHPT, a multimodality approach that utilizes the expertise of high-volume centers can accurately localize persistent or recurrent disease and enable curative parathyroidectomy.

1. Introduction

Reoperation in patients with primary hyperparathyroidism (PHPT) presents unique challenges for both radiologists and surgeons. Although the vast majority of patients with PHPT undergo curative initial exploration, between 2 and 10% of patients develop persistent or recurrent disease after initial surgery [1–9]. Persistent PHPT (pPHPT) is defined as elevated serum calcium and parathyroid hormone (PTH) levels within 6 months of initial surgery. Recurrent PHPT (rPHPT) is defined as elevated serum calcium and PTH levels more than 6 months after successful surgery. Accurate preoperative localization has enabled minimally invasive parathyroidectomy to be as successful as traditional bilateral approaches [2, 4, 10]. In the reoperative setting, repeat surgery is not recommended unless the lesion can be well-localized.

In this article, we review the localization of parathyroid disease in the reoperative setting. We summarize the relevant imaging modalities, compare their accuracy in identifying reoperative disease, and outline their advantages and disadvantages.

2. Common Causes of Initial Postsurgical Failure

The most common causes of failed initial parathyroidectomy include missed orthotopic adenoma, ectopic adenoma, and multigland disease (encompassing both multiple adenomas and multigland hyperplasia), whereas less common causes include parathyroid carcinoma, regrowth of a partially resected gland, and parathyromatosis from inadvertent seeding of parathyroid cells during prior exploration [1, 11–17]. While some studies report that multigland disease accounts for more than half of all reoperative cases [3, 11], most studies attribute the majority of reoperative cases (as high as 79%) to the failed detection of a single adenoma [1, 13, 15–19]. Although ectopic adenomas may be up to four times as common in the reoperative setting than in the primary setting [11, 18, 20, 21], the majority of missed single adenomas are orthotopic [4, 14, 19, 22, 23]. Multiple endocrine neoplasia type 1 (MEN1) specifically accounts for between 8.5 and 10.3% of all reoperative cases, causing both pPHPT and rPHPT [11, 15]. More than one-third of patients with MEN1 are undiagnosed upon initial operation, and approximately half develop persistent disease after initial operation [24]. Rarer causes of initial failure include parathyromatosis (Figure 1), parathyroid carcinoma, and adenoma arising from autotransplanted parathyroid glands following surgical exploration (Figures 1 and 2), each accounting for ≤3% of reoperative cases [12, 19, 25, 26]. The development of a second adenoma in a previously normal gland is rare except for in patients with prior neck radiation [27].

3. Role of Preoperative Imaging

Imaging is not diagnostic of PHPT but is used to localize disease prior to surgical exploration. Indications for preoperative imaging include determining candidacy for minimally invasive parathyroidectomy, assessing for ectopic glands, assessing for concurrent thyroid neoplasia, and evaluating persistent or recurrent disease after prior parathyroidectomy [28, 29]. Accurate preoperative localization identifies ectopic glands, decreases operating time, decreases the likelihood of surgical complications, and improves the success rate of parathyroidectomy [11, 30, 31]. Meanwhile, negative or discordant preoperative imaging is a risk factor for persistent disease after surgical exploration [3, 32], with initial surgical failure rates higher than those for well-localized glands [28, 32]. Rates of inconclusive first-line imaging have been reported as high as 63% in the reoperative setting [12]. Particularly in this challenging population, the expertise of high-volume centers may increase the yield from preoperative imaging modalities [33].

4. Surgical Reexploration

Before proceeding to repeat surgical exploration, patients with pPHPT or rPHPT should have their diagnosis biochemically reconfirmed and undergo additional (repeat) preoperative imaging localization, alongside a full review of prior imaging and operative findings [34]. In addition, patients need to be reassessed for symptoms associated with PHPT to ensure that they have an indication for reoperation.

Reoperation can be technically challenging due to scarring and obliteration of tissue planes, obscuring of normal anatomy of recurrent and superior laryngeal nerves, and encasement of abnormal parathyroid glands in scar tissue following initial surgery [4, 29]. Due to the difficulties of localizing and excising abnormal glands in the reoperative setting, repeat parathyroidectomy used to have operative success rates between 82 and 90%, lower than the analogous rates for initial exploration [35, 36]. Today, however, surgical cure rates in the reoperative setting are reported between 86 and 100%, with a meta-analysis by Singh Ospina and colleagues reporting a cure rate of 98% with bilateral neck exploration and 97% with minimally invasive parathyroidectomy [4, 12, 13, 37–41]. Common complications after reoperation include injury to the recurrent laryngeal nerve and permanent hypoparathyroidism, the reported frequencies of which vary widely from 0 to 15% for each [4, 12, 22, 40–42]. Given the challenges that accompany reoperative parathyroidectomy, it is crucial to seek the expertise of high-volume and experienced parathyroid surgeons when assessing a patient with pPHPT or rPHPT [7, 34].

5. Ultrasound

Ultrasound is a common first-line modality used to preoperatively localize parathyroid adenomas. Ultrasound localization requires examination of the anterior cervical region using a high-frequency linear transducer. Parathyroid adenomas appear round or ovoid, well-circumscribed, homogeneous, and hypoechoic relative to thyroid tissue (Figure 1). Doppler interrogation often identifies a polar vessel or peripheral rim of vascularity surrounding the adenomatous gland (Figure 1). Ultrasound also guides fine-needle aspiration of possible parathyroid lesions, albeit accompanied by the risk of causing fibrosis of the adenoma and surrounding tissues. Meta-analysis of preoperative ultrasound has determined a pooled sensitivity of 76% and a pooled positive predictive value (PPV) of 93% for localizing abnormal parathyroid glands in *de novo* patients with PHPT [43]. However, the accuracy of ultrasound decreases in the reoperative setting. In patients with pPHPT or rPHPT undergoing reoperative parathyroidectomy, the sensitivity of ultrasound for localizing abnormal glands ranges between 54 and 68% [4, 15, 23, 44]. Although there are studies that report analogous sensitivities between 20 and 40%, such studies include very few reoperative patients [45] or use samples that specifically required a second-line modality for accurate localization [37]. Furthermore, ultrasound possesses significantly lower sensitivity (often reported near 40%) in patients with multigland disease, a population that frequently requires reoperation [2, 37, 39, 45]. A systematic review of 20,225 cases of PHPT determined that the sensitivity of preoperative ultrasound is 79% for localizing solitary adenomas but decreases to 34.9% for localizing

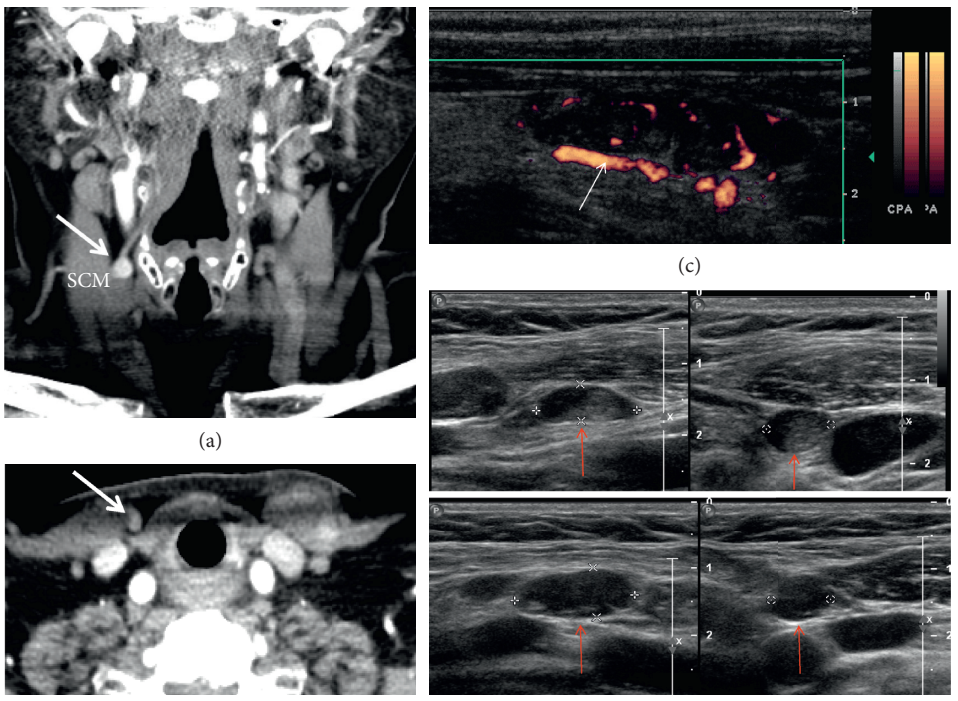

Figure 1: Autotransplanted parathyroid gland and parathyromatosis. A 70-year-old female presents with hyperparathyroidism after remote thyroidectomy. Coronal (a) and axial (b) four-dimensional computed tomography (4DCT) shows a hyperenhancing parathyroid gland (thick arrows) superficial to the right sternocleidomastoid muscle (SCM). Power Doppler ultrasound (c) of the autotransplanted hypoechoic nodule shows a polar feeding vessel (thin arrow) and peripheral rim of vascularity. Additional well-circumscribed mostly hypoechoic nodules consistent with multiple implants of parathyroid tissue (d) (red arrows) are also visualized.

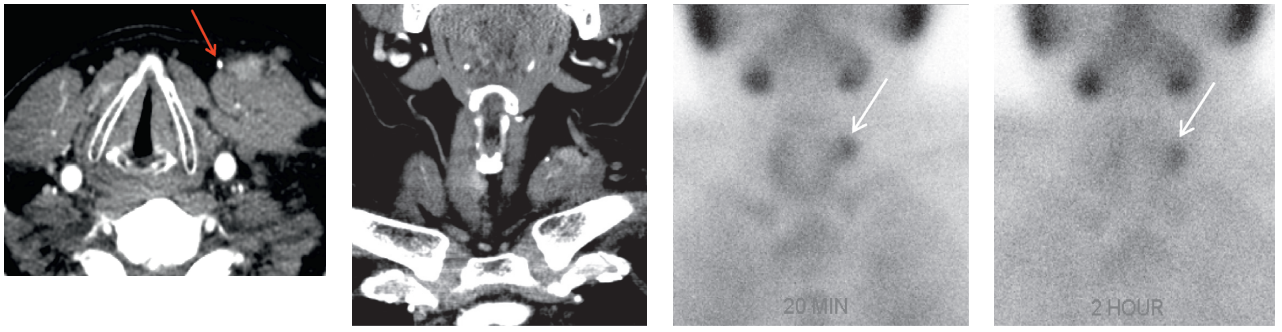

Figure 2: Hyperfunctioning autotransplanted parathyroid remnant. A 50-year-old male with multiple endocrine neoplasia type 1 (MEN1) presents with recurrent disease after prior parathyroidectomy. Axial (a) and coronal (b) four-dimensional computed tomography (4DCT) images show an irregular enhancing focus (white arrows) superficial to the left SCM muscle, lateral to a surgical clip (red arrow). Planar immediate (c) (20 minutes) and delayed (d) (two hours) single-photon emission computed tomography (SPECT) images demonstrate focal radiotracer accumulation (white arrows) in the left lateral neck that persists on delayed images and confirms the diagnosis of the hyperfunctioning parathyroid gland.

multigland hyperplasia and 16.2% for localizing double adenomas [2].

Ultrasound is an attractive first-line modality because it is inexpensive, accessible, and radiation-free. It also enables fine-needle aspiration of suspected parathyroid lesions and evaluation of concurrent thyroid pathology. However, ultrasound is subject to several limitations. It is highly operator-dependent and is often insensitive to multigland parathyroid disease [2, 28, 37, 39, 45–47]. Ultrasound frequently fails to localize adenomatous glands in obese patients or in sonographically inaccessible locations (e.g., mediastinal, tracheoesophageal groove, retroesophageal, and retroclavicular) [21, 28, 46, 47]. Ultrasound is well-suited as a first-line modality in both primary and reoperative settings, particularly at high-volume institutions where radiologists and surgeons have familiarity and confidence with the

modality. Nevertheless, patients with pPHPT or rPHPT should still undergo additional imaging studies for more accurate preoperative localization.

6. Sestamibi Scintigraphy

Sestamibi scintigraphy is frequently used to identify abnormal parathyroid glands. The most common protocol consists of dual-phase single-isotope scintigraphy using the ^{99m}Tc sestamibi radiotracer. The radiotracer concentrates in the mitochondria of metabolically active tissues, such as the mitochondria-rich oxyphil cells of hyperfunctioning parathyroid glands [48]. The early phase (15 minutes after injection) demonstrates radiotracer uptake in both thyroid and parathyroid glands. The delayed phase (120 minutes after injection) demonstrates washout of the radiotracer from normal tissue but retention of the radiotracer in hyperfunctioning parathyroid glands (Figures 2 and 3). Meta-analysis of dual-phase ^{99m}Tc sestamibi scintigraphy has demonstrated a pooled sensitivity of 63% and a pooled PPV of 90% for localizing abnormal glands in patients with PHPT [49]. However, like that of ultrasound, the accuracy of sestamibi scintigraphy decreases in the reoperative setting (Figure 4). In patients with pPHPT or rPHPT undergoing reoperative parathyroidectomy, the sensitivity of ^{99m}Tc sestamibi scintigraphy for localizing parathyroid adenomas ranges from 53 to 74% [4, 23, 50]. Single-photon emission computed tomography (SPECT) and hybrid imaging with both SPECT and computed tomography (SPECT/CT) offer additional anatomic visualization that aids in surgical planning (Figure 3). However, the addition of SPECT and SPECT/CT does not markedly change the sensitivity of the technique (between 69 and 74%) [44, 51]. A small number of studies have investigated the use of ^{123}I/^{99m}Tc subtraction scintigraphy in the reoperative setting with sensitivities reported as high as 81%, leading some to advocate for its use over traditional single-tracer scintigraphy (Figure 5) [15, 40, 50, 52]. Dual-phase ^{99m}Tc sestamibi scintigraphy is significantly less accurate at localizing multigland disease as compared to single-gland disease, with sensitivities reported between 23 and 45% [2, 37, 39, 45, 50]. A 2005 meta-analysis reported that the sensitivity of preoperative sestamibi scintigraphy decreases from 88.4% for localizing solitary adenomas to 44.5% for localizing multigland hyperplasia and 30.0% for localizing double adenomas [2].

Sestamibi scintigraphy is an operator-independent modality that offers both functional and anatomic information when supplemented by computed tomography as in SPECT/CT. Although sestamibi scintigraphy is a commonly used first-line modality in both primary and reoperative settings, it possesses clear limitations. Sestamibi scintigraphy requires relatively long imaging times as well as radiation exposure. It also requires experience to interpret accurately, underscoring the importance of seeking a high-volume radiologist. It is quite limited in both its anatomic resolution and its ability to localize small parathyroid glands or multigland disease (in which glands tend to be only mildly enlarged) [14, 28, 53–55]. There are several factors that may explain why the accuracy of preoperative sestamibi scintigraphy decreases in the setting of persistent or recurrent disease. Dual-phase sestamibi techniques often fail to localize hyperplastic glands (which are a common cause for reoperation) because they do not retain the radiotracer during the late phase [56–59]. Patients having undergone prior exploration may exhibit distorted anatomy, altered perfusion of remaining glands, and interference of ^{99m}Tc uptake, all of which decrease the accuracy of sestamibi scintigraphy in the reoperative setting [60–62]. Despite these drawbacks, sestamibi scintigraphy still possesses a higher sensitivity than ultrasound for localizing reoperative disease, ectopic disease, and multigland disease [2, 4, 21, 37, 46]. Consequently, sestamibi scintigraphy remains an adequate first-line modality for preoperatively localizing reoperative disease.

7. Four-Dimensional Computed Tomography

The advent of four-dimensional computed tomography (4DCT) has facilitated accurate preoperative localization of abnormal parathyroid glands. 4DCT consists of multiphase computed tomography—often using noncontrast, arterial, and delayed (venous) phases—to detect changes in enhancement over time. Parathyroid adenomas exhibit low attenuation (compared to normal thyroid tissue) on noncontrast images, peak enhancement during the arterial phase, and washout of contrast in the delayed phase (Figures 6 and 7). As a first-line study in *de novo* or uncomplicated patients with PHPT, 4DCT has sensitivity to localization between 62 and 92% and a PPV between 88 and 94% [28]. In the reoperative setting, 4DCT has sensitivity for localization as high as 93% and sensitivity for lateralization as high as 97% [28, 37, 60, 63–65]. However, this modality exhibits variable accuracy in patients with multigland disease (Figure 6). Although 4DCT can correctly predict multigland disease in 80 to 90% of patients with surgically proven multigland disease (in studies that pooled both *de novo* and reoperative patients) [60, 65], its sensitivity for accurate localization of multigland disease ranges from 43 to 69% [37, 45, 66, 67]. Between 57 and 75% of lesions missed by 4DCT in the reoperative setting constitute multigland disease [64, 68]. In addition to comprising a substantial proportion of reoperative patients, patients with multigland disease are also more likely to have milder hypercalcemia and smaller lesions than patients with single-gland disease [67, 69]. 4DCT is significantly more accurate than sestamibi scintigraphy at lateralizing parathyroid lesions in patients with mild hypercalcemia (<10.8 mg/dL) and low gland weights (<0.5 g) [70]. Another risk factor for requiring reoperation is nonlocalizing, inconclusive, or discordant first-line imaging studies (Figure 4). When used as a second-line modality in patients with nonlocalizing, inconclusive, or discordant prior imaging, 4DCT has sensitivity for localization between 67 and 89% and a PPV between 65 and 87% (Figure 4) [28, 45, 71]. In a study of reoperative patients specifically with negative ultrasound and sestamibi scintigraphy, 4DCT had sensitivity for localization of 50% and a PPV of 100% [72].

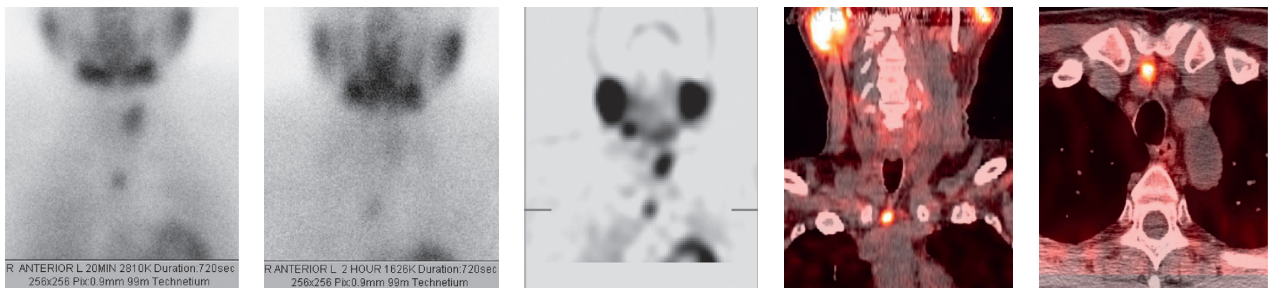

(a) (b) (c) (d) (e)

Figure 3: Ectopic mediastinal adenoma. A 56-year-old female presents with persistent hyperparathyroidism after prior four-gland parathyroidectomy and right thyroid lobectomy. Planar sestamibi scintigraphy at 20 minutes (a) and two hours (b) and coronal single-photon emission computed tomography (SPECT) (c) show a hypermetabolic mediastinal gland. Coronal (d) and axial (e) hybrid SPECT and computed tomography (SPECT/CT) confirm an ectopic and adenomatous fifth gland in the anterior mediastinum.

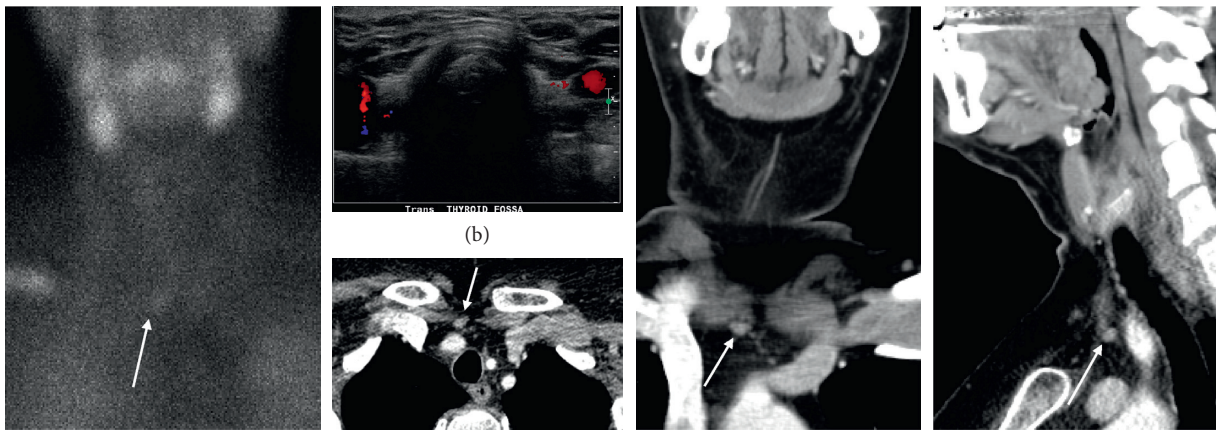

(a) (b) (c) (d) (e)

Figure 4: Inconclusive sestamibi scintigraphy versus ultrasound with successful localization by four-dimensional computed tomography (4DCT). A 49-year-old female with multiple endocrine neoplasia type 1 (MEN1) and remote prior three-gland parathyroidectomy presents with recurrent hyperparathyroidism. Planar delayed (two hours) sestamibi scintigraphy (a) shows a questionable-inconclusive enlarged right hypermetabolic parathyroid gland in the superior mediastinum (white arrow). Ultrasound with Doppler interrogation (b) is negative for recurrence. Axial (c), coronal (d), and sagittal (e) arterial phase 4DCT was performed to clarify discordant first-line findings and confirm a small hyperenhancing and ectopic right intrathymic parathyroid adenoma (white arrows).

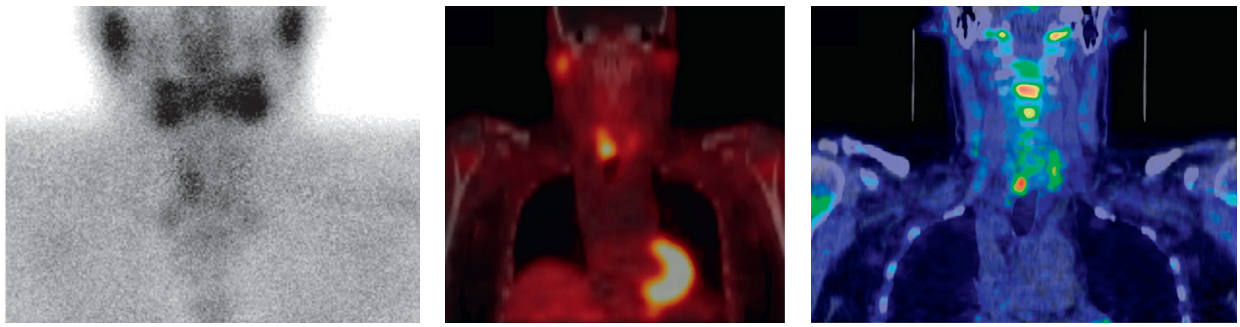

(a) (b) (c)

Figure 5: Persistent hyperparathyroidism. Preoperative $^{123}I/^{99m}Tc$ subtraction scintigraphy (a), ^{99m}Tc sestamibi hybrid single-photon emission computed tomography and computed tomography (SPECT/CT) (b), and ^{11}C-methionine hybrid positron emission tomography and computed tomography (PET/CT) (c) correctly localized the pathologic parathyroid gland (bottom right). Histology demonstrated parathyroid glandular hyperplasia (figure reused with permission).

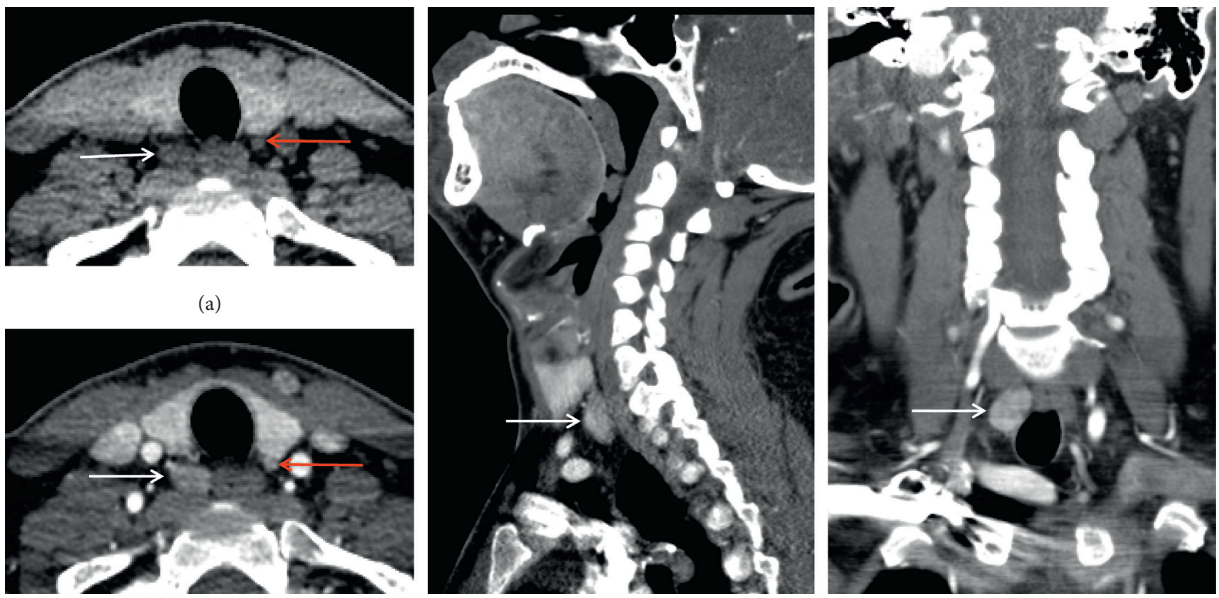

Figure 6: Multigland disease on four-dimensional computed tomography (4DCT). A 44-year-old female presents with recurrent hyperparathyroidism after prior right inferior parathyroidectomy. Axial precontrast (a) and postcontrast (b) early arterial phases show a moderately enhancing overly descended right superior parathyroid adenoma (white arrows) and a small hyperenhancing orthotopic left inferior parathyroid adenoma (red arrows). Coronal (c) and sagittal (d) views similarly demonstrate the overly descended right superior parathyroid adenoma (white arrows).

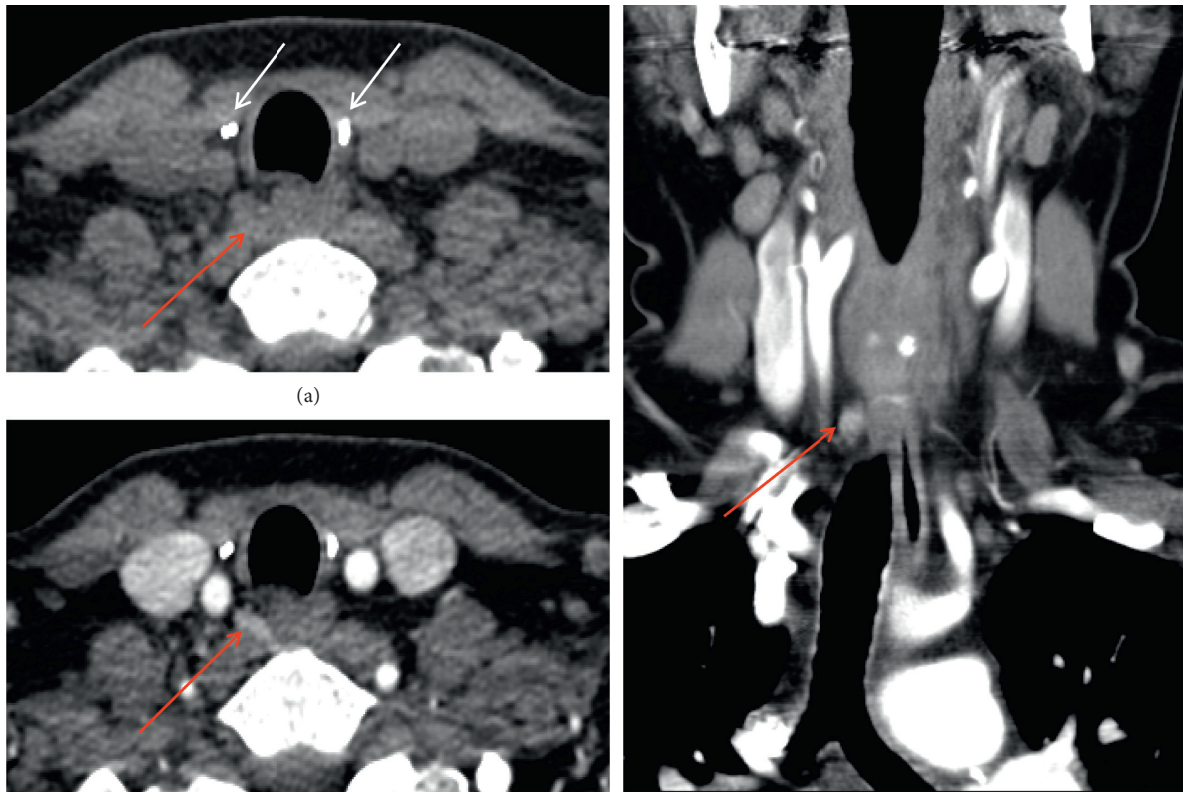

Figure 7: Ectopic parathyroid adenoma on four-dimensional computed tomography (4DCT). A patient presents with recurrent hyperparathyroidism after prior total thyroidectomy with benign pathology and prior bilateral inferior parathyroidectomy. Axial precontrast 4DCT (a) shows ectopic adenoma (red arrow) in the right para-retroesophageal region almost at the prevertebral fascia, deep to right surgical clips (white arrows). The ectopic adenoma is hyperenhancing on axial postcontrast (b) and coronal (c) early arterial phases (red arrows).

4DCT has many strengths that make it well-suited for the reoperative setting. Due to its very high spatial resolution, 4DCT delineates important anatomic landmarks and structures surrounding the diseased gland(s), thereby providing critical information that can guide surgical reexploration. It requires short imaging times and can capably localize ectopic adenomas (Figure 7) [21, 46]. 4DCT also has important disadvantages. It confers ionizing radiation, uses iodinated contrast, and requires radiologist experience to accurately interpret the modality. 4DCT has limited accuracy in patients with multigland disease, small glands, or concomitant thyroid pathology [73]. Nevertheless, 4DCT has emerged as a useful and sensitive modality in the setting of reoperation. Unlike ultrasound and sestamibi scintigraphy, 4DCT does not significantly differ in accuracy between unexplored patients and reoperative patients [63]. The modality is also superior to ultrasound and sestamibi scintigraphy in the preoperative localization of persistent or recurrent disease [37, 64, 71, 74, 75]. In addition, 4DCT accurately identifies parathyroid disease in challenging reoperative patients, such as those with negative first-line imaging or multigland disease [28, 37, 45, 66, 67, 72]. Finally, because it can differentiate unilateral and bilateral disease in up to 96% of reoperative patients, 4DCT can enable targeted parathyroidectomies in difficult reoperative cases [37, 39, 76]. Thus, 4DCT possesses several attributes that make it an accurate and informative modality for the preoperative localization of persistent or recurrent disease.

8. Magnetic Resonance Imaging

Magnetic resonance imaging (MRI) is occasionally used as a second-line modality to identify lesions that have been otherwise poorly or inconclusively localized by prior studies. Conventional MRI protocols for preoperatively localizing parathyroid lesions include small field-of-view precontrast axial T1- and T2-weighted sequences and postcontrast T1-weighted images with fat saturation. Parathyroid adenomas appear isointense to the muscle on T1-weighted images, hyperintense on T2-weighted images, and strongly and rapidly enhancing on postcontrast fat-saturated T1-weighted images (Figures 8 and 9) [44]. Such protocols have demonstrated sensitivities as high as 91% for localizing abnormal glands in patients with PHPT [46]. The addition of MRI to the combination of ultrasound and sestamibi scintigraphy significantly increases the sensitivity for localization from 75% to 92% [44]. In the reoperative setting, meanwhile, multiple investigations have reported the sensitivity of conventional MRI for localizing parathyroid adenomas to be 82% [44, 77]. A small number of studies have investigated the role of dynamic MRI. Dynamic 4D contrast-enhanced (DCE) MRI is a multiphase (4-phase) contrast-enhanced high spatial and temporal resolution T1-weighted sequence with fat suppression. Like 4DCT, dynamic MRI makes use of the hypervascular behavior of parathyroid adenomas. DCE provides quantitative perfusion parameters that enable differentiation between parathyroid adenomas, lymph nodes, and thyroid tissue. On dynamic MRI, parathyroid adenomas exhibit significantly faster arterial enhancement and higher wash-in and higher washout compared to lymph nodes and thyroid tissue (Figure 9) [78]. In unselected patients with PHPT, dynamic MRI has a reported sensitivity of 91% for detecting parathyroid adenomas [78]. In reoperative patients, dynamic MRI has a sensitivity of 90% for localizing adenomas; although this sensitivity is higher than that of conventional MRI in the reoperative setting (82%), this difference was not statistically significant [44]. The addition of dynamic magnetic resonance angiography (MRA) has also been investigated as a localizing modality for parathyroid adenomas. MRA constitutes a contrast-enhanced 3D angiographic acquisition. Parathyroid adenomas appear hyperenhancing during the early arterial phase, while thyroid tissue enhances during subsequent phases. In a study of 30 patients with hyperparathyroidism and prior neck surgery, MRI with dynamic MRA had sensitivity for localization of 93% [53].

Unlike sestamibi scintigraphy and 4DCT, MRI does not confer ionizing radiation, nor does it have significantly lower sensitivity in patients with concomitant thyroid pathology [44]. MRI also possesses specific advantages that make it well-suited to evaluate reoperative disease. MRI does not significantly differ in sensitivity between unexplored patients and reoperative patients, as reported by Kluijfhout and colleagues in a study of 41 unexplored and 84 reoperative patients with PHPT [44]. The addition of MRI to first-line modalities significantly increases the sensitivity to adenoma localization [44]. Although this increase was shown in a sample consisting of both initial and reoperative patients, it is reasonable to conclude that MRI provides an added benefit in the reoperative setting, where the accuracy of ultrasound and sestamibi scintigraphy markedly suffer. While the use of dynamic MRI does not confer a significant benefit over conventional MRI in the reoperative setting, the addition of dynamic MRA might, as it enables the detection of smaller adenomas than conventional MRI alone [53]. Yet, these strengths must be weighed against both the drawbacks of the modality and the limitations in evidence supporting it. MRI is more costly, inaccessible, and time-consuming than 4DCT and would be inappropriate as a first-line imaging modality. Only a small handful of investigations with narrow samples support the use of dynamic MRI or dynamic MRA in preoperatively localizing persistent or recurrent disease. Despite the high sensitivities of MRI for localizing reoperative lesions, further investigation is necessary before conclusively establishing the role of MRI in patients with persistent or recurrent disease.

9. Positron Emission Tomography and Hybrid PET/CT

In positron emission tomography (PET), patients undergo injection of a radiotracer that demonstrates avidity for metabolically active tissues. Hyperfunctioning tissues such as parathyroid adenomas appear as focal areas of radiotracer uptake. Compared to the aforementioned modalities, PET and hybrid imaging with both PET and low-dose computed tomography (PET/CT) are relatively new localization

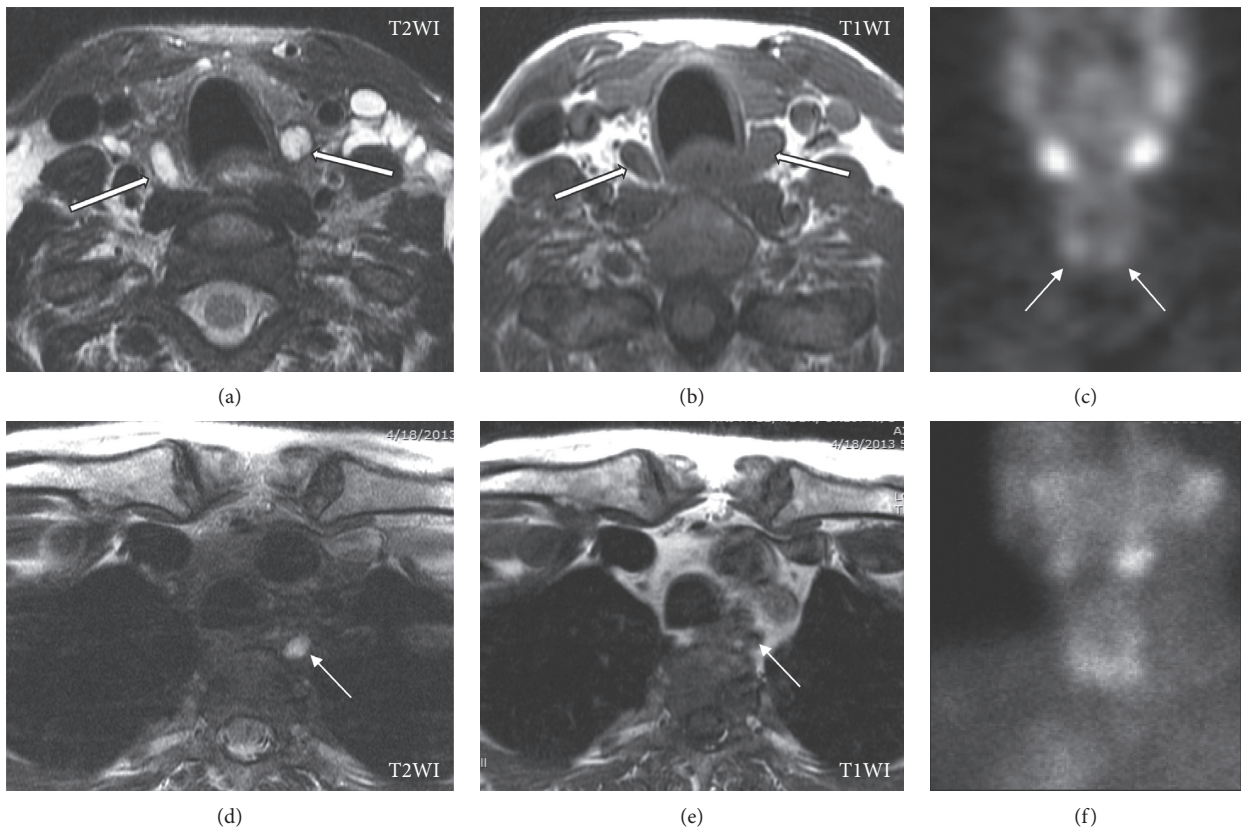

Figure 8: Parathyroid adenomas on magnetic resonance imaging (MRI). A 67-year-old female presents with persistent hyperparathyroidism after initial bilateral inferior parathyroidectomy. Unenhanced MRI (due to allergy to iodine- and gadolinium-based contrast materials) shows well-circumscribed bilateral inferior T2WI hyperintense (a) and T1WI hypointense (b) adenomas (white arrows) posterior to the inferior thyroid lobes. Planar delayed (two hours) single-photon emission computed tomography (SPECT) (c) demonstrates focal radiotracer accumulation (white arrows) along the inferior margin of the thyroid lobes. Further review of the MRI reveals small T2WI hyperintense (d) and poorly defined T1WI hypointense (e) nodules in the left posterior mediastinum/prevertebral region corresponding to an overly descended left superior parathyroid adenoma not demonstrated on initial SPECT studies (c, f).

techniques. In a pooled sample of both unexplored and reoperative patients, meta-analysis of ^{11}C-methionine (^{11}C-MET) PET showed a pooled sensitivity for localizing abnormal parathyroid glands of 77% and a pooled PPV of 98% [79]. Specifically in reoperative patients with PHPT, ^{11}C-MET PET has a sensitivity between 75 and 88% [80–84]. Analogously, ^{18}F-fluorodeoxyglucose (^{18}F-FDG) PET has a sensitivity of 62% in the reoperative setting [85]. Meanwhile, hybrid imaging with PET/CT offers high-resolution anatomic information in addition to the functional information provided by PET alone. ^{11}C-MET PET/CT has a sensitivity of 61% in reoperative patients, though this figure may be as low as 40% in challenging subgroups such as those with negative sestamibi scintigraphy (Figure 5) [40, 86]. However, ^{18}F-fluoromethylcholine (^{18}F-FCH) PET/CT demonstrates strong potential for localizing persistent or recurrent disease with sensitivities between 96 and 100% (albeit in studies with small sample sizes) [22, 87]. In patients with multigland disease, ^{18}F-FCH PET/CT has a reported sensitivity of 79% and PPV of 100% [87]. Moreover, the use of both ^{18}F-FDG and ^{18}F-FCH in hybrid PET/CT has proven useful in evaluating parathyroid carcinoma for the extent of primary disease, metastases, and recurrence (Figure 10) [88, 89].

Preoperative localization with PET and PET/CT possesses distinct advantages. First, PET offers better spatial and temporal resolution than SPECT, thus enabling the detection of very small pathologic glands [79]. Analogously, ^{18}F-FCH PET/CT has higher spatial resolution, lower radiation burden (2.8 mSv), and shorter total study time (38 minutes) than SPECT/CT (11.8 mSv, total study time 120 minutes) [90–92]. In a study of 29 patients undergoing reoperation for PHPT, ^{18}F-FCH PET/CT was more sensitive than ultrasound, sestamibi scintigraphy, and 4DCT for localizing parathyroid disease; however, it is likely that patients who proceed to PET/CT have negative or discordant results from more commonly utilized modalities in the first place [22]. Moreover, ^{18}F-FCH PET/CT often fails to detect hyperplastic glands and ectopic adenomas, both of which constitute common causes of reoperation [87, 93–95]. PET/CT is also an infrequently used modality and can be quite costly. Additional studies with larger samples are necessary before definitively establishing the role of PET/CT in localizing persistent or recurrent disease. Nevertheless, PET/CT may be a promising second-line modality in the reoperative setting as evidenced by its very high sensitivities, particularly when first-line imaging modalities are discordant or inconclusive.

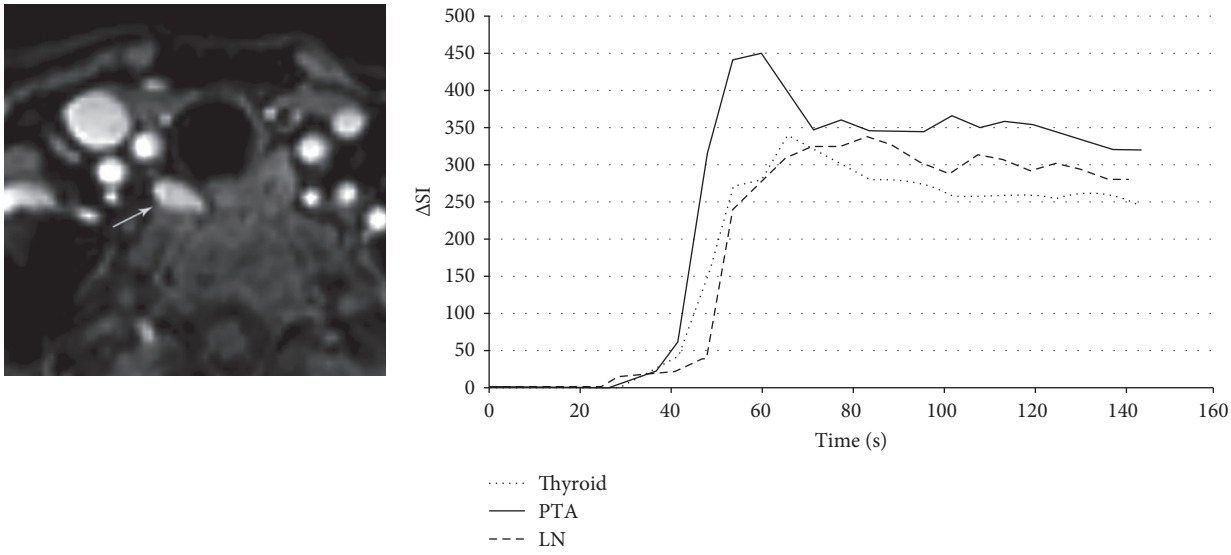

(a) (b)

Figure 9: Parathyroid adenoma on dynamic 4D contrast-enhanced magnetic resonance imaging (MRI). A 68-year-old female presents with primary hyperparathyroidism. An axial arterial phase contrast-enhanced image from magnetic resonance perfusion demonstrates a parathyroid adenoma (arrow) in the right tracheoesophageal groove. Concentration-time curve analysis from regions of interest placed over the parathyroid adenoma (arrow), thyroid gland, and a jugulodigastric lymph node shows significantly faster time-to-peak (TTP) and higher wash-in and washout values of the parathyroid adenoma compared to the thyroid gland and cervical lymph node. Parathyroid adenoma: TTP, 37 seconds; wash-in, 7.8; washout, 0.58. Thyroid: TTP, 42 seconds; wash-in, 5.4; washout, 0.46. Lymph node: TTP, 60 seconds; wash-in, 4.8; washout, 0.29. ΔSI indicates the change in signal intensity. Wash-in is the initial upslope of the concentration-time curve (slope from the end of the baseline to the peak of the curve). Washout is the downslope of the concentration-time curve (negative slope from the peak to the last acquisition time point) (figure reused with permission).

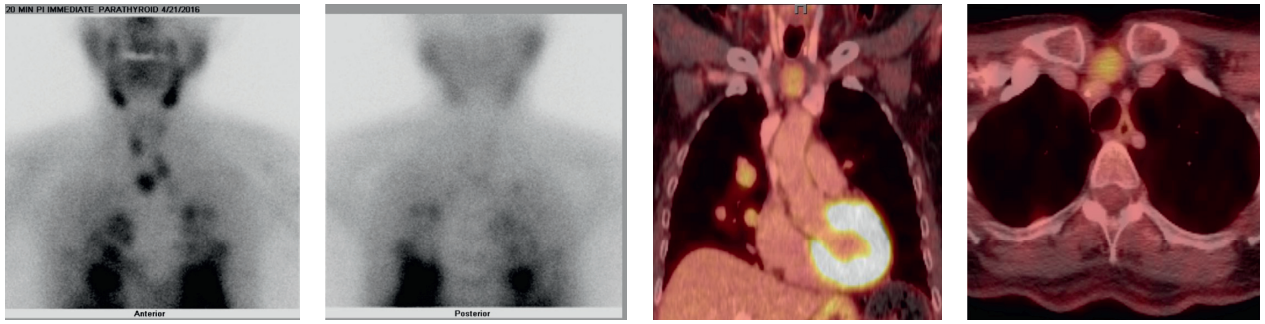

(a) (b) (c) (d)

Figure 10: Parathyroid carcinoma. A 68-year-old female presents with recurrent hyperparathyroidism due to recurrent parathyroid carcinoma. Planar anterior (a) and posterior (b) sestamibi scintigraphy at 20 minutes and ^{18}F-fluorodeoxyglucose (^{18}F-FDG) hybrid positron emission tomography and computed tomography (PET/CT) show multiple marked FDG-avid lesions (c, d) attributable to both local recurrence and multiple local and lung metastases.

10. Selective Venous Sampling

In the reoperative setting, noninvasive imaging modalities frequently fail to definitively localize disease and often demonstrate low concordance with operative findings [1, 23]. Patients with pPHPT or rPHPT as well as non-localizing, equivocal, or discordant noninvasive imaging studies may undergo invasive localization in the form of selective venous sampling (SVS) for PTH. SVS involves selective catheterization of neck and mediastinal veins (e.g., internal jugular veins, brachiocephalic veins, azygos vein, and vertebral veins) with PTH sampling. A PTH level in a selected vein at least twice the systemic level is considered localizing for abnormal parathyroid glands. A 2018 meta-analysis of SVS in both *de novo* (minority) and reoperative (majority) patients reported a pooled sensitivity of 74% for localizing parathyroid adenomas [96]. Among reoperative patients with inconclusive noninvasive imaging studies, the sensitivity of SVS ranges from 75 to 93% [1, 6, 41, 72]. Additionally, in reoperative patients with negative or

nonlocalizing first-line imaging, the combination of 4DCT and SVS has a sensitivity of 95% and is significantly more sensitive than 4DCT alone [72]. The recent adoption of superselective venous sampling (SSVS) has increased the accuracy of invasive PTH sampling. SSVS obtains samples from smaller neck and upper chest veins (e.g., superior, middle, and inferior thyroid veins; main inferior thyroid trunk; thymic vein; superior intercostal veins; and occasionally internal mammary veins) to enable more precise localization of parathyroid pathology. In the reoperative setting, meta-analysis of SSVS has found a pooled sensitivity of 90% for localizing parathyroid adenomas [96]. Among reoperative patients with inconclusive first-line imaging, SSVS has a sensitivity of 96% and a PPV of 84%, which is significantly more accurate than routine SVS [97].

The benefits of invasive localization should be measured against its costs and limitations. Meta-analysis has shown that SVS is more sensitive than noninvasive imaging modalities at localizing adenomas in patients with pPHPT or rPHPT undergoing reoperation [96]. Yet, this higher sensitivity of SVS may be attributable to the fact that the patients enrolled in comparative studies only underwent invasive imaging because their noninvasive imaging studies were inconclusive to begin with. Localization using SVS can be inaccurate when veins drain bilaterally or in patients with altered venous anatomy and drainage patterns (as is seen in the reoperative setting). As a result, SVS may occasionally demonstrate low concordance with surgical findings in reoperative patients [98]. SVS also requires the expertise of interventional radiology and carries procedural risks that do not accompany noninvasive localization techniques. Although the combination of 4DCT and SVS and the advent of SSVS exhibit strong potential, their utility must be carefully weighed against their costs, the risks of invasive localization, and the risk of inaccurate results due to postoperative anatomic changes. As a result, SVS should be reserved for challenging reoperative cases in which noninvasive modalities are negative or discordant.

11. Intraoperative PTH Monitoring

Intraoperative PTH monitoring (IOPTH) is frequently utilized as a surgical adjunct to determine if all abnormal parathyroid glands have been resected. Its use has enabled minimally invasive or focused parathyroidectomy in initial explorations, as it can determine whether the remaining unexplored parathyroid glands are producing physiologic amounts of PTH. Due to the short half-life of PTH, a decrease of >50% in intact PTH from preexcision levels in a sample of peripheral blood collected 5 and 10 minutes after excision of suspected abnormal parathyroid tissue is associated with a high rate of cure. Furthermore, a decrease in IOPTH levels into the normal range provides reliable evidence that the remaining unexplored parathyroid glands are producing physiologic amounts of PTH, thus making further exploration unnecessary. Meanwhile, a persistently elevated IOPTH level may predict multigland disease in the setting of a focused exploration or may predict an ectopic adenoma in the setting of a four-gland exploration. In the reoperative setting, IOPTH has been reported to have sensitivity for predicting cure between 99 and 100% and has been shown to be a statistically significant predictor of operative success [4, 15, 23, 51]. Specifically in reoperative patients with MEN1, IOPTH has a sensitivity of 92% and accurately distinguishes patients with previously undetected multigland disease [24]. Existing literature provides mixed evidence regarding the influence of IOPTH on the rates of cure and complications [4, 15, 16]. Nevertheless, IOPTH provides critical information during the surgical exploration of challenging reoperative patients.

12. Radiation Dose Exposure and Associated Cancer Risks

Concerns over radiation exposure have prompted several investigations into the radiation doses conferred by preoperative imaging modalities. Sestamibi scintigraphy has an effective dose between 3.3 and 13.7 mSv, with SPECT/CT conferring more radiation than SPECT and planar scintigraphy [45, 92, 99, 100]. Undergoing a sestamibi scintigraphy study increases a patient's lifetime attributable risk for cancer incidence over baseline by 0.19% [92]. 4DCT exhibits a wide range of effective doses varying from 5.6 mSv to 28.5 mSv, with most studies reporting doses <15 mSv and two- and three-phase protocols conferring less radiation than four-phase protocols [45, 65, 92, 99–102]. Undergoing a 4DCT study increases a patient's lifetime attributable risk for cancer incidence over baseline by 0.52% [92]. Efforts to reduce the radiation dose from four-phase 4DCT protocols have spurred the use of two-phase protocols (consisting of precontrast and early arterial phases only) or even a single-phase protocol [103]. When used as a second-line modality, there is no significant difference in ability to lateralize parathyroid lesions between four-phase protocols and two- or three-phase protocols, including in reoperative patients and patients with multigland disease [63, 65]. Lastly, ^{18}F-FCH PET/CT possesses an effective dose of 2.8 mSv [90]. Radiation doses exhibit a large range because protocols are highly specialized and vary from institution to institution. Nevertheless, the aforementioned imaging modalities are considered safe because the annual background radiation in the United States is 3 mSv and additional exposures of less than 15 mSv are considered low risk for carcinogenesis [99, 102].

13. Cost

Studies investigating the cost of preoperative imaging modalities are limited both in number and in the availability of cost data. A 2013 study examining Medicare payments and institutional charges calculated the costs of thin-cut 4DCT and sestamibi scintigraphy to be $1296 and $1112, respectively [99]. Meanwhile, the limited availability and high cost of PET radiotracers make PET unwarranted in uncomplicated or unexplored patients. Lubitz and colleagues concluded that ultrasound alone as a first-line modality followed by 4DCT in inconclusive cases is the most cost-effective strategy given the superior ability of 4DCT to enable

minimally invasive parathyroidectomy [104]. Similarly, Wang and colleagues concluded that ultrasound and SPECT together as a first-line modality is the most cost-effective strategy, followed by 4DCT if the two initial studies are discordant [105]. The costs of imaging studies must be weighed against the benefits of highly sensitive preoperative localization, reductions in operating time, and increases in the likelihood of surgical cure.

14. Conclusion

The evaluation of persistent or recurrent disease in reoperative patients presents challenges for radiologists and surgeons alike. Accurate localization by preoperative imaging is a predictor of operative success. Inversely, negative or discordant preoperative imaging is a risk factor for operative failure, thus underscoring the importance of pursuing additional localization studies when first-line studies are inconclusive.

In this article, we review the common imaging modalities used to preoperatively localize parathyroid adenomas in the reoperative setting. We present the technique, accuracy, advantages, and disadvantages of each modality with respect to localizing persistent or recurrent disease. Unfortunately, there is no clear standard of care for the imaging localization of reoperative parathyroid pathology. Nevertheless, the present literature review enables us to recommend the following approach. Imaging in the reoperative setting should depend on which modalities were used during the patient's initial workup. First-line modalities in the reoperative setting should consist of both ultrasound and 4DCT, particularly in patients with rPHPT for whom evaluation of thyroid pathology is contributory to surgical management. Sestamibi scintigraphy is also an accurate initial modality in the reoperative setting. However, in practice, sestamibi scintigraphy is not repeated in patients with pPHPT or recent recurrence. Unfortunately, first-line imaging modalities are often negative or discordant in the reoperative setting, leaving many patients without curative options unless additional localization studies are pursued. Reoperative patients with negative or discordant first-line imaging should subsequently undergo PET/CT or conventional MRI before attempting invasive localization with SVS, which should be reserved for challenging cases in which several noninvasive modalities are inconclusive. When used in concert, the aforementioned techniques identify operative targets in challenging reoperative patients and thereby enable safe and curative parathyroidectomy.

Disclosure

With regard to Figure 5, this research was originally published by Schalin-Jäntti C et al. Planar scintigraphy with ^{123}I/^{99m}Tc-sestamibi, ^{99m}Tc-sestamibi SPECT/CT, ^{11}C-methionine PET/CT, or selective venous sampling before reoperation of primary hyperparathyroidism?. *J Nucl Med*. 2013; 5: 739–47. © SNMMI. With regard to Figure 9: this research was originally published by Nael K et al. Dynamic 4D MRI for characterization of parathyroid adenomas: multiparametric analysis. *AJNR*. 2015, 36 (11) 2147–2152.

Conflicts of Interest

The authors RHG and FEM are employees of Baylor College of Medicine. The other author declares no conflicts of interest regarding the publication of this paper.

References

[1] N. Jaskowiak, J. A. Norton, H. R. Alexander et al., "A prospective trial evaluating a standard approach to reoperation for missed parathyroid adenoma," *Annals of Surgery*, vol. 224, no. 3, pp. 308–322, 1996.

[2] J. M. Ruda, C. S. Hollenbeak, and B. C. Stack, "A systematic review of the diagnosis and treatment of primary hyperparathyroidism from 1995 to 2003," *Otolaryngology—Head and Neck Surgery*, vol. 132, no. 3, pp. 359–372, 2005.

[3] A. Bagul, H. P. Patel, D. Chadwick, B. J. Harrison, and S. P. Balasubramanian, "Primary hyperparathyroidism: an analysis of failure of parathyroidectomy," *World Journal of Surgery*, vol. 38, no. 3, pp. 534–541, 2014.

[4] P. P. Parikh, J. C. Farra, B. J. Allan, and J. I. Lew, "Long-term effectiveness of localization studies and intraoperative parathormone monitoring in patients undergoing reoperative parathyroidectomy for persistent or recurrent hyperparathyroidism," *The American Journal of Surgery*, vol. 210, no. 1, pp. 117–122, 2015.

[5] J. E. Witteveen, J. Kievit, A. R. van Erkel, H. Morreau, J. A. Romijn, and N. A. T. Hamdy, "The role of selective venous sampling in the management of persistent hyperparathyroidism revisited," *European Journal of Endocrinology*, vol. 163, no. 6, pp. 945–952, 2010.

[6] J. J. Jones, L. Brunaud, C. F. Dowd, Q.-Y. Duh, E. Morita, and O. H. Clark, "Accuracy of selective venous sampling for intact parathyroid hormone in difficult patients with recurrent or persistent hyperparathyroidism," *Surgery*, vol. 132, no. 6, pp. 944–951, 2002.

[7] M. W. Yeh, J. E. Wiseman, S. D. Chu et al., "Population-level predictors of persistent hyperparathyroidism," *Surgery*, vol. 150, no. 6, pp. 1113–1119, 2011.

[8] D. K. Bartsch and M. Rothmund, "Reoperative surgery for primary hyperparathyroidism," *British Journal of Surgery*, vol. 96, no. 7, pp. 699–701, 2009.

[9] C. A. Patow, J. A. Norton, and M. F. Brennan, "Vocal cord paralysis and reoperative parathyroidectomy: a prospective study," *Annals of Surgery*, vol. 203, no. 3, pp. 282–285, 1986.

[10] C. R. Baliski, J. K. Stewart, D. W. Anderson, S. M. Wiseman, and S. P. Bugis, "Selective unilateral parathyroid exploration: an effective treatment for primary hyperparathyroidism," *The American Journal of Surgery*, vol. 189, no. 5, pp. 596–600, 2005.

[11] I. Gough, "Reoperative parathyroid surgery: the importance of ectopic location and multigland disease," *ANZ Journal of Surgery*, vol. 76, no. 12, pp. 1048–1050, 2006.

[12] C. McIntyre, J. Allen, V. Constantinides, J. Jackson, N. Tolley, and F. Palazzo, "Patterns of disease in patients at a tertiary referral centre requiring reoperative parathyroidectomy," *The Annals of the Royal College of Surgeons of England*, vol. 97, no. 8, pp. 598–602, 2015.

[13] R. Udelsman, "Approach to the patient with persistent or recurrent primary hyperparathyroidism," *The Journal of*

Clinical Endocrinology & Metabolism, vol. 96, no. 10, pp. 2950–2958, 2011.

[14] J. E. Witteveen, J. Kievit, M. P. M. Stokkel, H. Morreau, J. A. Romijn, and N. A. T. Hamdy, "Limitations of Tc^{99m}-MIBI-SPECT imaging scans in persistent primary hyperparathyroidism," *World Journal of Surgery*, vol. 35, no. 1, pp. 128–139, 2011.

[15] M. L. Richards, G. B. Thompson, D. R. Farley, and C. S. Grant, "Reoperative parathyroidectomy in 228 patients during the era of minimal-access surgery and intraoperative parathyroid hormone monitoring," *The American Journal of Surgery*, vol. 196, no. 6, pp. 937–943, 2008.

[16] E. Karakas, H.-H. Müller, T. Schlosshauer, M. Rothmund, and D. K. Bartsch, "Reoperations for primary hyperparathyroidism-improvement of outcome over two decades," *Langenbeck's Archives of Surgery*, vol. 398, no. 1, pp. 99–106, 2013.

[17] L. Rotstein, J. Irish, P. Gullane, M. A. Keller, and K. Sniderman, "Reoperative parathyroidectomy in the era of localization technology," *Head & Neck*, vol. 20, no. 6, pp. 535–539, 1998.

[18] E. J. Silberfein, "Reoperative parathyroidectomy: location of missed glands based on a contemporary nomenclature system," *Archives of Surgery*, vol. 145, no. 11, p. 1065, 2010.

[19] I. Nawrot, W. Chudziński, T. Ciąćka, M. Barczyński, and J. Szmidt, "Reoperations for persistent or recurrent primary hyperparathyroidism: results of a retrospective cohort study at a tertiary referral center," *Medical Science Monitor*, vol. 20, pp. 1604–1612, 2014.

[20] W. S. Duke, H. M. Vernon, and D. J. Terris, "Reoperative parathyroidectomy: overly descended superior adenoma," *Otolaryngology—Head and Neck Surgery*, vol. 154, no. 2, pp. 268–271, 2016.

[21] A. M. Parikh, J. W. Suliburk, and F. E. Morón, "Imaging localization and surgical approach in the management of ectopic parathyroid adenomas," *Endocrine Practice*, vol. 24, no. 6, pp. 589–598, 2018.

[22] C. Amadou, G. Bera, M. Ezziane et al., "^{18}F-Fluorocholine PET/CT and parathyroid 4D computed tomography for primary hyperparathyroidism: the challenge of reoperative patients," *World Journal of Surgery*, vol. 43, no. 5, pp. 1232–1242, 2019.

[23] T. W. F. Yen, T. S. Wang, K. M. Doffek, E. A. Krzywda, and S. D. Wilson, "Reoperative parathyroidectomy: an algorithm for imaging and monitoring of intraoperative parathyroid hormone levels that results in a successful focused approach," *Surgery*, vol. 144, no. 4, pp. 611–621, 2008.

[24] X. M. Keutgen, N. Nilubol, S. Agarwal et al., "Reoperative surgery in patients with multiple endocrine neoplasia type 1 associated primary hyperparathyroidism," *Annals of Surgical Oncology*, vol. 23, no. S5, pp. 701–707, 2016.

[25] Y. Hu, T. Ondracek, and F. Chen, "Parathyroid adenoma arising from autotransplanted parathyroid tissue in sternocleidomastoid muscle: a case report with review of the literature," *North American Journal of Medicine & Science*, vol. 8, no. 2, pp. 89–91, 2015.

[26] P. Touska, A. Srikanthan, K. Amarasinghe, and S. Jawad, "Parathyroid adenoma arising within the sternocleidomastoid muscle: a rare complication of autotransplantation," *BMJ Case Reports*, vol. 2016, Article ID bcr2015213184, 2016.

[27] J.-F. Henry, "Reoperation for primary hyperparathyroidism: tips and tricks," *Langenbeck's Archives of Surgery*, vol. 395, no. 2, pp. 103–109, 2010.

[28] P. M. Bunch and H. R. Kelly, "Preoperative imaging techniques in primary hyperparathyroidism: a review," *JAMA Otolaryngology—Head & Neck Surgery*, vol. 144, no. 10, p. 929, 2018.

[29] A. Simental and R. L. Ferris, "Reoperative parathyroidectomy," *Otolaryngologic Clinics of North America*, vol. 41, no. 6, pp. 1269–1274, 2008.

[30] C. Hasse, H. Sitter, M. Brune, I. Wollenteit, C. Nies, and M. Rothmund, "Quality of life and patient satisfaction after reoperation for primary hyperparathyroidism: analysis of long-term results," *World Journal of Surgery*, vol. 26, no. 8, pp. 1029–1036, 2002.

[31] W. Shen, M. Düren, E. Morita et al., "Reoperation for persistent or recurrent primary hyperparathyroidism," *Archives of Surgery*, vol. 131, no. 8, pp. 861–867, 1996.

[32] A. O. J. Bergenfelz, G. Wallin, S. Jansson et al., "Results of surgery for sporadic primary hyperparathyroidism in patients with preoperatively negative sestamibi scintigraphy and ultrasound," *Langenbeck's Archives of Surgery*, vol. 396, no. 1, pp. 83–90, 2011.

[33] M. C. Singer, D. Pucar, M. Mathew, and D. J. Terris, "Improved localization of sestamibi imaging at high-volume centers: high-volume sestamibi," *The Laryngoscope*, vol. 123, no. 1, pp. 298–301, 2013.

[34] S. M. Wilhelm, T. S. Wang, D. T. Ruan et al., "The American association of endocrine surgeons guidelines for definitive management of primary hyperparathyroidism," *JAMA Surgery*, vol. 151, no. 10, p. 959, 2016.

[35] M. F. Brennan and J. A. Norton, "Reoperation for persistent and recurrent hyperparathyroidism," *Annals of Surgery*, vol. 201, no. 1, pp. 40–44, 1985.

[36] J. Järhult, J. Nordenströ, and L. Perbeck, "Reoperation for suspected primary hyperparathyroidism," *British Journal of Surgery*, vol. 80, no. 4, pp. 453–456, 1993.

[37] M. M. Mortenson, D. B. Evans, J. E. Lee et al., "Parathyroid exploration in the reoperative neck: improved preoperative localization with 4D-computed tomography," *Journal of the American College of Surgeons*, vol. 206, no. 5, pp. 888–895, 2008.

[38] N. M. Singh Ospina, R. Rodriguez-Gutierrez, S. Maraka et al., "Outcomes of parathyroidectomy in patients with primary hyperparathyroidism: a systematic review and meta-analysis," *World Journal of Surgery*, vol. 40, no. 10, pp. 2359–2377, 2016.

[39] C. C. Lubitz, G. J. Hunter, L. M. Hamberg et al., "Accuracy of 4-dimensional computed tomography in poorly localized patients with primary hyperparathyroidism," *Surgery*, vol. 148, no. 6, pp. 1129–1138, 2010.

[40] C. Schalin-Jantti, E. Ryhanen, I. Heiskanen et al., "Planar scintigraphy with ^{123}I/^{99m}Tc-Sestamibi, ^{99m}Tc-sestamibi SPECT/CT, ^{11}C-methionine PET/CT, or selective venous sampling before reoperation of primary hyperparathyroidism?," *Journal of Nuclear Medicine*, vol. 54, no. 5, pp. 739–747, 2013.

[41] P. Y. Sun, S. M. Thompson, J. C. Andrews et al., "Selective parathyroid hormone venous sampling in patients with persistent or recurrent primary hyperparathyroidism and negative, equivocal or discordant noninvasive imaging," *World Journal of Surgery*, vol. 40, no. 12, pp. 2956–2963, 2016.

[42] C. Guerin, N. C. Paladino, A. Lowery, F. Castinetti, D. Taieb, and F. Sebag, "Persistent and recurrent hyperparathyroidism," *Updates in Surgery*, vol. 69, no. 2, pp. 161–169, 2017.

[43] K. Cheung, T. S. Wang, F. Farrokhyar, S. A. Roman, and J. A. Sosa, "A meta-analysis of preoperative localization techniques for patients with primary hyperparathyroidism," *Annals of Surgical Oncology*, vol. 19, no. 2, pp. 577–583, 2012.

[44] W. P. Kluijfhout, S. Venkatesh, T. Beninato et al., "Performance of magnetic resonance imaging in the evaluation of first-time and reoperative primary hyperparathyroidism," *Surgery*, vol. 160, no. 3, pp. 747–754, 2016.

[45] Y. Tian, S. T. Tanny, P. Einsiedel et al., "Four-dimensional computed tomography: clinical impact for patients with primary hyperparathyroidism," *Annals of Surgical Oncology*, vol. 25, no. 1, pp. 117–121, 2018.

[46] S. Liddy, D. Worsley, W. Torreggiani, and J. Feeney, "Preoperative imaging in primary hyperparathyroidism: literature review and recommendations," *Canadian Association of Radiologists Journal*, vol. 68, no. 1, pp. 47–55, 2017.

[47] N. A. Johnson, M. E. Tublin, and J. B. Ogilvie, "Parathyroid imaging: technique and role in the preoperative evaluation of primary hyperparathyroidism," *American Journal of Roentgenology*, vol. 188, no. 6, pp. 1706–1715, 2007.

[48] H. K. Eslamy and H. A. Ziessman, "Parathyroid scintigraphy in patients with primary hyperparathyroidism: ^{99m}Tc sestamibi SPECT and SPECT/CT," *RadioGraphics*, vol. 28, no. 5, pp. 1461–1476, 2008.

[49] W.-J. Wei, C.-T. Shen, H.-J. Song, Z.-L. Qiu, and Q.-Y. Luo, "Comparison of SPET/CT, SPET and planar imaging using ^{99m}Tc-MIBI as independent techniques to support minimally invasive parathyroidectomy in primary hyperparathyroidism: a meta-analysis," *Hellenic Journal of Nuclear Medicine*, vol. 18, no. 2, pp. 127–135, 2015.

[50] C. C. Chen, M. C. Skarulis, D. L. Fraker, R. Alexander, S. J. Marx, and A. M. Spiegel, "Technetium-99m-sestamibi imaging before reoperation for primary hyperparathyroidism," *Journal of Nuclear Medicine: Official Publication, Society of Nuclear Medicine*, vol. 36, no. 12, pp. 2186–2191, 1995.

[51] A. C. Powell, H. R. Alexander, R. Chang et al., "Reoperation for parathyroid adenoma: a contemporary experience," *Surgery*, vol. 146, no. 6, pp. 1144–1155, 2009.

[52] E. Hindie, P. Zanotti-Fregonara, A. Tabarin et al., "The role of radionuclide imaging in the surgical management of primary hyperparathyroidism," *Journal of Nuclear Medicine*, vol. 56, no. 5, pp. 737–744, 2015.

[53] R. Aschenbach, S. Tuda, E. Lamster et al., "Dynamic magnetic resonance angiography for localization of hyperfunctioning parathyroid glands in the reoperative neck," *European Journal of Radiology*, vol. 81, no. 11, pp. 3371–3377, 2012.

[54] E. Moralidis, "Radionuclide parathyroid imaging: a concise, updated review," *Hellenic Journal of Nuclear Medicine*, vol. 16, no. 2, pp. 125–133, 2013.

[55] J. M. Jones, C. F. J. Russell, W. R. Ferguson, and J. D. Laird, "Pre-operative sestamibi-technetium subtraction scintigraphy in primary hyperparathyroidism: experience with 156 consecutive patients," *Clinical Radiology*, vol. 56, no. 7, pp. 556–559, 2001.

[56] R. Taillefer, Y. Boucher, C. Potvin, and R. Lambert, "Detection and localization of parathyroid adenomas in patients with hyperparathyroidism using a single radionuclide imaging procedure with technetium-99m-sestamibi (double-phase study)," *Journal of Nuclear Medicine: Official Publication, Society of Nuclear Medicine*, vol. 33, no. 10, pp. 1801–1807, 1992.

[57] D. Martin, I. B. Rosen, and M. Ichise, "Evaluation of single isotope technetium ^{99}M-sestamibi in localization efficiency for hyperparathyroidism," *The American Journal of Surgery*, vol. 172, no. 6, pp. 633–636, 1996.

[58] Pattou, Huglo, and Proye, "Radionuclide scanning in parathyroid diseases," *British Journal of Surgery*, vol. 85, no. 12, pp. 1605–1616, 1998.

[59] M. A. Muros, J. B. Soto, J. M. López Ruiz et al., "Two-phase scintigraphy with technetium ^{99}m-sestamibi in patients with hyperparathyroidism due to chronic renal failure," *The American Journal of Surgery*, vol. 193, no. 4, pp. 438–442, 2007.

[60] S. Cham, A. R. Sepahdari, K. E. Hall, M. W. Yeh, and A. Harari, "Dynamic parathyroid computed tomography (4DCT) facilitates reoperative parathyroidectomy and enables cure of missed hyperplasia," *Annals of Surgical Oncology*, vol. 22, no. 11, pp. 3537–3542, 2015.

[61] L. F. Morris, S. Lee, C. L. Warneke et al., "Fewer adverse events after reoperative parathyroidectomy associated with initial minimally invasive parathyroidectomy," *The American Journal of Surgery*, vol. 208, no. 5, pp. 850–855, 2014.

[62] R. Mihai, F. Gleeson, I. D. Buley, D. E. Roskell, and G. P. Sadler, "Negative imaging studies for primary hyperparathyroidism are unavoidable: correlation of sestamibi and high-resolution ultrasound scanning with histological analysis in 150 patients," *World Journal of Surgery*, vol. 30, no. 5, pp. 697–704, 2006.

[63] H. R. Kelly, L. M. Hamberg, and G. J. Hunter, "4D-CT for preoperative localization of abnormal parathyroid glands in patients with hyperparathyroidism: accuracy and ability to stratify patients by unilateral versus bilateral disease in surgery-naïve and Re-exploration patients," *American Journal of Neuroradiology*, vol. 35, no. 1, pp. 176–181, 2014.

[64] M. Hamidi, M. Sullivan, G. Hunter et al., "4D-CT is superior to ultrasound and sestamibi for localizing recurrent parathyroid disease," *Annals of Surgical Oncology*, vol. 25, no. 5, pp. 1403–1409, 2018.

[65] A. G. Ramirez, A. L. Shada, A. N. Martin et al., "Clinical efficacy of 2-phase versus 4-phase computed tomography for localization in primary hyperparathyroidism," *Surgery*, vol. 160, no. 3, pp. 731–737, 2016.

[66] J. L. Chazen, A. Gupta, A. Dunning, and C. D. Phillips, "Diagnostic accuracy of 4D-CT for parathyroid adenomas and hyperplasia," *American Journal of Neuroradiology*, vol. 33, no. 3, pp. 429–433, 2012.

[67] S. Sho, M. Yilma, M. W. Yeh et al., "Prospective validation of two 4D-CT-based scoring systems for prediction of multigland disease in primary hyperparathyroidism," *American Journal of Neuroradiology*, vol. 37, no. 12, pp. 2323–2327, 2016.

[68] L. Galvin, J. D. Oldan, M. Bahl, J. D. Eastwood, J. A. Sosa, and J. K. Hoang, "Parathyroid 4D CT and scintigraphy: what factors contribute to missed parathyroid lesions?," *Otolaryngology—Head and Neck Surgery*, vol. 154, no. 5, pp. 847–853, 2016.

[69] M. Parikshak, E. D. Castillo, M. F. Conrad, and G. B. Talpos, "Impact of hypercalcemia and parathyroid hormone level on the sensitivity of preoperative sestamibi scanning for primary hyperparathyroidism," *The American Surgeon*, vol. 69, no. 5, pp. 393–398, 2003.

[70] L. I. Eichhorn-Wharry, A. M. Carlin, and G. B. Talpos, "Mild hypercalcemia: an indication to select 4-dimensional computed tomography scan for preoperative localization of

parathyroid adenomas," *The American Journal of Surgery*, vol. 201, no. 3, pp. 334–338, 2011.

[71] K. M. Day, M. Elsayed, M. D. Beland, and J. M. Monchik, "The utility of 4-dimensional computed tomography for preoperative localization of primary hyperparathyroidism in patients not localized by sestamibi or ultrasonography," *Surgery*, vol. 157, no. 3, pp. 534–539, 2015.

[72] M. Ginsburg, G. A. Christoforidis, S. P. Zivin et al., "Adenoma localization for recurrent or persistent primary hyperparathyroidism using dynamic four-dimensional CT and venous sampling," *Journal of Vascular and Interventional Radiology*, vol. 26, no. 1, pp. 79–86, 2015.

[73] S. Sho, A. D. Yuen, M. W. Yeh, M. J. Livhits, and A. R. Sepahdari, "Factors associated with discordance between preoperative parathyroid 4-dimensional computed tomographic scans and intraoperative findings during parathyroidectomy," *JAMA Surgery*, vol. 152, no. 12, p. 1141, 2017.

[74] A. M. Hinson, D. R. Lee, B. A. Hobbs, R. T. Fitzgerald, D. L. Bodenner, and B. C. Stack, "Preoperative 4D CT localization of nonlocalizing parathyroid adenomas by ultrasound and SPECT-CT," *Otolaryngology-Head and Neck Surgery*, vol. 153, no. 5, pp. 775–778, 2015.

[75] Y. J. Suh, J. Y. Choi, S.-J. Kim et al., "Comparison of 4D CT, ultrasonography, and ^{99m}Tc sestamibi SPECT/CT in localizing single-gland primary hyperparathyroidism," *Otolaryngology—Head and Neck Surgery*, vol. 152, no. 3, pp. 438–443, 2015.

[76] M. D. Beland, W. W. Mayo-Smith, D. J. Grand, J. T. Machan, and J. M. Monchik, "Dynamic MDCT for localization of occult parathyroid adenomas in 26 patients with primary hyperparathyroidism," *American Journal of Roentgenology*, vol. 196, no. 1, pp. 61–65, 2011.

[77] M. B. Gotway, G. P. Reddy, W. R. Webb, E. T. Morita, O. H. Clark, and C. B. Higgins, "Comparison between MR imaging and ^{99m}Tc MIBI scintigraphy in the evaluation of recurrent or persistent hyperparathyroidism," *Radiology*, vol. 218, no. 3, pp. 783–790, 2001.

[78] K. Nael, J. Hur, A. Bauer et al., "Dynamic 4D MRI for characterization of parathyroid adenomas: multiparametric analysis," *American Journal of Neuroradiology*, vol. 36, no. 11, pp. 2147–2152, 2015.

[79] W. P. Kluijfhout, J. D. Pasternak, F. T. Drake et al., "Use of PET tracers for parathyroid localization: a systematic review and meta-analysis," *Langenbeck's Archives of Surgery*, vol. 401, no. 7, pp. 925–935, 2016.

[80] O. Hessman, P. Stålberg, A. Sundin et al., "High success rate of parathyroid reoperation may be achieved with improved localization diagnosis," *World Journal of Surgery*, vol. 32, no. 5, pp. 774–781, 2008.

[81] D. Otto, A. R. Boerner, M. Hofmann et al., "Pre-operative localisation of hyperfunctional parathyroid tissue with ^{11}C-methionine PET," *European Journal of Nuclear Medicine and Molecular Imaging*, vol. 31, no. 10, 2004.

[82] A. Sundin, C. Johansson, P. Hellman et al., "PET and parathyroid L-[carbon-11]methionine accumulation in hyperparathyroidism," *Journal of Nuclear Medicine: Official Publication, Society of Nuclear Medicine*, vol. 37, no. 11, pp. 1766–1770, 1996.

[83] G. Cook, J. Wong, W. Smellie, A. Young, M. Maisey, and I. Fogelman, "[^{11}C]Methionine positron emission tomography for patients with persistent or recurrent hyperparathyroidism after surgery," *European Journal of Endocrinology*, vol. 139, no. 2, pp. 195–197, 1998.

[84] T. Weber, G. Cammerer, C. Schick et al., "C-11 methionine positron emission tomography/computed tomography localizes parathyroid adenomas in primary hyperparathyroidism," *Hormone and Metabolic Research*, vol. 42, no. 3, pp. 209–214, 2010.

[85] D. R. Neumann, C. B. Esselstyn, W. J. MacIntyre, E. Q. Chen, R. T. Go, and A. A. Licata, "Regional body FDG-PET in postoperative recurrent hyperparathyroidism," *Journal of Computer Assisted Tomography*, vol. 21, no. 1, pp. 25–28, 1997.

[86] T. Traub-Weidinger, M. E. Mayerhoefer, O. Koperek et al., "^{11}C-Methionine PET/CT imaging of ^{99m}Tc-MIBI-SPECT/CT-negative patients with primary hyperparathyroidism and previous neck surgery," *The Journal of Clinical Endocrinology & Metabolism*, vol. 99, no. 11, pp. 4199–4205, 2014.

[87] S. Grimaldi, J. Young, P. Kamenicky et al., "Challenging presurgical localization of hyperfunctioning parathyroid glands in primary hyperparathyroidism: the added value of ^{18}F-Fluorocholine PET/CT," *European Journal of Nuclear Medicine and Molecular Imaging*, vol. 45, no. 10, pp. 1772–1780, 2018.

[88] N. T. K. Thanseer, A. Parihar, A. Sood et al., "Evaluation of recurrent parathyroid carcinoma: a new imaging tool in uncommon entity," *World Journal of Nuclear Medicine*, vol. 18, no. 2, p. 198, 2019.

[89] D. Deandreis, M. Terroir, A. Al Ghuzlan et al., "^{18}Fluorocholine PET/CT in parathyroid carcinoma: a new tool for disease staging?," *European Journal of Nuclear Medicine and Molecular Imaging*, vol. 42, no. 12, pp. 1941-1942, 2015.

[90] S. Rep, M. Hocevar, J. Vaupotic, U. Zdesar, K. Zaletel, and L. Lezaic, "^{18}F-choline PET/CT for parathyroid scintigraphy: significantly lower radiation exposure of patients in comparison to conventional nuclear medicine imaging approaches," *Journal of Radiological Protection*, vol. 38, no. 1, pp. 343–356, 2018.

[91] W. P. Kluijfhout, M. R. Vriens, G. D. Valk, R. E. Barth, I. H. M. Borel Rinkes, and B. de Keizer, "^{18}F-Fluorocholine PET-CT enables minimal invasive parathyroidectomy in patients with negative sestamibi SPECT-CT and ultrasound: a case report," *International Journal of Surgery Case Reports*, vol. 13, pp. 73–75, 2015.

[92] J. K. Hoang, R. E. Reiman, G. B. Nguyen et al., "Lifetime attributable risk of cancer from radiation exposure during parathyroid imaging: comparison of 4D CT and parathyroid scintigraphy," *American Journal of Roentgenology*, vol. 204, no. 5, pp. W579–W585, 2015.

[93] L. Michaud, A. Burgess, V. Huchet et al., "Is ^{18}F-Fluorocholine-Positron emission tomography/computerized tomography a new imaging tool for detecting hyperfunctioning parathyroid glands in primary or secondary hyperparathyroidism?," *The Journal of Clinical Endocrinology & Metabolism*, vol. 99, no. 12, pp. 4531–4536, 2014.

[94] L. Michaud, S. Balogova, A. Burgess et al., "A pilot comparison of ^{18}F-fluorocholine PET/CT, ultrasonography and ^{123}I/^{99m}Tc-sestaMIBI dual-phase dual-isotope scintigraphy in the preoperative localization of hyperfunctioning parathyroid glands in primary or secondary hyperparathyroidism: influence of thyroid anomalies," *Medicine (Baltimore)*, vol. 94, no. 41, Article ID e1701, 2015.

[95] M. Hocevar, L. Lezaic, S. Rep et al., "Focused parathyroidectomy without intraoperative parathormone testing is safe after pre-operative localization with ^{18}F-Fluorocholine PET/

CT," *European Journal of Surgical Oncology (EJSO)*, vol. 43, no. 1, pp. 133–137, 2017.

[96] K. Ibraheem, E. A. Toraih, A. B. Haddad, M. Farag, G. W. Randolph, and E. Kandil, "Selective parathyroid venous sampling in primary hyperparathyroidism: a systematic review and meta-analysis: selective parathyroid venous sampling," *The Laryngoscope*, vol. 128, no. 11, pp. 2662–2667, 2018.

[97] P. Habibollahi, B. Shin, S. P. Shamchi, H. Wachtel, D. L. Fraker, and S. O. Trerotola, "Eleven-year retrospective report of super-selective venous sampling for the evaluation of recurrent or persistent hyperparathyroidism in 32 patients," *CardioVascular and Interventional Radiology*, vol. 41, no. 1, pp. 63–72, 2018.

[98] L. F. Morris, C. Loh, K. Ro et al., "Non-super-selective venous sampling for persistent hyperparathyroidism using a systemic hypocalcemic challenge," *Journal of Vascular and Interventional Radiology*, vol. 23, no. 9, pp. 1191–1199, 2012.

[99] C. A. Madorin, R. Owen, B. Coakley et al., "Comparison of radiation exposure and cost between dynamic computed tomography and sestamibi scintigraphy for preoperative localization of parathyroid lesions," *JAMA Surgery*, vol. 148, no. 6, p. 500, 2013.

[100] A. Mahajan, L. F. Starker, M. Ghita, R. Udelsman, J. A. Brink, and T. Carling, "Parathyroid four-dimensional computed tomography: evaluation of radiation dose exposure during preoperative localization of parathyroid tumors in primary hyperparathyroidism," *World Journal of Surgery*, vol. 36, no. 6, pp. 1335–1339, 2012.

[101] M. J. Campbell, P. Sicuro, A. Alseidi, C. C. Blackmore, and J. A. Ryan, "Two-phase (low-dose) computed tomography is as effective as 4D-CT for identifying enlarged parathyroid glands," *International Journal of Surgery*, vol. 14, pp. 80–84, 2015.

[102] S. Moosvi, S. Smith, J. Hathorn, and T. Groot-Wassink, "Evaluation of the radiation dose exposure and associated cancer risks in patients having preoperative parathyroid localization," *The Annals of The Royal College of Surgeons of England*, vol. 99, no. 5, pp. 363–368, 2017.

[103] F. Morón, A. Delumpa, J. Chetta, D. Guffey, and D. Dunaway, "Single phase computed tomography is equivalent to dual phase method for localizing hyperfunctioning parathyroid glands in patients with primary hyperparathyroidism: a retrospective review," *PeerJ*, vol. 5, Article ID e3586, 2017.

[104] C. C. Lubitz, A. E. Stephen, R. A. Hodin, and P. Pandharipande, "Preoperative localization strategies for primary hyperparathyroidism: an economic analysis," *Annals of Surgical Oncology*, vol. 19, no. 13, pp. 4202–4209, 2012.

[105] T. S. Wang, K. Cheung, F. Farrokhyar, S. A. Roman, and J. A. Sosa, "Would scan, but which scan? A cost-utility analysis to optimize preoperative imaging for primary hyperparathyroidism," *Surgery*, vol. 150, no. 6, pp. 1286–1294, 2011.

Hindawi
International Journal of Endocrinology
Volume 2019, Article ID 7617254, 7 pages
https://doi.org/10.1155/2019/7617254

Research Article

Symptomatic Hypercalcemia in Patients with Primary Hyperparathyroidism Is Associated with Severity of Disease, Polypharmacy, and Comorbidity

C. Aresta,[1] E. Passeri,[2] and S. Corbetta[2,3]

[1]*Endocrine Unit, IRCCS Istituto Auxologico Italiano, Milan, Italy*
[2]*Endocrinology and Diabetology Service, IRCCS Istituto Ortopedico Galeazzi, Milan, Italy*
[3]*Department of Biomedical, Surgical and Dental Sciences, University of Milan, Milan, Italy*

Correspondence should be addressed to S. Corbetta; sabrina.corbetta@unimi.it

Received 8 August 2019; Revised 28 November 2019; Accepted 10 December 2019; Published 30 December 2019

Academic Editor: Maria L. Dufau

Current primary hyperparathyroidism (PHPT) clinical presentation is asymptomatic in more than 90% of patients, while symptoms concern osteoporosis and rarely kidney stones. Here, we retrospectively investigated the prevalence of PHPT patients presenting with hypercalcemic-related symptoms (HS-PHPT) as cognitive impairment, changes in sensorium, proximal muscle weakness, nausea and vomiting, constipation, and severe dehydration, in a single center equipped with an emergency department and described their clinical features and outcome in comparison with a series of asymptomatic PHPT out-patients (A-PHPT). From 2006 to 2016, 112 PHPT patients were consecutively diagnosed: 16% ($n = 18$, 3M/15F) presented with hypercalcemic-related symptoms. Gastrointestinal symptoms occurred in 66% of HS-PHPT patients and cognitive impairment in 44%; one woman experienced hypertensive heart failure. Two-thirds of HS-PHPT patients were hospitalized due to the severity of symptoms. Comparing the clinical features of HS-PHPT patients with A-PHPT patients, no gender differences were detected in the two groups, while HS-PHPT patients were older at diagnosis (71 (61–81) vs. 64 (56–74) years, $P = 0.04$; median (IQR)). HS-PHPT patients presented higher albumin-corrected calcium levels (12.3 (11.3–13.7) vs. 10.6 (10.3–11.3) mg/dl, $P < 0.001$); 4 HS-PHPT presented corrected calcium levels >14 mg/dl. Serum PTH levels and total alkaline phosphatase activity were higher in HS-PHPT. Reduced kidney function (eGFR < 45 ml/min) was prevalent in HS-PHPT patients (42% vs. 5%, $P = 0.05$). No differences in kidney stones and osteoporosis were detected, as well as in the rates of cardiovascular comorbidities and main cardiovascular risk factors. HS-PHPT patients had an age-adjusted Charlson Comorbidity Index higher than that of the A-PHPT patients and were on chronic therapy with a greater number of medications than A-PHPT patients. In conclusion, hypercalcemic-related symptoms occurred in 16% of PHPT patients. Risk factors were severity of the parathyroid tumor function, multimorbidity, and polypharmacy.

1. Introduction

Primary hyperparathyroidism (PHPT) is the third most common endocrine disorder, after diabetes and thyroid diseases, characterized by an inappropriate secretion of parathyroid hormone (PTH) from parathyroid glands. The incidence of PHPT significantly increased in the last decades in western countries, probably due to the inclusion of serum calcium level determination in biochemical screening tests for osteoporosis evaluation [1]. As a result, even the PHPT clinical presentation has changed from symptomatic disorder, primarily characterized by overt skeletal fragility, kidney stones, and hypercalcemic symptoms, to asymptomatic one, that accounts for more than 90% of cases in USA. Due to poor clinical symptoms, PHPT is often an incidental diagnosis during routine evaluation for osteoporosis in postmenopausal women.

PHPT is the most common cause of hypercalcemia [2], although a normocalcemic variant has been established. Hypercalcemia may be associated with a spectrum of clinical

manifestations that usually correlate with the absolute level of serum calcium and the rapidity of onset. Mild calcium levels elevation is often well tolerated, with, when present, aspecific symptoms as fatigue or constipation. More severe clinical presentation, including polyuria, dehydration, anorexia, nausea, and changes in sensorium can be associated with a severe and/or acute rise in serum calcium levels, and patients with severe clinical conditions may require acute hospitalization for the management. However, most PHPT patients are nowadays managed as out-patients.

The aims of the study were (1) to determine the prevalence of PHPT patients presenting with symptomatic hypercalcemia (HS-PHPT) at a single center equipped with an emergency department; (2) to describe their clinical and biochemical features and outcomes in comparison with a series of asymptomatic PHPT (A-PHPT) out-patients.

2. Patients and Methods

2.1. Patients. We retrospectively analyzed data from 112 consecutive patients with PHPT (21 males and 91 females) referred to the single academic center (IRCCS Policlinico San Donato, San Donato Milanese, Milan, Italy) from 2006 to 2016. All patients were white Caucasians.

PHPT was diagnosed when hypercalcemia, namely elevated albumin-corrected serum calcium and/or ionized calcium, and elevated or inappropriately normal PTH level occurred. Patients with normocalcemic PHPT, characterized by elevated PTH levels and normal serum calcium levels, in the absence of any other causes for secondary elevation of PTH, such as severe vitamin D deficiency or renal failure [3], were included.

Symptomatic hypercalcemia was defined as occurrence of hypercalcemic-related symptoms, namely cognitive impairment, severe nausea and vomiting, proximal muscle hypostenia, and hemodynamic instability in patients with diagnosis of PHPT.

The study was conducted in accordance with the Declaration of Helsinki. This study was carried out in accordance with the recommendations of IRCCS Ospedale San Raffaele Milan Ethical Committee with written informed consent from all subjects. All subjects gave written informed consent in accordance with the Declaration of Helsinki. The protocol was approved by the local Ethical Committee.

2.2. Methods. Data were retrospectively collected from the medical record including details on hospital admission, personal and familial medical history, anthropometric measurements, including height and weight, and detailed medication lists. We distinguished hypercalcemia-related symptoms in four main categories: gastrointestinal manifestations (anorexia, nausea, vomiting, abdominal pain, and constipation), neurologic symptoms (cognitive impairment, irritability, and changes in sensorium), musculoskeletal manifestations (fatigue and proximal muscle weakness), and hemodynamic instability (dehydration and hypotension).

Weight was measured on a standard balance beam scale; height was measured using a calibrated, wall-mounted Harpenden stadiometer. Body mass index (BMI) was calculated.

Age-adjusted Charlson Comorbidity Index (ACCI) was determined for each patient by taking into account the occurrence of specific pathologic conditions, with additional points added for age (https://www.mdcalc.com/charlson-comorbidity-index-cci) [4].

Overnight fasting biochemical evaluation included serum and 24-hour urinary calcium, serum albumin, ionized calcium, serum and 24-hour urinary phosphate, total alkaline phosphatase, bone alkaline phosphatase isoenzymes, glucose, insulin, total and HDL cholesterol, triglycerides, and creatinine. Biochemical parameters were assayed by routine methods (Roche modular platform, Roche Diagnostics, Mannheim, Germany); in particular, albumin was measured immunoturbidimetrically, providing measurements similar to those obtained by the bromocresol purple (BCP)-based method [5]. The albumin-corrected serum calcium was calculated according to the following formula: serum total calcium (mg/dL) $- 0.8 \times$ (serum albumin (g/dL) $- 4.0$). Ionized calcium concentrations were assayed by Liquichek Blood Gas (IL Synthesis Series, BioRad Laboratories, Segrate, MI, Italy). Hormonal parameters, namely serum intact PTH and 25-hydroxyvitamin D (25OHD) were assayed by Electrochemiluminescence on an Elecsys 2010 (Roche Diagnostics, Mannheim, Germany) (mean intra-assay and interassay coefficients of variation (CV) of 2.3% and 3%, respectively) and LIAISON® 25OHvitamin D total assay (DiaSorin Inc., Stillwater, MN, USA) with mean intra- and interassay CVs of 4.5% and 7.5%, respectively. The estimated glomerular filtration rate (eGFR) was calculated by the CKD-EPI creatinine equation [6]. Insulin resistance was evaluated according to the HOMA-IR formula [7].

All patients were evaluated with a dual-energy X-ray absorptiometry (DXA) to measure BMD at the lumbar spine (LS), total femur (FT), and femoral neck (FN). Osteoporosis was diagnosed by a BMD T-score lower than -2.5 in postmenopausal patients and by a BMD Z-score lower than -2.0 in premenopausal patients according to the World Health Organization criteria [8]. Ultrasound kidney examination was obtained in all patients.

2.3. Statistical Analysis. The normality of distribution was tested by the Kolmogorov–Smirnov test. Data were nonparametric and were presented as median and interquartile (IQ) range for continuous parameters. Categorical data were presented as percentages. Differences between non-normally distributed parameters were investigated by the Mann–Whitney U test. Differences between frequencies were analysed by the Fischer exact test. The receiver operating characteristic (ROC) curve analysis was performed to assess for each parameter found to be statistically different between HS-PHPT and A-PHPT patients and the predictivity of the occurrence of the hypercalcemia-related symptoms. The logistic regression analysis assessed the association between polypharmacy and age-adjusted Charlson index and the risk to develop hypercalcemic-related symptoms, after adjustment for age and eGFR. A P

value less than 0.05 was considered significant. Statistical analysis was performed using Prism 6.0.

3. Results

3.1. Prevalence of Symptomatic Hypercalcemia in the Series of PHPT Patients. Eighteen patients experienced symptomatic hypercalcemia out of a total of 112 newly diagnosed PHPT patients, indicating a prevalence of 16%. The clinical severity of the SH required hospitalization in the two thirds of cases ($n = 12$).

The most frequent manifestations were gastrointestinal symptoms, occurring in 66% of hypercalcemic-related symptomatic patients (HS-PHPT), the leading ones being nausea and anorexia. Neurologic symptoms, most commonly mild cognitive impairment and irritability, occurred in 50% of cases. Musculoskeletal manifestations were present in 5 patients (27%), and hemodynamic instability, namely lipothymic episodes, was reported in 5 patients (27%). One woman presented hypertensive congestive heart failure, while sepsis occurred in one 50-year-old woman.

3.2. Managing HS-PHPT Patients. Parathyroidectomy was performed in 10 out of 18 (55%) HS-PHPT patients: 9 patients were diagnosed with parathyroid adenoma, and one patient affected with chronic renal failure presented diffuse parathyroid hyperplasia. One patient died 20 days after parathyroidectomy due to major hemorrhagic stroke. Transient hypoparathyroidism, resolving within six months, occurred in 8 patients, whereas only one patient resulted with permanent hypoparathyroidism. The patient with parathyroid hyperplasia experienced a reduction in calcium levels, without complete normalization.

Five HS-PHPT patients were not suitable to parathyroidectomy due to high surgical risk and were successfully treated with oral cinacalcet HCl. Two patients presented mildly elevated calcium levels (less than 11.0 mg/dl) after the resolution of the precipitating event and dehydration. One patient was lost at the follow-up.

3.3. Comparison between HS-PHPT and A-PHPT Patients. Data are presented in Table 1. HS-PHPT patients were significantly older than A-PHPT patients, while no gender differences were detected in the two groups. Multiple endocrine neoplasia type 1 (MEN1) syndrome was diagnosed in 8 (7%) PHPT patients, though none of the MEN1-related PHPT patients experienced SH.

HS-PHPT patients presented significantly higher median albumin-corrected calcium levels than A-PHPT patients, and 4 patients had albumin-corrected calcium levels above 14.0 mg/dl. Moreover, median serum ionized calcium, PTH levels, and total alkaline phosphatase (ALP) were higher in HS-PHPT patients (Figures 1(a)–1(c), panels). Estimated glomerular filtration rate (eGFR) was significantly lower in HS-PHPT (Figure 1(d), panel), and reduced kidney function (eGFR < 45 ml/min; CKD stage G3b and severer) was about 8 folds more frequently detected in HS-PHPT patients. Median serum 25OHD levels were similar in the two groups of PHPT patients, as well as median serum phosphate and 24-hours urinary calcium levels, while median 24-hours urine phosphate levels were lower in HS-PHPT vs. A-PHPT patients, likely related to the lower eGFR.

Received operator characteristic curve (ROC curve) analysis showed that serum calcium levels were significantly associated with hypercalcemic-related symptoms in PHPT patients (area 0.866, $P < 0.0001$), and the threshold of 12.0 mg/dl predicted the occurrence of hypercalcemic-related symptoms with a sensitivity of 93.6% and a specificity of 61.1%. Moreover, serum PTH and ALP levels were associated with hypercalcemic-related symptoms (area 0.880 and 0.702, $P < 0.0001$ and $P = 0.010$, respectively).

Considering PHPT clinical features, the prevalence of kidney stones and osteoporosis were similar in HS-PHPT and A-PHPT patients. Hypertension had the same rate in the two groups (66% vs. 60%, HS-PHPT vs. A-PHPT), and no difference in smoking habit was detected.

Regarding metabolic status, serum glucose and insulin levels, as well as HOMA-IR and occurrence of overt diabetes mellitus did not differ in the two groups. Moreover, though the prevalence of overt dyslipidemia was similarly detected in about one-third of PHPT patients, median serum LDL cholesterol level was slightly but significantly lower in HS-PHPT patients (Figure 1(e), panel).

Finally, we calculated the age-adjusted Charlson comorbidity index, which is considered an indicator of patients' health status. The index was significantly higher in HS-PHPT patients (Table 1 and Figure 2(a), panel), suggesting that HS-PHPT patients had multiple concomitant comorbidities. Additionally, SH-PHPT patients were on chronic therapy with a greater number of medications than A-PHPT patients (Table 1 and Figure 2(b), panel).

Received operator characteristic curve (ROC curve) analysis confirmed the ability of the parameters age (area 0.665, $P = 0.028$), eGFR (area 0.685, $P = 0.016$), polypharmacy (area 0.728, $P = 0.001$), and age-adjusted Charlson index (area 0.732, $P = 0.002$) to be predictive of symptomatic hypercalcemia. The logistic regression analysis considering as dependent variable the occurrence of hypercalcemic-related symptoms and as independent variables age, serum calcium, PTH and ALP levels, eGFR, polypharmacy and age-adjusted Charlson index, showed that serum calcium levels were the strongest predictor of hypecalcemic-related symptoms in PHPT patients with an Odd Ratio (OR) of 2.73 ($P = 0.013$), though polypharmacy and age-adjusted Charlson index also were predictive of hypercalcemic-related symptoms with ORs of 1.50 ($P = 0.05$) and 2.46 ($P = 0.05$), respectively.

4. Discussion

The consensus statements from the first PARAT workshop, a new European Society of Endocrinology program, aiming to identify unmet scientific and educational needs of parathyroid disorders, held in September 2018, highlighted that evidence concerning the natural history of PHPT and whether morbidity and long-term outcomes are related to hypercalcemia or plasma PTH concentrations, or both, is

Table 1: Clinical and biochemical differences between PHPT patients experiencing hypercalcemic-related symptoms and asymptomatic PHPT patients.

	Reference range	HS-PHPT	A-PHPT	*P*
Patients, *n*		18	94	
Age, years		73.0 (81.5–91.5)	65.0 (55.5–74.0)	**0.026**
Gender, M/F		3/15	18/76	0.805
BMI, kg/m^2		25.0 (21.0–28.6)	26.5 (23.2–29.7)	0.504
MEN1-related PHPT, %		0.0	8.5	1.000
Calcium phosphate metabolism-related biochemical parameters				
Serum calcium, mg/dl*	8.4–10.4	12.5 (11.3–13.7)	10.6 (10.3–11.3)	**0.001**
Ionized calcium, mmol/L	1.18–1.30	1.52 (1.43–1.91)	1.39 (1.28–1.47)	**0.001**
PTH, pg/ml	10.0–65.0	422.0 (200.0–704.0)	130.0 (90.7–189.8)	**0.001**
25OHD, ng/ml	>30.0	14.0 (7.1–22.2)	20.1 (10.3–26.7)	0.126
Total ALP, U/L		104.0 (92.2–122.3)	79.5 (60.2–116.0)	**0.009**
Bone-specific ALP, μg/L	6.0–26.0	33.8 (19.9–42.1)	14.8 (10.8–28.2)	**0.010**
eGFR, ml/min		71.0 (43.0–96.0)	90.5 (71.8–104.8)	**0.015**
eGFR < 45 ml/min, %		42.0	5.0	**0.050**
Serum phosphate, mg/dl	3.50–5.00	2.40 (2.08–2.71)	2.60 (2.20–2.90)	0.371
Urine calcium, mg/kg/24 h	<4.00	4.59 (2.85–6.98)	4.10 (2.80–5.76)	0.520
Urine phosphate, g/24 h	<1.00	0.49 (0.36–0.86)	0.73 (0.56–0.89)	**0.028**
PHPT-related clinical features				
Kidney stones, %		44.0	51.0	0.615
Osteoporosis, %		50.0	52.0	1.000
Hypertension, %		66.0	60.0	0.611
Smokers, %		8.3	13.5	1.000
Metabolic status				
Glucose, mg/dl	>100.0	91.0 (81.0–104.5)	90.0 (81.0–96.3)	0.921
Insulin, mU/L	5–25	11.0 (5.9–15.3)	7.3 (2.8–11.6)	0.146
HOMA-IR	<2.5	2.56 (1.09–3.53)	1.62 (0.52–2.85)	0.219
Overt diabetes, %		16.7	5.3	0.087
Total cholesterol, mg/dl	<200.0	188.5 (150.5–211.8)	195.5 (172.8–223.0)	0.130
HDL cholesterol, mg/dl	>40M, >50F	59.0 (46.2–73.7)	56.0 (47.2–67.5)	0.691
LDL cholesterol, mg/dl	<130.0	106.1 (75.9–117.9)	114.1 (94.8–139.9)	**0.033**
Triglycerides, mg/dl	<150.0	117.0 (92.2–135.5)	98.5 (74.5–123.3)	0.118
Overt dyslipidemia, %		27.0	36.0	0.593
PHPT patients' health status				
Age-adjusted Charlson comorbidity index		3.5 (2.7–5.0)	2.0 (1.0–3.0)	**0.001**
Chronic medications, *n*		5.0 (2.2–6.8)	2.0 (0.0–4.0)	**0.001**

HS-PHPT, hypercalcemic-related symptomatic PHPT patients; A-PHPT, asymptomatic PHPT patients; M/F, male/female; *albumin-corrected serum calcium; PTH, parathormone; ALP, alkaline phosphatase; eGFR, estimated glomerular filtration rate; and 25OHD, 25hydroxy-vitamin D.

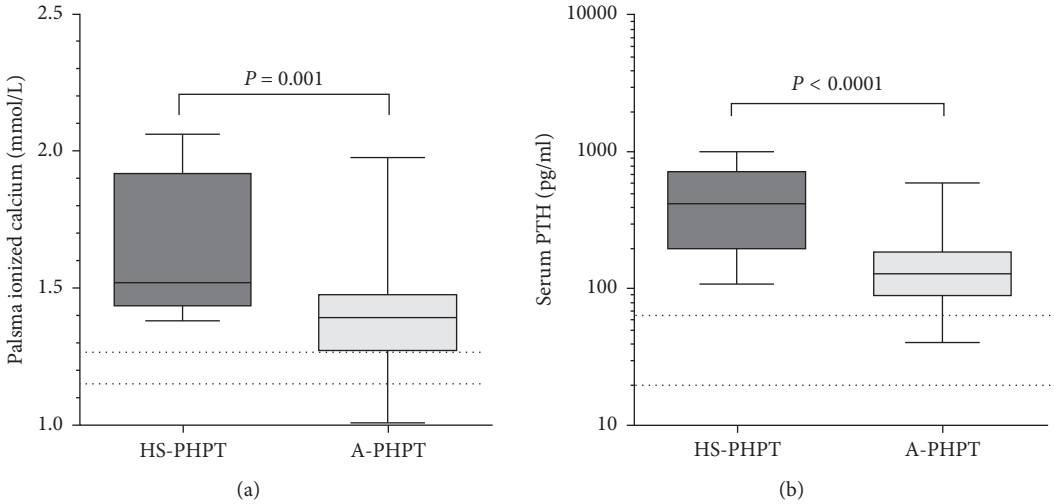

Figure 1: Continued.

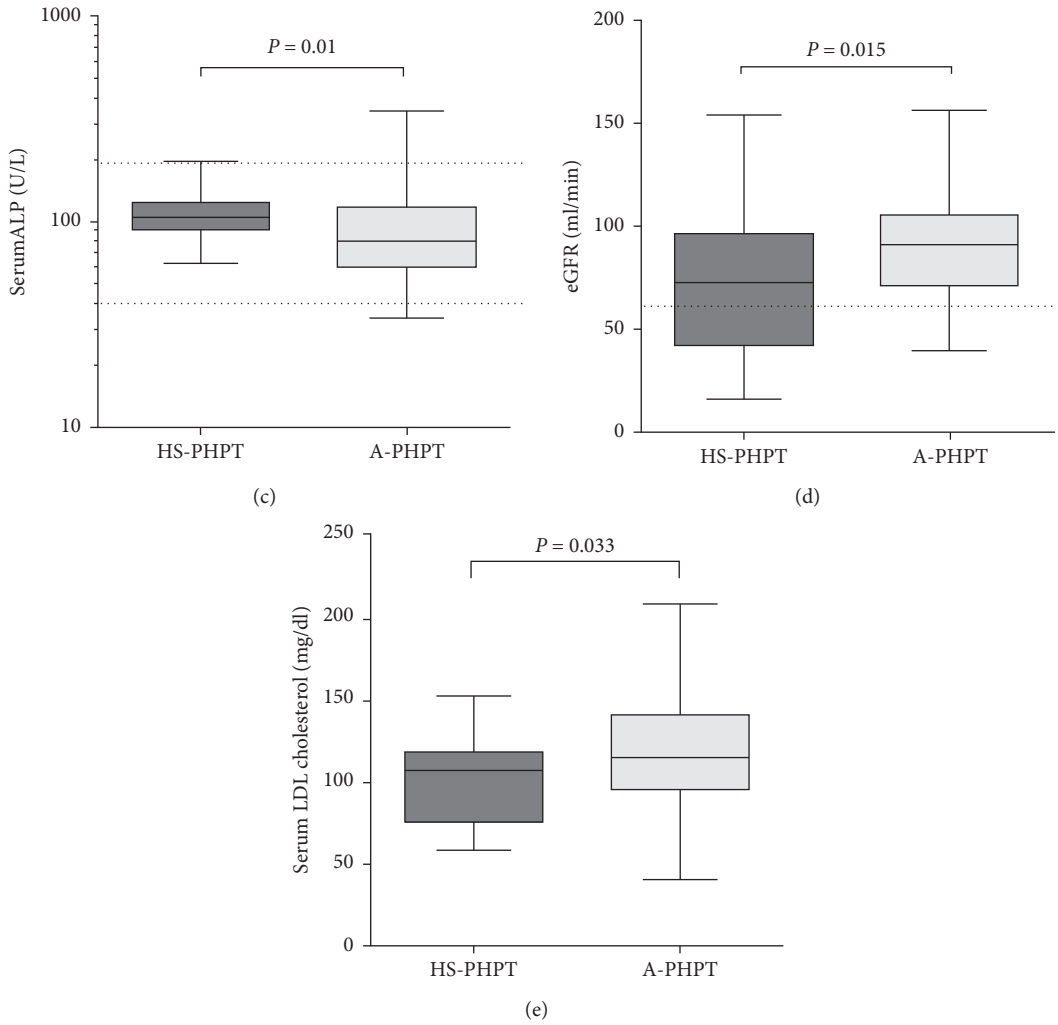

Figure 1: Differences in biochemical parameters between HS-PHPT and A-PHPT. Median plasma ionized calcium (a), serum PTH (b), serum total ALP activity (c), eGFR (d), and LDL cholesterol (e) significantly differed between HS-PHPT and A-PHPT patients. Dashed lines indicate normal reference ranges. Data are presented as median and range interquartile by box, and wisker plots represent minimum and maximum values. Statistical significance was determined by the Mann–Whitney test. HS-PHPT, hypercalcemic-related symptomatic PHPT (dark grey boxes); A-PHPT, asymptomatic PHPT (light grey boxes); PTH, parathormone; ALP, alkaline phosphatase; eGFR, estimated glomerular filtration rate; and LDL, low density lipoprotein.

yet sparse [9]. Present data aimed to contribute to these concerns. PHPT patients attending with asymptomatic primary hyperparathyroidism (PHPT) are common occurrence in the outpatient endocrine setting, and clinicians may be no longer usual in recognizing hypercalcemia-related symptoms in PHPT patients, leading to underrate the prevalence. In the present Italian series of PHPT patients, consecutively enrolled in a single academic hospital equipped with emergency department, hypercalcemia-related symptoms occurred in 16% of cases, suggesting that in this setting, hypercalcemia-related symptoms are not unusual. Main symptoms were gastrointestinal, neurologic, and cognitive impairment, while heart failure and sepsis may occur. The clinical severity of the symptoms required hospitalization in two-thirds of cases. Nonetheless, short-term hypercalcemia-related mortality was low (1 out of 18 cases).

Investigating the clinical characteristics of the patients experiencing symptomatic hypercalcemia (HS-PHPT) compared with A-PHPT patients, HS-PHPT patients emerged as older and presented with a more severe hyperparathyroidism, in terms of higher serum calcium, PTH, and total ALP levels, suggesting that hypercalcemia-related symptoms are positively correlated with the parathyroid tumor activity. At variance, classical PHPT-related symptoms, namely kidney stone and osteoporosis, occurred with similar rates in HS-PHPT and A-PHPT patients, in line with recent reports, where end-organ PHPT manifestations (osteoporosis, nephrolithiasis, and hypercalciuria) developed before biochemical diagnosis or within 5 years in most patients, regardless of severity of hypercalcemia [10, 11].

Of note, kidney function was markedly reduced in HS-PHPT. This might be related to older ages and PHPT clinical severity, as hypercalciuria-induced nephrogenic diabetes

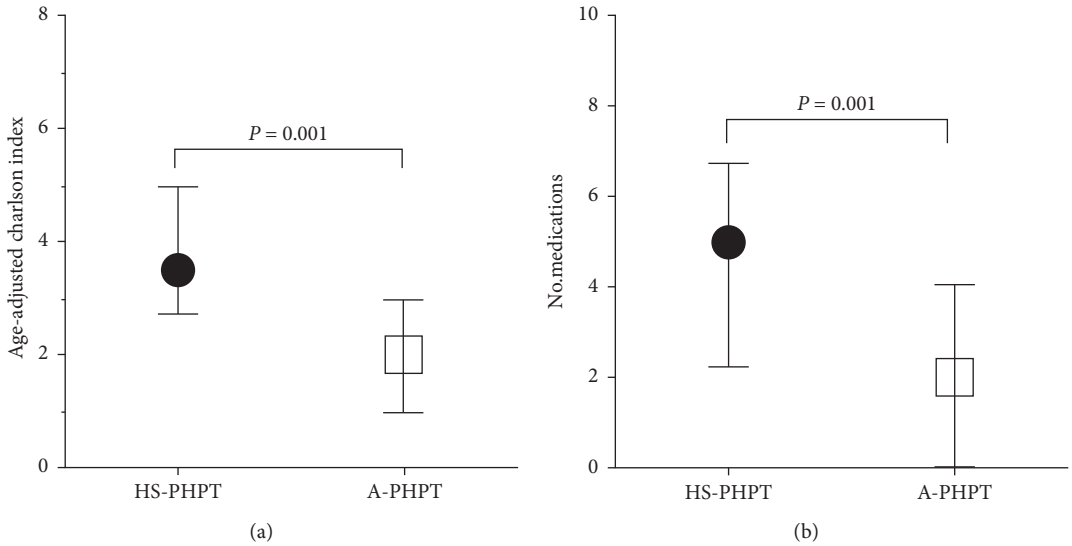

Figure 2: Differences in multimorbidity and polypharmacy between HS-PHPT and A-PHPT. Median values of age-adjusted Charlson index (a) and of the number of medications (b) differed between HS-PHPT and A-PHPT patients. Data are presented as median and range interquartile by box, and wisker plots represent minimum and maximum values. Statistical significance was determined by the Mann–Whitney test. HS-PHPT, hypercalcemic-related symptomatic PHPT (black circles); A-PHPT, asymptomatic PHPT (grey squares).

insipidus often results in polyuria leading to volume depletion and a reduction in the glomerular filtration rate, which may lead to a further increase in calcium concentration [12]. Similarly, a retrospective study of 160 PHPT cases managed at a regional centre in the United Kingdom reported that higher peak calcium concentration was an independent predictor of acute kidney injury [13].

Therefore, patients experiencing symptomatic hypercalcemia were older, with a reduced kidney function, experiencing higher comorbidity score and treated with a higher number of drugs. In this analysis, we operationally define multiple chronic diseases, using the Charlson comorbidity index, intrinsically a measure of aggregate chronic disease burden, developed to predict survival and validated for diseases, like cancers and diabetes [4]. Multimorbidity and polypharmacy are associated with mortality, incident disability, hospitalization, and emergency department visits in frail and prefrail older adults [14–16]. Indeed, after adjustment for age and eGFR, logistic regression analysis showed that serum calcium levels are predictive of the risk to develop symptomatic hypercalcemia; however, polypharmacy and multimorbidity are factors contributing to the risk.

Therefore, data from the present series suggested that patients with severe PHPT should be carefully evaluated for concomitant multimorbidity and polypharmacy in order to estimate the risk of symptomatic hypercalcemia.

Treatment of symptomatic PHPT was surgical in more than a half of HS-PHPT patients: success rate was high, determining serum calcium normalization in more than 90% of cases. In patients contraindicated for or refusing parathyroidectomy, medical treatment with cinacalcet HCl was effective in controlling calcemia. We are tempted to suggest that patients with multimorbidity and polypharmacy at diagnosis of PHPT should be surgically treated, in agreement with recent advice [17], or, if contraindicated or refused, should be carefully followed-up for the development of symptomatic hypercalcemia. Cinacalcet HCl may be considered a therapeutic option to avoid symptomatic hypercalcemia.

5. Conclusions

PHPT patients experiencing hypercalcemia-related symptoms are not uncommon. Hypercalcemia-related symptoms are associated with severity of the parathyroid tumor function, multimorbidity, and polypharmacy. Clinicians should investigate all these factors in PHPT patients in order to estimate the risk of developing hypercalcemic-related symptoms and to consider parathyroid surgery.

Data Availability

The datasets generated during and/or analysed during the current study are available from the corresponding author on reasonable request.

Conflicts of Interest

The authors declare no conflicts of interest.

Authors' Contributions

CS conceived the study and established the protocol; AC and PE managed patients and collected clinical and biochemical data. SC and PE reviewed the data and wrote the manuscript. All the co-authors reviewed the manuscript and approved the final submitted version.

Acknowledgments

This work was supported by the Italian Ministry of Health.

References

[1] J. P. Bilezikian, N. E. Cusano, A. A. Khan, J.-M. Liu, C. Marcocci, and F. Bandeira, "Primary hyperparathyroidism," *Nature Reviews Disease Primers*, vol. 2, no. 1, Article ID 16033, 2016.

[2] C. Marcocci and F. Cetani, "Primary hyperparathyroidism," *New England Journal of Medicine*, vol. 365, no. 25, pp. 2389–2397, 2011.

[3] N. E. Cusano, S. J. Silverberg, and J. P. Bilezikian, "Normocalcemic primary hyperparathyroidism," *Journal of Clinical Densitometry*, vol. 16, no. 1, pp. 33–39, 2013.

[4] M. Charlson, T. P. Szatrowski, J. Peterson, and J. Gold, "Validation of a combined comorbidity index," *Journal of Clinical Epidemiology*, vol. 47, no. 11, pp. 1245–1251, 1994.

[5] J. Helmersson-Karlqvist, M. Flodin, A. M. Havelka, X. Y. Xu, and A. Larsson, "The roche immunoturbidimetric albumin method on cobas c 501 gives higher values than the abbott and roche BCP methods when analyzing patient plasma samples," *Journal of Clinical Laboratory Analysis*, vol. 30, no. 5, pp. 677–681, 2016.

[6] A. S. Levey, L. A. Stevens, C. H. Schmid et al., "A new equation to estimate glomerular filtration rate," *Annals of Internal Medicine*, vol. 150, no. 9, pp. 604–612, 2009.

[7] D. R. Matthews, J. P. Hosker, A. S. Rudenski, B. A. Naylor, D. F. Treacher, and R. C. Turner, "Homeostasis model assessment: insulin resistance and β-cell function from fasting plasma glucose and insulin concentrations in man," *Diabetologia*, vol. 28, no. 7, pp. 412–419, 1985.

[8] J. A. Kanis, L. J. Melton III, C. Christiansen, C. C. Johnston, and N. Khaltaev, "The diagnosis of osteoporosis," *Journal of Bone and Mineral Research*, vol. 9, no. 8, pp. 1137–1141, 1994.

[9] J. Bollerslev, C. Schalin-Jantti, L. Rejnmark et al., "Management of endocrine disease: unmet therapeutic, educational and scientific needs in parathyroid disorders," *European Journal of Endocrinology*, vol. 181, no. 3, pp. 1–9, 2019.

[10] Y. Assadipour, H. Zhou, E. J. Kuo, P. I. Haigh, A. L. Adams, and M. W. Yeh, "End-organ effects of primary hyperparathyroidism: a population-based study," *Surgery*, vol. 165, no. 1, pp. 99–104, 2019.

[11] H. Yan, N. Calcatera, T. A. Moo-Young, R. A. Prinz, and D. J. Winchester, "Degree of hypercalcemia correlates with parathyroidectomy but not with symptoms," *The American Journal of Surgery*, vol. 217, no. 3, pp. 437–440, 2019.

[12] D. A. Bushinsky and R. D. Monk, "Calcium," *The Lancet*, vol. 352, no. 9124, pp. 306–311, 1998.

[13] J. M. Pappachan, M. N. Elnaggar, R. Sodi, K. Jbeili, P. R. Smith, and I. M. Lahart, "Primary hyperparathyroidism: findings from the retrospective evaluation of cases over a 6-year period from a regional UK centre," *Endocrine*, vol. 62, no. 1, pp. 174–181, 2018.

[14] K.-U. Saum, B. Schöttker, A. D. Meid et al., "Is polypharmacy associated with frailty in older people? results from the ESTHER cohort study," *Journal of the American Geriatrics Society*, vol. 65, no. 2, pp. e27–e32, 2017.

[15] B. Bonaga, P. M. Sánchez-Jurado, M. Martínez-Reig et al., "Frailty, polypharmacy, and health outcomes in older adults: the frailty and dependence in albacete study," *Journal of the American Medical Directors Association*, vol. 19, no. 1, pp. 46–52, 2018.

[16] M. Q. Thompson, O. Theou, S. Yu, R. J. Adams, G. R. Tucker, and R. Visvanathan, "Frailty prevalence and factors associated with the frailty phenotype and frailty index: findings from the north west adelaide health study," *Australasian Journal on Ageing*, vol. 37, no. 2, pp. 120–126, 2018.

[17] I.-L. Nilsson, "Primary hyperparathyroidism: should surgery be performed on all patients? current evidence and residual uncertainties," *Journal of Internal Medicine*, vol. 285, no. 2, pp. 149–164, 2019.

Hindawi
International Journal of Endocrinology
Volume 2019, Article ID 1761030, 8 pages
https://doi.org/10.1155/2019/1761030

Review Article

Clinical Features, Treatment, and Surveillance of Hyperparathyroidism-Jaw Tumor Syndrome: An Up-to-Date and Review of the Literature

Francesca Torresan and Maurizio Iacobone

Endocrine Surgery Unit, Department of Surgery, Oncology and Gastroenterology, University of Padova, Via Giustiniani 2, 35128 Padova, Italy

Correspondence should be addressed to Maurizio Iacobone; maurizio.iacobone@unipd.it

Received 5 September 2019; Accepted 11 November 2019; Published 18 December 2019

Guest Editor: Vito Guarnieri

Hyperparathyroidism-jaw tumor (HPT-JT) syndrome is an autosomal dominant disorder characterized by parathyroid tumors in association with fibro-osseous jaw tumors and uterine and renal lesions. HPT-JT syndrome is caused by germline mutations of the cell division cycle 73 (*CDC73*) gene that encodes the parafibromin, a 531-amino acid protein with antiproliferative activity. Primary hyperparathyroidism is the main finding of HPT-JT syndrome, usually caused by a single-gland parathyroid involvement (80% of cases), at variance with other variants of hereditary hyperparathyroidism, in which a multiglandular involvement is more frequent. Moreover, parathyroid carcinoma may occur in approximately 20% of cases. Surgery is the treatment of choice for primary hyperparathyroidism, but the extent of surgery remains controversial, varying between bilateral neck and focused exploration, with subtotal or limited parathyroidectomy. Recently, more limited approaches and parathyroid excisions have been suggested in order to decrease the risk of permanent hypoparathyroidism, the main surgical morbidity following more extensive surgical approaches. Ossifying fibromas of the mandible or maxilla may present only in a minority of cases and, even if benign, they should be surgically treated to avoid tumor growth and subsequent functional limitations. Benign and malignant uterine involvement (including leiomyomas, endometrial hyperplasia, adenomyosis, multiple adenomyomatous polyps, and adenosarcomas) is the second most common clinical feature of the syndrome, affecting more than 50% of *CDC73*-carrier women. Genetic testing should be performed in all family members of affected individuals, in young patients undergoing surgery for primary hyperparathyroidism, or in presence of other associated tumors, allowing early diagnosis and prompt treatment with more tailored surgery. Moreover, *CDC73* mutation carriers should be also periodically screened for primary hyperparathyroidism and the other associated tumors. The present review was aimed to summarize the main clinical features of HPT-JT syndrome, focusing on genetic screening and surgical treatment, and to revise the available literature.

1. Introduction

Hyperparathyroidism-jaw tumor syndrome (HPT-JT) (OMIM#145001) is a rare autosomal dominant disorder with incomplete penetrance characterized by the development of parathyroid tumors, ossifying fibromas of the mandible and maxilla, cystic and neoplastic renal abnormalities, and hyperplastic and neoplastic uterine involvement [1, 2].

HPT-JT syndrome is caused by germline mutations of the *CDC73* gene that encodes the parafibromin, a ubiquitously expressed, predominantly nuclear protein with antiproliferative properties [3–6].

Despite the nomenclature of the syndrome, jaw tumors may be found only in approximately one third of cases, while the most common, and sometimes the only feature of HPT-JT, is primary hyperparathyroidism (pHPT). At variance with other forms of hereditary pHPT in which parathyroid tumors are generally benign, HPT-JT is associated with a higher prevalence of atypical adenomas and carcinomas [7, 8].

Genetic testing is required to confirm the hereditary nature of pHPT in HPT-JT, and it is crucial for the optimal clinical and surgical management of the affected individuals; moreover, a molecular genetic testing should be obtained in at risk relatives in order to identify the gene carriers as early as possible to start surveillance and early treatment [9].

The aim of this review is to summarize the current knowledge on HPT-JT syndrome including clinical features, genetic, and treatments and to revise the available literature.

2. Etiology and Diagnosis

HPT-JT is linked to germline-inactivating mutations in the tumor suppressor gene *CDC73* (formerly *HRPT2*), which is comprised of 17 exons on chromosome 1q31.2 and encodes for the predominantly nuclear, 531-amino acid protein, parafibromin [10]. Parafibromin is ubiquitously expressed in a variety of human tissues, including kidney, liver, stomach, renal cortex tubules, and the pars intermedia of the hypophysis [11].

Parafibromin is associated with other proteins in the polymerase-associated factor (PAF1) and induces the downregulation of cyclin D1 expression and direct interaction with *ß*-catenin, resulting in the activation of transcription of target genes. Studies of the PAF1 complex in yeast and *Drosophila*, as well as in mammalian cells, have revealed that parafibromin, as part of the PAF1 complex, induces histone modification, transcription elongation, and chromatin remodeling [12–14].

About 75% of HPT-JT patients have germline *CDC73* mutations within the coding region, and the majority (>80%) are frameshift or nonsense mutations that determine the functional loss of parafibromin by causing a premature truncation of this protein or a rapid loosing of the translated protein via nonsense-mediated mRNA decay. Therefore, the expression of parafibromin is completely lost in HPT-JT-associated tumor tissues. Immunohistochemical staining of parafibromin in parathyroid tumors and other HPT-JT-associated tumors is an indirect method to recognize HPT-JT syndrome patients. The remaining 25% of HPT-JT patients may have abnormalities in *CDC73* promoter regions, whole exon or gene deletions, mutations in unidentified genes, or epigenetic modifications [15].

As in all tumor suppressor genes, the first mutation is usually inherited by one of the parents or, in very rare cases, developed *de novo* at embryo level; the second allele-inactivating mechanism is a novel acquired somatic mutation or a loss of heterozygosity in HPT-JT tumor-related tissues, consistent with Knudson's two-hit hypothesis [7–16].

Even in presence of a *CDC73* mutation, the penetrance of pHPT is incomplete and no genotype-phenotype correlations have been fully established to date. However, it has been suggested that missense mutations are more likely to be associated with the disease without typical associated features (familial isolated pHPT), whereas mutations causing gross parafibromin disruption are more likely associated with the classical HPT-JT phenotype [9].

The diagnosis of HPT-JT must be confirmed by genetic testing. The screening for *CDC73* germline mutations is indicated in presence of familial pHPT, in case of pHPT with young age onset (<40 years), multiglandular involvement, cystic, atypical, or malignant parathyroid involvements, or in presence of coexistence ossifying jaw fibroma, renal, or uterine tumors [9, 17]. As in the original description of HPT-JT syndrome, where it was characterized as cystic parathyroid adenomatosis, the adenomas may be cystic, either with micro- or macrocysts, and similar cystic changes can also be present in the normal parathyroid glands in these patients [18].

Following the initial diagnosis, the associated jaw tumors and renal and uterine lesions should be systematically searched [3–6].

Genetic screening for identifying the gene carrier and/or affected family members should be performed in all family members to start a specific HPT-JT screening program [19]. In *CDC73* mutation carrier families, the screening should be performed also in children before the age of 10 since malignant pHPT has been sometimes described at very early age.

3. Clinical Features

3.1. pHPT. pHPT is the main finding of HPT-JT syndrome and is found in almost 100% of mutation carriers typically in late adolescence or early adulthood. The earliest reported age of hypercalcemia is seven years [20]. The median age of diagnosis of pHPT reported was 27 years (range 12–58) [21], and the mean age ranged between 32 years and 36 years [4, 22]. In a report of a three large kindred, *CDC73*-related pHPT occurred in 87.5% of cases among patients older than 20 years [9], while penetrance of pHPT in a Dutch population was shown to increase with age (8%, 53%, and 75% at ages 25, 50, and 70, respectively) [22]. To date, 154 HPT-JT kindreds have been reported in the literature (Table 1), including 365 patients affected by pHPT. At variance with other forms of hereditary pHPT, in HPT-JT, a single-gland parathyroid involvement has been reported more frequently (86.1%). Multiglandular involvement occurs rarely at initial surgery (13.9% of cases); recurrences of pHPT may occur metachronously in 20% of cases. At pathology, a single benign parathyroid adenoma is usually found; however, parathyroid carcinoma may be found in 23% of cases [2–82].

pHPT is usually mild and/or asymptomatic, but, in the case of parathyroid carcinoma, severe hypercalcemic crises may occur [83]. Hence, in presence of abnormal high serum calcium concentration (>12 mg/dL) and iPTH levels (>3 times the upper limit of normal) and parathyroid lesions larger than 3 cm, parathyroid carcinomas should be suspected, even if nonfunctioning parathyroid malignancy may very rarely occur in *CDC73*-related disorder [35, 82]. Moreover, parathyroid carcinoma can present as palpable neck mass associated with hoarseness, difficulty speaking or swallowing, muscle weakness, nausea/vomiting, altered mental status, bone pain, and/or pathologic bone fractures [7, 17, 22, 23, 38].

Given the rarity of the disease and the heterogeneity of the phenotype, the optimal surgical approach to *CDC73*-related

Table 1: Review of the literature focusing on HPT-JT syndrome.

Author (year)	Kindred (n =)	pHPT (n =)	Single-gland pHPT (n =)	Synchronous multiglandular pHPT (n =)	Recurrences (n =)	Parathyroid carcinoma (n =)	Jaw tumor (n =)	Renal lesions (n)	Uterine lesions (n)
Carpten et al. (2002) [7]	14	66	NA	NA	NA	11	30	18	NA
Shattuck et al. (2003) [23]	3	3	NA	NA	NA	3	NA	NA	NA
Howell et al. (2003) [24]	3	7	NA	NA	0	3	0	0	NA
Simonds et al. (2004) [25]	1	4	4	0	0	1	0	0	NA
Cetani et al. (2004) [17]	2	4	3	1	NA	0	0	0	NA
Villablanca et al. (2004) [26]	2	9	7	2	3	0	0	0	NA
Cavaco et al. (2004) [27]	6	9	5	1	0	0	2	2	NA
Howell et al. (2004) [28]	1	2	2	0	NA	0	1	NA	NA
Bradley et al. (2005) [2]	2	9	NA	NA	NA	2	11	0	6
Moon et al. (2005) [29]	1	2	2	0	NA	2	1	NA	NA
Gimm et al. (2006) [30]	1	3	1	1	1	1	NA	NA	NA
Mizusawa et al. (2006) [31]	3	7	6	0	1	1	1	0	0
Aldred et al. (2006) [32]	1	3	3	0	0	0	2	NA	NA
Bradley et al. (2006) [33]	5	5	4	1	NA	0	2	0	1
Juhlin et al. (2006) [34]	1	1	1	NA	NA	0	NA	NA	NA
Guarnieri et al. (2006) [35]	1	4	4	0	1	1	NA	0	2
Kelly et al. (2006) [8]	1	3	2	1	2	2	NA	NA	NA
Yamashita et al. (2007) [36]	1	1	1	0	0	0	1	NA	NA
Cetani et al. (2007) [37]	1	1	1	0	1	0	0	0	NA
Cetani et al. (2007) [38]	2	3	NA	NA	NA	3	NA	NA	NA
Raue et al. (2007) [39]	1	2	1	1	NA	1	1	NA	NA
Cetani et al. (2008) [40]	1	1	1	0	NA	1	0	NA	NA
Sarquis et al. (2008) [41]	3	11	5	6	6	1	1	4	5
Guarnieri et al. (2008) [42]	3	3	3	0	1	3	0	3	3
Howell et al. (2009) [43]	1	1	1	0	0	NA	NA	NA	NA
Silveira et al. (2008) [44]	1	9	3	6	6	1	0	4	5
Schmidt et al. (2009) [45]	1	1	1	0	0	0	1	NA	NA
Rekik et al. (2010) [46]	1	1	1	0	0	0	1	0	1
Panicker et al. (2010) [47]	1	5	NA	NA	NA	0	1	0	1
Veiguela et al. (2010) [48]	1	7	NA	NA	NA	1	3	0	2
Cavaco et al. (2011) [49]	2	2	2	0	1	2	0	0	0
Pichardo-Lowden et al. (2011) [20]	1	1	1	0	1	0	0	1	NA
Frank-Raue et al. (2011) [50]	7	11	9	1	1	3	8	0	2
Cascón et al. (2011) [10]	1	3	NA	NA	NA	0	3	NA	NA
Siu et al. (2011) [51]	2	2	2	0	0	1	0	0	NA
Domingues et al. (2012) [52]	1	1	1	0	0	0	0	0	NA
Guerrouani et al. (2013) [53]	1	1	1	0	NA	0	1	NA	NA
Bricaire et al. (2013) [21]	NA	19	NA	NA	NA	5	4	4	6
Kutcher et al. (2013) [54]	1	1	0	1	0	1	1	1	NA
Ghemigian et al. (2013) [55]	1	3	3	0	0	0	0	NA	NA
Abdulla et al. (2013) [56]	1	1	0	1	1	0	1	NA	NA
Pazienza et al. (2013) [57]	3	7	7	0	0	0	0	1	1
Kong et al. (2014) [58]	1	2	0	2	1	0	1	NA	2
Chiofalo et al. (2014) [59]	1	2	2	0	0	1	1	0	NA
Korpi-Hyövälti et al. (2014) [60]	1	7	NA	NA	NA	2	NA	2	NA
Sriphrapradang et al. (2014) [61]	1	1	1	0	NA	1	1	0	NA
Mehta[a] et al. (2014) [62]	7	16	11	5	4	6	2	3	2
Parfitt et al. (2015) [63]	1	1	1	0	0	1	1	0	0
Shibata et al. (2015) [64]	1	1	1	0	1	0	0	0	0

Table 1: Continued.

Author (year)	Kindred (n =)	pHPT (n =)	Single-gland pHPT (n =)	Synchronous multiglandular pHPT (n =)	Recurrences (n =)	Parathyroid carcinoma (n =)	Jaw tumor (n =)	Renal lesions (n)	Uterine lesions (n)
Khadilkar et al. (2015) [65]	4	6	6	0	2	1	2	3	2
Marchiori et al. (2015) [66]	1	1	1	0	0	1	1	0	0
Bellido et al. (2016) [67]	1	1	1	0	0	0	1	NA	NA
Ennazk et al. (2016) [68]	1	1	1	0	0	0	1	NA	NA
Mathews et al. (2016) [69]	1	1	1	0	0	0	1	NA	NA
Mele et al. (2016) [70]	1	1	1	0	1	1	1	NA	0
Piciu et al. (2016) [71]	1	1	1	0	0	0	1	0	1
Guarnieri et al. (2017) [72]	1	3	3	0	0	1	0	0	1
Mamedova et al. (2017) [73]	6	6	6	0	1	4	0	0	0
van der Tuin et al. (2017) [22]	12	32	32	0	NA	5	6	10	1
Dhas et al. (2017) [74]	1	1	1	0	0	0	1	0	1
Rubinstein et al. (2017) [75]	1	1	1	0	0	0	0	0	1
Koikawa et al. (2018) [76]	1	1	1	0	0	0	1	0	1
Bachmeier et al. (2018) [77]	1	1	1	0	0	0	0	0	0
Kapur et al. (2018) [78]	1	1	1	0	NA	1	0	0	0
Ciuffi et al. (2019) [79]	1	1	1	0	NA	1	1	NA	0
Russo et al. (2019) [80]	1	1	1	0	1	1	1	NA	NA
Gill et al. (2019) [81]	13	16	15	1	3	4	1	NA	NA
Iacobone et al. (2019) [82]	5	20	19	1	6	3	2	1	14
Total n = (%)	154	365	198 (86.1%)	32 (13.9%)	46 (20%)	84 (23%)	104 (28.4%)	57 (15.6%)	60 (45.1%)

[a]Some cases have been previously included in Carpten et al. [7]. NA = not available; pHPT = primary hyperparathyroidism.

pHPT has not yet been established and remains controversial, varying between bilateral or targeted neck exploration and extensive or limited parathyroidectomy [9].

In the past, prophylactic subtotal or total parathyroidectomy has been suggested to reduce the risk of recurrences and parathyroid carcinoma in HPT-JT syndrome and therefore to obtain a definitive cure; however, total parathyroidectomy is clearly not always successful and leads to an increased morbidity due to the permanent postsurgical hypoparathyroidism that is difficult to treat especially in young patients. For these reasons, subtotal parathyroidectomy or total parathyroidectomy with autotransplantation has been suggested in the same setting of other variants of hereditary pHPT, even if autotransplantation has been advocated to theoretically cause tumor dissemination in case of malignant involvement [82]. Moreover, because of the reported high prevalence of uniglandular involvement at onset, targeted approaches and selective parathyroid excisions have recently been proposed in order to achieve, whenever possible, the longest possible normocalcemia without permanent hypoparathyroidism, minimizing surgical morbidity and facilitating eventual future surgery for recurrent disease [4].

In 2008, Sarquis et al. have observed, in a series of 11 *CDC73* germline mutated patients from 3 kindreds, a synchronous multiglandular involvement at initial operation in 54.5% of cases, parathyroid malignancy in 9%, and an overall persistence/recurrence rate of 80%; thus, a bilateral exploration with subtotal parathyroidectomy was suggested as the initial approach [41].

In 2014, Mehta et al. suggested a bilateral neck exploration with selective removal only of abnormal gland/s in HPT-JT syndrome patients, given the high frequency of benign single-gland involvement (69%) and relatively low rate of reoccurences (20%) found in their multicentric cohort of 16 individuals from seven families [62].

More recently, Iacobone et al. reported, in a cohort of 20 HPT-JT syndrome patients from five large families, a 95% rate of single-gland involvement. Therefore, in case of preoperative imaging techniques localizing concordantly, a single-gland involvement and in absence of suspicion of parathyroid malignancy, a focused approach with selective parathyroidectomy has been proposed. In case of absent or discordant preoperative localization, a subtotal parathyroidectomy was suggested because of the increased risk of multiglandular involvement and recurrent pHPT [82]. Regardless of the surgical approach, the risk of recurrences is estimated, according to the review of the literature (Table 1), to be about 25%, thus requiring a regular lifelong pHPT biochemical and instrumental monitoring.

If parathyroid carcinoma is clinically suspected (large tumor at imaging, palpable neck mass, and biochemical and clinical presentation of severe pHPT), an en bloc resection of the mass with the ipsilateral thyroid lobe, possibly also including the ipsilateral normal parathyroid and the

surrounding lymph fatty tissue, should be performed, in order to avoid tumor seeding and achieve a "complete unilateral parathyroidectomy," and finally avoiding the risk of reoperation in a scarred area [4, 82–84].

Cinacalcet hydrochloride, a calcimimetic that binds to the calcium-sensing receptor, has been approved for the long-term control of hypercalcemia secondary to pHPT in individuals who are unable to undergo parathyroidectomy and for the treatment of parathyroid carcinoma-related hypercalcemia, in case of unresectable or metastatic disease.

For severe or symptomatic hypercalcemia, individuals can be treated with an infusion of zoledronic acid or denosumab for acute management.

3.2. Jaw Tumors. Jaw tumors in HPT-JT are fibro-osseous lesions that typically involve the maxilla or mandible that occur in about 30% of cases (Table 1), often prior to the third decade of life.

The majority of the reported jaw tumors in HPT-JT syndrome are ossifying fibromas, benign and generally slow-growing tumors arising from the periodontal ligament in molar or premolar areas [85]. Even if specific features of ossifying fibroma in HPT-JT syndrome are not well defined, most often they appear to be radiographically radiolucent compared to the mixed radiolucent/radiopaque lesions in the sporadic variants [32]. They may present as an enlarging visible or palpable mass, or in some cases, they are only detected on dental X-ray imaging.

Although benign, ossifying fibroma can disrupt normal dentition and impair breathing, causing functional and cosmetic symptoms. Moreover, ossifying fibroma in HPT-JT syndrome may be bilateral/multifocal and may recur. For these reasons, complete surgical removal is the recommended treatment based on the size, location, and symptoms of the lesion. Individuals with a history of jaw tumors should be followed closely because of the possibility of recurrence [86].

3.3. Renal Involvement. The kidney is involved in a limited subset of patients with HPT-JT (approximately 15% of cases). Cystic kidney disease is the most common renal manifestation of this syndrome.

In addition to renal cysts, some patients often develop hamartomas and rare renal tumors, such as adult Wilms's tumors and mixed epithelial-stromal tumors (MEST). Wilms's tumors in HPT-JT have been identified in the fifth decade of life, are usually bilateral, poorly circumscribed, of smaller sizes compared to the classical childhood form, and they usually do not metastasize. Moreover, they had also distinctive histological features from the childhood form, such as a low number of mitoses, lack of necrosis and hemorrhages, large mesenchymal components, and the presence of cysts [87].

The association between MEST, a predominantly benign tumor characterized by both epithelial and spindle cell stromal components, and HPT-JT syndrome is poorly reported in the literature.

Since HPT-JT patients may be at risk for multiple, bilateral renal tumors potentially requiring multiple renal surgeries over their lifetime, nephron-sparing surgery rather than radical surgery is advocated, in order to preserve renal function [88]. Moreover, given the malignant potential, sarcomatoid differentiation, and metastatic spread, surgery represents the treatment of choice [89].

Papillary renal cell carcinoma have also been described, albeit rarely, in HPT-JT [4, 90].

3.4. Uterine Involvement. Uterine tumors have been described in association with HPT-JT and are the most common clinical feature after pHPT, affecting more than 50% of HPT-JT female patients in some cohorts [9].

Most women present with menorrhagia that may require hysterectomy at an early age (mean 35 years). Affected women often have a history of miscarriage and a significantly impaired ability to bear children when compared with their unaffected female relatives [33]. Histological analysis of the uterine specimens revealed both benign and malignant tumors, such as adenomyosis, adenofibromas, leiomyomas, endometrial hyperplasia, adenosarcomas, or tumors arising from the Müllerian duct system.

No treatment guidelines for uterine manifestations associated with HPT-JT syndrome have been proposed to date. Individuals with evidence of a uterine tumor should be managed by a gynecologist on a case-by-case basis.

3.5. Other Features. Thyroid carcinoma, thyrotoxicosis, colon carcinoma, cholangiocarcinoma, chronic lymphatic leukemia, pancreatic adenocarcinoma, and pituitary cyst have also been described, but the association between these less common tumors and HPT-JT syndrome remains unclear [4, 42, 90].

3.6. Surveillance. Even if there are no well-established surveillance guidelines, according to the literature we suggest that *CDC73* mutation carriers should undergo the following screening:

(i) Biannual evaluation of serum calcium and PTH for pHPT screening, possibly starting at the age of five, and periodic parathyroid ultrasound examination

(ii) Panoramic X-ray dental imaging at least every five years

(iii) Monitor for kidney lesions by periodic renal ultrasound examination, magnetic resonance imaging, or computed tomography scan at least every 5 years, starting at the age of diagnosis

(iv) Starting at the reproductive age, women with a *CDC73*-related disorder should undergo regular gynecologic care, including pelvic ultrasound examination with eventually further imaging studies if clinically indicated.

Conflicts of Interest

The authors declare that there are no conflicts of interest regarding the publication of this paper.

References

[1] T. Carling and R. Udelsman, "Parathyroid surgery in familial hyperparathyroid disorders," *Journal of Internal Medicine*, vol. 257, no. 1, pp. 27–37, 2005.

[2] K. J. Bradley, M. R. Hobbs, I. D. Buley et al., "Uterine tumours are a phenotypic manifestation of the hyperparathyroidism-jaw tumour syndrome," *Journal of Internal Medicine*, vol. 257, no. 1, pp. 18–26, 2005.

[3] M. Iacobone, L. Barzon, A. Porzionato et al., "Parafibromin expression, single-gland involvement, and limited parathyroidectomy in familial isolated hyperparathyroidism," *Surgery*, vol. 142, no. 6, pp. 984–991, 2007.

[4] M. Iacobone, G. Masi, L. Barzon et al., "Hyperparathyroidism-jaw tumor syndrome: a report of three large kindred," *Langenbeck's Archives of Surgery*, vol. 394, no. 5, pp. 817–825, 2009.

[5] G. Masi, L. Barzon, M. Iacobone et al., "Clinical, genetic, and histopathologic investigation of *CDC73*-related familial hyperparathyroidism," *Endocrine Related Cancer*, vol. 15, no. 4, pp. 1115–1126, 2008.

[6] G. Masi, M. Iacobone, A. Sinigaglia et al., "Characterization of a new *CDC73* missense mutation that impairs parafibromin expression and nucleolar localization," *PLoS One*, vol. 9, no. 5, Article ID e97994, 2014.

[7] J. D. Carpten, C. M. Robbins, A. Villablanca et al., "*HRPT2*, encoding parafibromin, is mutated in hyperparathyroidism-jaw tumor syndrome," *Nature Genetics*, vol. 32, no. 4, pp. 676–680, 2002.

[8] T. G. Kelly, T. M. Shattuck, M. Reyes-Mugica et al., "Surveillance for early detection of aggressive parathyroid disease: carcinoma and atypical adenoma in familial isolated hyperparathyroidism associated with a germline *HRPT2* mutation," *Journal of Bone and Mineral Research*, vol. 21, no. 10, pp. 1666–1671, 2006.

[9] M. Iacobone, B. Carnaille, F. Palazzo, and M. Vriens, "Hereditary hyperparathyroidism—a consensus report of the European Society of Endocrine Surgeons (ESES)," *Langenbeck's Archives of Surgery*, vol. 400, no. 8, pp. 867–886, 2015.

[10] A. Cascón, C. V. Huarte-Mendicoa, L. Javier Leandro-García et al., "Detection of the first gross *CDC73* germline deletion in an HPT-JT syndrome family," *Genes, Chromosomes and Cancer*, vol. 50, no. 11, pp. 922–929, 2011.

[11] A. Porzionato, V. Macchi, L. Barzon et al., "Immunohistochemical assessment of parafibromin in mouse and human tissues," *Journal of Anatomy*, vol. 209, no. 6, pp. 817–827, 2006.

[12] O. Rozenblatt-Rosen, C. M. Hughes, S. J. Nannepaga et al., "The parafibromin tumor suppressor protein is part of a human Paf1 complex," *Molecular and Cellular Biology*, vol. 25, no. 2, pp. 612–620, 2005.

[13] A. Yart, M. Gstaiger, C. Wirbelauer et al., "The *HRPT2* tumor suppressor gene product parafibromin associates with human PAF1 and RNA polymerase II," *Molecular and Cellular Biology*, vol. 25, no. 12, pp. 5052–5060, 2005.

[14] C. Mosimann, G. Hausmann, and K. Basler, "Parafibromin/hyrax activates wnt/wg target gene transcription by direct association with β-catenin/armadillo," *Cell*, vol. 125, no. 2, pp. 327–341, 2006.

[15] P. J. Newey, M. R. Bowl, T. Cranston, and R. V. Thakker, "Cell division cycle protein 73 homolog (*CDC73*) mutations in the hyperparathyroidism-jaw tumor syndrome (HPT-JT) and parathyroid tumors," *Human Mutation*, vol. 31, no. 3, pp. 295–307, 2010.

[16] G. V. Walls, M. Stevenson, K. E. Lines et al., "Mice deleted for cell division cycle 73 gene develop parathyroid and uterine tumours: model for the hyperparathyroidism-jaw tumour syndrome," *Oncogene*, vol. 36, no. 28, pp. 4025–4036, 2017.

[17] F. Cetani, E. Pardi, S. Borsari et al., "Genetic analyses of the *HRPT2* gene in primary hyperparathyroidism: germline and somatic mutations in familial and sporadic parathyroid tumors," *The Journal of Clinical Endocrinology & Metabolism*, vol. 89, no. 11, pp. 5583–5591, 2004.

[18] L. E. Mallette, S. Malini, M. P. Rappaport, and J. L. Kirkland, "Familial cystic parathyroid adenomatosis," *Annals of Internal Medicine*, vol. 107, no. 1, pp. 54–60, 1987.

[19] S. M. Hyde, T. A. Rich, S. G. Waguespack, N. D. Perrier, and M. I. Hu, "*CDC73*-related disorders," in *GeneReviews® [Internet]*, R. A. Pagon, M. P. Adam, H. H. Ardinger et al., Eds., University of Washington, Seattle, WA, USA, 2019.

[20] A. Pichardo-Lowden, A. Manni, B. Saunders, and M. Baker, "Familial hyperparathyroidism due to a germline mutation of the *CDC73* gene: implications for management and age-appropriate testing of relatives at risk," *Endocrine Practice*, vol. 17, no. 4, pp. 602–609, 2011.

[21] L. Bricaire, M.-F. Odou, C. Cardot-Bauters et al., "Frequent large germline *HRPT2* deletions in a French national cohort of patients with primary hyperparathyroidism," *The Journal of Clinical Endocrinology & Metabolism*, vol. 98, no. 2, pp. E403–E408, 2013.

[22] K. van der Tuin, C. M. J. Tops, M. A. Adank et al., "*CDC73*-related disorders: clinical manifestations and case detection in primary hyperparathyroidism," *The Journal of Clinical Endocrinology & Metabolism*, vol. 102, no. 12, pp. 4534–4540, 2017.

[23] T. M. Shattuck, S. Välimäki, T. Obara et al., "Somatic and germ-line mutations of the *HRPT2* gene in sporadic parathyroid carcinoma," *New England Journal of Medicine*, vol. 349, no. 18, pp. 1722–1729, 2003.

[24] V. M. Howell, C. J. Haven, K. Kahnoski et al., "*HRPT2* mutations are associated with malignancy in sporadic parathyroid tumours," *Journal of Medical Genetics*, vol. 40, no. 9, pp. 657–663, 2003.

[25] W. F. Simonds, C. M. Robbins, S. K. Agarwal, G. N. Hendy, J. D. Carpten, and S. J. Marx, "Familial isolated hyperparathyroidism is rarely caused by germline mutation in *HRPT2*, the gene for the hyperparathyroidism-jaw tumor syndrome," *The Journal of Clinical Endocrinology & Metabolism*, vol. 89, no. 1, pp. 96–102, 2004.

[26] A. Villablanca, A. Calender, L. Forsberg et al., "Germline and de novo mutations in the *HRPT2* tumour suppressor gene in familial isolated hyperparathyroidism (FIHP)," *Journal of Medical Genetics*, vol. 41, no. 3, p. e32, 2004.

[27] B. M. Cavaco, L. Guerra, K. J. Bradley et al., "Hyperparathyroidism-jaw tumor syndrome in Roma families from Portugal is due to a founder mutation of the *HRPT2* gene," *The Journal of Clinical Endocrinology & Metabolism*, vol. 89, no. 4, pp. 1747–1752, 2004.

[28] V. M. Howell, R. T. Zori, H. J. Stalker et al., "A molecular diagnosis of hyperparathyroidism—jaw tumor syndrome in an adolescent with recurrent kidney stones," *The Journal of Pediatrics*, vol. 145, no. 4, p. 567, 2004.

[29] S.-D. Moon, J.-H. Park, E.-M. Kim et al., "A novel IVS2-1G>A mutation causes aberrant splicing of the *HRPT2* gene in a family with hyperparathyroidism-jaw tumor syndrome," *The Journal of Clinical Endocrinology & Metabolism*, vol. 90, no. 2, pp. 878–883, 2005.

[30] O. Gimm, K. Lorenz, P. Nguyen Thanh et al., "Das familiäre nebenschilddrüsenkarzinom," *Der Chirurg*, vol. 77, no. 1, pp. 15–24, 2006.

[31] N. Mizusawa, S. Uchino, T. Iwata et al., "Genetic analyses in patients with familial isolated hyperparathyroidism and hyperparathyroidism-jaw tumour syndrome," *Clinical Endocrinology*, vol. 65, no. 1, pp. 9–16, 2006.

[32] M. J. Aldred, A. A. Talacko, R. Savarirayan et al., "Dental findings in a family with hyperparathyroidism-jaw tumor syndrome and a novel *HRPT2* gene mutation," *Oral Surgery, Oral Medicine, Oral Pathology, Oral Radiology, and Endodontology*, vol. 101, no. 2, pp. 212–218, 2006.

[33] K. J. Bradley, B. M. Cavaco, M. R. Bowl et al., "Parafibromin mutations in hereditary hyperparathyroidism syndromes and parathyroid tumours," *Clinical Endocrinology*, vol. 64, no. 3, pp. 299–306, 2006.

[34] C. Juhlin, C. Larsson, T. Yakoleva et al., "Loss of parafibromin expression in a subset of parathyroid adenomas," *Endocrine-Related Cancer*, vol. 13, pp. 509–523, 2006.

[35] V. Guarnieri, A. Scillitani, L. A. Muscarella et al., "Diagnosis of parathyroid tumors in familial isolated hyperparathyroidism with *HRPT2* mutation: implications for cancer surveillance," *The Journal of Clinical Endocrinology & Metabolism*, vol. 91, no. 8, pp. 2827–2832, 2006.

[36] Y. Yamashita, T. Akiyama, N. Mizusawa, K. Yoshimoto, and M. Goto, "A case of hyperparathyroidism-jaw tumour syndrome found in the treatment of an ossifying fibroma in the maxillary bone," *International Journal of Oral and Maxillofacial Surgery*, vol. 36, no. 4, pp. 365–369, 2007.

[37] F. Cetani, E. Pardi, E. Ambrogini et al., "Different somatic alterations of the *HRPT2* gene in a patient with recurrent sporadic primary hyperparathyroidism carrying an *HRPT2* germline mutation," *Endocrine-Related Cancer*, vol. 14, no. 2, pp. 493–499, 2007.

[38] F. Cetani, E. Ambrogini, P. Viacava et al., "Should parafibromin staining replace HRTP2 gene analysis as an additional tool for histologic diagnosis of parathyroid carcinoma?," *European Journal of Endocrinology*, vol. 156, no. 5, pp. 547–554, 2007.

[39] F. Raue, C. Haag, and K. Frank-Raue, "Hyperparathyreoidismus-kiefertumor-syndrom," *DMW—Deutsche Medizinische Wochenschrift*, vol. 132, no. 27, pp. 1459–1462, 2007.

[40] F. Cetani, E. Pardi, E. Ambrogini et al., "Hyperparathyroidism 2 gene (*HRPT2*, *CDC73*) and parafibromin studies in two patients with primary hyperparathyroidism and uncertain pathological assessment," *Journal of Endocrinological Investigation*, vol. 31, no. 10, pp. 900–904, 2008.

[41] M. S. Sarquis, L. G. Silveira, F. J. Pimenta et al., "Familial hyperparathyroidism: surgical outcome after 30 years of follow-up in three families with germline *HRPT2* mutations," *Surgery*, vol. 143, no. 5, pp. 630–640, 2008.

[42] V. Guarnieri, M. Bisceglia, N. Bonfitto et al., "Re: familial hyperparathyroidism: surgical outcome after 30 years of follow-up in three families with germline *HRPT2* mutations," *Surgery*, vol. 144, no. 5, pp. 839-840, 2008.

[43] V. M. Howell, A. Gill, A. Clarkson et al., "Accuracy of combined protein gene product 9.5 and parafibromin markers for immunohistochemical diagnosis of parathyroid carcinoma," *The Journal of Clinical Endocrinology & Metabolism*, vol. 94, no. 2, pp. 434–441, 2009.

[44] L. G. Silveira, E. P. Dias, B. C. G. Marinho, R. S. Gomez, L. De Marco, and M. S. Sarquis, "*HRPT2*-related familial isolated hyperparathyroidism: could molecular studies direct the surgical approach?," *Arquivos Brasileiros de Endocrinologia & Metabologia*, vol. 52, no. 8, pp. 1211–1220, 2008.

[45] B. P. Schmidt, J. P. Bradrick, and A. Gabali, "Hyperparathyroidism-jaw tumor syndrome: a case report," *Journal of Oral and Maxillofacial Surgery*, vol. 67, no. 2, pp. 423–427, 2009.

[46] N. Rekik, B. Ben Naceur, M. Mnif et al., "Hyperparathyroidism-jaw tumor syndrome: a case report," *Annales d'Endocrinologie*, vol. 71, no. 2, pp. 121–126, 2010.

[47] L. M. Panicker, J.-H. Zhang, P. K. Dagur, M. J. Gastinger, and W. F. Simonds, "Defective nucleolar localization and dominant interfering properties of a parafibromin L95P missense mutant causing the hyperparathyroidism-jaw tumor syndrome," *Endocrine-Related Cancer*, vol. 17, no. 2, pp. 513–524, 2010.

[48] B. Veiguela, M. L. Isidro, S. Jorge, and B. Ruano, "Una causa rara de hipercalcemia: carcinoma sincrónico de dos paratiroides en el contexto del síndrome de hiperparatiroidismo familiar-tumor mandibular," *Endocrinología y Nutrición*, vol. 57, no. 8, pp. 391–393, 2010.

[49] B. M. Cavaco, R. Santos, A. Félix et al., "Identification of de novo germline mutations in the *HRPT2* gene in two apparently sporadic cases with challenging parathyroid tumor diagnoses," *Endocrine Pathology*, vol. 22, no. 1, pp. 44–52, 2011.

[50] K. Frank-Raue, G. Leidig-Bruckner, A. Lorenz et al., "Hereditäre formen des primären hyperparathyreoidismus," *DMW—Deutsche Medizinische Wochenschrift*, vol. 136, no. 38, pp. 1889–1894, 2011.

[51] W. K. Siu, C. Y. Law, C. W. Lam et al., "Novel nonsense *CDC73* mutations in Chinese patients with parathyroid tumors," *Familial Cancer*, vol. 10, no. 4, pp. 695–699, 2011.

[52] R. Domingues, R. A. Tomaz, C. Martins, C. Nunes, M. J. Bugalho, and B. M. Cavaco, "Identification of the first germline *HRPT2* whole-gene deletion in a patient with primary hyperparathyroidism," *Clinical Endocrinology*, vol. 76, no. 1, pp. 33–38, 2012.

[53] A. Guerrouani, A. Rzin, and K. El Khatib, "Hyperparathyroidism jaw tumour syndrome detected by aggressive generalized osteitis fibrosa cystica," *Clinical Cases in Mineral and Bone Metabolism*, vol. 10, no. 1, pp. 65–67, 2013.

[54] M. R. Kutcher, M. H. Rigby, M. Bullock, J. Trites, S. M. Taylor, and R. D. Hart, "Hyperparathyroidism-jaw tumor syndrome," *Head & Neck*, vol. 35, no. 6, pp. E175–E177, 2013.

[55] A. Ghemigian, M. Ghemigian, I. Popescu et al., "Familial isolated primary hyperparathyroidism due to *HRPT2* mutation," *Hormones*, vol. 12, no. 3, pp. 454–460, 2013.

[56] A. Abdulla, E. O'Leary, J. Isorena, M. Diaz, and M. Yeh, "Recurrent hyperparathyroidism and a novel nonsense mutation in a patient with hyperparathyriodism-jaw tumor syndrome," *Endocrine Practice*, vol. 19, no. 6, pp. e134–e137, 2013.

[57] V. Pazienza, A. La Torre, F. Baorda et al., "Identification and functional characterization of three NoLS (nucleolar localisation signals) mutations of the *CDC73* gene," *PLoS One*, vol. 8, no. 12, Article ID e82292, 2013.

[58] J. Kong, O. Wang, M. Nie et al., "Familial isolated primary hyperparathyroidism/hyperparathyroidism-jaw tumour syndrome caused by germline gross deletion or point mutations of *CDC73* gene in Chinese," *Clinical Endocrinology*, vol. 81, no. 2, pp. 222–230, 2014.

[59] M. G. Chiofalo, A. Sparaneo, M. Chetta et al., "A novel *CDC73* gene mutation in an Italian family with hyperparathyroidism-

jaw tumour (HPT-JT) syndrome," *Cellular Oncology*, vol. 37, no. 4, pp. 281–288, 2014.

[60] E. Korpi-Hyövälti, T. Cranston, E. Ryhänen et al., "*CDC73* intragenic deletion in familial primary hyperparathyroidism associated with parathyroid carcinoma," *The Journal of Clinical Endocrinology & Metabolism*, vol. 99, no. 9, pp. 3044–3048, 2014.

[61] C. Sriphrapradang, P. Sornmayura, N. Chanplakorn, O. Trachoo, P. Sae-Chew, and R. Aroonroch, "Fine-needle aspiration cytology of parathyroid carcinoma mimic hürthle cell thyroid neoplasm," *Case Reports in Endocrinology*, vol. 2014, Article ID 680876, 7 pages, 2014.

[62] A. Mehta, D. Patel, A. Rosenberg et al., "Hyperparathyroidism-jaw tumor syndrome: results of operative management," *Surgery*, vol. 156, no. 6, pp. 1315–1325, 2014.

[63] J. Parfitt, M. Harris, J. M. Wright, and S. Kalamchi, "Tumor suppressor gene mutation in a patient with a history of hyperparathyroidism-jaw tumor syndrome and healed generalized osteitis fibrosa cystica: a case report and genetic pathophysiology review," *Journal of Oral and Maxillofacial Surgery*, vol. 73, no. 1, pp. 194.e1–194.e9, 2015.

[64] Y. Shibata, M. Yamazaki, M. Takei, S. Uchino, A. Sakurai, and M. Komatsu, "Early-onset, severe, and recurrent primary hyperparathyroidism associated with a novel *CDC73* mutation," *Endocrine Journal*, vol. 62, no. 7, pp. 627–632, 2015.

[65] K. S. Khadilkar, S. R. Budyal, R. Kasliwal, A. R. Lila, T. Bandgar, and N. S. Shah, "*HRPT2*- (*CDC73*) related hereditary hyperparathyroidism: a case series from Western India," *Endocrine Practice*, vol. 21, no. 9, pp. 1010–1016, 2015.

[66] É. C. Marchiori, B. A. Isom, and A. T. Indresano, "Management of ossifying fibroma in a suspicious case of hyperparathyroid-jaw tumor syndrome," *Craniomaxillofacial Trauma & Reconstruction*, vol. 8, no. 3, pp. 228–233, 2015.

[67] V. Bellido, I. Larrañaga, M. Guimón et al., "A novel mutation in a patient with hyperparathyroidism-jaw tumour syndrome," *Endocrine Pathology*, vol. 27, no. 2, pp. 142–146, 2016.

[68] L. Ennazk, G. El Mghari, and N. El Ansari, "Jaw tumor in primary hyperparathyroidism is not always a brown tumor," *Clinical Cases in Mineral and Bone Metabolism*, vol. 13, no. 1, pp. 64–66, 2016.

[69] J. W. Mathews, R. Winchester, N. Alsaygh, A. M. Bartlett, and L. Luttrell, "Hyperparathyroidism-jaw tumor syndrome: an overlooked cause of severe hypercalcemia," *The American Journal of the Medical Sciences*, vol. 352, no. 3, pp. 302–305, 2016.

[70] M. Mele, L. Rolighed, M. Jespersen et al., "Recurrence of hyperparathyroid hypercalcemia in a patient with the HRPT-2 mutation and a previous parathyroid carcinoma in hyperparathyroidism-jaw tumor syndrome," *International Journal of Endocrinology and Metabolism*, vol. 14, no. 2, Article ID e35424, 2016.

[71] D. Piciu, A. Piciu, E. Barbus, C. Pestean, M. I. Larg, and B. Fetica, "Primary hyperparathyroidism-jaw tumor syndrome: a confusing and forgotten diagnosis," *Medicine and Pharmacy Reports*, vol. 89, no. 4, pp. 555–558, 2016.

[72] V. Guarnieri, R. M. Seaberg, C. Kelly et al., "Large intragenic deletion of *CDC73* (exons 4–10) in a three-generation hyperparathyroidism-jaw tumor (HPT-JT) syndrome family," *BMC Medical Genetics*, vol. 18, no. 1, p. 83, 2017.

[73] E. Mamedova, N. Mokrysheva, E. Vasilyev et al., "Primary hyperparathyroidism in young patients in Russia: high frequency of hyperparathyroidism-jaw tumor syndrome," *Endocrine Connections*, vol. 6, no. 8, pp. 557–565, 2017.

[74] M. P. R. Dhas, K. S. Karthiga, J. E. Tatu, and S. J. Eugenia, "Hyper parathyroidisim jaw tumor syndrome: a rare condition of incongruous features," *Ethiopian Journal of Health Sciences*, vol. 27, no. 3, pp. 309–313, 2017.

[75] J. C. Rubinstein, S. K. Majumdar, W. Laskin et al., "Hyperparathyroidism-jaw tumor syndrome associated with large-scale 1q31 deletion," *Journal of the Endocrine Society*, vol. 1, no. 7, pp. 926–930, 2017.

[76] K. Koikawa, Y. Okada, H. Mori, M. Kawaguchi, S. Uchino, and Y. Tanaka, "Hyperparathyroidism-jaw tumor syndrome confirmed by preoperative genetic testing," *Internal Medicine*, vol. 57, no. 6, pp. 841–844, 2018.

[77] C. Bachmeier, C. Patel, P. Kanowski, and K. Sangla, "Should all patients with hyperparathyroidism be screened for a *CDC73* mutation?," *Endocrinology, Diabetes & Metabolism Case Reports*, vol. 2018, Article ID EDM170164, 2018.

[78] A. Kapur, N. Singh, O. Mete, R. A. Hegele, and I. G. Fantus, "A young male with parafibromin-deficient parathyroid carcinoma due to a rare germline *HRPT2*/*CDC73* mutation," *Endocrine Pathology*, vol. 29, no. 4, pp. 374–379, 2018.

[79] S. Ciuffi, L. Cianferotti, G. Nesi et al., "Characterization of a novel *CDC73* gene mutation in a hyperparathyrodism-jaw tumor patient affected by parathyroid carcinoma in the absence of somatic loss of heterozygosity," *Endocrine Journal*, vol. 66, no. 4, pp. 319–327, 2019.

[80] M. Russo, G. Borzì, M. Ilenia, F. Frasca, P. Malandrino, and D. Gullo, "Challenges in the treatment of parathyroid carcinoma: a case report," *Hormones*, vol. 18, no. 3, pp. 325–328, 2019.

[81] A. J. Gill, G. Lim, V. K. Y. Cheung et al., "Parafibromin-deficient (HPT-JT type, *CDC73* mutated) parathyroid tumors demonstrate distinctive morphologic features," *The American Journal of Surgical Pathology*, vol. 43, no. 1, pp. 35–46, 2019.

[82] M. Iacobone, V. Camozzi, C. Mian et al., "Long-term outcomes of parathyroidectomy in hyperparathyroidism-jaw tumor syndrome: analysis of five families with *CDC73* mutations," *World Journal of Surgery*, 2019.

[83] M. Iacobone, F. Lumachi, and G. Favia, "Up-to-date on parathyroid carcinoma: analysis of an experience of 19 cases," *Journal of Surgical Oncology*, vol. 88, no. 4, pp. 223–228, 2004.

[84] M. Iacobone, C. Ruffolo, F. Lumachi, and G. Favia, "Results of iterative surgery for persistent and recurrent parathyroid carcinoma," *Langenbeck's Archives of Surgery*, vol. 390, no. 5, pp. 385–390, 2005.

[85] J. D. Chen, C. Morrison, C. Zhang, K. Kahnoski, J. D. Carpten, and B. T. Teh, "Hyperparathyroidism-jaw tumour syndrome," *Journal of Internal Medicine*, vol. 253, no. 6, pp. 634–642, 2003.

[86] Y. Teh, D. Y. Hu, T. T. Wang et al., "*CDC73* gene mutations in sporadic ossifying fibroma of the jaws," *Diagnostic Pathology*, vol. 11, no. 1, p. 91, 2016.

[87] J. Szabó, B. Heath, V. M. Hill et al., "Hereditary hyperparathyroidism-jaw tumor syndrome: the endocrine tumor gene *HRPT2* maps to chromosome 1q21–q31," *American Journal of Human Genetics*, vol. 56, pp. 944–950, 1995.

[88] C. D. Vocke, C. J. Ricketts, M. W. Ball et al., "*CDC73* germline mutation in a family with mixed epithelial and stromal tumors," *Urology*, vol. 124, pp. 91–97, 2019.

[89] W. L. Xie, J. Y. Lian, B. Li, X. Y. Tian, and Z. Li, "Mixed epithelial and stromal tumor of kidney with renal vein extension: an unusual case report and review of literature," *Histology and Histopathology*, vol. 32, no. 4, pp. 361–369, 2017.

[90] C. J. Haven, F. K. Wong, E. W. C. M. van Dam et al., "A genotypic and histopathological study of a large Dutch kindred with hyperparathyroidism-jaw tumor syndrome1," *The Journal of Clinical Endocrinology & Metabolism*, vol. 85, no. 4, pp. 1449–1454, 2000.

Hindawi
International Journal of Endocrinology
Volume 2019, Article ID 4687951, 7 pages
https://doi.org/10.1155/2019/4687951

Research Article

Intraoperative Near-Infrared Autofluorescence and Indocyanine Green Imaging to Identify Parathyroid Glands: A Comparison

Max Lerchenberger,[1] Norah Al Arabi,[1] Julia K. S. Gallwas,[2] Herbert Stepp,[3] Klaus K. J. Hallfeldt,[1] and Roland Ladurner[1]

[1]*Department of Surgery, Ludwig Maximilians University Munich, Innenstadt Medical Campus, Nussbaumstrasse 20, 80336 Munich, Germany*
[2]*Department of Obstetrics and Gynecology, Ludwig Maximilians University Munich, Maistr. 11, 80337 Munich, Germany*
[3]*Laser-Research Laboratory, LIFE-Center and Department of Urology, Ludwig Maximilians University Munich, Grosshadern Medical Campus, Feodor-Lynen-Str. 19, 81377 Munich, Germany*

Correspondence should be addressed to Klaus K. J. Hallfeldt; klaus.hallfeldt@med.uni-muenchen.de

Received 31 May 2019; Accepted 11 September 2019; Published 25 September 2019

Academic Editor: Maria G. Chiofalo

Objective. To investigate the feasibility of near-infrared autofluorescence (AF) and indocyanine green (ICG) fluorescence to identify parathyroid glands intraoperatively. *Methods*. Fluorescence imaging was carried out during open parathyroid and thyroid surgery. After visual identification, parathyroid glands were exposed to near-infrared (NIR) light with a wavelength between 690 and 770 nm. The camera of the Storz® NIR/ICG endoscopic system used detects NIR light as a blue signal. Therefore, parathyroid AF was expected to be displayed in the blue color channel in contrast to the surrounding tissue. Following AF imaging, a bolus of 5 mg ICG was applied intravenously. ICG fluorescence was detected using the same NIR/ICG imaging system. Well-vascularized parathyroid glands were expected to show a strong fluorescence in contrast to surrounding lymphatic and adipose tissue. *Results*. We investigated 78 parathyroid glands from 50 patients. 64 parathyroid glands (82%) displayed AF showing the typical bluish violet color. 63 parathyroid glands (81%) showed a strong and persistent fluorescence after application of ICG. The sensitivity of identifying a parathyroid gland by AF was 82% (64 true positive and 14 false negative results), while ICG imaging showed a sensitivity of 81% (63 true positive and 15 false negative results). The Fisher exact test revealed no significant difference between both groups at $p < 0.05$. Neither lymph nodes nor adipose tissue revealed substantial AF or ICG fluorescence. *Conclusion*. AF and ICG fluorescence reveal a high degree of sensitivity in identifying parathyroid glands. Further, ICG imaging facilitates the assessment of parathyroid perfusion. However, in the current setting both techniques are not suitable as screening tools to identify parathyroid glands at an early stage of the operation.

1. Introduction

Difficulties in accurately localizing parathyroid glands during thyroid surgery may result in the disruption of the parathyroid vasculature. Despite refined operation techniques, postoperative temporary hypocalcemia remains the most common complication after total thyroidectomy [1–4]. The standard procedure to identify and save parathyroid glands is just by visual inspection, and the result largely depends on the surgeon's experience. Most endocrine surgeons would agree that there is a great demand for a simple and reliable technique to identify parathyroid glands intraoperatively. To date, numerous localization techniques have been proposed to facilitate intraoperative parathyroid identification.

The idea of using a dye or a fluorophore in order to visualize parathyroid glands is not new. Back in 1971, Dudley described the application of methylene blue as an exogenous contrast agent [5]. 30 years later, van der Vorst et al. investigated near-infrared fluorescence imaging based on the intravenous application of small doses of methylene blue [6], and 20 years ago, Prosst et al. proposed

aminolevulinic acid (ALA) as a contrast agent [7]. Although these methods proved to be effective in trials, they could not become generally accepted, and the clinical approach to parathyroid identification remained stagnant [8–10]. Rubinstein et al. have been the first to visualize parathyroid glands by applying optical coherence tomography (OCT), a noninvasive high-resolution imaging technique that permits characterization of microarchitectural features up to 2 mm in depth [11]. OCT images of lymph nodes and parathyroid, thyroid, and adipose tissue display typical characteristics for each entity, facilitating a reliable differentiation. Conti de Freitas et al. and our research group were able to confirm these favorable results ex vivo [12–14]. However, due to technical problems, handling the OCT probe covered with a sterile sheath it was impossible to obtain similar results in vivo [15].

The recent discovery of parathyroid autofluorescence by a research team of biomedical engineers and endocrine surgeons from Nashville, Tennessee has renewed the interest in intraoperative parathyroid imaging [16]. At an excitation wavelength in the near-infrared (NIR), parathyroid tissue exhibits a unique autofluorescence up to 11 times higher than that of the surrounding tissue. As most tissue types are more or less completely void of autofluorescence in this wavelength range, even a weak fluorescence signal can provide a high contrast. Furthermore, this wavelength range is characterized by a high penetration depth and allows for the recognition of fluorescent tissue. In the meantime, a large number of studies have confirmed the excellent detection rates initially described by McWade et al. [17–26].

In 2016, Zaidi et al. described the use of indocyanine green (ICG) fluorescence imaging during parathyroid and thyroid surgery [27, 28]. In these prospective studies, over 90% of parathyroid glands were reliably identified by their ICG uptake. In the same year, Fortuny et al. reported on a study using ICG angiography in order to assess parathyroid vascularization [29]. By now, the high sensitivity in detecting parathyroid glands using ICG imaging and just as well screening their vascularization has been supported by numerous studies [30–32].

Autofluorescence and ICG fluorescence imaging represent the techniques most intensively investigated at present. In this in vivo study we compare the different approaches and try to assess their differences.

2. Materials and Methods

This prospective in vivo study was approved by the institutional ethical review board of the Medical faculty of the University of Munich. Patients undergoing open hemithyroidectomy or total thyroidectomy and patients undergoing open parathyroidectomy with complete cervical exploration were eligible for enrollment. Informed consent was obtained from all patients.

2.1. Imaging System. Parathyroid ICG fluorescence was visualized using a commercially available near-infrared/indocyanine green (NIR/ICG) endoscopic system (Karl Storz, Tuttlingen, Germany). The system comprises a high-end full high-definition camera system (Image1 H3-Z 3-Chip Full HD camera, Karl Storz) connected to a 10 mm 0° ICG telescope (Hopkins™ II, Karl Storz). The camera is sensitive for NIR light with its blue channel, due to the spectral properties of the dielectric coatings of the color beamsplitter. The telescope is equipped with a specific filter for optimal detection of white light and NIR fluorescence, while completely blocking out NIR excitation light. In the NIR excitation mode, the light source also emits low-intensity light in the green and red spectral ranges to enable orientation during NIR fluorescence imaging. The system's xenon light source (D-Light P, Karl Storz) provides both visible and NIR excitation light at a wavelength of 690 nm to 790 nm. The surgeon can use a footswitch to change from white light to NIR. Parathyroid autofluorescence was detected using the same NIR/ICG endoscopic system as its excitation wavelength in the near-infrared is around 800 nm, and autofluorescence is emitted at around 820 nm. However, as autofluorescence is considerably weaker than ICG fluorescence and previous investigations showed a notable amount of light being backscattered and recorded in the blue channel, a second xenon light source (D-Light P, Karl Storz) was modified by interposing an additional longpass filter. Further, a bandpass filter was added to reduce the light in the green and red spectral region [20].

2.2. Intraoperative Imaging. Autofluorescence and ICG imaging were carried out during open thyroid and parathyroid surgery for benign and malignant disease. After lateral mobilization of the thyroid and exposure of the recurrent laryngeal nerve, the parathyroid glands were visualized. However, we did not search for a gland when it was not apparent during initial thyroid dissection. Using magnifying glasses special care was taken to preserve the vascular pedicles. Only parathyroid glands that were definitely identified by an experienced endocrine surgeon were considered for fluorescence imaging. First, white light images were collected. Second, with all operating room lights turned off, the parathyroid gland as well as the surrounding tissue were exposed to near-infrared (NIR) light. The tip of the laparoscope was held stationary approximately 5 cm above the tissue. With the light source in fluorescence mode, NIR light was detected as a blue signal by the camera, and in contrast to the surrounding tissue the parathyroid gland was expected to be displayed in the blue color channel. The autofluorescent effect was photo-documented for each parathyroid gland.

For ICG fluorescence imaging, 25 mg of the fluorophore ICG-Pulsion® (Diagnostic Green GmbH, Aschheim-Dornach, Germany) was dissolved in 5 ml sterile water and 5 mg (1 ml) injected intravenously. ICG fluorescence became apparent after 1-2 minutes. The progression was video-documented over 3–5 minutes. To allow a direct comparison between autofluorescence and ICG fluorescence, we investigated only one side in each patient. Measuring autofluorescence after application of ICG on the contralateral side would have falsified the results for AF imaging.

When a parathyroid gland revealed at least the same fluorescence than the surrounding thyroid tissue, ICG fluorescence was regarded as being positive. In most cases, the fluorescence even persisted after the decrease of thyroid fluorescence. A negative result was defined as parathyroid fluorescence being completely missing or being significantly less compared to the surrounding thyroid tissue.

3. Results

Between October 2017 and May 2018, 78 parathyroid glands from 50 patients who underwent open thyroid or parathyroid surgery were examined with regard to their autofluorescence and ICG fluorescence. The demographic and clinical details are shown in Table 1.

64 parathyroid glands (82%) displayed NIR autofluorescence showing the typical bluish violet color as described in previous studies [20–22]. The intensity of their fluorescence enabled a sharp distinction from surrounding structures, especially lymph nodes, thyroid tissue, and adipose tissue (Figure 1(a)). Regarding the extent of autofluorescence, we could not observe noticeable differences between vascular and avascular glands. Autofluorescence imaging was especially helpful in identifying inferior parathyroid glands during central lymph node dissection. In 14 cases (18%) we were unable to visualize autofluorescence despite unambiguous visual identification of the parathyroid gland (Table 2). The sensitivity of identifying a parathyroid gland by autofluorescence was 82%. ICG imaging was carried out subsequent to autofluorescence imaging. 63 parathyroid glands (81%) showed a persistent fluorescence after the decrease of thyroid fluorescence. This effect was seen 2-3 min after i.v. ICG application (Figure 2). In 11 cases (14%) fluorescence was not observed, although visual inspection suggested a good vascularity of the parathyroid tissue, and no change of color was noted during the operation (Figures 1(b) and 1(c)). 4 parathyroid glands showed a distinct darkening of color following dissection.

The subsequent ICG application did not induce a noticeable fluorescence, and we had to assume a damage to parathyroid vascularization. These glands were autotransplanted into the sternocleidomastoid muscle. Two of these patients developed transient hypocalcemia postoperatively which was treated with calcium effervescent tablets 4×500 mg/die and alfacalcidol capsules $1\,\mu$g/die. Further, all patients with thyroidectomy and central lymph node dissection received this medication on a routine basis as well as 3 patients with Graves' disease and moderate ICG fluorescence, where we had to dissect the inferior parathyroid glands from the thyroid capsule.

The sensitivity of identifying a parathyroid gland by autofluorescence was 82% (64 true positive and 14 false negative results) while ICG imaging showed a sensitivity of 81% (63 true positive and 15 false negative results). The Fisher exact test revealed no significant difference between both groups at $p < 0.05$. However, the quoted sensitivity of ICG imaging must be judged with caution as the technique relies on well-vascularized tissue, and a compromised circulation falsifies the results.

Table 1: Descriptive data.

Number of patients	50
Mean age	47.2 years
Sex (female/male)	36/14
Type of operation	(*n*)
Open parathyroidectomies	17
Thyroidectomies—Goiter	7
Thyroidectomies—Graves' disease	9
Thyroidectomies—Carcinoma	8
Plus central LN dissection	4
Hemithyroidectomies	5

Regarding the extra time necessary to perform AF imaging, we required approximately 3–5 minutes to prepare the imaging system and 2-3 min to visualize both parathyroid glands on one side. ICG imaging was more time-consuming with around 3 extra minutes to see the peak of parathyroid fluorescence emission.

4. Discussion

The study demonstrates that both imaging techniques examined are helpful in identifying parathyroid glands intraoperatively. Autofluorescence and ICG imaging showed a sensitivity of 82% and 85%, respectively. There was no statistically significant difference between both groups. These results are consistent with observations made by other authors who reported detection rates of 77–100% with AF [19–22, 25] and 84–100% with ICG fluorescence [29–31, 33, 34].

However, both techniques are currently not sufficiently sensitive to operate as screening tools helping to localize parathyroid tissue at an early stage of the operation. The initial goal, the precise and rapid detection of parathyroid glands by way of screening the surgical site, cannot be achieved. Frequently, parathyroid glands are covered by a sheath of adipose tissue which needs to be removed in order to display autofluorescence. We experienced similar problems with ICG imaging, where adipose tissue but also even minor bleeding at the operating site may obscure the fluorescence. AF and ICG imaging may be helpful to confirm the presence of a parathyroid gland, but in their present utilization the techniques will not be effective to replace accurate dissection by an experienced surgeon. Regarding AF, more sensitive imaging systems than those available at present could lead to an effective screening at an early stage of the operation and replace the present strategy of confirming the presence of a visually identified parathyroid gland. For ICG imaging we used a small dose of 5 mg indocyanine per patient. In our opinion, it would be of interest to investigate whether higher doses increase parathyroid fluorescence and thereby allow an early detection. The cause for the longer persistence of ICG-fluorescence in parathyroid glands as compared to the thyroid is not known to us. A possible explanation may be a slower venous blood flow.

Table 3 summarizes advantages and disadvantages of autofluorescence and ICG imaging as experienced in our study. All investigations were carried out using a

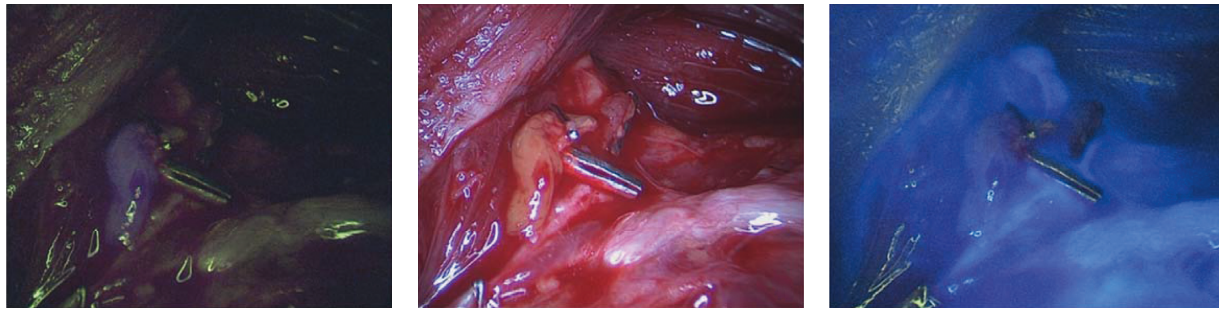

(a) (b) (c)

Figure 1: Parathyroid gland. (a) Autofluorescence image that displays the typical bluish violet color of the gland. (b) The parathyroid gland in normal white light. (c) 2 min after i.v. application of 5 mg ICG. The gland shows hardly any ICG fluorescence, and it can be assumed that it is devascularized.

Table 2: Comparison of autofluorescence (AF) and indocyanine green (ICG) fluorescence.

	AF positive	AF negative	Total
ICG positive	56	7	63
ICG negative	8 (4 devas.)	7	15
Total	64	14	78

78 parathyroid glands were examined. 64 showed autofluorescence (sensitivity 82%) and 63 ICG fluorescence (sensitivity 85%). 7 glands were negative both for AF and ICG fluorescence. 4 ICG negative glands showed a darkening of color intraoperatively and we had to assume their devascularization. The Fisher exact test did not reveal significant differences between both the groups.

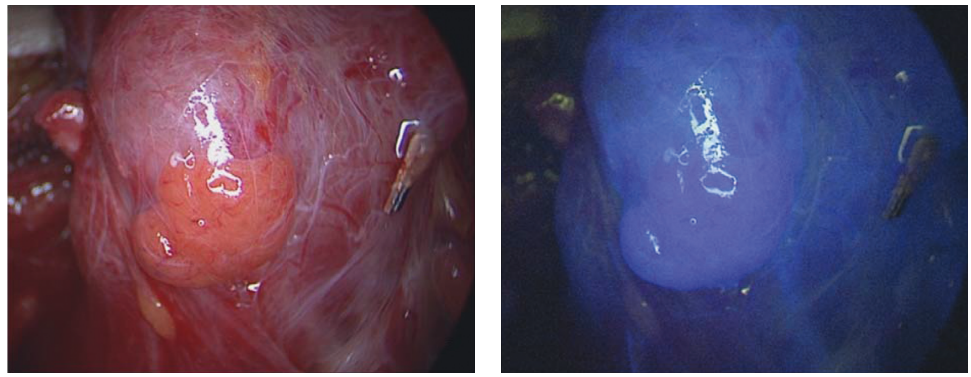

(a) (b)

Figure 2: Parathyroid gland exposed to normal white light (a) and near-infrared light 2 min after i.v. application of 5 mg ICG (b). The gland displays a strong fluorescence indicating a good vascularity. The surrounding structures, especially the thyroid, are less fluorescent.

commercially available Storz ICG imaging system (Karl Storz GmbH, Tuttlingen, Germany) with only slight modifications to the light source for autofluorescence imaging. Irrespective of their ICG components, camera and light source provide the same features as the standard laparoscopic equipment and can be used for routine laparoscopic surgery. The additional costs for the NIR imaging capability amount to approximately 4000 Euro. A 25 mg vial of indocyanine green (ICG-Pulsion®, Diagnostic Green GmbH) costs around 70 Euro.

The commercially available Fluobeam® 800 system (Fluoptics, Grenoble, France) represents another, meanwhile well-established, device to detect parathyroid autofluorescence. A laser provides an irradiance of 5 mW/cm^2 at 750 nm and collects the optical signal for wavelengths above 800 nm [24–26]. At an experimental level, Kim et al. introduced a new technique to visualize both parathyroid glands and the surrounding tissue in a single image, using a 780 nm collimated light-emitting diode (Thorlabs, Newton, NJ, USA) with an excitation filter appropriate for parathyroid autofluorescence, an illuminator (INFRALUX-300, Daekyoung, Korea) for reflection of the entire surgical area, and a digital single-lens reflex camera (Canon, EOS REBEL T3, Ota, Tokyo, Japan) [23, 27].

Other commercially available devices used for ICG fluorescence imaging were the Novadaq® Pinpoint system (Novadaq®, Mississauga, On, Canada) and the Striker® endoscopic near-infrared visualization(ENV) system (Stryker® Endoscopy, San Jose, CA, USA). The main difference of these devices compared to the Storz ICG imaging

Table 3: Comparison of autofluorescence and ICG imaging of parathyroid glands.

Autofluorescence imaging	ICG imaging
Confirmation of parathyroid tissue after identification of the gland by the naked eye	Confirmation of parathyroid tissue after identification of the gland by the naked eye
No screening tool	No screening tool
No administration of a pharmaceutical	Intravenous administration of a fluorophore with potential side effects. Not approved for this indication in Europe.
Fluorescence imaging with a modified ICG system	Fluorescence imaging with a standard ICG system
No assessment of parathyroid perfusion	Assessment of parathyroid perfusion possible
No appraisal of vascular anatomy	Evaluation of vascular anatomy possible
Additional operating time: 5–10 min	Additional operating time: 8–13 min
No additional costs	Additional costs of 70 EUR (ICG)

system is the use of a NIR laser instead of a xenon light source. To our knowledge, no studies exist that directly compare their performance.

Along with higher costs, longer operating times may be an obstacle to incorporate a new technique to conventional surgery. In our experience, the additional time needed for AF imaging and ICG imaging amounts to 5–10 min and 8–13 min, respectively. This includes setting up the endoscopic system, darkening the operating room, and endoscopically localizing the parathyroid glands. With extended i.v. lines, as in our setting due to the positioning of the arms, an extra 3 min was needed to follow ICG enhancement in the tissue with the peak to be seen in the parathyroid glands after 2-3 min. AF reveals no difference between vascularized and devascularized glands. In contrast, ICG imaging depends on tissue vascularity and as described by several authors it is well possible to identify devascularized glands (Figure 2) and thus, simplifying the decision for autotransplantation. In the present series, 15 out of 78 parathyroid glands did not reveal an adequate ICG fluorescence, most likely caused by insufficient vascularization. As we did not notice a change of color in 11 of these glands, during the further course of the operation we refrained from autotransplantation. We believe, the disruption may have been temporarily, for instance by vascular compression or traction on the thyroid lobe. A complete separation of the parathyroid vessels would have been very unlikely at the early stage of the operation when ICG imaging was carried out.

Apart from assessing parathyroid vascularization intraoperatively, ICG imaging may be helpful to visualize the exact vascular anatomy before dissection close to the gland begins. This could be a major advantage in order to avoid hypoparathyroidism, especially if parathyroid glands are attached to the thyroid or possess a long vascular pedicle [35].

A limitation of the present study is that we had to rely on the visual evaluation of parathyroid glands. Although we carried out measurements only in situations where we were absolutely sure to have identified parathyroid tissue, 11 of the 15 ICG negative results and especially the 7 ICG and AF negative results must be questioned. As already discussed in previous studies [20–22], we cannot explain why in our series AF imaging failed in around 15% of cases. The cause could be our imaging system, originally destined to provide ICG imaging but not to display the considerably weaker parathyroid autofluorescence. Further, in a recent article McWade et al. noted that different probe placements could lead to different measurements from the same gland [19]. These differences were attributed to intraglandular heterogeneity. In our experience, AF becomes more difficult to detect when the glands are embedded in adipose tissue or seem to contain a high amount of adipose cells. Regarding parathyroid vascularity, we noticed substantial differences between our visual impression and ICG imaging. 11 parathyroid glands showed no darkening in color despite a missing or poor contrasting after application of indocyanine green. This suggests that ICG imaging may be more precise to evaluate parathyroid vascularity and that a missing change of color does not imply good vascularization.

In practical terms, we found it difficult to apply the ICG 0–2 scoring system proposed by Fortuny et al. [30] and especially to distinguish between grey, grey/black, and entirely black parathyroid glands. This may be due to a lack of experience and certainly this new technique involves a learning curve. In this study, the indication for autotransplantation still depended on the visual impression of the gland, and it was not our intention to correlate ICG fluorescence and postoperative hypocalcemia.

As mentioned before, both techniques are not screening tools, and parathyroid glands need to be identified beforehand with the naked eye. AF imaging allows to localize parathyroid glands even though the tissue is devascularized. We found this helpful in surgery with central lymph node dissection, either to verify their localization or to confirm their identity before autotransplantation. For ICG imaging, parathyroid glands need to be vascularized. This circumstance may be used to predict postoperative parathyroid function [30, 31, 33, 34] or in future to assist the decision making whether an autotransplantation should be carried out.

5. Conclusions

Although most parathyroid and thyroid operations are uncomplicated, difficult situations occur regularly, and it may be crucial to identify and preserve parathyroid tissue. It seems to be premature to assume that AF imaging or ICG imaging will play a major role regarding the intraoperative

identification of parathyroid glands. However, both techniques have so far shown to be fairly reliable. They can be easily applied intraoperatively and require only moderate expenditure. However, the main issue, the precise and rapid detection of parathyroid glands by way of screening the surgical site, cannot be achieved.

Data Availability

The data used to support the findings of this study are included within the article.

Conflicts of Interest

Karl Storz® GmbH provided a laparoscopic system with a special light source and camera free of charge to R. Ladurner and K. Hallfeldt. Karl Storz® GmbH had no role in the design of the study, in the collection, analyses, or interpretation of data; in the writing of the manuscript, and in the decision to publish the results. N. Al Arabi, M. Lerchenberger, J. Gallwas and H. Stepp have no conflicts of interest or financial ties to disclose.

References

[1] D. T. Lin, S. G. Patel, A. R. Shaha, B. Singh, and J. P. Shah, "Incidence of inadvertent parathyroid removal during thyroidectomy," *The Laryngoscope*, vol. 112, no. 4, pp. 608–611, 2002.

[2] O. Thomusch, A. Machens, C. Sekulla, J. Ukkat, M. Brauckhoff, and H. Dralle, "The impact of surgical technique on postoperative hypoparathyroidism in bilateral thyroid surgery: a multivariate analysis of 5846 consecutive patients," *Surgery*, vol. 133, no. 2, pp. 180–185, 2003.

[3] A. Bergenfelz, S. Jansson, A. Kristoffersson et al., "Complications to thyroid surgery: results as reported in a database from a multicenter audit comprising 3,660 patients," *Langenbeck's Archives of Surgery*, vol. 393, no. 5, pp. 667–673, 2008.

[4] J. P. Bilezikian, A. Khan, J. T. Potts et al., "Hypoparathyroidism in the adult: epidemiology, diagnosis, pathophysiology, target-organ involvement, treatment, and challenges for future research," *Journal of Bone and Mineral Research*, vol. 26, no. 10, pp. 2317–2337, 2011.

[5] N. E. Dudley, "Methylene blue for rapid identification of the parathyroids," *BMJ*, vol. 3, no. 5776, pp. 680-681, 1971.

[6] J. R. van der Vorst, B. E. Schaafsma, F. P. R. Verbeek et al., "Intraoperative near-infrared fluorescence imaging of parathyroid adenomas with use of low-dose methylene blue," *Head and Neck*, vol. 36, no. 6, pp. 853–858, 2014.

[7] R. L. Prosst, J. Weiss, L. Hupp, F. Willeke, and S. Post, "Fluorescence-guided minimally invasive parathyroidectomy: clinical experience with a novel intraoperative detection technique for parathyroid glands," *World Journal of Surgery*, vol. 34, no. 9, pp. 2217–2222, 2010.

[8] N. Han, J. M. Bumpous, R. E. Goldstein, M. M. Fleming, and M. B. Flynn, "Intra-operative parathyroid identification using methylene blue in parathyroid surgery," *The American Surgeon*, vol. 73, no. 8, pp. 820–823, 2007.

[9] T. Suzuki, T. Numata, and M. Shibuya, "Intraoperative photodynamic detection of normal parathyroid glands using 5-aminolevulinic acid," *The Laryngoscope*, vol. 121, no. 7, pp. 1462–1466, 2011.

[10] H. P. Patel, D. R. Chadwick, B. J. Harrison, and S. P. Balasubramanian, "Systematic review of intravenous methylene blue in parathyroid surgery," *British Journal of Surgery*, vol. 99, no. 10, pp. 1345–1351, 2012.

[11] M. Rubinstein, W. B. Armstrong, K. Naemi, S. B. Keel, B. J. F. Wong, and J. H. Kim, "Intraoperative use of OCT in endocrine surgery," in *Proceedings of the AAO-HNSF Annual Meeting*, Boston, MA, USA, September 2010.

[12] L. C. Conti de Freitas, E. Phelan, L Liu et al., "Optical coherence tomography imaging during thyroid and parathyroid surgery: a novel system of tissue identification and differentiation to obviate tissue resection and frozen section," *Head and Neck*, vol. 36, no. 9, pp. 1329–1334, 2014.

[13] R. Ladurner, K. K. J. Hallfeldt, N. Al Arabi, H. Stepp, S. Mueller, and J. K. S. Gallwas, "Optical coherence tomography as a method to identify parathyroid glands," *Lasers in Surgery and Medicine*, vol. 45, no. 10, pp. 654–659, 2013.

[14] S. Sommerey, R. Ladurner, N. Al Arabi, U. Mortensen, K. Hallfeldt, and J. Gallwas, "Backscattering intensity measurements in optical coherence tomography as a method to identify parathyroid glands," *Lasers in Surgery and Medicine*, vol. 47, no. 6, pp. 526–532, 2015.

[15] S. Sommerey, N. Al Arabi, R. Ladurner et al., "Intraoperative optical coherence tomography imaging to identify parathyroid glands," *Surgical Endoscopy*, vol. 29, no. 9, pp. 2698–2704, 2015.

[16] C. Paras, M. Keller, L. White, J. Phay, and A. Mahadevan-Jansen, "Near-infrared auto-fluorescence for the detection of parathyroid glands," *Journal of Biomedical Optics*, vol. 16, no. 6, Article ID 067012, 2011.

[17] M. A. McWade, C. Paras, L. M. White, J. E. Phay, A. Mahadevan-Jansen, and J. T. Broome, "A novel optical approach to intraoperative detection of parathyroid glands," *Surgery*, vol. 154, no. 6, pp. 1371–1377, 2013.

[18] M. A. McWade, C. Paras, L. M. White et al., "Label-free intraoperative parathyroid localization with near-infrared autofluorescence imaging," *The Journal of Clinical Endocrinology and Metabolism*, vol. 99, no. 12, pp. 4574–4580, 2014.

[19] M. A. McWade, M. E. Sanders, J. T. Broome, C. C. Solórzano, and A. Mahadevan-Jansen, "Establishing the clinical utility of autofluorescence spectroscopy for parathyroid detection," *Surgery*, vol. 159, no. 1, pp. 193–203, 2016.

[20] R. Ladurner, S. Sommerey, N. Arabi Al, K. K. J. Hallfeldt, H. Stepp, and J. K. S. Gallwas, "Intraoperative near-infrared autofluorescence imaging of parathyroid glands," *Surgical Endoscopy*, vol. 31, no. 8, pp. 3140–3145, 2017.

[21] R. Ladurner, N. Al Arabi, U. Guendogar, K. K. J. Hallfeldt, H. Stepp, and J. K. S. Gallwas, "Near-infrared autofluorescence imaging to detect parathyroid glands in thyroid surgery," *The Annals of The Royal College of Surgeons of England*, vol. 100, no. 1, pp. 33–36, 2018.

[22] R. Ladurner, M. Lerchenberger, N. Al Arabi, J. K. S. Gallwas, H. Stepp, and K. K. J. Hallfeldt, "Parathyroid autofluorescence-how does it affect parathyroid and thyroid surgery? A 5 year experience," *Molecules*, vol. 24, no. 14, p. 2560, 2019.

[23] S. W. Kim, H. S. Lee, and K. D. Lee, "Intraoperative real-time localization of parathyroid gland with near infrared fluorescence imaging," *Gland Surgery*, vol. 6, no. 5, pp. 516–524, 2017.

[24] F. Benmiloud, S. Rebaudet, A. Varoquaux, G. Penaranda, M. Bannier, and A. Denizot, "Impact of autofluorescence-based identification of parathyroids during total thyroidectomy on postoperative hypocalcemia: a before and after controlled study," *Surgery*, vol. 163, no. 1, pp. 23–30, 2018.

[25] J. Falco, F. Dip, P. Quadri, M. de la Fuente, M. Prunello, and R. J. Rosenthal, "Increased identification of parathyroid glands using near infrared light during thyroid and parathyroid surgery," *Surgical Endoscopy*, vol. 31, no. 9, pp. 3737–3742, 2017.

[26] B. Kahramangil, F. Dip, F. Benmiloud et al., "Detection of parathyroid autofluorescence using near-infrared imaging: a multicenter analysis of concordance between different surgeons," *Annals of Surgical Oncology*, vol. 25, no. 4, pp. 957–962, 2018.

[27] S. W. Kim, H. S. Lee, Y.-C. Ahn et al., "Near-infrared autofluorescence image-guided parathyroid gland mapping in thyroidectomy," *Journal of the American College of Surgeons*, vol. 226, no. 2, pp. 165–172, 2018.

[28] N. Zaidi, E. Bucak, P. Yazici et al., "The feasibility of indocyanine green fluorescence imaging for identifying and assessing the perfusion of parathyroid glands during total thyroidectomy," *Journal of Surgical Oncology*, vol. 113, no. 7, pp. 775–778, 2016.

[29] N. Zaidi, E. Bucak, A. Okoh, P. Yazici, H. Yigitbas, and E. Berber, "The utility of indocyanine green near infrared fluorescent imaging in the identification of parathyroid glands during surgery for primary hyperparathyroidism," *Journal of Surgical Oncology*, vol. 113, no. 7, pp. 771–774, 2016.

[30] J. V. Fortuny, V. Belfontali, S. M. Sadowski, W. Karenovics, S. Guigard, and F. Triponez, "Parathyroid gland angiography with indocyanine green fluorescence to predict parathyroid function after thyroid surgery," *British Journal of Surgery*, vol. 103, no. 5, pp. 537–543, 2016.

[31] M. Lavazza, X. Liu, C. Wu et al., "Indocyanine green-enhanced fluorescence for assessing parathyroid perfusion during thyroidectomy," *Gland Surgery*, vol. 5, no. 5, pp. 512–521, 2016.

[32] P. Jitpratoom and A. Anuwong, "The use of ICG enhanced fluorescence for the evaluation of parathyroid gland preservation," *Gland Surgery*, vol. 6, no. 5, pp. 579–586, 2017.

[33] J. V. Fortuny, S. M. Sadowski, V. Belfontali et al., "Randomized clinical trial of intraoperative parathyroid gland angiography with indocyanine green fluorescence predicting parathyroid function after thyroid surgery," *British Journal of Surgery*, vol. 105, no. 4, pp. 350–357, 2018.

[34] B. Kahramangil and E. Berber, "Comparison of indocyanine green fluorescence and parathyroid autofluorescence imaging in the identification of parathyroid glands during thyroidectomy," *Gland Surgery*, vol. 6, no. 6, pp. 644–648, 2017.

[35] S. M. Sadowski, J. V. Fortuny, and F. Triponez, "A reappraisal of vascular anatomy of the parathyroid gland based on fluorescence techniques," *Gland Surgery*, vol. 6, no. 1, pp. S30–S37, 2017.